Functional characterization of pathogenicity genes in *Fusarium circinatum*

by

Mmatshepho Malekgale Phasha

Submitted in partial fulfillment of the requirements for the degree

Philosophiae doctor (Microbiology)

In the faculty of Natural and Agricultural Sciences

University of Pretoria

Pretoria

24 May 2021

Supervisor: Prof. E.T. Steenkamp

Co-supervisor: Prof. B.D. Wingfield

Co-supervisor: Prof. M.P.A. Coetzee

Co-supervisor: Prof. M.J. Wingfield

Declaration

I, Mmatshepho Malekgale Phasha declare that the thesis, which I hereby submit for the degree Philosophiae doctor (Microbiology) at the University of Pretoria, is my own work and has not been submitted by me for a degree at this or any other tertiary institution.

SIGNATURE: 

DATE: 24 May 2021

Acknowledgements

I would like to acknowledge the following people and funding bodies:

- **Primary supervisor Prof. Emma Steenkamp** for contributing greatly towards the standard of this thesis by making sure results and answers to research questions were communicated and discussed clearly.

- **Co-supervisor Prof. Brenda Wingfield** for inspiring and supporting the molecular techniques used to answer the research questions presented in this thesis.

- **Co-supervisor Prof. Martin Coetzee** for contributing significantly towards the readability of each chapter of this thesis.

- **Co-supervisor Prof. Mike Wingfield** for his great contribution towards the clarity of this thesis.

- **Co-authors** of papers from this thesis, and **various researchers** from the University of Pretoria and other universities for all their contributions towards my academic journey.

- The **University of Pretoria**, the National Research Foundation (**NRF**), the Forestry and Agricultural Biotechnology Institute (**FABI**), the Tree Protection Cooperative Programme (**TPCP**), and the DSI-NRF South African Research Chairs Initiative (**SARChI**) Chair in Fungal Genomics for the financial support that enabled the research presented in this thesis.

- **Ms. Emily Mokhehle**, **Ms. Eva Muller** and **Ms. Heidi Fysh** for all the administrative support during the course of this degree.

- **My brothers and friends** (in and outside FABI) for their motivation and encouragements during this degree.

- **My Mother and Father** for being unconditionally supportive and setting great examples for me. I learnt from them that persistence and following through pays off. Hunadi le Ngaketse, ke a leboga!

- **My husband** for his encouragement and talking me out of quitting when it was difficult to keep going.

- **My Heavenly Father** for this great achievement! I am humbled.

Table of Contents

Preface

Fungal phytopathogens cause destructive plant diseases, many of which have huge health and economic implications globally. *Fusarium* species are among the most destructive phytopathogens that affect agricultural and forestry crops. In many cases, the infection biology of these fungi is well understood, but the molecular basis and mechanisms the fungi use to infect, colonize and survive in their hosts are ill-understood. Because of their importance, whole genome sequences for various *Fusarium* species have been determined, which has aided the identification of numerous putative pathogenicity and virulence factor genes in some of these fungi. Although extensive genomic resources are also available for the pine pitch canker fungus, *Fusarium circinatum*, few pathogenicity and virulence factor genes have been identified.

The identification of putative fungal pathogenicity and virulence factor genes provides clues of the molecular basis of these traits, while knowledge of the exact roles of such genes helps us better understand the molecular mechanisms these fungi use to overcome defences of hosts, infect and colonize the hosts. However, relative to the number of pathogenicity and virulence factor genes identified so far, very few have been characterized functionally. This is primarily due to the lack of fast and efficient genetic engineering methods to generate mutants in many non-model phytopathogenic fungi. Improvements in some of the existing methods have contributed to increased efficiency and turn-around time in the characterization of pathogenicity and virulence factor genes in some fungi, including *F. circinatum*. Moreover, advancements in transcriptome sequencing have enabled the elucidation of signalling pathways that control development and pathogenesis, as well as genes under the direct control of these pathways. The use of such genetic engineering and transcriptome sequencing technologies is thus essential to ultimately improve our understanding of pathogenesis in fungal plant pathogens.

The pine pitch canker fungus, *F. circinatum*, causes devastating disease and economic losses to the forestry industry. It is thus important to understand how this fungus attacks pine. The overall goal of this thesis was to gain knowledge on the molecular basis of the pathogenicity and virulence in *F. circinatum*. Particularly, we sought to understand the role of two putative *F. circinatum* pathogenicity genes (*RAS2* and *FUB1*) during pine infection using knockout mutants. In addition,

we wanted to decipher other putative pathogenicity genes directly or indirectly controlled by the products of *RAS2* and *FUB1*.

Chapter 1 of this thesis provides a review of available literature on pathogenicity and virulence factors in filamentous phytopathogenic fungi. Illustrative examples involved during the different stages of the infection process are discussed. The genomic organization as well as the evolution of pathogenicity and virulence factor genes are also considered. Finally methods used to characterize these genes are discussed. Recent advancements in such methods are also highlighted.

In **Chapter 2**, the function of the putative pathogenicity gene *RAS2* was investigated in *F. circinatum*. To accomplish this, knockout and complement mutants were generated using the split-marker method, and their phenotypes were compared to those of *F. circinatum* wild type strain FSP34. The phenotypes included hyphal growth, conidiation, fertility and virulence on *Pinus patula* seedlings. Results from this chapter will shed light on the role of the Ras2 protein in the growth, development and pathogenicity of *F. circinatum*.

In **Chapter 3**, the function of the putative pathogenicity and polyketide synthase gene *FUB1* was investigated in *F. circinatum*. Here, a knockout mutant strain was also generated using the split-marker method, and its phenotypes were compared to those of *F. circinatum* wild type strain FSP34. The investigated phenotypes included the ability to produce the phytotoxin fusaric acid (for which the polyketide synthase encoded by *FUB1* is a key player) and virulence on *P. patula* seedlings. Furthermore, the transcriptomes of this mutant and the wild type strains were sequenced to facilitate a better understanding of the role of this gene in the pathogenesis of *F. circinatum*. Findings from this work will provide us with knowledge on the role of the polyketide synthase encoded by the *FUB1* gene in *F. circinatum*.

In **Chapter 4**, genes under the control of *F. circinatum* Ras2 and the signalling pathway by which these genes are regulated by Ras2 were elucidated. To achieve this, the transcriptomes of the *ras2* knockout and complement mutants and wild type strain FSP34 of this fungus were sequenced. This was done in triplicate, and expression studies were conducted to determine genes differentially expressed between the strains. Genes found to be differentially expressed were

further investigated for their potential roles in pathogenicity and development. The differential expression data was also used to determine the most likely signalling pathway by which Ras2 regulates these genes, and thus pathogenesis in *F. circinatum*. Knowledge of the exact genes under the control of Ras2, as well as the pathway by which this protein regulates pathogenicity will shed light on the molecular mechanisms underpinning this trait in *F. circinatum*.

Note: The Supplementary (excel) files for Chapters 3 and 4 are located in the CD or zipped folder provided along with this thesis.

Chapter 1

Literature review: Pathogenicity and virulence factors in phytopathogenic filamentous fungi

Abstract

Phytopathogenic filamentous fungi cause some of the most destructive diseases of plants including trees globally. Understanding the molecular basis and mechanisms underlying pathogenesis in these organisms is thus important. The advent of high throughput sequencing technologies has accelerated the identification of many genes potentially involved in this process, although the exact roles of many have not yet been determined and/or proven. This is due to time-consuming laboratory-based methods to functionally characterize these genes. However, new methods such as the CRISPR/Cas9 genome editing technology offers efficient functional characterization, enabling high throughput genome editing experiments. This review covers various pathogenicity and virulence factors of agriculturally and economically important plant pathogens involved in different stages of the infection process. The components of the major pathways controlling the expression of these genes are also discussed. The last section of the review considers different approaches used to identify and characterize pathogenicity and virulence factors. Only by understanding the identity and roles of these factors, will we gain better knowledge of why and how fungal pathogens thrive on and in their host plants, which is in turn fundamental to the development of efficient strategies for combatting fungal diseases.

1. Introduction

The term "fungal pathogenesis" refers to the entire array of processes that allow a pathogen to cause disease on its host plant (i.e., adhesion, recognition and penetration of the host, invasive growth within the host, production and dispersal of infectious particles) (reviewed by Shapiro-Ilan et al., 2005). Within this context, the term "pathogenicity" refers to the ability of an organism to cause disease on a susceptible host organism (reviewed by Thomas and Elkinton, 2004 and Agrios, 2005). This ability is a complex trait that is governed by a plethora of genes, the products of which are often referred to as pathogenicity factors (van de Wouw and Howlett, 2011; Rauwane et al., 2020). These factors play key roles during specific stages of the overall pathogenesis process (Yoder and Turgeon, 2001; Rauwane et al., 2020). Their expression depends largely on the host and its response to infection, as well as environmental conditions (van der Does and Rep, 2007; Li et al., 2020), which taken together, dictate the pathogen's virulence, i.e., degree of damage caused to a host by the pathogen (Steinhaus and Martignoni, 1970; Aizawa, 1971; Fuxa and Tanada, 1987; Lacey, 1997; Thomas and Elkinton, 2004; van der Does and Rep, 2007).

To date, numerous pathogenicity and virulence factor genes have been identified in the genomes and proteomes of phytopathogenic fungi (reviewed by Idnurm and Howlett, 2001 and Pontes et al., 2020). Some of these are highly variable and encode proteins needed for host recognition,

attachment and penetration, suppression of host defensive compounds, plant cell wall degradation, transport, defence, and secondary metabolism, among others (reviewed by Idnurm and Howlett, 2001 and Pontes et al., 2020). Other pathogenicity and virulence factor genes may be highly conserved, both in terms of sequence and of function. Fitting examples of these are those encoding signalling pathways, where G-proteins (also referred to as GTPases: guanosine triphosphatases) relay specific gene expression cues via the mitogen-activated protein kinase (MAPK) and cyclic adenosyl monophosphate (cAMP) pathways (Lengeler et al., 2000; Xu, 2000). Therefore, despite being highly conserved and ubiquitous in fungi (i.e., also occurring in non-pathogens), G-proteins and the proteins of the MAPK and cAMP pathways are also regarded as virulence factors because their activation leads to the expression of genes involved in pathogenicity and virulence (Idnurm and Howlett, 2001).

Pathogenicity and virulence factor genes in fungi often have particular genomic organisation and distribution, and some evolve faster than other genes within the same genome (Reviewed by van der Does and Rep, 2007). For example, pathogenicity and virulence factor genes may be organised in clusters across genomes while others are present near telomeres or on accessory chromosomes (van der Does and Rep, 2007; Rep and Kistler, 2010; Ma et al., 2010). Such clustering is thought to mediate coordinated expression of the genes (Gasch et al., 2000; Kamper et al., 2006; Ellison et al., 2014), while their position near/in telomeres and on accessory chromosomes may increase their mutation rates (van der Does and Rep, 2007; Rep and Kistler, 2010). The trigger for mutation can be due to host plants changing their defence factors to evade the fungal pathogen (van der Does and Rep, 2007; Li et al., 2020). Irrespective of its origin, rapid evolution of pathogenicity and virulence factors enable pathogens to constantly overcome host defence responses thereby successfully colonising the host (van der Does and Rep, 2007; Rep and Kistler, 2010).

The number of identified fungal pathogenicity and virulence genes is increasing rapidly due to the ever-reducing costs of whole genome sequencing (Tang et al., 2018). Consequently, researchers are inundated with the need to characterize and confirm their function (reviewed by Larrondo et al., 2009), and to decipher their relationships and the networks of which they are part. Traditionally, the main approaches for characterising new genes would have been reverse genetics strategies such as targeted gene replacement/disruption, gene silencing and site directed mutagenesis, while northern blotting, expressed sequence tag studies, microarrays and real time polymerase chain reaction studies would have been used for determining gene expression and for investigating their relationships and the networks they may be part of (Gasch et al., 2000; Bhadauria et al., 2009; Tan et al., 2009; Ellison et al., 2014). However, the complexities and time-intensive nature of these standard reverse genetics approaches generally limit the number of genes that can be fully

functionally characterized (Bhadauria et al., 2009; Tan et al., 2009). Recently, on-going developments in some of these approaches are making it easier to characterise a greater number of genes and to do this more rapidly. In addition, more recent technologies such as transcriptome sequencing are making it possible to discover a myriad of genes belonging to pathways and networks rapidly and efficiently (Nagalakshmi et al., 2008; Meijueiro et al., 2014).

This review considers the role of pathogenicity and virulence factors of agriculturally and economically important plant pathogens at different stages of the infection process. Where relevant, examples of genes identified and functionally characterized in various filamentous fungi using knockout mutant strains are also provided. The two major pathways (MAPK and cAMP) by which these pathogenicity and virulence factor genes are activated as well as their genomic organisation and evolution are also discussed. Furthermore, methods used to identify and characterize these genes, and their relevance in this era of rapidly evolving technologies, are reviewed. Where applicable, ways in which these methods can be efficiently applied to better understand the molecular basis and mechanisms of pathogenicity and virulence in fungal phytopathogens are highlighted.

2. Fungal pathogenicity and virulence factors

Despite each having its own definition, it can be difficult to make a clear separation between a pathogenicity and virulence factor. At the molecular level, this confusion is often due to the fact that homologous proteins can have different roles or effects depending on the infected host and environmental conditions at play, while non-homologous proteins can have the same function (Tudzynski and Sharon, 2003). Furthermore, some genes can have more than one role in the same organism depending, for example, on the stage in the infection process (Liu et al., 2011; Anjago et al., 2018). However, a considerable number of functional characterization studies has been conducted on numerous genes in fungi (see Table 1 for notable examples). Illustrative examples of those involved in signalling, host attachment and penetration, host tissue colonization, and suppression of host defensive compounds in some of the best studied agriculturally and economically important phytopathogenic fungi are discussed in this section.

2.1. Components of signalling pathways

In phytopathogenic fungi, infection of a susceptible host is largely driven by signal cascade pathways (Tudzynski and Sharon, 2003). Examples of these pathways include the cAMP and MAPK signalling pathways, which are the two most studied signalling pathways associated with pathogenesis in fungi (Lowy, 1993; Stepien and Lalak-Kanczugowska, 2020). Shortly after a fungal pathogen perceives molecules and material (i.e., growth factors) on a plant surface with its receptors

(i.e., growth factor receptors), the cAMP and MAPK signalling pathways are activated (Kronstadt, 1997; Stepien and Lalak-Kanczugowska, 2020; Figure 1). This interaction between the growth factor receptors and growth factors causes conformational change and phosphorylation of the receptors, which usually activates a master regulatory protein. This protein then triggers a cascade of phosphorylation reactions between proteins of the cAMP and MAPK signalling pathways, which in turn cause activation of transcriptional regulators to ultimately culminate in the expression of a myriad of genes involved in the pathogenesis (Kronstadt, 1997; Tudzynski and Sharon, 2003; van de Wouw and Howlett, 2011; Figure 1).

In phytopathogenic fungi, the most common master regulators of pathogenesis-related processes are small G-proteins belonging to the Ras superfamily of proteins (Zhu et al., 2009). This superfamily is divided into five main groups (i.e., Rab, Ran, Ras, Rho, and Sar/Arf) based on sequence and function (Bourne et al., 1991; Cox and Der, 2010). They all have in common the core G domain that provides the GTPase and nucleotide exchange activity (Barbacid, 1987; de Vos et al., 1988; Pai et al., 1989; Tong et al., 1989; Cox and Der, 2010). In the case of Ras, the protein also has a C-terminal membrane targeting region to allow its proper processing and subcellular localization (Spence and Casey, 2001; Young et al., 2001). Like other members of the superfamily, Ras proteins have "on" and "off" states – when GTP is bound to the G domain the protein is active, and inactive when guanosine diphosphate (GDP) occupies this position (Kronstadt, 1997; Tudzynski and Sharon, 2003).

Although the cAMP and MAPK pathways are conserved, some components of these pathways can be divergent, making it important to study them in many fungi (Martinez-Soto and Ruiz-Herrera, 2017). Also, signal transduction via both pathways can become complicated because, depending on the growth factor encountered, the Ras protein can activate both or either pathway (Lengeler et al., 2000). Moreover, the components of these pathways can also be affected differently (Lengeler et al., 2000). The next sections provide a discussion of some of the characterised genes and proteins that are part of the cAMP and MAPK pathways in different fungi.

2.1.1. The MAPK pathway

In addition to pathogenesis, the MAPK signalling pathway affects diverse biological processes in fungi (reviewed by Martinez-Soto and Ruiz-Herrera, 2017). The pathway consists of a MAPK kinase kinase (MAPKKK) protein (that receives signals directly from Ras), followed by a MAPK kinase (MAPKK), and a MAPK that activates one or more transcriptional regulators. These regulators direct the expression of genes involved in various cellular processes including growth, development, sporulation and virulence, among others (Kronstadt, 1997; Tudzynski and Sharon, 2003; Martinez-Soto and Ruiz-Herrera, 2017; Stepien and Lalak-Kanczugowska, 2020; Figure 1).

MAPK pathways affecting pathogenicity have been identified in fungi such as *Magnaporthe grisea* (Xu, 2000), *Cochliobollus heterostrophus* (Lev et al., 1999), *Botrytis cinerea* (Zheng et al., 2000), *Ustilago maydis*, and *Fusarium* spp (reviewed by Tudzynski and Sharon, 2003) The core MAPK genes identified in these fungi include *PMK1* (Xu, 2000) and *MPS1* (Lev et al., 1999), *BMP1* (Zheng et al., 2000), *KPP2* (Muller et al., 1999), *FMK1* (Di Pietro et al., 2001), respectively. In *M. grisea* mutants of genes *PKM1* and *MPS1* are defective in appressorium formation and invasive growth, and in penetration, respectively (Xu, 2000). Lev et al. (1999) found that *C. heterostrophus* knockout mutants of the *PKM1* gene produce reduced lesion sizes on maize leaves compared to the wild type strain, while Zheng et al. (2000) found that *bmp1* knockout mutants of *B. cinerea* showed loss of pathogenicity to tomato. In *U. maydis*, mutants of the *KPP2* gene were defective in mating and vegetative growth, but only had slight reduction in virulence on maize (Muller et al., 1999). Inactivation of the *FMK1* gene of *F. oxysporum* f. sp. *lycopersici* resulted in mutants that were near non-pathogenic on tomato due to inability to grow invasively during infection (Di Pietro et al., 2001), and deletion of this gene in *F. verticillioides* (i.e., *FvMK1*) affected microconidium production and virulence on maize (Zhang et al., 2011). Most recently, the MAPK gene of the tree pathogen *F. circinatum* was suggested to play a role in vegetative growth and virulence of the fungus on *Pinus patula* seedlings (Phasha et al., 2021).

2.1.2. The cAMP pathway

As with the MAPK pathway, the components and typical sequence of signal relay through the cAMP pathway are well established (Kronstadt, 1997; Figure 1). Two proteins form this pathway, namely adenylate cyclase and protein kinase A (PKA). Following growth factor perception, the Ras protein activates adenylate cyclase, causing it to convert ATP to cAMP (Kronstadt, 1997). This causes an activation of PKA, which in turn activates transcriptional regulators that induce the expression of particular genes involved in different stages of fungal pathogenesis, including appressorial differentiation, conidial development and hyphal growth among others (Kang et al., 1999; Kruger et al., 2000; Tudzynski and Sharon, 2003; Zhang et al., 2011; Figure 1).

Functional characterization studies have shown that both the adenylate cyclase and PKA influence pathogenicity/virulence in some fungi (Kang et al., 1999; Fillinger et al., 2002; Schumacher et al., 2008; Choi and Xu, 2010). For example, deletion of the adenylate cyclase gene (*cyaA*) and the catalytic subunit of the PKA gene (*pkaA*) in *Aspergillus nidulans* resulted in smaller colonies and fewer conidiophores in *cyaA* mutants, and slower conidial germination in *pkaA* mutants than in the wild type strain (Fillinger et al., 2002). Disruption of the PKA gene of *M. grisea* caused a delay in appressorium formation, thereby affecting the pathogen's ability to cause disease (Kang et al., 1999). Deletion of the catalytic subunit gene of PKA (i.e., gene *FAC1*) in *F. verticillioides* resulted

in mutants that are defective in microconidium and macroconidium production, and have reduced virulence on corn stalks (Choi and Xu, 2010). In *B. cinerea*, deletion of PKA's catalytic and regulatory subunits (*bcpka1* and *bcpkaR*) caused slow lesion development compared to the wild type strain (Schumacher et al., 2008). Interestingly, a study conducted in *F. graminearum RAS* mutants did not find evidence showing that genes of the cAMP pathway play a role in vegetative growth, conidiation and virulence in this fungus on wheat (Bluhm et al., 2007).

2.2. Genes involved in host attachment and penetration

Recognition of a susceptible host plant by a fungal pathogen marks the onset of processes needed for attachment to and penetration of the host (reviewed by Deising et al., 2000; Tudzynski and Sharon, 2003). Accordingly, genes involved in these processes are among the first to be expressed shortly after the compatible plant-pathogen interaction has been established (Dean, 1997; Tudzynski and Sharon, 2003). The products of these genes enable the pathogen to attach and cross the cuticle and cell wall barriers of the plant, constituting the first line of defence against infection (Horbach et al., 2011). Depending on the lifestyle of a fungus (i.e., biotroph, hemibiotroph or necrotroph), force and/or chemicals are needed to cross these barriers (Demoor et al., 2019). For example, in obligate biotrophs such as powdery mildew pathogens, an appressorium is required for penetration (Horbach et al., 2011). Hemibiotrophic fungi such as *Magnaporthe* and *Colletotrichum* also have appressoria enabling them to gain access into the plant host, although they also employ cell wall degrading enzymes (CWDEs) for this purpose (Talbot, 2003; Horbach et al., 2011). For necrotrophs, CWDEs are vital for entry into the plant host cell, although some pathogens in this group (e.g., certain species of *Fusarium, Botrytis*, *Alternaria* and *Cercospora*) also produce appressorium-like structures (Horbach et al., 2011; Kubicek et al., 2014). Whatever the strategy, without efficient attachment to and penetration of the physical barriers of the host plant's tissue, successful infection cannot occur (Deising et al., 2000). Considerable knowledge regarding infection biology can thus be gained by studying genes that encode infection structures and CWDEs in phytopathogenic fungi.

2.2.1. Genes involved in appressorium formation

Since the first discovery of appressoria (Frank, 1883), the genes that regulate their formation and function have received considerable attention (Deising et al., 2000; Demoor et al., 2019). Thus, many fungi previously thought not to produce these structures (e.g., *Podospora anserina*; Brun et al., 2009) are now known to produce appressoria and/or encode the genes thought to be required for their formation (Lambou et al., 2008; Marschall et al., 2016; Galhano et al., 2017). This has raised questions regarding the presence, role and regulation of appressorial genes during the infection process in phytopathogenic fungi not known to produce these structures (Demoor et al., 2019).

Nevertheless, these genes have been extensively studied and characterized in agriculturally important hemibiotrophs such as *M. grisea* and *M. oryzae*, and species of *Colletotrichum* (Tang et al., 2018). As a consequence, a wealth of information has been generated about the molecular basis of appressorium formation in these fungi, mainly because of their experimental tractability (Tang et al., 2018). For example, they are much easier to culture and work with in the laboratory than obligate biotrophs, and they form more conspicuous appressoria than the so-called "infection cushions" or inconspicuous appressoria formed by certain other pathogens (Perpetua et al., 1996; Kamakura et al., 2002; Wanjiru et al., 2002; Talbot, 2019).

Based on the current body of knowledge, Tudzynski and Sharon (2003) separated appressorial genes into three categories: i) genes expressed prior to the formation of the appressorium, ii) genes expressed in the appressorium and, iii) genes involved in the germination of the appressorium and penetration of the host (Tudzynski and Sharon, 2003). However, the last two categories of genes are often difficult to distinguish and, technically, both groups are expressed in the appressorium. Therefore, to simplify the discussion in this section, appressorial genes were considered as being part of two broad groups (Groups 1 and 2). Those in Group 1 are expressed before appressorium formation, and Group 2 includes genes expressed in the appressorium during its formation, germination and host penetration.

Group 1 often contains genes encoding components of signalling pathways, which is despite the fact that these genes also represent pathogenicity factors involved in additional cellular processes (Tudzynski and Sharon, 2003; Bruno et al., 2004; Liu et al., 2011). Signalling genes form part of Group 1, because appressoria are formed in response to particular physical and chemical cues such as plant surface hardness, the presence of cutin monomers, etc. (Frank, 1883 as quoted by Talbot, 2019). For instance, the product of the previously mentioned MAPK gene (*PMK1*) of *M. grisea* (Xu et al., 1996) can also relay signals generated from the hydrophobicity of leaf surfaces, which culminate in the germination of conidia that differentiate into appressoria (Sabnam and Barman, 2017). In this fungus, it was found that *PMK1* is essential for appressorium formation, particularly in developing conidia prior to forming appressoria as well as in developing appressoria (Bruno et al., 2004). Although conserved, *PMK1* orthologs in many fungi have not been reported to play a role in appressorium differentiation and formation (Liu et al., 2011), thus highlighting the fact that knowledge gained using one pathosystem is often not transferrable to another.

Other pathogenicity factors included in Group 1 are those involved in chitin biosynthesis. This likely reflects the need for chitin production in conidia destined to develop into appressoria. In *M. oryzae*, the chitin synthase gene *CHS7* is highly expressed in conidia and essential for the production of conidial germ tubes from which appressoria are formed (Kong et al., 2012). Also in

M. grisea, another Group 1 gene encodes the chitin-binding protein CBP1 which affects spore adhesion and appressorial differentiation (Kamakura et al., 2002). In this fungus, the *CBP1* gene was shown to be expressed in the cell walls of germ tubes, further indicating its involvement in the conversion of chitin to chitosan during conidial differentiation into appressoria (Kuroki et al., 2017).

Known genes included in Group 2 are those involved in creating turgor pressure needed to puncture the plant surface, as well germination of the appressorium and development of a penetration peg (Tudzynski and Sharon, 2003). Turgor pressure is primarily dependent on biosynthesis of glycerol and melanin within appressoria (Tudzynski and Sharon, 2003). Examples of the latter thus include the melanin biosynthesis genes *PKS1* and *THR1* (encoding a polyketide synthase and trihydroxynaphthalene reductase, respectively) in *Colletotrichum lagenarium* that are essential for host plant infection (Takano et al., 1995; Perpetua et al., 1996; Tudzynski and Sharon, 2003). An example of glycerol biosynthesis regulation is the serine/threonine kinase gene, *MGATG1*, that allows *M. grisea* to penetrate its plant host by contributing to the generation of turgor in appressoria by controlling formation of lipid droplets in these structures (Liu et al., 2007). Other interesting Group 2 pathogenicity factor genes include *GAS1* and *GAS2* that are expressed in appressoria of *M. grisea*. In this case, deletion mutants are incapable of appressorial penetration of rice and barley tissue, despite retaining the ability to form appressoria (Xue et al., 2002). The *PIC5* gene (i.e., Pmk1-interacting clone 5) encoded downstream of *PMK1* of *M. oryzae* is also a Group 2 pathogenicity factor gene, which affects germ tube formation and appressorial differentiation, with mutants not being able to penetrate the host tissue (Zhang et al., 2011).

Although numerous appressorial genes are well characterized and more are being discovered (e.g., the *CLU5* gene cluster in *Colletotrichum graminicola*; Eisermann et al., 2019), it is still not well understood how the exact switch from polarized hyphal cell growth to the non-polarized growth of appressoria occurs (Talbot, 2019). The mechanism ensuring that the penetration peg emerges from the correct side of the appressorium is also not understood (Talbot, 2019). Although some of the genes characterized in *Magnaporthe* and *Colletotrichum* are conserved among Sodariomycetes (in some cases among both pathogens and saprotrophs) (Eisermann et al., 2019), functional characterization is needed for them and other appressoria-associated genes to better understand their role in fungal pathogenesis.

2.2.2. Genes involved in plant cell wall degradation

Plants use the cell wall and cuticle as a physical barrier against pathogens (De Lorenzo et al., 1997; Hematy et al., 2009). To overcome this complex barrier consisting of various organic polymers (e.g., pectin, lignin, structural proteins, cellulose), phytopathogenic fungi utilize various CWDEs

(Leslie and Xu, 2010). Thus, following recognition of a susceptible plant host, the pathogen secretes one or more suitable CWDEs to depolymerize the plant cell wall, thereby allowing it access into the plant cell (Kubicek et al., 2014; Figure 1). It is consequently not surprising that fungi can produce vast arrays of CWDEs. For example, the genomes of single necrotrophs harbour between 400 and 900 genes encoding carbohydrate active enzymes (CAZymes), many of which represent CWDEs (Zhao et al., 2013). Although CWDEs are utilised by all phytopathogens during late stages of infection, necrotrophs, due to their dependence on these enzymes to enter plant cells, encode many more CWDE genes than hemibiotrophs and biotrophs (Horbach et al., 2011; Kubicek et al., 2014). Also, not all CWDE genes of phytopathogenic fungi affect pathogenicity, and these genes are also found in saprotrophs and endophytes (Bakri et al., 2014). Moreover, within particular fungal genomes, CWDE genes may have a high level of redundancy (Isshiki et al., 2001; Leslie and Xu, 2010). Given these reasons, functional studies of CWDE genes and proving their specific roles in pathogenicity/virulence are often challenging.

By making use of gene knockout or replacement mutants, a number of CWDEs have been shown to represent pathogenicity/virulence factors. For example, when the endo-β-1,4-xylanase encoding gene *VmXyl1* in the apple tree pathogen, *Valsa mali*, is disrupted, the mutant strain formed fewer pycnidia and was less virulent than the wild type strain (Yu et al., 2018). Also making use of mutants, ten Have et al. (1998) and Isshiki et al. (2001) demonstrated that polygalacturonases encoded by *Bcpg1* in *B. cinerea* and *Acpg* in *Alternaria citri* contributed to the pathogens' virulence on tomato and citrus, respectively. However, deletion of the *Acpg* homolog in *A. alternata* (i.e., *Aapg*) did not affect virulence, showing that this pathogen was able to produce other enzymes that compensated for this function (Isshiki et al., 2001).

In *Fusarium*, several studies with knockout mutants of CWDE genes have shown that these enzymes do not affect pathogenicity as much as they do in the other fungi discussed here (e.g., Rogers et al., 1994; Garcia-Maceira et al., 2001; Gomez-Gomez et al., 2002). Interestingly, however, a study in *F. graminearum* with a double knockout of the genes *Pg1* and *xyr1* (encoding an endo-polygalacturonase CWDE and a transcriptional regulator of xylanase genes, respectively) found that the mutant was significantly less virulent on wheat than the wild type strain, whereas the independent disruption of the two genes did not affect the mutants' virulence (Paccanaro et al., 2017). This suggests that CWDEs could be working in synergy with the products of other genes during depolymerisation of the plant cell wall in some fungi (Paccanaro et al., 2017), and sets a precedent for research in other *Fusarium* species, and probably most fungi where single knockouts did not affect virulence.

2.3. Genes involved in host colonization

After breaching the plant cuticle and cell wall, fungal pathogens need to colonize the host tissues. For example, obligate biotrophs use nutrition cells called haustoria to gain access into host cells without destroying the cells (Horbach et al., 2011). Necrotrophs, however, colonise the host cells by producing phytotoxins that destroy the cell membranes (Horbach et al., 2011). Although their mode of action is not always known, it appears that certain pathogenic fungi produce some of these toxins in a host-specific manner and also use them to disable the defence system of the host during colonisation (Horbach et al., 2011; van de Wouw and Howlett, 2011). Nevertheless, these pathogenicity/virulence factors often represent secondary metabolites produced by non-ribosomal peptide synthetases (NRPSs) and/or polyketide synthases (PKSs), which are low molecular weight enzymes containing multiple domains (Figure 2) involved in the polymerization of the core components of the toxins (Keller et al., 2005; van de Wouw and Howlett, 2011).

NRPSs and PKSs-encoding genes involved in the production of pathogenicity and virulence factors have been identified in various fungi (Ahn and Walton, 1996; Yoder et al., 1997; Wiemann et al., 2013). In many cases, both NRPS and PKS genes, as well as some of their accessory genes, have been shown to play vital roles in fungal virulence (Horbach et al., 2011). For example, certain strains of *C. heterostrophus* produce a polyketide toxin (T-toxin) (Kono et al., 1981), making them more virulent than those that do not produce the toxin (Yoder et al., 1997). Also, *C. heterostrophus* mutants carrying a deletion in any of the T-toxin biosynthesis genes (i.e., *PKS1*, *PKS2* and *DEC1*) cause only small lesions on maize compared to wild type strains (Yang et al., 1996; Rose et al., 2002; Baker et al., 2006). In *Cochliobolus carbonum*, gene knockout studies have shown the NRPS-encoded HC toxin is needed for virulence specifically on maize (Ahn and Walton, 1996; Walton, 2006), which is also true for the *TOXF* gene product responsible for regulating the HC toxin biosynthesis gene cluster (Cheng et al., 1999). Other examples of host-selective toxins are ToxA produced by *Pyrenophora tritici-repentis* (Friesen et al., 2006) and AAL produced by *A. alternata* (Akamatsu et al., 1997). ToxA is encoded by the *TOXA* gene and confers *P. tritici-repentis* with virulence specifically to wheat (Friesen et al., 2006), while AAL is a polyketide that confers *A. alternata* with virulence specifically to tomato (Akamatsu et al., 1997).

Phytotoxins produced by *Fusaruim* species represent some of the best studied virulence and pathogenicity factors in phytopathogenic fungi. For example, enniatin-producing strains of *F. avenaceum* are more efficient in colonizing potato tubers (Herrmann et al., 1996). The genus *Fusarium* contains an exceptionally rich reservoir of genes encoding a diversity of secondary metabolite pathways (Wiemann et al., 2013). Trichothecenes are among the best-known and most studied toxins in the genus, particularly among members of the *F. sambucinum* species complex

(Perincherry et al., 2019). The trichothecene deoxynivalenol produced by *F. graminearum* has been shown to have cytotoxic effects on cereals (Proctor et al., 1995). Mutants carrying a disrupted *Tri5* gene encoding an enzyme (trichodiene synthase) required for the initial steps during biosynthesis of this toxin were less virulent on wheat and rye than the wild type strain (Proctor et al., 1995). Some of the best characterized phytotoxins in the *F. fujikuroi* and *F. oxysporum* species complexes include fumonisin, fusaric acid and bikaverin (Berthiller et al., 2013; Perincherry et al., 2019). The production of these toxins has been correlated with virulence of *F. oxysporum* f. sp. *lycopersici* on tomato (Lopez-Diaz et al., 2018), *F. oxysporum* f. sp. *vasinfectum* (Bell et al., 2003) on cotton and *F. verticillioides* on maize (Glenn et al., 2008), respectively, and the genes encoding the enzymes that produce these secondary metabolites have also been functionally characterized. However, as stated earlier, presence of homologs of toxin genes in related species do not always correlate with biosynthesis of these important secondary metabolites. Therefore, future studies on toxins and the concomitant genes in other fungi affecting different plant hosts will lead to a better understanding of the activities of toxins and their role in pathogenesis.

2.4. Genes involved in the suppression of host defense compounds

The evasion or suppression of antifungal compounds produced by plants is one of the key strategies used by phytopathogens to overcome host defence responses and thus to facilitate efficient colonisation of the plant tissue (Tudzynski and Sharon, 2003). Some of the most common antifungal compounds employed by plants against phytopathogens are phytoalexins (Hammerschmidt, 1999; Figure 1). In turn, fungal phytopathogens employ two main mechanisms to evade the effects of these phytoalexins during infection. The first mechanism involves detoxification of the antifungal compounds, while the second involves their export out of the cell (Leslie and Xu, 2010; Figure 1). Genes involved in these two processes have been identified and characterized in a number of fungal phytopathogens including *Fusarium* species (Wasmann and VanEtten, 1996; Andrade et al., 2000; Sun et al., 2006; de Waard et al., 2006; Coleman et al., 2011).

Various proteins that detoxify phytoalexins have been shown to represent pathogenicity or virulence factors. For example, in *F. solani*, knockout mutants of the pisatin demethylase gene (*PDA1*) display reduced virulence on pea. This is because the protein product of this gene is a cytochrome P450 monooxygenase and is essential for degrading pisatin (Wasmann and VanEtten, 1996; van den Brink et al., 1998; Driessen et al., 2000). Similarly, *TOM1* mutants of *F. oxysporum* f. sp. *lycopersici* are highly sensitive to the phytoalexin α-tomatine and show delayed disease progression on tomato (Pareja-Jaime et al., 2008). In this case, a functional *TOM1* gene product is needed to detoxify the antifungal compound by removing one or more sugar residues from it (Pareja-Jaime et al., 2008). Numerous other cytochrome P450 monooxygenase genes thought to be

involved in the detoxification of phytoalexins have been identified in fungi, but their function in phytoalexin detoxification remains unconfirmed, partly due to the fact that numerous of these genes encode redundant products (reviewed by Shin et al., 2018).

As with phytoalexin detoxifying genes, many proteins responsible for the efflux of these antifungal compounds are also regarded as pathogenicity or virulence factors. An example is an ATP-binding cassette (ABC) transporter of *F. sambucinum* (encoded by *GpABC1*) that has been shown to be important for pathogenicity on potato, where knockout mutants are not effective at infecting potato tubers and have increased sensitivity to the phytoalexin rishitin (Fleibner et al., 2002). Other examples where ABC transporters are involved in phytopathogenesis by providing tolerance to the cytotoxic environment during plant infection include those encoded by the *ABC1*, *ABC3* and *ABC4* genes of *M. grisea* (Urban et al., 1999; Sun et al., 2006; Gupta and Chattoo, 2008) the *atrB* gene of *B. cinerea* (Schoonbeek et al., 2001) and the *atr4* gene of *Zymoseptoria tritici* (Stergiopoulos et al., 2003). In some fungi, similar effects can also be achieved with Major Facilitator Superfamily (MFS) transporters, with the transporter encoded by *mfsG* of *B. cinerea* representing a notable example (Vela-Corcía et al., 2019). In this system, the MfsG protein provides efflux of the glucosinolates produced by cruciferous plants such as *Arabidopsis thaliana*, which reduces the negative effect of the glucosinolates and thus enhances virulence of the pathogen (Vela-Corcía et al., 2019).

With the growing number of sequenced fungal genomes and the advent of transcriptomics, hundreds of new genes involved in the evasion and suppression of antifungal compound genes are being identified per genome (Sang et al., 2018; Carreon-Anguiano et al., 2020). In addition to their abundance, many of these genes are poorly conserved, making it essential to validate and characterize them so as to improve our understanding of their roles and contribution to fungal pathogenesis (Carreon-Anguiano et al., 2020). The characterization of these genes will likely also contribute greatly to the development of strategies to combat plant diseases caused by fungal pathogens.

3. Genome organization and evolution of pathogenicity and virulence factor genes

Fungal genes involved pathogenesis and virulence often have higher mutations rates than those involved in housekeeping processes (van der Does and Rep, 2007). From an evolutionary biology point of view, such patterns may be explained by the so-called “evolutionary arms race” between pathogens and their plant hosts (Maor and Shirasu, 2005). For example, when a pathogen secretes effectors during the early stages of infection, the host’s defence response is triggered, causing the

plant to express and produce proteins or metabolites to counter the pathogen (Maor and Shirasu, 2005). In turn, and over time, the pathogen adapts by accumulating mutations in the genes encoding the proteins targeted by the plant's defence response, which leads to an altered protein or metabolite allowing the pathogen to avoid or overcome the host defence response (Maor and Shirasu, 2005; van der Does and Rep, 2007). However, these genes can mutate to such an extent that they ultimately lose their function or they are lost, which is not favourable for the pathogen (van der Does and Rep, 2007). To compensate for this loss over evolutionary time, some phytopathogenic fungi appear capable of or at least to have benefited from novel gene acquisitions via horizontal gene transfer (HGT) (van der Does and Rep, 2007). In fact, some fungi seem to have specifically evolved the ability to take up genes via HGT and maintain them (van der Does and Rep, 2007).

The variation in mutation rates between housekeeping and pathogenesis-related genes in filamentous fungi results in so-called two-speed or "multiple speed" genomes (Dong et al., 2015; Frantzeskakis et al., 2019). Genes with housekeeping functions form part of the core subgenomic compartment, while pathogenicity and virulence factor genes, together with others that confer ecological benefits, are often encoded on the more dynamic accessory subgenomic compartment (Dong et al., 2015; Frantzeskakis et al., 2019). To this effect, Croll et al. (2021) referred to the accessory genome as the "cradle of adaptive evolution". The genes in the accessory genome commonly have uneven distribution within genera and moderate synteny within species (van der Does and Rep, 2007; Frantzeskakis et al., 2019). The main parts of fungal genomes that form the accessory genome include dispensable or accessory chromosomes, telomeric regions and other accessory regions (van der Does and Rep, 2007), and pathogenicity and virulence factor genes occupying them are sometimes clustered (van der Does and Rep, 2007). The next sections provide a brief overview of the distribution of pathogenicity and virulence genes across filamentous phytopathogenic fungal genomes and those known to have been acquired through HGT.

3.1. Genomic distribution of pathogenicity and virulence factor genes

Analyses of genomes of phytopathogenic fungi have revealed several virulence factor genes located on conditionally dispensable chromosomes (Fedorova et al., 2008; Ma et al., 2010). These fungi include species in the genera *Pyrenophora, Colletotrichum*, *Ustilago*, *Magnaporthe*, *Alternaria*, *Cochliobolus*, *Leptospheria*, and *Fusarium*, among others (reviewed by van der Does and Rep, 2007 and Bertazzoni et al., 2018). Furthermore, some of the pathogenicity/virulence genes on these chromosomes have been reported to have a patchy distribution within and between genera (van der Does and Rep, 2007). Examples are the pea pathogenicity (*PEP*) and pisatin demethylase (*PDA*) genes of *F. solani* (Han et al., 2001). *PEP1* has a homolog in *F. graminearum*, but none in other fungi, while *PEP2* has homologs in many fungal species (van der Does and Rep, 2007). Homologs

of *PDA* are absent in several related species and present in some strains of *F. oxysporum* (Temporini and VanEtten, 2004). Another example is the *TOXA* gene in *P. tritici-repentis*, which is absent in close relatives of *P. tritici-repentis*, but present in another wheat pathogen, *Stagonospora nodorum* (Friesen et al., 2006). The distribution of these genes can be linked to host-specificity in some of these fungi (van der Does and Rep, 2007).

In addition to their location on dispensable chromosomes, studies have reported pathogenicity/virulence genes located on telomeric and sub-telomeric regions in various filamentous fungi (Cuomo et al., 2007). For example, in *M. oryzae* virulence genes (*AVR-Pita1* and *AVR-Pita2*) encoding effectors (that interact with *Pi-ta* genes in resistance rice cultivars) are located on telomeres where they are flanked by repetitive elements (Orbach et al., 2000; Khang et al., 2008). Like many other virulence factors found in the accessory genome, these genes have no homologs in other fungal species (Khang et al., 2008). Another example is the *SIX8* gene of *F. oxysporum* (secreted in xylem), which is present in multiple identical copies at telomeric regions in the genome of this pathogen (Rep and Kistler, 2010). In *F. oxysporum* f. sp. *lycopersici*, pathogenesis-related genes are also believed to be located on sub-telomeric regions (Ma et al., 2010; Bertazzoni et al., 2018). This is not surprising as sub-telomeric and telomeric regions are known to be conducive to duplications and gene conversions, making them a favourable location for virulence genes encoding effectors (Rep and Kistler, 2010).

Fungal pathogenicity and virulence genes encoding the machinery to synthesize secondary metabolites are often organized in clusters (reviewed by Keller et al., 2005). Examples include the *Fusarium* genes *FUB1*, *FUM1*, and *BIK1*, which exist in tandem with the accessory genes required to synthesize and transport fusaric acid, fumonisin, and bikaverin, respectively (Wiemann et al., 2013). In *F. oxysporum*, five putative tomatinase genes (i.e., *TOM1* - *TOM5*), reportedly involved in disease development, also belong to a cluster (Pareja-Jaime et al., 2008). Interestingly, many other secondary metabolites that have no proven role in fungal pathogenicity and virulence are produced by proteins encoded by gene clusters, underscoring the evolutionary advantage of gene clustering, which is that genes in clusters have co-regulated expression thereby facilitating efficient host colonization (Zhang et al., 2004; Keller et al., 2005; Wiemann et al., 2013).

The dispensable chromosomes and telomeric regions on which the genes discussed in this section are located, are often rich in transposable elements (TEs) and/or repetitive sequences (Faino et al., 2016; Frantzeskakis et al., 2019). As a result, these regions are "hot spots" for mutations, either those caused by the TEs and repeats themselves (Wöstemeyer and Kreibich, 2002; Thon et al., 2006; van der Does and Rep, 2007) or that are induced by genome protection pathways such as RIP (repeat-induced point mutation) (van Wyk et al., 2021). Consequently, pathogenicity and virulence

genes in these regions have higher mutation rates while new genes can also arise from such mechanisms (van der Does and Rep, 2007; Rep and Kistler, 2010; Frantzeskakis et al., 2019).

3.2. HGT of pathogenicity and virulence factor genes

HGT is the exchange of genes between two members of a species or unrelated species that leads to stable integration of such genetic material into the recipient genome (Walton, 2000). Since the early experimental demonstration of horizontal transfer of chromosomes (HCT) in *Colletotrichum* (He et al., 1998), many phytopathogenic fungi have been the subject of studies investigating horizontal transfer of genetic material (e.g., Liu et al., 2003; Ma et al., 2010). It has been reported that the evolution of HGT in phytopathogenic fungi succeeds because of the need to compensate for loss of pathogenicity and virulence factor genes (van der Does and Rep, 2007). In other instances, phytopathogenic fungi have specifically evolved the ability to acquire ecologically beneficial genes via HGT (van der Does and Rep, 2007). Nevertheless, maintenance of horizontally acquired genes and chromosomes is driven by the selective advantage such genetic material confers to recipient fungi (reviewed by Walton, 2000).

Generally, horizontally acquired genes are characterized by the compartments of the genome they occupy as well as the sequence content of these regions. For instance, a number of such genes are found near TEs and regions with GC content different to that of the rest of the genome (van der Does and Rep, 2007). The same applies for horizontally gained chromosomes that have TEs and a different GC content. Due to their lateral acquisition, dispensable genes and chromosomes often have a patchy distribution within and between genera (van der Does and Rep, 2007). Additionally, genes acquired via HGT are often clustered, thereby enhancing the possibility that entire pathways or processes may be acquired via HGT (Walton, 2000). Laboratory experimentation together with these characteristics make it possible to identify fungal genetic material laterally acquired.

A few notable examples of pathogenesis-related genetic material of phytopathogenic fungi acquired via HGT exist. The *PEP* virulence genes in *F. solani*, which are clustered, are located on a conditionally dispensable chromosome that has many TEs and a GC content different to that of indispensable chromosomes, which strongly suggests horizontal acquisition of these genes (Liu et al., 2003). The *BIK* gene cluster encoding the phytotoxin bikaverin found in some *Fusarium* species is another example of clustered genes thought to have been gained horizontally (from *B. cinerea*) (Campbell et al., 2012; Schumacher et al., 2013). The *TOXA* gene that renders *P. tritici-repentis* pathogenic to wheat and is absent in related species of *Pyrenophora* has been reported to have been horizontally transferred from *S. nodorum* (Friesen et al., 2006). In *F. oxysporum*, an experimentally transferred conditionally dispensable chromosome of *F. oxysporum* that conferred pathogenicity to a non-pathogenic strain showed evidence of HCT origin in this species (Ma et al., 2010).

Continuous research and experiments involving HGT and HCT in fungi in which such experiments have not yet been explored will help us better understand these phenomena and the extent to which they occur across fungal phytopathogens.

4. Methods to identify and characterise pathogenicity and virulence factors

To understand pathogenicity and virulence factors, we need to functionally characterize them. Characterization is usually preceded by the identification of a putative pathogenicity gene. Various methods can be used for both the identification and functional characterization of these genes. Methods for identification include construction of genetic linkage maps (forward genetics technique), targeted sequencing, whole genome sequencing, transcriptome sequencing, while reverse genetics techniques such as genetic engineering are used for functional characterization (Tang et al., 2018). Selecting the appropriate method to efficiently study genes of interest and their associated phenotypes is vital, especially in this era of 'omics' characterized by rapid advancements in technology.

Gene identification with forward genetic techniques entails the use of an observed phenotype to determine the gene(s) controlling it (Russell, 2006). First, sexual crosses between individuals differing in a phenotype (i.e., quantitative or qualitative trait- such as virulence and pathogenicity) of interest is performed, followed by screening of the progeny, and the construction of genetic linkage maps to determine the location of genes or markers in a genome (i.e., quantitative trait loci; Russell, 2006). Initially methods such as amplified fragment length polymorphisms (AFLPs), restriction fragment length polymorphisms (RFLPs), and simple sequence repeats (SSRs) were used for this purpose (De Vos et al., 2007; Foulongne-Oriol, 2012). For example, AFLP-based linkage maps are available for various fungi (Xu and Leslie, 1996; Kema et al., 2002; Jurgenson et al., 2002; Gale et al., 2005; Gale et al., 2005; Hamwieh et al., 2005; Lind et al., 2005). Likewise, quantitative trait loci (QLTs) influencing pathogenicity have been identified for fungi such as *F. graminearum* and the basidiomycete *Heterobasidion annosum* (Cumagun et al., 2004; Lind et al., 2007). With the advent of next generation sequencing technologies, it became possible to construct high-resolution genetic linkage maps and identify pathogenicity/virulence QTLs using genome wide single nucleotide polymorphism (SNP) data such as has been achieved in the *Ceratocystis* pathogens of sweet potato and *Acacia* (Fourie et al., 2019).

On its own, genome sequencing is also a powerful tool to identify putative pathogenicity and virulence factors (Tang et al., 2018). Genes can be identified from sequence data by making use of gene prediction software or performing homology searches. Comparative genomic analyses of species or strains with different lifestyles is also a powerful pathogenicity gene identification

approach (e.g., Fourie et al., 2020). With the availability of thousands of whole genome sequence information for fungi across various freely available online databases (e.g., approximately 2000 genome assemblies in the MycoCosm database; https://mycocosm.jgi.doe.gov/fungi/fungi.info.html), the number of identified putative genes involved in filamentous fungal pathogenesis has increased greatly (Ma et al., 2010; Rep and Kistler, 2010; Ma et al., 2013; Rauwane et al., 2020). However, this technology is not without challenges. The massive amounts of data generated often requires complex bioinformatic analysis software and advanced skills to correctly and accurately interpret the data. This challenge has partially been mitigated by the development of automated pipelines. But this is not always the case for non-model organisms including many filamentous fungi. There is consequently a need to develop suitable pipelines for these fungi to enable accurate identification of pathogenicity and virulence factors.

The sequencing of transcriptomes is another powerful approach used for gene discovery (Tan et al., 2009; Meijueiro et al., 2014). Unlike whole genome sequencing, this approach enables the discovery of genes associated with an observed phenotype under certain conditions. For example, sequencing and studying transcriptomes of knockout mutants in various filamentous pathogenic fungi has revealed hundreds of genes under the control of single genes as well as gene networks (e.g., Pham et al., 2015; Gilbert et al. 2016; Tannous et al., 2018; Jones et al., 2019). Entire signalling pathways such as the MAPK pathway have also been determined in these fungi using a similar approach (e.g., Wang et al., 2016). Challenges associated with transcriptome sequencing include obtaining high quality RNA and the need for validation of gene expression data using quantitative reverse-transcriptase polymerase chain reaction or RNA blotting methods. Although the latter challenge can be overcome by including adequate biological and/or technical replicates (during laboratory experimentation and sequencing) and using statistical tests, the former is more difficult to overcome as many factors can affect the stability of RNA at any step of the workflow prior to sequencing. Therefore, suitable RNA extraction methods have to be determined for fungi being investigated.

Overall, the field of reverse genetics offers various genetic engineering approaches to functionally characterize putative pathogenesis-related genes. These include the use of i) knockout mutants generated by deleting, disrupting, or mutating a gene of interest, ii) knock-in mutants made by the insertion of a foreign gene into the genome of an organism of interest, and iii) knockdown mutants generated by gene silencing through RNA interference (RNAi) (Larrondo et al., 2009). Knockout experiments, being the most popular of the three for studies on filamentous fungi, involves the generation of a knockout construct containing partial sequences of the gene of interest and a selectable marker (e.g., antibiotic resistance gene) and the transformation of the fungus of interest

with the construct. These constructs can also contain the GFP (green fluorescent protein) gene for studying the localization of expressed proteins. The construct is then delivered into the fungal genome using transformation of fungal protoplasts or via infection with transformed *Agrobacterium* (reviewed by Weld et al., 2006). Integration of the construct into the genome of the fungus is facilitated by homologous recombination between the partial sequences of the gene of interest in the construct and the gene of interest at its locus (Figure 3A). The majority of the pathogenicity genes discussed in this review were characterised using knockout mutants generated by either gene deletion or disruption.

Although reverse genetics-based methods provide the most accurate means to functionally characterize genes, the experimentation required for many of these methods can be cumbersome and time consuming (Shi et al., 2017). This is due to the low efficiency of homologous recombination that often results in ectopic integration of knockout constructs in the fungal genome of interest. This means that multiple experiments are required to successfully knock out a gene. Although Catlett et al. (2003) developed a split-marker method where an additional homologous recombination event is required for construct integration at the correct locus to mitigate this (Figure 3B), low levels of recombination still occur in some filamentous fungi (Wilson and Wingfield, 2020).

More recent genetic engineering approaches such as CRISPR/Cas9 offer better homologous recombination frequencies across filamentous fungi (Shi et al., 2017; Ding et al., 2019; Wilson and Wingfield, 2020). This feature of CRISPR/Cas9 is especially important for high throughput genome editing experiments, which would otherwise have taken long periods of time using traditional methods (Ding et al., 2019). Although not yet applied to many pathogenicity genes, this technology has recently been used to successfully edit the gibberellin pathway in *F. fujikuroi* to enhance its production (Shi et al., 2019). Using CRISPR/Cas9 or a related technology to study the role of putative pathogenicity and virulence genes will undoubtedly also accelerate the rate at which we generate knowledge about these genes and thus better understand pathogenesis in these fungi.

5. Conclusions and future prospects

Phytopathogenic fungi pose a major threat to plant health, thus impacting negatively on food security and industries that rely on plant production. Accordingly, studies focussed on understanding fungal pathogenesis have received much attention. Although a considerable body of knowledge has been generated regarding the biology of many plant pathogenic fungi, the molecular processes and mechanisms underlying pathogenicity and virulence is less well understood. This is especially true in the case of unculturable fungi and forest tree pathogens. The emergence of whole

genome and transcriptome sequencing has enabled plant pathologists and molecular geneticists to decipher the molecular basis of pathogenesis and virulence in numerous previously poorly studied fungi. However, a full understanding of how most phytopathogenic fungi overcome and colonize their hosts requires functional characterization of putative pathogenicity and virulence factor genes.

Traditional genetic engineering methods makes the characterization of putative pathogenicity and virulence factor genes difficult. However, recent advances, particularly pertaining the CRISPR technology, promise accelerated experimentation and thus increased knowledge generation in the field of fungal pathogenesis. The success of this will depend strongly on optimization of this technology for use with non-model fungal species. It is clear that lessons learned from studying one particular species of a fungal pathogen cannot always be applied to another. Thus, greater effort will need to be applied to develop this technology for non-model fungi, including most phytopathogens of economic importance. This will consequently contribute to better design of effective responses and methods to prevent, combat or minimise fungal plant diseases.

References

Agrios, G., 2005. Plant Pathology, fifth ed. Amsterdam, Netherlands, Elsevier Academic Press.

Ahn, J.H., Walton, J.D., 1996. Chromosomal organization of TOX2, a complex locus controlling host-selective toxin biosynthesis in *Cochliobolus carbonum*. The Plant Cell Online, 8, 887-897.

Aizawa, K., 1971. Strain improvement and preservation of virulence of pathogens. Burges, HD Microbial control of insects and mites.

Akamatsu, H., Itoh, Y., Kodama, M., Otani, H., Kohmoto, K., 1997. AAL-toxin deficient mutants of *Alternaria alternata* tomato pathotype by restriction enzyme-mediated integration. Phytopathol. 87, 967-72.

Andrade, A.C., Del Sorbo, G., Van Nistelrooy, J.G. and De Waard, M.A., 2000. The ABC transporter AtrB from *Aspergillus nidulans* mediates resistance to all major classes of fungicides and some natural toxic compounds. Microbiol. 146, 1987-1997.

Anjago, W.M., Zhou, T., Zhang, H., Shi, M., Yang, T., Zheng, H., Wang, Z., 2018. Regulatory network of genes associated with stimuli sensing, signal transduction and physiological transformation of appressorium in *Magnaporthe oryzae*. Mycology, 9, 211-222.

Baker, S.E., Kroken, S., Inderbitzin, P., Asvarak, T., Li, B.Y., Shi, L., et al., 2006. Two polyketide synthase-encoding genes are required for biosynthesis of the polyketide virulence factor. T-toxin, by *Cochliobolus heterostrophus*. Mol. Plant-Microbe Interact. 19, 139–49.

Bakri, Y., Jawhar, M., Arabi M.I.E., 2014. Enzymatic activity of the endophytic *Fusarium* species strains isolated from wheat. Adv. Hort. Sci., 28, 129-132.

Barbacid, M. Ras genes. Annu. Rev. Biochem. 1987, 56, 779-827.

Bell, A.A., Wheeler, M.H., Liu, J., Stipanovic, R.D., Puckhaber, L.S., Orta, H., 2003. United States Department of Agriculture - Agricultural Research Service studies on polyketide toxins of *Fusarium oxysporum* f. sp. *vasinfectum*: potential targets for disease control. Pest Manag. Sci. 59, 736-747.

Bertazzoni, S., Williams, A.H., Jones, D.A., Syme, R.A., Tan, K., Hane, J.K., 2018. Accessories Make the Outfit: Accessory Chromosomes and Other Dispensable DNA Regions in Plant-Pathogenic Fungi. Mol. Plant-Microbe Interact. 31, 779-788.

Berthiller, F., Crews, C., Dall'Asta, C., De Saeger, S., Haesaert, G., Karlovsky, P., Oswald, I.P., Seefelder, W., Speijers, G., Stroka, J., 2013. Masked mycotoxins: A review. Mol. Nutr. Food Res. 57, 165–186.

Bhadauria, V., Banniza, S., Wei, Y. and Peng, Y.L., 2009. Reverse genetics for functional genomics of phytopathogenic fungi and oomycetes. Comp. Funct. Genom. 2009, 1-11.

Bluhm, B., Zhao, X., Flaherty, J., Xu, J.R., Dunkle, L., 2007. RAS2 regulates growth and pathogenesis in *Fusarium graminearum*. Mol. Plant-Microbe Interact. 20, 627-636.

Bourne, H.R., Sanders, D.A., McCormick, F., 1991. The GTPase superfamily: conserved structure and molecular mechanism. Nature 349, 117.

Brun, S., Malagnac, F., Bidard, F., Lalucque, H., Silar, P., 2009. Functions and regulation of the Nox family in the filamentous fungus *Podospora anserina*: a new role in cellulose degradation. Mol. Microbiol. 74, 480–496.

Bruno, K.S., Tenjo, F., Li, L., Hamer, J.E., Xu, J.R., 2004. Cellular localization and role of kinase activity of PMK1 in *Magnaporthe grisea*. Eukaryot. Cell 3, 1525-1532.

Campbell, M.A., Rokas, A., Slot, J.C., 2012. Horizontal transfer and death of a fungal secondary metabolic gene cluster. Genome Biol. Evol. 4, 289-293.

Carreon-Anguiano, K.G., Islas-Flores, I., Vega-Arreguín, J., Sáenz-Carbonell, L. Canto-Canché, B., 2020. EffHunter: A tool for prediction of effector protein candidates in fungal proteomic databases. Biomolecules, 10, 712.

Catlett, N.L., Lee, B.N., Yoder, O., Turgeon, B.G., 2003. Split-marker recombination for efficient targeted deletion of fungal genes. Fungal Genet. Rep. 50, 9-11.

Cheng, Y.Q., Ahn, J.H., Walton, J.D., 1999. A putative branched-chain-amino-acid transaminase gene required for HC-toxin biosynthesis and pathogenicity in *Cochliobolus carbonum*. Microbiology 145, 3539-3546.

Choi, Y.E., and Xu, J.R., 2010. The cAMP signaling pathway in *Fusarium verticillioides* is important for conidiation, plant infection, and stress responses but not fumonisin production. Mol. Plant-Microbe Interact. 23, 522-533.

Coleman, J.J., White, G.J., Rodriguez-Carres, M. and VanEtten, H.D., 2011. An ABC transporter and a cytochrome P450 of *Nectria haematococca* MPVI are virulence factors on pea and are the major tolerance mechanisms to the phytoalexin pisatin. Mol. Plant-Microbe Interact. 24, 368-376.

Cox, A.D., Der, C.J., 2010. Ras history: The saga continues. Small GTPases. 1, 2-27.

Croll, D., McDonald, B.A., 2012. The accessory genome as a cradle for adaptive evolution in pathogens. PLoS Pathog. 8, e1002608.

Cumagun, C. J. R., Bowden, R. L., Jurgenson, J. E., Leslie, J. F. and Miedaner, T., 2004. Genetic mapping of pathogenicity and aggressiveness of *Gibberella zeae* (*Fusarium graminearum*) toward wheat. Phytopathol. 94, 520-526.

Cuomo, C.A., Güldener, U., Xu, J.R., Trail, F., Turgeon, B.G., Di Pietro, A., Walton, J.D., Ma, L.J., Baker, S.E., Rep, M., 2007. The *Fusarium graminearum* genome reveals a link between localized polymorphism and pathogen specialization. Science 317, 1400-1402.

De Lorenzo, G., Castoria, R., Bellincampi, D.; Cervone, F., 1997. Fungal invasion enzymes and their inhibition. Plant Relationships. Springer.

de Vos, A.M., Tong, L., Milburn, M.V., Matias, P.M., Jancarik, J., Noguchi, S., et al., 1988. Three-dimensional structure of an oncogene protein: catalytic domain of human c-H-ras p21. Science 239, 888-893.

De Vos, L., Myburg, A. A., Wingfield, M. J., Desjardins, A. E., Gordon, T. and Wingfield, B. D., 2007. Complete genetic linkage maps from an interspecific cross between *Fusarium circinatum* and *Fusarium subglutinans*. Fungal Genet. Biol. 44, 701-714.

de Waard MA, Andrade AC, Hayashi K, Schoonbeek H, Stergiopoulos I, Zwiers L, 2006. Impact of fungal drug transporters on fungicide sensitivity, multidrug resistance and virulence. Pest Manag. Sci. 62, 195-207.

Dean, R.A., 1997. Signal pathways and appressorium morphogenesis. Annu. Rev. Phytopathol. 35, 211-234.

Deising, H.B., Werner, S., Wernitz, M., 2000. The role of fungal appressoria in plant infection. Microbes Infect. 2, 1631-1641.

Demoor, A., Silar, P. and Brun, S., 2019. Appressorium: the breakthrough in Dikarya. J. Fungi 53, 72.

Di Pietro F, García-Maceira I, Méglecz E, and Roncero MIG., 2001. A MAP kinase of the vascular wilt fungus *Fusarium oxysporum* is essential for root penetration and pathogenesis. Mol. Microbiol. 39, 1140-1152.

Ding, Y., Wang, K.F., Wang, W.J., Ma, Y.R., Shi, T.Q., Huang, H. and Ji, X.J., 2019. Increasing the homologous recombination efficiency of eukaryotic microorganisms for enhanced genome engineering. Appl. Microbiol. Biotechnol. 103, 4313-4324.

Dong, S., Raffaele S., Kamoun. S., 2015. The two-speed genomes of filamentous pathogens: Waltz with plants. Curr. Opin. Genet. Dev. 35, 57-65.

Driessen, A.J.M., Rosen, B.P., and Konings, W.N., 2000. Diversity of transport mechanisms: common structural principles. Trends Biochem. Sci. 25, 397-401.

Eisermann, I., Weihmann, F., Krijger, J.J., Kröling, C., Hause, G., Menzel, M., Pienkny, S., Kiesow, A., Deising, H.B., Wirsel, S.G., 2019. Two genes in a pathogenicity gene cluster encoding secreted proteins are required for appressorial penetration and infection of the maize anthracnose fungus *Colletotrichum graminicola*. Environ. Microbiol. 21, 4773-4791.

Ellison, C. E., Kowbel, D., Glass, N. L., Taylor, J. W. and Brem, R. B., 2014. Discovering functions of unannotated genes from a transcriptome survey of wild fungal isolates. mBio 5, 1-13.

Faino, L., Seidl, M.F., Shi-Kunne, X., Pauper, M., van den Berg, G.C.M.M., Wittenberg, A.H.J.J., Thomma, B.P.H.J.H.J., 2016. Transposons passively and actively contribute to evolution of the two-speed genome of a fungal pathogen. Genome Res. 26, 1091-1100.

Fedorova, N. D., Khaldi, N., Joardar, V. S., Maiti, R., Amedeo, P., Anderson, M. J., Crabtree, J., Silva, J. C., Badger, J. H.; Albarraq, A., 2008. Genomic islands in the pathogenic filamentous fungus *Aspergillus fumigatus*. PLoS Genet. 4, e1000046.

Fillinger, S., Chaveroche, M.K., Shimizu, K., Keller, N., d'Enfert, C., 2002. cAMP and ras signalling independently control spore germination in the filamentous fungus *Aspergillus nidulans*. Mol. Microbiol. 44, 1001-1016.

Fleibner, A., Sopalla, C.; Weltring, K.M., 2002. An ATP-binding cassette multidrug-resistance transporter is necessary for tolerance of *Gibberella pulicaris* to phytoalexins and virulence on potato tubers. Mol. Plant-Microbe Interact. 15, 102-108.

Foulongne-Oriol, M., 2012. Genetic linkage mapping in fungi: current state, applications, and future trends. Appl. Microbiol. Biotechnol. 95, 891-904.

Fourie, A., de Jonge, R., van der Nest, M. A., Duong, T. A., Wingfield, M. J., Wingfield, B. D. and Barnes, I., 2020. Genome comparisons suggest an association between *Ceratocystis* host adaptations and effector clusters in unique transposable element families. Fungal Genet. Biol. 143, 103433.

Fourie, A., van der Nest, M. A., De Vos, L., Wingfield, M. J., Wingfield, B. D. and Barnes, I., 2019. QTL mapping of mycelial growth and aggressiveness to distinct hosts in *Ceratocystis* pathogens. Fungal Genet. Biol. 131, 103242.

Frank, B., 1883. Ueber einige neue und weniger bekannte Pflanzenkrankheiten, Ber. Deutsch. Bot. Gesell. 1, 29–34.

Frantzeskakis, L., Kusch, S., Panstruga, R., 2019. The need for speed: compartmentalized genome evolution in filamentous phytopathogens. Mol. Plant Pathol. 20, 3-7.

Friesen, T. L., Stukenbrock, E. H., Liu, Z., Meinhardt, S., Ling, H., Faris, J. D., Rasmussen, J. B., Solomon, P. S., Mcdonald, B. A.; Oliver, R. P., 2006. Emergence of a new disease as a result of interspecific virulence gene transfer. Nat. Genet. 38, 953-956.

Fuxa, J.R., Tanada, Y., 1987. Epizootiology of Insect Diseases. Wiley, New York.

Gale, L.R., Bryant, J.D., Calvo, S., Giese, H., Katan, T., ODonnell, K. Suga, H. Taga, M. Usgaard, T.R. Ward T.J., Kistler, H.C., 2005. Chromosome complement of the fungal plant pathogen *Fusarium graminearum* based on genetic and physical mapping and cytological observations. Genetics 171, 985-1001.

Galhano, R., Illana, A., Ryder, L.S., Rodríguez-Romero, J., Demuez, M., Badaruddin, M., Martinez-Rocha, A.L., Soanes, D.M., Studholme, D.J., Talbot, N.J., et al., 2017. Tpc1 is an important Zn(II)2Cys6 transcriptional regulator required for polarized growth and virulence in the rice blast fungus. PLoS Pathog. 13, e1006516.

Garcia-Maceira, F.I., Di Pietro, A., Huertas-González, M.D., Ruiz-Roldán, M.C., Roncero, M.I.G., 2001. Molecular characterization of an endopolygalacturonase from *Fusarium oxysporum* expressed during early stages of infection. Applied and Environ. Microbiol. 67, 2191-2196.

Gasch, A.P., Spellman, P.T., Kao, C.M., Carmel-Harel, O., Eisen, M.B., Storz, G., Botstein, D., Brown, P.O., 2000. Genomic expression programs in the response of yeast cells to environmental changes. Mol. Biol. Cell. 11, 4241-4257.

Gilbert, M.K., Mack, B.M., Wei, Q., Bland, J.M., Bhatnagar, D. and Cary, J.W., 2016. RNA sequencing of an *nsdC* mutant reveals global regulation of secondary metabolic gene clusters in *Aspergillus flavus*. Microbiol. Res. 182, 150-161.

Glenn, A.E., Zitomer, N.C., Zimeri, A.M., Williams, L.D., Riley, R.T., et al., 2008. Transformation-mediated complementation of a FUM gene cluster deletion in *Fusarium verticillioides* restores both fumonisin production and pathogenicity on maize seedlings. Mol. Plant-Microbe Interact. 21, 87-97.

Gomez-Gomez, E., Ruız-Roldan, M., Di Pietro, A., Roncero, M.; Hera, C., 2002. Role in Pathogenesis of Two Endo-β-1, 4-xylanase Genes from the Vascular Wilt Fungus *Fusarium oxysporum*. Fungal Genet. Biol. 35, 213-222.

Gupta, A., Chattoo, B.B., 2008. Functional analysis of a novel ABC transporter ABC4 from *Magnaporthe grisea*. FEMS Micro-biol. Lett. 278, 22-28.

Hammerschmidt, R., 1999. Phytoalexins: what have we learned after 60 years? Annu. Rev. Phytopathol. 37, 285-306.

Hamwieh, A., Udupa, S., Choumane, W., Sarker, A., Dreyer, F., Jung, C. and Baum, M., 2005. A genetic linkage map of Lens sp. based on microsatellite and AFLP markers and the localization of *Fusarium* vascular wilt resistance. Theor. Appl. Genet. 110, 669-677.

Han, Y., Liu, X., Benny, U., Kistler, H.C., VanEtten, H.D., 2001. Genes determining pathogenicity to pea are clustered on a supernumerary chromosome in the fungal plant pathogen *Nectria haematococca*. The Plant J. 25, 305-314.

ten Have, A.T., Mulder, W., Visser, J., van Kan, J.A.L., 1998. The endopolygalacturonase gene Bcpg1 is required for full virulence of *Botrytis cinerea*. Mol. Plant-Microb. Inter. 11, 1009–1016.

He, C., Rusu, A.G., Poplawski, A.M., Irwin, J.A.G., Manners, J.M., 1998. Transfer of a supernumerary chromosome between vegetatively incompatible biotypes of the fungus *Colletotrichum gloeosporioides*. Genetics 150, 1459-1466.

Hematy, K., Cherk, C., Somerville, S., 2009. Host-pathogen warfare at the plant cell wall. Curr. Opin. Plant Biol. 12, 406-13.

Herrmann, M., Zocher, R., Haese, A., 1996. Effect of disruption of the enniatin synthetase gene on the virulence of *Fusarium avenaceum*. Mol. Plant-Microbe Interact. 9, 226-232.

Horbach, R., Navarro-Quesada, A. R., Knogge, W.; Deising, H. B., 2011. When and how to kill a plant cell: infection strategies of plant pathogenic fungi. J. Plant Physiol. 168, 51-62.

Idnurm, A.; Howlett, B. J., 2001. Pathogenicity genes of phytopathogenic fungi. Mol. Plant Pathol. 2, 241-255.

Isshiki, A., Akimitsu, K., Yamamoto, M., Yamamoto, H., 2001. Endopolygalacturonase is essential for citrus black rot caused by *Alternaria* citri but not brown spot caused by *Alternaria alternata*. Mol. Plant-Microbe Interact. 14, 749-57.

Jones, D.A., John, E., Rybak, K., Phan, H.T., Singh, K.B., Lin, S.Y., Solomon, P.S., Oliver, R.P., Tan, K.C., 2019. A specific fungal transcription factor controls effector gene expression and orchestrates the establishment of the necrotrophic pathogen lifestyle on wheat. Sci. Rep. 9, 1-13.

Jurgenson, J.E., Zeller, K.A., Leslie, J.F., 2002. Expanded genetic map of *Gibberella moniliforme* (*Fusarium verticillioides*). Appl. Environ. Microbiol. 68, 1972-1979.

Kamakura, T., Yamaguchi, S., Saitoh, K.I., Teraoka, T.; Yamaguchi, I., 2002. A novel gene, CBP1, encoding a putative extracellular chitin-binding protein, may play an important role in the hydrophobic surface sensing of *Magnaporthe grisea* during appressorium differentiation. Mol. Plant-Microbe Interact. 15, 437-444.

Kamper, J., Kahmann, R., Bölker, M., Ma, L.J., Brefort, T., Saville, B. J., Banuett, F., Kronstad, J. W., Gold, S. E. and Müller, O., 2006. Insights from the genome of the biotrophic fungal plant pathogen *Ustilago maydis*. Nature 444, 97-101.

Kang, S. H., Khang, C. H.; Lee, Y. H., 1999. Regulation of cAMP-dependent protein kinase during appressorium formation in *Magnaporthe grisea*. FEMS Microbiol. Lett. 170, 419-423.

Keller, N.P., Turner, G., Bennett, J.W., 2005. Fungal secondary metabolism - from biochemistry to genomics. Nat. Rev. Microbiol., 3, 937-947.

Kema, G.H., Goodwin, S.B., Hamza, S., Verstappen, E.C., Cavaletto, J.R., Van der Lee, T.A., de Weerdt, M., Bonants, P.J. and Waalwijk, C., 2002. A combined amplified fragment length polymorphism and randomly amplified polymorphism DNA genetic linkage map of *Mycosphaerella graminicola*, the *Septoria tritici* leaf blotch pathogen of wheat. Genetics 161, 1497-1505.

Khang, C.H., Park, S.Y., Lee, Y.H., Valent, B., Kang, S., 2008. Genome organization and evolution of the AVR-Pita avirulence gene family in the *Magnaporthe grisea* species complex. Mol. Plant-Microbe Interact. 21, 658-670.

Kong, L.A., Yang, J., Li, G.T., Qi, L.L., Zhang, Y.J., Wang, C.F., Zhao, W.S., Xu, J.R., Peng, Y.L., 2012. Different chitin synthase genes are required for various developmental and plant infection processes in the rice blast fungus *Magnaporthe oryzae*. PLoS Pathog. 8, e1002526.

Kono, Y., Knoche, H.W., Daly, J.M., 1981. Structure: Fungal host-specific, in: R.D. Durbin, (Ed), Toxins in Plant Disease. Academic Press, New York, pp. 221-257.

Kronstad, J., 1997. Virulence and cAMP in smuts, blasts and blights. Trends Plant Sci. 2, 193-199.

Kruger, J., Loubradou, G., Wanner, G., Regenfelder, E., Feldbrügge, M., Kahmann, R., 2000. Activation of the cAMP pathway in *Ustilago maydis* reduces fungal proliferation and teliospore formation in plant tumors. Mol. Plant-Microbe Interact. 13, 1034-1040.

Kubicek, C.P., Starr, T.L. and Glass, N.L., 2014. Plant cell wall–degrading enzymes and their secretion in plant-pathogenic fungi. Annu. Rev. Phytopathol. 52, 427-451.

Kuroki, M., Okauchi, K., Yoshida, S., Ohno, Y., Murata, S., Nakajima, Y., Nozaka, A., Tanaka, N., Nakajima, M. and Taguchi, H., 2017. Chitin-deacetylase activity induces appressorium differentiation in the rice blast fungus *Magnaporthe oryzae*. Sci. Rep. 7, 1-8.

Lacey, L.A., 1997. Manual of Techniques in Insect Pathology. Academic Press, Boston.

Lambou, K., Malagnac, F., Barbisan, C., Tharreau, D., Lebrun, M.H., Silar, P., 2008. The crucial role of the Pls1 tetraspanin during ascospore germination in *Podospora anserina* provides an example of the convergent evolution of morphogenetic processes in fungal plant pathogens and saprobes. Eukaryot. Cell 7, 1809–1818.

Larrondo, L. F., Colot, H. V., Baker, C. L., Loros, J. J. and Dunlap, J. C., 2009. Fungal functional genomics: tunable knockout-knock-in expression and tagging strategies. Eukaryot. Cell 8, 800-804.

Lengeler, K.B., Davidson, R.C., D'Souza, C., Harashima, T., Shen, W., Wang, P., et al., 2000. Signal transduction cascades regulating fungal development and virulence. Microbiol. Mol. Biol. Rev. 64, 746-785.

Leslie, J.F., Xu, J.R., 2010. *Fusarium* genetics and pathogenicity, in: Borkovich, K.A., Ebbole, D.J. (Eds), Cellular and Molecular Biology of Filamentous Fungi. John Wiley & Sons, Inc., pp. 607-621.

Lev, S., Sharon, A., Hadar, R., Ma, H.; Horwitz, B. A., 1999. A mitogen-activated protein kinase of the corn leaf pathogen *Cochliobolus heterostrophus* is involved in conidiation, appressorium formation, and pathogenicity: diverse roles for mitogen-activated protein kinase homologs in foliar pathogens. PNAS 96, 13542-13547.

Li, J., Cornelissen, B., Rep, M., 2020. Host-specificity factors in plant pathogenic fungi. Fungal Genet. Biol. 144, 103447-103458.

Lind, M., Dalman, K., Stenlid, J., Karlsson, B. and Olson, A., 2007. Identification of quantitative trait loci affecting virulence in the basidiomycete *Heterobasidion annosum sl*. Curr. Genet. 52, 35-44.

Lind, M., Olson, A., Stenlid, J., 2005. An AFLP-markers based genetic linkage map of *Heterobasidion annosum* locating intersterility genes. Fungal Genet. Biol. 42, 519-527.

Liu, W., Zhou, X., Li, G., Li, L., Kong, L., Wang, C., Zhang, H., Xu, J.R., 2011. Multiple plant surface signals are sensed by different mechanisms in the rice blast fungus for appressorium formation. PLoS Pathog. 7, e1001261.

Liu, X., Inlow, M.; VanEtten, H.D., 2003. Expression profiles of pea pathogenicity (PEP) genes in vivo and in vitro, characterization of the flanking regions of the PEP cluster and evidence that the PEP cluster region resulted from horizontal gene transfer in the fungal pathogen *Nectria haematococca*. Curr. Genet. 44, 95-103.

Liu, X.H., Lu, J.P., Zhang, L., Dong, B., Min, H., Lin F.C., 2007. Involvement of a *Magnaporthe grisea* serine/threonine kinase gene, mgatg1, in appressorium turgor and pathogenesis. Eukaryot. Cell, 6, 997-1005.

Lopez-Diaz, C., Rahjoo, V., Sulyok, M., Ghionna, V., Martín-Vicente, A., Capilla, J., Di Pietro, A., Lopez-Berges, M.S., 2018. Fusaric acid contributes to virulence of *Fusarium oxysporum* on plant and mammalian hosts. Mol. Plant Pathol. 19, 440-453.

Lowy, D. R. and Willumsen, B. M., 1993. Function and regulation of ras. Annu. Rev. Biochem. 62, 851-891.

Ma, L.J., Geiser, D.M., Proctor, R.H., Rooney, A.P., O'Donnell, K., Trail, F., Gardiner, D.M., Manners, J.M. and Kazan, K., 2013. *Fusarium* pathogenomics. Annu. Rev. Microbiol. 67, 399-416.

Ma, L.J., van Der Does, H. C., Borkovich, K. A., Coleman, J. J., Daboussi, M.J., Di Pietro, A., Dufresne, M., Freitag, M., Grabherr, M.; Henrissat, B., 2010. Comparative genomics reveals mobile pathogenicity chromosomes in *Fusarium*. Nature 464, 367-373.

Maor, R., Shirasu, K., 2005. The arms race continues: battle strategies between plants and fungal pathogens. Curr. Opin. Microbiol. 8, 399-404.

Marschall, R., Tudzynski, P., 2016. Reactive oxygen species in development and infection processes. Semin. Cell Dev. Biol. 57, 138-146.

Martinez-Soto, D., Ruiz-Herrera, J., 2017. Functional analysis of the MAPK pathways in fungi. Rev Iberoam Micol. 34, 192–202.

Meijueiro, M.L., Santoyo, F., Ramírez, L. and Pisabarro, A.G., 2014. Transcriptome characteristics of filamentous fungi deduced using high-throughput analytical technologies. Brief. Funct. Genomics 13, 440-450.

Muller, P., Aichinger, C., Feldbrügge, M. and Kahmann, R., 1999. The MAP kinase kpp2 regulates mating and pathogenic development in *Ustilago maydis*. Mol. Microbiol. 34, 1007-1017.

Nagalakshmi, U., Wang, Z., Waern, K., Shou, C., Raha, D., Gerstein, M. and Snyder, M., 2008. The transcriptional landscape of the yeast genome defined by RNA sequencing, Science 320, 1344-1349.

Orbach, M.J., Farrall, L., Sweigard, J.A., Chumley, F.G., Valent, B., 2000. A telomeric avirulence gene determines efficacy for the rice blast resistance gene Pi-ta. Plant Cell 12, 2019-2032.

Paccanaro, M.C., Sella, L., Castiglioni, C., Giacomello, F., Martínez-Rocha, A.L., D'Ovidio, R., Schäfer, W., Favaron, F., 2017. Synergistic effect of different plant cell wall–degrading enzymes is important for virulence of *Fusarium graminearum*. Mol. Plant-Microbe Interact. 30, 886-895.

Phasha, M., Wingfield, M., Wingfield, B., Coetzee, M., Hallen-Adams, H., Fru, F., Swalarsk-Parry, B., Yilmaz, N., Duong, T., Steenkamp, E., 2021. Ras2 is important for growth and pathogenicity in *Fusarium circinatum*. Fungal Genet. Biol. 150, 103541-103550.

Pai, E.F., Kabsch, W., Krengel, U., Holmes, K.C., John, J., Wittinghofer, A., 1989. Structure of the guanine-nucleotidebinding domain of the Ha-ras oncogene product p21 in the triphosphate conformation. Nature, 341, 209-14.

Pareja-Jaime, Y., Roncero, M. I. G.; Ruiz-Roldán, M. C., 2008. Tomatinase from *Fusarium oxysporum* f. sp. *lycopersici* is required for full virulence on tomato plants. Mol. Plant-Microbe Interact. 21, 728-736.

Perincherry, L., Lalak-Kanczugowska, J. and Stępien, L., 2019. *Fusarium*-produced mycotoxins in plant-pathogen interactions. Toxins 11, 664.

Perpetua, N.S., Kubo, Y., Yasuda, N., Takano, Y.; Furusawa, I., 1996. Cloning and characterization of a melanin biosynthetic THR1 reductase gene essential for appressorial penetration of *Colletotrichum lagenarium*. Molecular plant-microbe interactions: Mol. Plant-Microbe Interact. 9, 323-329.

Pham, K.T.M., Inoue, Y., Vu, B.V., Nguyen, H.H., Nakayashiki, T., Ikeda, K.I. and Nakayashiki, H., 2015. MoSET1 (histone H3K4 methyltransferase in *Magnaporthe oryzae*) regulates global gene expression during infection-related morphogenesis. PLoS Genet. 11, e1005385.

Pontes, J.G.M., Fernandes, L.S., dos Santos, R.V., Tasic L., Fill, T.P., 2020. Virulence Factors in the Phytopathogen−Host Interactions: An Overview. J. Agric. Food Chem. 68, 7555−7570.

Proctor, R.H., Hahn, T.M., McCormick, S.P., 1995. Reduced virulence of *Gibberella zeae* caused by disruption of a trichothecene toxin biosynthetic gene. Mol. Plant-Microbe Interact. 8, 598-601.

Rauwane, M.E., Ogugua, U.V., Kalu, C.M., Ledwaba, L.K., Woldesemayat, A.A., Ntushelo, K., 2020. Pathogenicity and virulence factors of *Fusarium graminearum* including factors discovered using next generation sequencing technologies and proteomics. Microorganisms 8, 305-333.

Rep, M., Kistler, H.C., 2010. The genomic organization of plant pathogenicity in *Fusarium* species. Curr. Opin. Plant Biol. 13, 420-426.

Rogers, L. M., Flaishman, M. A.; Kolattukudy, P. E., 1994. Cutinase gene disruption in *Fusarium solani* f. sp, *pisi* decreases its virulence on pea. The Plant Cell 6, 935-945.

Rose, M.S., Yun, S.H., Asvarak, T., Lu, S.W., Yoder, O.C., Turgeon, B.G., 2002. A decarboxylase encoded at the *Cochliobolus heterostrophus* translocation-associated Tox1B locus is required for polyketide biosynthesis and high virulence on maize. Mol. Plant- Microbe Interact. 15, 883–93.

Russell, P. J., 2006. iGenetics: a Mendelian approach, Benjamin-Cummings Publishing Company, Pearson Education, Inc., San Francisco.

Sabnam, N., Barman, S.R., 2017. WISH, a novel CFEM GPCR is indispensable for surface sensing, asexual and pathogenic differentiation in rice blast fungus. Fungal Genet. Biol. 105, 37-51.

Sang, H., Hulvey, J.P., Green R., Xu, H., Im, J., Chang, T., Jung, G., 2018. A xenobiotic detoxification pathway through transcriptional regulation in filamentous fungi. mBio 9.

Schoonbeek, H., Del Sorbo, G., De Waard, M.A., 2001. The ABC transporter B catrB affects the sensitivity of *Botrytis cinerea* to the phytoalexin resveratrol and the fungicide fenpiclonil. Mol. Plant-Microbe Interact. 14, 562-571.

Schumacher, J., Gautier, A., Morgant, G., Studt, L., Ducrot, P., et al., 2013. A functional bikaverin biosynthesis gene cluster in rare strains of *Botrytis cinerea* is positively controlled by VELVET. PloS One 8, e53729.

Schumacher, J., Kokkelink, L., Huesmann, C., Jimenez-Teja, D., Collado, I. G., Barakat, R., Tudzynski, P., and Tudzynski, B., 2008. The cAMP-dependent signaling pathway and its role in conidial germination, growth, and virulence of the gray mold *Botrytis cinerea*. Mol. Plant-Microbe Interact. 21, 1443-1459.

Shapiro-Ilan, D.I., Fuxa, J.R., Lacey, L.A., Onstad, D.W., Kaya, H.K., 2005. Definitions of pathogenicity and virulence in invertebrate pathology. J. Invert. Pathol. 88, 1-7.

Shi, T.Q., Gao, J., Wang, W.J., Wang, K.F., Xu, G.Q., Huang, H. and Ji, X.J., 2019. CRISPR/Cas9-based genome editing in the filamentous fungus *Fusarium fujikuroi* and its application in strain engineering for gibberellic acid production. ACS Synth. Biol. 445-454.

Shi, T.Q., Liu, G.N., Ji, R.Y., Shi, K., Song, P., Ren, L.J., Huang, H. and Ji, X.J., 2017. CRISPR/Cas9-based genome editing of the filamentous fungi: the state of the art. Appl. Microbiol. Biotechnol. 101, 7435-7443.

Shin, J., Kim, J., Lee, Y., Son, H., 2018. Fungal Cytochrome P450s and the P450 Complement (CYPome) of *Fusarium graminearum*. Toxins 10, 112.

Spence, R., Casey, P.J., 2001. Mechanism of catalysis by protein farnesyltransferase, in: Tamanoi, F., Sigman, D. (Eds.), The Enzymes. Academic Press, New York, pp. 1-18.

Steinhaus, E.A., Martignoni, M.E., 1970. An Abridged Glossary of Terms Used in Invertebrate Pathology. U.S. PNW Forest Stations.

Stepien, L. and Lalak-Kanczugowska, J., 2020. Signaling pathways involved in virulence and stress response of plant-pathogenic *Fusarium* species. Fungal Biol. Rev. 35; 27-39.

Stergiopoulos, I., van Nistelrooy, J.G., Kema, G.H., De Waard, M.A., 2003. Multiple mechanisms account for variation in base-line sensitivity to azole fungicides in field isolates of *Mycosphaerella graminicola*. Pest Manag. Sci. 59, 1333-1343.

Sun, C.B., Suresh, A., Deng, Y.Z. and Naqvi, N.I., 2006. A multidrug resistance transporter in *Magnaporthe* is required for host penetration and for survival during oxidative stress, The Plant Cell 18, 3686-3705.

Takano, Y., Kubo, Y., Shimizu, K., Mise, K., Okuno, T., Furusawa, I., 1995. Structural analysis of PKS1, a polyketide synthase gene involved in melanin biosynthesis in *Colletotrichum lagenarium*. Mol. Gen. Genet. 249, 162-7.

Talbot, N.J., 2003. On the trail of a cereal killer: exploring the biology of *Magnaporthe grisea*. Annu. Rev. Microbiol. 57, 177-202.

Talbot, N.J., 2019. Appressoria, Curr. Biol. 29, R144-R146.

Tan, K.C., Ipcho, S.V., Trengove, R.D., Oliver, R.P. and Solomon, P.S, 2009. Assessing the impact of transcriptomics, proteomics and metabolomics on fungal phytopathology. Mol. Plant Pathol. 10, 703-715.

Tang, C., Xu, Q., Zhao, M., Wang, X. and Kang, Z., 2018. Understanding the lifestyles and pathogenicity mechanisms of obligate biotrophic fungi in wheat: The emerging genomics era. The Crop J. 6, 60-67.

Tannous, J., Kumar, D., Sela, N., Sionov, E., Prusky, D. and Keller, N.P., 2018. Fungal attack and host defence pathways unveiled in near-avirulent interactions of *Penicillium expansum creA* mutants on apples. Mol. Plant Pathol. 19, 2635-2650.

Temporini, E.D., VanEtten, H.D., 2004. An analysis of the phylogenetic distribution of the pea pathogenicity genes of *Nectria haematococca* MPVI supports the hypothesis of their origin by horizontal transfer and uncovers a potentially new pathogen of garden pea: *Neocosmospora boniensis*. Curr. Genet. 46, 29-36.

Thomas, S.R., Elkinton, J.S., 2004. Pathogenicity and virulence. J. Invertebr. Pathol. 85, 146-151.

Thon, M.R., Pan, H.Q., Diener, S., Papalas, J., Taro, A., Mitchell, T.K., and Dean, R.A., 2006. The role of transposable element clusters in genome evolution and loss of synteny in the rice blast fungus *Magnaporthe oryzae*. Genome Biol. 7, R16.

Tong, L., Milburn, M.V., de Vos, A.M., Kim, S.H., 1989. Structure of ras proteins. Science 1989, 245, 244.

Tudzynski, P.; Sharon, A., 2003. Fungal pathogenicity genes. Appl. Mycol. Biotech. 3, 187-212.

Urban, M., Bhargava, T., Hamer, J.E., 1999. An ATP-driven efflux pump is a novel pathogenicity factor in rice blast disease. EMBOJ. 18, 512-521.

van de Wouw, A. P., Howlett, B. J., 2011. Fungal pathogenicity genes in the age of 'omics'. Mol. Plant Pathol. 12, 507-514.

van den Brink, H.J.M., van Gorcom, R.F.M., van den Hondel, C.A.M.J.J., Punt P. J., 1998. Cytochrome P450 Enzyme Systems in Fungi. Fungal Genet. Biol. 23, 1-17.

van der Does, H. C., Rep, M., 2007. Virulence genes and the evolution of host specificity in plant-pathogenic fungi. Mol. Plant-Microbe Interact. 20, 1175-1182.

van Wyk, S., Wingfield, B.D., De Vos, L., van der Merwe, N.A, Steenkamp, E.T., 2021. Genome-Wide Analyses of Repeat-Induced Point Mutations in the Ascomycota. Front. Microbiol. 11, 622368.

Vela-Corcía, D., Aditya Srivastava, D., Dafa-Berger, A. et al., 2019. MFS transporter from *Botrytis cinerea* provides tolerance to glucosinolate-breakdown products and is required for pathogenicity. Nat. Commun. 10, 2886.

Walton, J.D., 2000. Horizontal Gene Transfer and the Evolution of Secondary Metabolite Gene Clusters in Fungi: An Hypothesis. Fungal Genet. Biol. 30, 167-171.

Walton, J.D., 2006. HC-toxin. Phytochem. 67, 1406-1413.

Wang, Y., Tian, L., Xiong, D., Klosterman, S.J., Xiao, S. and Tian, C., 2016. The mitogen-activated protein kinase gene, VdHog1, regulates osmotic stress response, microsclerotia formation and virulence in *Verticillium dahliae*. Fungal Genet. Biol. 88, 13-23.

Wanjiru, W.M., Zhensheng, K., Buchenauer, H., 2002. 'Importance of cell wall degrading enzymes produced by *Fusarium graminearum* during infection of wheat heads. Eur. J. Plant Pathol. 108, 803-810.

Wasmann, C., VanEtten, H.D., 1996. Transformation-mediated chromosome loss and disruption of a gene for pisatin demethylase decrease the virulence of *Nectria haematococca* on pea. Mol. Plant Microbe Interact. 9, 793-803.

Weld, R.J., Plummer, K.M., Carpenter, M.A. and Ridgway, H. J., 2006. Approaches to functional genomics in filamentous fungi. Cell Res. 16, 31-44.

Wiemann, P., Sieber, C.M.K., von Bargen, K.W., Studt, L., Niehaus, E.M. et al., 2013. Deciphering the Cryptic Genome: Genome-wide Analyses of the Rice Pathogen *Fusarium fujikuroi* Reveal Complex Regulation of Secondary Metabolism and Novel Metabolites. PLoS Pathog. 9, e1003475.

Wilson, A. M. and Wingfield, B. D., 2020. CRISPR-Cas9-Mediated Genome Editing in the Filamentous Ascomycete *Huntiella omanensis*. J. Visual. Experim. e61367.

Wöstemeyer, J., and Kreibich, A., 2002. Repetitive DNA elements in fungi (Mycota): Impact on genomic architecture and evolution. Curr. Genet. 41, 189-198.

Xu, J.F., Leslie, A., 1996. Genetic map of *Gibberella fujikuroi* mating population A (*Fusarium moniliforme*). Genetics 143, 175-189.

Xu, J.R., 2000. MAP kinases in fungal pathogens. Fungal Genet. Biol. 31, 137-152.

Xu, J.R., Hamer, J.E., 1996. MAP kinase and cAMP signaling regulate infection structure formation and pathogenic growth in the rice blast fungus *Magnaporthe grisea*. Genes Dev. 10, 2696-2706.

Xue, C.Y., Park, G., Choi, W.B., Zeng, L., Dean, R.A., Xu, J.R., 2002. Two novel fungal virulence genes specifically expressed in appressoria of the rice blast fungus. Plant Cell 14, 2107-2119.

Yang, G., Rose, M.S., Turgeon, B.G., Yoder, O.C., 1996. A polyketide synthase is required for fungal virulence and production of the polyketide T-toxin. Plant Cell 8, 2139-50.

Yoder, O.; Turgeon, B. G., 2001. Fungal genomics and pathogenicity. Curr. Opin. Plant Biol. 4, 315-321.

Yoder, O.C., Macko, V., Wolpert, T.J., Turgeon, B.G., 1997. *Cochliobolus* spp. and their host-specific toxins. In: Carroll G, Tudzynski P, editors. The Mycota VA: Plant Relationships. Berlin: Springer; 145-166.

Young, S.G., Ambroziak, P., Kim, E., Clarke, S., 2001. Postisoprenylation protein processing: CXXX CaaX endoproteases and isoprenylcysteine carboxyl methyltransferase, in: Tamanoi, F., Sigman, D.S. (Eds.), The Enzymes. Academic Press, New York, pp. 155-213.

Yu, C., Li, T., Shi, X., Saleem, M., Li, B., Liang, W., Wang, C., 2018. Deletion of endo-β-1, 4-xylanase VmXyl1 impacts the virulence of *Valsa mali* in apple tree. Front. Plant Sci. 9, 663.

Zhang Y. Choi Y. Zou X.; Xu J., 2011. The FvMK1 mitogen-activated protein kinase gene regulates conidiation, pathogenesis, and fumonisin production in *Fusarium verticillioides*. Fungal Genet. Biol. 48, 71-79.

Zhang, H., Xue, C., Kong, L., Li, G., Xu, J., 2011. A Pmk1-Interacting gene is involved in appressorium differentiation and plant infection in *Magnaporthe oryzae*. Eukaryot. Cell 10, 1535-9778.

Zhang, Y., Wilkinson, H., Keller, N., Tsitsigiannis, D., An, Z. 2004. Secondary metabolite gene clusters. New York: Marcel Dekker.

Zhao, Z., Liu, H., Wang, C., Xu, JR., 2013. Comparative analysis of fungal genomes reveals different plant cell wall degrading capacity in fungi. BMC Genomics 14, 274.

Zheng, L., Campbell, M., Murphy, J., Lam, S.; Xu, J.R., 2000. The BMP1 gene is essential for pathogenicity in the gray mold fungus *Botrytis cinerea*. Mol. Plant-Microbe Interact. 13, 724-732.

Zhu, Y., Fang, H.M., Wang, Y.M., Zeng, G.S., Zheng, X.D., Wang, Y., 2009. Ras1 and Ras2 play antagonistic roles in regulating cellular cAMP level, stationary-phase entry and stress response in *Candida albicans*. Mol. Microbiol. 74, 862-875.

Tables

Table 1. Overview information for the known pathogenicity and virulence factors discussed in this review.

Role during infection	Gene name	Gene product	Species	Reference
Signal transduction	*RAS2*	Guanosine triphosphatase	*Fusarium graminearum*	Bluhm et al. (2007)
	RAS2	Guanosine triphosphatase	*Fusarium circinatum*	Phasha et al. (2021)
	PMK1	Map kinase	*Magnaporthe grisea*	Xu (2000)
	MPS1	Map kinase	*Cochliobollus heterostrophus*	Lev et al. (1999)
	BMP1	Map kinase	*Botrytis cinerea*	Zheng et al. (2000)
	KPP2	Map kinase	*Ustilago maydis*	Muller et al. (1999)
	FMK1	Map kinase	*Fusarium* spp.	Di Pietro et al. (2001)
	cyaA	Adenylate cyclase	*Aspergillus nidulans*	Fillinger et al. (2002)
	pkaA	Protein kinase	*Aspergillus nidulans*	Fillinger et al. (2002)
	FAC1	Protein kinase catalytic subunit	*Fusarium verticillioides*	Choi and Xu (2010)
	bcpka1	Protein kinase catalytic subunit	*Botrytis cinerea*	Schumacher et al. (2008)
	bcpkaR	Protein kinase catalytic subunit	*Botrytis cinerea*	Schumacher et al. (2008)
Host penetration	*CHS7*	Chitin synthase	*Magnaporthe oryzae*	Kong et al. (2012)
	PMK1	Map kinase	*Magnaporthe grisea*	Xu et al. (1996), Xu and Hamer (1996), Bruno et al. (2004), Sabnam and Barman (2017)
	CBP1	Chitin-binding protein	*Magnaporthe grisea*	Kamakura et al. (2002)

Table 1. Continued.

Role during infection	Gene name	Gene product	Species	Reference
	CBP1	Chitin-binding protein	*Magnaporthe oryzae*	Kuroki et al. (2017)
	PKS1	Polyketide synthase	*Cochliobollus lagenarium*	Takano et al. (1995)
	THR1	Reductase	*Cochliobollus lagenarium*	Perpetua et al. (1996)
	MGATG1	Serine/threonine kinase	*Magnaporthe grisea*	Liu et al. (2007)
	GAS1	Uncharacterized protein	*Magnaporthe grisea*	Xue et al. (2002)
	GAS2	Uncharacterized protein	*Magnaporthe grisea*	Xue et al. (2002)
	PIC5	Uncharacterized with transmembrane domain	*Magnaporthe oryzae*	Zhang et al. (2011)
	CLU5	Uncharacterized secreted protein	*Cochliobollus graminocala*	Eisermann et al. (2019)
Cell wall degradation	*Bcpg1*	Polygalacturosane	*Botrytis cinerea*	ten Have et al. (1998)
	Acpg	Polygalacturosane	*Alternaria citri*	Isshiki et al. (2001)
	VmXyl1	Endo-β-1,4-xylanase	*Valsa mali*	Yu et al. (2018)
	Pg1	Endo- Polygalacturosane	*Fusarium graminearum*	Paccanaro et al. (2017)
	xyr1	Transcriptional regulator	*Fusarium graminearum*	Paccanaro et al. (2017)
Host colonization	*PKS1*	Polyketide synthase	*Cochliobollus heterostrophus*	Yang et al. (1996)
	PKS2	Polyketide synthase	*Cochliobollus heterostrophus*	Baker et al. (2006)
	DEC1	Decarboxylase	*Cochliobollus heterostrophus*	Rose et al. (2002)

Table 1. Continued.

Role during infection	Gene name	Gene product	Species	Reference
	TOXF	Transaminase	*Cochliobollus carbonum*	Cheng et al. (1999)
	ALT1	Polyketide synthase	*Alternaria alternata*	Akamatsu et al. (1997)
	TOXA	Secreted ToxA protein	*Pyrenophora tritici-repentis*	Friesen et al. (2006)
	FUM1	Polyketide synthase	*Fusarium verticillioides*	Glenn et al. (2008)
	FUB1	Polyketide synthase	*Fusarium oxysporum* f. sp. *lycopersici*	Lopez-Diaz et al. (2018)
	BIK	Polyketide synthase	*Fusarium oxysporum* f. sp. *vasinfectum*	Bell et al. (2003)
	Tri5	Trichodiene synthase	*Fusarium graminearum*	Proctor et al. (1995)
Suppression of defensive compounds	*PDA1*	Pisatin demethylase	*Fusarium solani*	Wasmann and VanEtten (1996)
	TOM1	Tomatinase	*Fusarium oxysporum*	Pareja-Jaime et al. (2008)
	GpABC1	ABC transporter	*Gibberella pulicans*	Fleibner et al. (2002)
	atrB	ABC transporter	*Aspergillus nidulans*	Andrade et al. (2000)
	ABC3	ABC transporter	*Magnaporthe grisea*	Sun et al. (2006)
	mfsG	MFS transporter	*Botrytis cinerea*	Vela-Corcía et al. (2019)

Figures

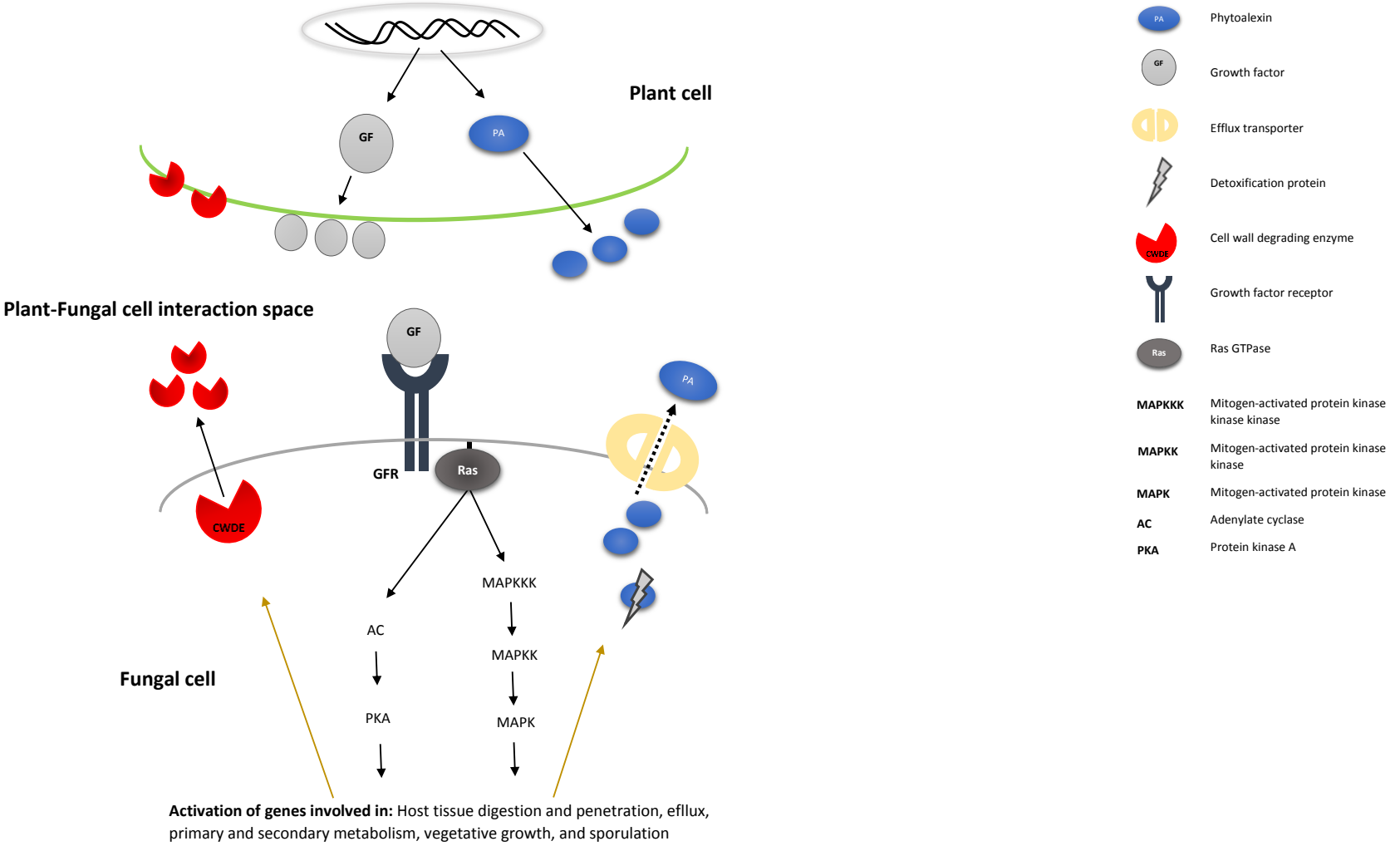

Figure 1. General MAPK and cAMP signalling pathways in phytopathogenic filamentous fungi. GF = growth factor, GFR = growth factor receptor, and MAPK = mitogen-activated protein kinase.

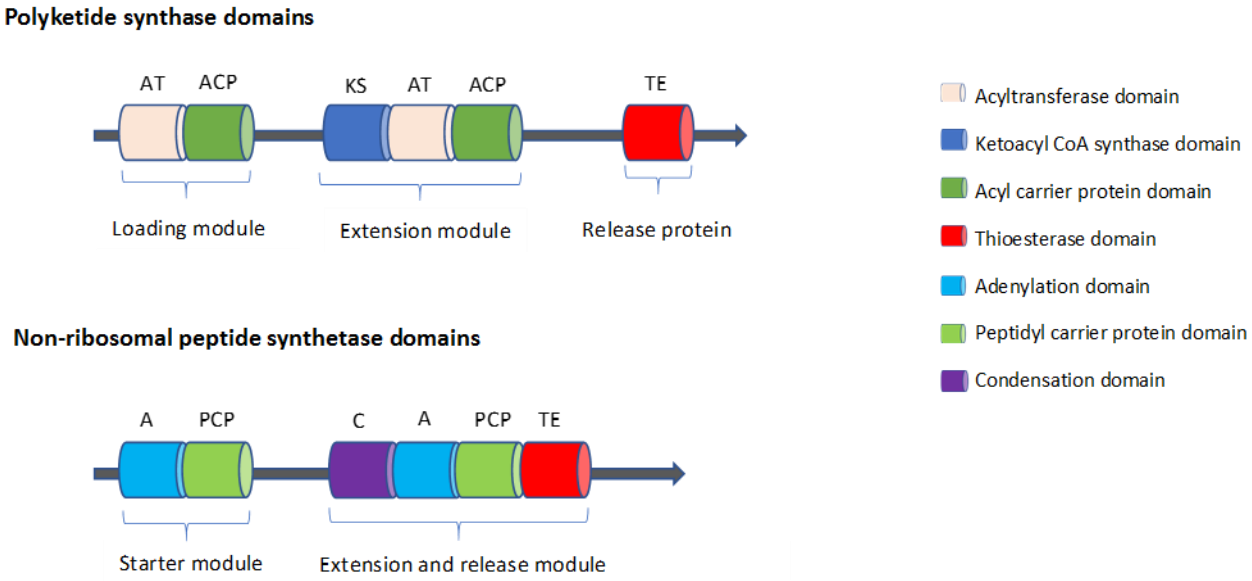

Figure 2. The basic domain structure of **(A)** a PKS (polyketide synthase) and **(B)** an NRPS (non-ribosomal peptide synthetase). AT = acyltransferase domain, KS = ketoacyl CoA synthase domain, ACP = Acyl carrier protein domain, TE = thioesterase domain, A = adenylation domain, PCP = peptidyl carrier protein domain, and C = condensation domain. Peptide synthesis starts from left to right (indicated by arrow).

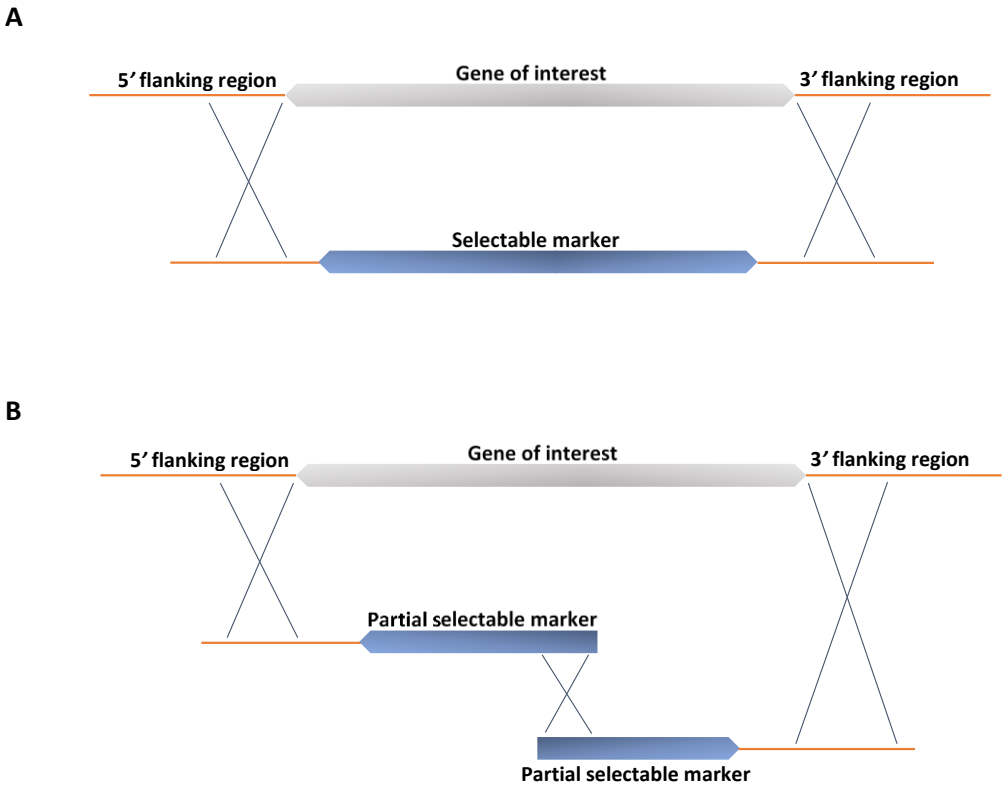

Figure 3. Approaches for generating a gene knockout. **A.** The conventional genomic integration method involving homologous recombination (HR) between partial sequences of the gene of interest that is part of a knockout construct and the gene of interest in the genome. **B.** The split-marker approach involving an additional HR event between two partial amplicons of a selectable marker to facilitate more precise genomic integration of the knockout construct. Homologous regions are coded with the same colour. Blue crosses indicate recombination events leading to gene deletion or disruption.

Chapter 2

Ras2 is important for growth and pathogenicity in *Fusarium circinatum*

Published: Phasha, M., Wingfield, M., Wingfield, B., Coetzee, M., Hallen-Adams, H., Fru, F., Swalarsk-Parry, B., Yilmaz, N., Duong, T., Steenkamp, E., 2021. Ras2 is important for growth and pathogenicity in *Fusarium circinatum*. Fungal Genet. Biol. 150, 103541-103550.

Abstract

In this study, we investigated the possible role of Ras2 in *Fusarium circinatum*- a fungus that causes pine pitch canker disease on many different pine species and has a wide geographic distribution. This protein is encoded by the *RAS2* gene and has been shown to control growth and pathogenicity in a number of fungi in a mitogen-activated protein kinase- and/or cyclic adenosyl monophosphate pathway-dependent manner. The aim was therefore to characterize the phenotypes of *RAS2* gene knockout and complementation mutants of *F. circinatum*. These mutants were generated by transforming protoplasts of the fungus with suitable split-marker constructs. The mutant strains, together with the wild type strain, were used in growth studies as well as pathogenicity assays on *Pinus patula* seedlings. Results showed that the knockout mutant strain produced significantly smaller lesions compared to the complementation mutant and wild type strains. Growth studies also showed significantly smaller colonies and delayed conidial germination in the knockout mutant strain compared to the complement mutant and wild type strains. Interestingly, the knockout mutant strain produced more macroconidia than the wild type strain. Collectively, these results showed that Ras2 plays an important role in both growth and pathogenicity of *F. circinatum*. Future studies will seek to determine the pathway(s) through which Ras2 controls these traits in *F. circinatum*.

1. Introduction

Signaling pathways that govern fungal pathogenesis and virulence have been the subject of numerous studies on important plant pathogens (Lengeler et al., 2000). This previous body of work has shown that these pathways are complex, involving many different proteins including receptors and transcription factors. The mitogen-activated protein kinase (MAPK) and cyclic adenosyl monophosphate (cAMP) pathways are among the most prominent known to be involved in fungal pathogenesis (Lengeler et al., 2000). They are activated by Ras proteins (Lengeler et al., 2000), which are not only important for the infection process, but in many cases also integral to growth and reproduction (Kronstad and Staben, 1997).

Ras proteins belong to a superfamily of small guanosine triphosphatases (GTPases) that act as molecular switches for signaling pathways in eukaryotes (Barbacid, 1987; Cox and Der, 2010). They transduce signals from external cues that culminate in the expression of genes involved in cellular functions such as growth, differentiation, metabolism and programmed cell death (Lowy and Willumsen, 1993). Overall, the Ras superfamily may be divided into five main groups based on sequence and function (i.e., Rab, Ran, Ras, Rho, and Sar/Arf), and of these the Ras group is by far the best characterized in multicellular eukaryotes (Bourne et al., 1991; Pentland et al., 2018). The Ras group proteins are encoded by *RAS* (rat sarcoma) genes, the first of which was characterized in rats where *RAS* mutations caused sarcomas due to constitutive activation of the Ras protein (Cox and Der, 2010). Because such mutations have also been linked to approximately 50% of all cancers in humans (Campbell et al., 2004), *RAS* genes form part of many molecular diagnostic cancer panels (Sokolenko and Imyanitov, 2018).

In fungi, the two Ras proteins that have been widely studied are Ras1 and Ras2, respectively encoded by *RAS1* and *RAS2* (Toda et al., 1985; Sun et al., 1994; Mosch et al., 1996; Fillinger et al., 2002; Waugh et al., 2002; Gourlay et al., 2006; Bluhm et al., 2007; Zhu et al., 2009; Zhou et al., 2014). Depending on the fungus examined, previous work has shown that the functions of these proteins may be redundant, overlapping and/or antagonistic. These proteins can also have high sequence similarity or differ significantly in the same fungus (Zhu et al., 2009). Moreover, the motif used for membrane anchorage (i.e., CAAX where C= Cysteine; AA= any two aliphatic amino acids; X= any amino acid), and where post-translational modifications occur for this purpose, can be the same or differ between the two proteins (Spence and Casey, 2001; Young, 2001; Krishnankutty et al., 2009). In *Saccharomyces cerevisiae* Ras1 and Ras2 are similar in length

and CAAX motif and thus have redundant roles (Hrycyna and Steven, 1992; Zhu et al., 2009), where both proteins are capable of activating the cAMP and MAPK pathways (Toda et al., 1985; Mosch et al., 1996). Interestingly, and contrary to the case in humans, hyper-activation of the Ras2 pathway in *S. cerevisiae* leads to apoptosis (Gourlay et al., 2006). In *Aspergillus nidulans*, RasA (a homologue of Ras1) controls asexual spore germination through activation of the cAMP pathway (Fillinger et al., 2002). The same has been observed for *Neurospora crassa* (Bruno et al., 1996), *S. cerevisiae* (Thevelein, 1984) and *Schizosaccharomyces pombe* (Hatanaka and Shimoda, 2001). In *Magnaporthe oryzae*, Ras1 plays a minor role in growth, whereas Ras2 plays a more critical role in the formation of the specialized cells (appressoria) needed for initiation of plant infection (Zhou et al., 2014). In *Candida albicans*, Ras1 and Ras2 have been shown to have antagonistic roles (Uhl et al., 2003; Zhu et al., 2009), while they have overlapping and unique roles in *Cryptococcus neoformans* (Waugh et al., 2002). In the latter fungus, both proteins are involved in growth, but only Ras1 is required for its growth at high temperatures (Waugh et al., 2002).

Few studies have investigated the role of Ras1 and Ras2 in the growth, development and infection biology of *Fusarium* species. This is despite the fact that members of this genus include some of the world's most important plant pathogens (Nelson et al., 1981). To the best of our knowledge, a Ras protein has been investigated in only one species of the genus, i.e., *Fusarium graminearum* (Bluhm et al., 2007). In this fungus, Ras2 was shown to control virulence, growth, spore germination and perithecium formation (Bluhm et al., 2007). The study also showed that, unlike in *S. cerevisiae*, Ras2 controls these traits in *F. graminearum* through the MAPK pathway only (Bluhm et al., 2007). In the current study, we focused on the *RAS2* gene of the globally important pine pathogen *Fusarium circinatum* (Wingfield et al., 2008; Drenkhan et al., 2020). Within the broader genus, *F. circinatum* is distantly related to *F. graminearum*, with the two fungi forming part of species complexes (i.e., *F. fujikuroi* and *F. sambucinum* species complexes, respectively) that diverged more than 30 million years ago (O'Donnell et al., 2013; Geiser et al., 2020).

The whole-genome sequence for *F. circinatum* has been determined (Wingfield et al., 2012), but not much is known about the molecular processes involved in its pathogenic behavior. Although a few studies have identified genes and gene clusters potentially involved in growth and pathogenicity (De Vos et al., 2011; Wiemann et al., 2013; Van Wyk et al., 2018; Munoz-Adalia et al., 2018a), only one has functionally characterized a gene involved in the growth of *F. circinatum* (Munoz-Adalia et al., 2018b). Also, nothing is known regarding the role of Ras2 in the biology of

F. circinatum. The aim of this study was therefore to characterize the role of Ras2 in *F. circinatum*. For this purpose, we first generated *RAS2* knockout and complement mutants using the split-marker construct protocol (Catlett et al., 2003). These mutants and the wild type strain were then used in an array of assays to assess the impact of Ras2 in growth and pathogenicity of the fungus. The findings of this study will thus increase our knowledge about the molecular basis and processes that underlie growth and pathogenicity in *F. circinatum* and likely other fungi in this genus.

2. Materials and Methods

2.1. Fungal isolates, growth conditions and DNA extractions

Four *F. circinatum* isolates were used in this study. Of the four, two originated from our previous work. These were isolates KS17 and FSP34 and are available as strains CMW 674 and CMW 53647, respectively, from the culture collection of the Forestry and Agricultural Biotechnology Institute, FABI, University of Pretoria, South Africa. These two isolates are sexually compatible and can produce fertile progeny, because KS17 is female fertile with MAT2 mating specificity and FSP34 is MAT1 and largely female sterile (Desjardins et al., 2000; Steenkamp et al., 2001; Van Wyk et al., 2018). The two remaining isolates used in this study represented *ras2* knockout (ΔFcras2; CMW 53644) and complement (ΔFcras2C; CMW 53645) mutants of FSP34, which were generated in this study (see below). Fungal strains were routinely grown on half strength Potato Dextrose Agar (PDA; Becton, Dickinson and Company, Franklin Lakes, NJ, USA) at 25 °C unless otherwise stated.

For the extraction of DNA, an agar block overgrown with mycelium was cut from a seven-day-old PDA culture and used to inoculate Potato Dextrose Broth (PDB; Becton, Dickinson and Company, Franklin Lakes, NJ, USA). The PDB cultures were incubated with shaking at approximately 200 rpm for seven days at room temperature. The cultures were then filtered through two layers of Miracloth (Calbiochem, La Jolla, CA, USA) to collect fungal biomass and then freeze dried. The freeze-dried material was then used to extract DNA using the CTAB (cetyltrimethylammonium bromide) protocol of Murray and Thompson (1980) with minor modifications (see Supplementary file S1).

2.2. Identification and analysis of *RAS* genes

To identify *RAS* genes in the genome of *F. circinatum*, the *F. graminearum RAS1* and *RAS2* gene sequences (FGSG_09778 and FGSG_10114; Bluhm et al., 2007) were used. They were retrieved from the nucleotide database of the National Center for Biotechnology Information (NCBI; https://www.ncbi.nlm.nih.gov) using NCBI accession numbers XM_011329611.1 and XM_011320750.1, respectively. The *F. graminearum* sequences were then used as queries in BLASTn searches against the genome of *F. circinatum* FSP34 (NCBI accession number AYJV00000000; Wingfield et al., 2012) using CLC Genomics Workbench (Version 8.0.3) with default settings. The protein sequences and CAAX motifs for these genes were compared using their inferred amino acid sequences and alignment in CLC Genomics Workbench.

We also subjected the *F. circinatum RAS2* gene to phylogenetic analysis. For this purpose, the *RAS2* coding sequences from various species of *Fusarium* (including those of the *F. fujikuroi* and *F. sambucinum* species complexes) and other fungi (i.e., *Colletotrichum higginsianum*, *M. oryzae* (*Pyricularia oryzae*), *Trichoderma reesei*, *Alternaria burnsii*, *A. nidulans*, and *N. crassa*) were retrieved from NCBI using the Ras2 sequence of *F. circinatum* and tBLASTn searches with default parameters. We then constructed multiple sequence alignments by aligning the coding nucleotide sequences based on their corresponding amino acid translations using MAFFT (Katoh et al., 2002) in the online version of TranslatorX (Abascal et al., 2010). Following visual inspection of the alignments in AliView version 1.26 (Larsson, 2014), a maximum likelihood phylogeny was determined using raxmlGUI version 2.0 (Edler et al., 2020). This analysis utilized the TIM2+G+I substitution model as determined with the "optimize" function in raxmlGUI. Nodal support values were calculated with bootstrap using the "thorough bootstrap" setting with 1000 replications. The tree was rooted with *Aspergillus nidulan*s and *Alternaria burnsii* as outgroup taxa.

2.3. Generation of *ras2* knockout and complementation constructs

Knockout constructs for *RAS2* gene replacement were generated using the split-marker construct protocol (Catlett et al., 2003; see Supplementary file S1). For this purpose, Polymerase Chain Reaction (PCR) amplification of the 5' flanking region of *RAS2* was done using primer set *Ras2*U F1 + *Ras2*U R1 (Table 1), and the 3' flank was amplified using primer set *Ras2*Dw F1 + *Ras2*Dw R1 (Table 1). We also produced two overlapping amplicons of the hygromycin resistance gene (*hygR*) by making use of two independent PCRs with primer sets HygR + ygF and HygF + hyR (Table 1; Zhou et al., 2010) that were performed directly on *Escherichia coli* colonies carrying plasmid pCB1004 (Carroll et al., 1994). All amplicons were generated using Phusion High-Fidelity

Master Mix (Thermo Fisher Scientific, Vilnius, Lithuania). The 5' *RAS2* flank was then fused to the first *hygR* amplicon using primer set *Ras2*U F1 + ygF (Table 1; Zhou et al., 2010), and the 3' *RAS2* flank was fused to the second *hygR* amplicon using primers *Ras2*Dw R1 and hyR. These amplicon fusion reactions were done using LongAmp® *Taq* 2X Master Mix (New England BioLabs, Ipswich, MA, USA).

A complementation construct of the *RAS2* gene was generated for random integration into the genome of the ΔFcras2 mutant. This was done by amplifying the FSP34 *RAS2* allele (the full gene sequence including the promoter and terminator regions) using Expand™ Long Range dNTPack (Sigma-Aldrich, Mannheim, Germany) with the primers *ras2*allele_F1 and *ras2*allele_R (Table 1; Supplementary file S1). This amplicon was then fused to a geneticin resistance cassette (i.e., *nptII*) which included a promoter and terminator. The cassette was amplified directly from *E. coli* colonies carrying plasmid pGEN-Not1 (Proctor et al., 2008) using Phusion High-Fidelity Master Mix and the primer set Not_1F_rp619 + Not_1R_rp620 (Table 1). Fusion of the *RAS2* allele to the geneticin resistance cassette was performed using LongAmp® *Taq* 2X Master Mix and the primers *ras2*allele_F1 and Not_1R_rp620.

2.4. Transformation of wild type and mutant strains

Protoplasts of *F. circinatum* FSP34 were generated using the protocol for *F. graminearum* (Hallen-Adams et al., 2011; Supplementary file S1). About 0.25-0.5 µg of the respective split-marker knockout constructs generated were incubated with *F. circinatum* FSP34 protoplasts in 9 ml of regeneration liquid medium with shaking at 75 rpm for about 18 hours. This mixture was then poured onto 90 mm Petri dishes (1 ml per plate) and mixed with 10 ml of regeneration agar medium containing 150 µg/ml of Hygromycin B solution from *Streptomyces hygroscopicus* (Sigma-Aldrich, Mannheim, Germany). Plates were incubated in the dark at room temperature for 14 days.

Screening for potential mutants was done by transferring grown colonies onto PDA medium containing 150 µg/ml of Hygromycin B and incubating them for seven days in the dark (Supplementary file S1). We then subjected putative transformants to PCR with primer sets *ras*2F + *ras*2R and HygF + HygR to confirm the presence of the *RAS2* and *hygR* genes, respectively (Table 1). To test for the replacement of *RAS2* by the *hygR* gene in mutants, PCR was done using primers that are complementary to the flanking regions of the 5' and 3' *ras2* flanks (i.e., *ras2*left_F1

and *ras2*right_R1; see Table 1) by employing the LongAmp® *Taq* 2X Master Mix. To determine the copy number of the *hygR* construct in genomes of the mutants, a Southern Blot analysis was done using a protocol adapted from Sambrook and Green (2012) and Eisel et al. (2008) (See Supplementary file S1). The primer set HygR + Hyg-int-R (Table 1) were used to synthesize the probe used during the Southern Blot analysis.

In order to produce complementation mutants, protoplasts were generated from ΔFcras2 and the protoplasts were transformed with the complementation construct as described above. However, the overnight cultures were mixed with regeneration agar medium containing 120 µg/ml of geneticin (G-418 sulfate; Thermo Fisher Scientific, Rockford, IL, USA). Further culturing of colonies was done on PDA augmented with 120 µg/ml of geneticin (G-418 sulfate) and incubated in the dark for seven days. To test for the presence of the *RAS2* gene in complementation transformants, colony PCR amplification was performed using *Ras2*_probeF1 and *Ras2*_probeR1 (Table 1) with the LongAmp® *Taq* 2X Master Mix.

2.5. Morphological traits of mutants and wild type strains

General colony morphology of the FSP34 wild type and the knockout and complement mutant strains were examined. After seven days of growth on Spezieller Nährstoffarmer Agar (SNA; Leslie and Summerell, 2006), agar discs overgrown with mycelium were punched out of each culture using a sterile hollow glass rod with 5 mm diameter. These discs were each placed onto 90 mm Petri dish plates containing PDA and incubated at 24 °C in i) darkness, ii) under continuous light, and iii) under a 12/12-hour light/dark cycle using near UV light. For assessments of fungal micromorphological structures, fungi were grown on Carnation Leaf Agar (CLA; Fisher et al. 1982) and SNA with sterile carnation leaves, and incubated at room temperature (22–24 °C) under a 12/12-hour near-UV light/dark cycle. Microscopic observations were made under a light microscope using a standard slide and water as a mounting medium. Photographs were captured at 63x magnification.

Colony growth of the FSP34 wild type and the knockout and complement mutant strains was measured. For this, 50 000 spores/ml spore suspensions were prepared by flushing 4 ml of sterile distilled water onto seven-day-old PDA cultures and enumerating the spores using a hemocytometer slide and 40x magnification under a light microscope. For each of the respective

strains, 10 µl of spore suspension was used to inoculate PDA medium. Following incubation at 25 °C for seven days, agar discs overgrown with mycelium were punched out of each culture using a sterile hollow glass rod with 5 mm diameter. These discs were each placed onto the center of 90 mm plates containing PDA and incubated under the following conditions: i) 25 °C under light, ii) 25 °C in darkness, iii) 15 °C under light and iv) 15 °C in darkness. Six replicates were used for each of the culturing conditions and perpendicular colony diameter measurements were taken after seven days. Similar sets of experiments were also used to evaluate growth rate, where inoculated plates were incubated for seven days and colony diameters recorded daily from days four to seven.

The number of conidia produced by the wild type and the knockout and complement mutant strains were examined. Conidial suspensions were prepared using 5 mm diameter discs overgrown with mycelium from 10-day-old PDA cultures incubated at 25 °C under light. These discs were placed in 2 ml tubes containing 1.5 ml sterile distilled water, and then agitated with a vortex mixer for 30 seconds to release spores into the water. The number of spores in 10 µl of each suspension was then quantified using a hemocytometer slide and 40x magnification under a light microscope. For these spore suspensions, the relative abundance of microconidia and macroconidia (the latter included mesoconidia) were also determined. This was done by placing 10 µl of the respective suspensions on standard microscope slides and counting the two conidial types using a light microscope. In all of these cases, three replicates were examined per strain.

Conidial germination was assessed for each of the wild type and the knockout and complement mutant strains. To this end, conidial suspensions were prepared by flushing 4 ml of sterile distilled water onto 10-day-old PDA cultures (incubated at 25 °C under light) of each strain. One milliliter of each suspension was then pipetted into sterile 12-well cell culture plates, which were then incubated with shaking (80 rpm) at 23 °C. Three replicate assessments were made for each strain. Following 24, 48 and 72 hours, 10 µl of the respective spore suspensions were collected and assessed under a light microscope by measuring the length of the hyphal strand that emerged from conidia of each strain during germination.

2.6. Fertility of wild type and mutants and sexual crosses

Sexual fertility of the FSP34 wild type and the knockout and complement mutant strains with *F. circinatum* KS17 was assessed. Because previous experiments have shown that FSP34 is

predominantly female sterile (Desjardins et al., 2000), the assessment focused on examination of the male fertility of FSP34 and its mutants. This was done by crossing each of the mutant strains and FSP34 with the female fertile isolate KS17. Accordingly, we cultivated KS17 on Carrot Agar (Leslie and Summerell, 2006) and the respective FSP34 wild type and mutant strains on Complete Medium (Leslie and Summerell, 2006) for seven days in the dark at room temperature. Spores produced by the Complete Medium cultures were then suspended in a 2.5 % Tween 20 solution (Sigma-Aldrich, Mannheim, Germany), of which about 1 ml was applied across the surface of a KS17 culture with a cell spreader. Perithecium formation was evaluated after six weeks following incubation at ±17 °C under near-UV light (Leslie and Summerell, 2006). The crosses were replicated four times for each of the FSP34 wild type and mutant strains.

2.7. Pathogenicity of wild type and mutants on pine seedlings

Pathogenicity of the FSP34 wild type and the knockout and complement mutant strains was tested on six-month-old *Pinus patula* seedlings. Conidial suspensions (50 000 conidia/ml) were prepared following the same procedure used for the growth study. Stem tips were removed five centimeters from the growth tip of the seedlings. To the cut plant surface, we then applied 10 µl of the prepared conidial suspension, while 10 µl of a 15% glycerol solution was used as control. Each strain was used to inoculate 40 *P. patula* seedlings and the same was also true for the control treatment. Inoculations were done in a randomized manner and the randomization layout design was done in Microsoft® Excel using the RAND function. Seedlings were watered once every day for six weeks after which lesion lengths (mm) were measured.

To meet the requirement of Koch's postulates, isolations were made from lesions on the inoculated seedlings. This was done by cutting diseased and non-diseased stem tips, removing the needles, and placing the stem tips into 90 mm Petri dishes containing *Fusarium* selective medium (FSM) (Leslie and Summerell, 2006). Following incubation for seven days at 25 °C in the dark, DNA was extracted (as described earlier) from the fungi growing on the FSM plates. These DNAs were then used to confirm that they represent *F. circinatum* using the diagnostic PCR protocol that uses *F. circinatum* species-specific primer set CIRC1A + CIRC4A (Table 1; Schweigkofler et al., 2004; Steenkamp et al., 2014) and *Taq* DNA polymerase (Roche Diagnostics, Mannheim Germany). We also confirmed presence/absence of the *RAS2* gene in these isolates using PCR with the primer set *ras2*_ProbeF1 + *ras2*_ProbeR1 (Table 1). The presence/absence of the hygromycin resistance gene

was also confirmed, using primers hy-R and HygF (Table 1), and the LongAmp® *Taq* 2X Master Mix.

2.8. Statistical analyses

To test for variation in lesion lengths between infected seedlings as well as variation in culture growth and conidial production in the FSP34 wild type and the knockout and complement mutant strains, analysis of variance (ANOVA) was used (http://astatsa.com/OneWay_Anova_with_TukeyHSD/). The null (H_o) hypothesis was tested using the *F* test where H_o was that all the (mean) lesion lengths produced by the different strains or their growth rates are equal (Samuels and Witmer, 2003). For this purpose, the *F* statistic was compared to an *F* distribution critical value at a 95% confidence level (*P* = probability = 0.05) (Samuels and Witmer, 2003). Tukey's Honestly Significant Difference (HSD) test was used to test which of the treatments were significantly different from each other. Tukey's statistic value equation $q = \frac{M1-M2}{\sqrt{MSw\ (\frac{1}{n})}}$ was used. In this equation, q is Tukey's statistic, M_1 and M_2 are the two means being tested, MS_w is the mean of squares within the data, and n is the number of samples per treatment group.

3. Results

3.1. Identification and analysis of *RAS* genes

The *RAS1* and *RAS2* genes were identified in the genome of *F. circinatum* wild type strain FSP34 using a BLASTn search with the *F. graminearum RAS1* and *RAS2* gene sequences as a query. This resulted in a hit to FCIRG_05034 and FCIRG_08573 (nucleotide sequence data for this gene are available in the Third Party Annotation Section of the DDBJ/ENA/GenBank databases under the accession number TPA: BK014288), respectively. The *F. circinatum RAS1* gene had 79% identity to that of *F. graminearum* (Expect-value = 0.0). The *RAS1* gene of *F. graminearum* is 892 base pairs (bp) in length, while *F. circinatum RAS1* is 891 bp long. Both genes have three introns at the same positions. The *F. circinatum RAS2* gene had 85% identity to that of *F. graminearum* (i.e., FGSG_10114; Expect-value = 0.0). The *RAS2* gene of *F. graminearum* is 708 bp in length, while its ortholog in *F. circinatum* is 773 bp long. This is due to a 65-bp intron in *RAS2* of *F. circinatum* compared to the *RAS2* of *F. graminearum*, which does not have that intron.

The *F. circinatum* and *F. graminearum RAS2* genes both coded for a protein containing 235 amino acids. Also, they shared 98.7% sequence similarity (differing with only 3 amino acids) and had the same CAAX motif (i.e., CVVL) at their C-terminals. The inferred Ras2 protein sequence further showed conservation (including in the CAAX motif) when compared with that of other *Fusarium* species and fungi such as *C. higginsianum*, *M. oryzae*, *T. reesei*, *A. burnsii*, *A. nidulans*, and *N. crassa* (not shown). However, comparison of the Ras2 protein sequence of *F. circinatum* with its Ras1 sequence showed only 50.2% similarity, while the *F. circinatum* and *F. graminearum* Ras1 protein sequences were highly similar (i.e., both consisting of 217 amino acids, at an identity of 99.5%, and with the CAAX motif of CVLM at the C-terminal). Phylogenetic analysis of the *RAS2* coding sequences clustered *F. circinatum* in a well-supported clade containing other representatives of the *F. fujikuroi* species complex and the closely related *F. oxysporum* species complex, while *F. graminearum* formed part of a separate clade containing other representatives of the *F. sambucinum* species complex (Geiser et al., 2020) (Supplementary figure S1). Within the *RAS2* phylogeny, these two species complexes formed sister clades, with a representative of the *F. solani* species complex at their base (Geiser et al., 2020; O'Donnell et al., 2020) (Supplementary figure S1).

3.2. Knockout and complementation of *RAS2*

The *RAS2* knockout experiment in *F. circinatum* yielded 13 potential transformants that grew on PDA supplemented with hygromycin B. Polymerase Chain Reaction experiments showed that *hygR* was present in nine of these, and in eight of these, *RAS2* was absent. Southern blot experiments showed the integration of only one copy of *hygR* into the genome of some of the latter eight isolates. Of the single-copy *hygR* mutant strains, one (ΔFcras2) was randomly selected for further phenotypic studies. Our PCR assays showed that *RAS2* had been replaced with *hygR* in the genome of ΔFcras2. Complementation of ΔFcras2 with the *RAS2* allele resulted in more than 20 colonies growing on PDA amended with geneticin, although only two of them contained the *RAS2* gene. One of these complements (ΔFcras2C) was selected for use in further phenotypic studies. In other words, all further studies considering the function of *RAS2* were conducted with strains ΔFcras2, ΔFcras2C and the wild type strain FSP34.

3.3. *RAS2* gene deletion affects the morphology and growth of *F. circinatum*

Overall morphological assessments showed differences between the knockout mutant strain ΔFcras2, the complement mutant ΔFcras2C and wild type strains FSP34 (Figure 1). Colonies of the knockout mutant strain appeared smaller than those of the wild type and complement strains (Figure 1A). The wild type and complement mutant strains produced sterile coils, while the knockout mutant strain ΔFcras2 did not (Figure 1B). Aerial conidia of FSP34 were predominantly produced by monophialides and those of the complement and knockout mutant strains were produced by mono- and polyphialides (Figure 1B). All strains produced both micro- and macroconidia, but ΔFcras2 also produced mesoconidia, which were not observed in the other two strains (Figure 1B).

The growth of the knockout mutant strain ΔFcras2 was significantly reduced compared to that of the wild type strain FSP34 and complement knockout strain ΔFcras2C (Figure 2, Table 2). These results were observed following incubation at 25 °C and at 15 °C in both light and darkness. In these experiments, the wild type strain FSP34 always formed the largest colonies. When comparing growth of the mutants under light and darkness at these temperatures, ΔFcras2 and ΔFcras2C always grew faster in the light than in the dark, with significant differences detected for all comparisons except when ΔFcras2C was grown at 15 °C. The wild type strain also grew more rapidly under light than in darkness at 15 °C, but at 25 °C it grew significantly faster in light. Additionally, the shape of the colonies produced by the knockout mutant strain ΔFcras2 were mostly asymmetrical whereas those of the wild type strain FSP34 were more symmetrical at 25 °C (Figure 3). This was evident from the differences between perpendicular colony diameter measurements that were substantially smaller in the case of FSP34 than for Fcras2 and Fcras2C. At 15 °C these differences were much less pronounced, but colonies of the two mutant strains were also more asymmetrical than those of the wild type strain (not shown).

3.4. Conidium production and germination are affected by *RAS2* gene deletion

The deletion of *RAS2* resulted in significant differences between wild type and mutant strains with regards to the production of conidia (Table 3). On average, the knockout mutant ΔFcras2 produced more conidia than either the complement mutant (ΔFcras2C) or the wild type strain (FSP34). However, for both mutant strains, most of these (44-49%) were represented by macroconidia. By

contrast, macroconidia represented only about 3% of the conidia produced by the wild type strain (Table 3).

Examination of conidial germination further showed that germination of conidia was delayed in ΔFcras2 compared to ΔFcras2C and FSP34. This pattern was observed at all time points investigated (24, 48 and 72 hours), although very little conidial germination occurred prior to 24 hours in strain ΔFcras2. Germination of conidia produced by ΔFcras2 resulted in significantly shorter hyphae or germination tubes than in the case of FSP34. However, no differences were observed in the germ tube lengths for the conidia of ΔFcras2C and FSP34 (Table 4). We did not observe notable differences in the amount of germinating conidia in the three strains (data not shown).

3.5. Deletion of *RAS2* reduces perithecial production

To determine whether *RAS2* deletion potentially impacts sexual reproduction in *F. circinatum*, a number of sexual crosses were performed by mating FSP34 and mutant strains with the female fertile MAT2 strain, KS17. Our results showed that the knockout mutant Fcras2 was generally less fertile as a male than the wild type in these crosses (Figure 4). In other words, mating of KS17 as the female parent with ΔFcras2 as the male parent generally resulted in the formation of substantially fewer perithecia (i.e., 12-45 perithecia per plate) than when FSP34 was used as the male parent (i.e., 32-73 perithecia per plate). However, large variations were observed between each set of four replicate plates, which precluded detection of statistically significant differences.

3.6. *RAS2* gene deletion affects the pathogenicity of *F. circinatum*

Six weeks post-inoculation, stems and needles of diseased seedlings inoculated with FSP34 and its mutants were discolored, wilted, and necrotic, while the set of seedlings in the control treatment appeared healthy (Figure 5A). Polymerase Chain Reaction analysis using the species-specific primer set CIRC1A + CIRC4A and DNAs extracted from isolates obtained from the diseased seedling tissue confirmed that the symptoms were caused by *F. circinatum*. Also, presence of amplicons of approximately 300 bp that were generated with primers *ras2*_ProbeF1 + *ras2*_ProbeR1 confirmed presence of the *RAS2* gene only in strains FSP34 and ΔFcras2C. Finally, amplicons of approximately 1000 bp that were generated with primers hy-R and HygF confirmed presence of the hygromycin resistance cassette only in strains ΔFcras2 and ΔFcras2C. These tests

thus proved that the differences observed in disease severity between treatments were due to the presence/absence of the *RAS2* gene in the different inoculum strains.

The lesions caused by FSP34 and the two mutants were all significantly longer than the 1 mm lesions obtained for the control treatment (i.e., inoculation of seedlings with 15% glycerol) (Figure 5B). However, the wild type strain (FSP34) produced significantly longer lesions on the pine seedlings than the knockout mutant ΔFcras2. The lesions induced by ΔFcras2 were on average 8 mm in length, while those caused by FSP34 had an average length of 31 mm. The latter were not significantly different from those produced by the complement strain ΔFcras2C.

4. Discussion

Our findings demonstrated that Ras2 plays an important role in the growth and pathogenicity of *F. circinatum*. The *RAS2* knockout mutant strain caused significantly smaller lesions on *P. patula* seedlings than the wild type and complementation mutant strains. The knockout mutant also grew significantly slower than the wild type and complementation mutant. Such reductions in virulence and growth rate, following deletion of *RAS2*, have also been reported for *F. graminearum* (Bluhm et al., 2007) and *U. maydis* (Lee and Kronstad, 2002). These mutant phenotypes are likely due to Ras2 not being available to relay crucial external stimuli (Pentland et al., 2018), which in turn impedes the activation of transcription factors responsible for the activation of genes involved in growth and virulence. In wild type cells, Ras proteins regulate cellular activities by cycling between GDP-bound and GTP-bound forms, where the GTP-bound Ras protein is active and the GDP-bound form is inactive (Boguski et al., 1993). In *F. graminearum* and *U. maydis*, Ras2 has been shown to regulate virulence and pathogenicity in a MAPK pathway-dependent manner (Lee and Kronstad, 2002; Bluhm et al., 2007). In these fungi and in *C. albicans*, growth is controlled in a similar manner (Lengeler et al., 2000; Lee and Kronstad, 2002; Bluhm et al., 2007). It is therefore likely that Ras2 impacts growth, virulence and pathogenicity in *F. circinatum* in a similar manner.

In *F. circinatum*, Ras2 appears to affect colony development under light and dark conditions. In contrast to the wild type that produced larger colonies in the dark than under light, both the *ras2* knockout and complementation mutants formed larger colonies when grown under light. Other *Fusarium* species have also been reported to have enhanced growth in the dark. These include *F. oxysporum*, *F. sacchari*, *F. globosum*, *F. proliferatum* and *F. solani* (Mohsen et al., 2016). Likewise, fungi such as the black mold *Stachybotrys chartarum*, a grain pathogen, have also been

shown to grow optimally in the dark (Curran, 1980). This has led to the hypothesis that some phytopathogenic fungi are adapted to grow optimally in darker environments because of the limited illumination in the plant tissues that they infect (Isaac, 1995). This could explain why the wild type of *F. circinatum* grows more rapidly in the dark, but there is no plausible molecular explanation for the increased growth exhibited by the *ras2* knockout mutant. Our results do, however, show that Ras2 plays an important role in mycelial growth of *F. circinatum* in the dark. The fact that the complementation mutant (ΔFcras2C) did not regain its ability to grow optimally in the dark is likely because the *RAS2* gene was randomly integrated into the knockout mutant's genome (and not in the same position as it is in the wild type strain). This positioning of the gene outside of its appropriate regulatory network could potentially explain why the phenotype of the complement strain was not restored fully. However, using our unpublished transcriptome data, we found no significant change in *RAS2* expression between the complement mutant and wild type strains, suggesting that the exact mechanism underlying partial restoration of some phenotypes of the complement mutant requires further exploration.

Deletion of *RAS2* impacts the shape of colonies produced by *F. circinatum* when it is grown on agar medium. Colonies produced by the wild type strain were symmetrically circular, while those produced by the knockout mutant were asymmetrical. A similar observation has been made for *F. oxysporum* following the disruption of *fga1* that encodes the alpha subunit of a G-protein (guanine nucleotide-binding protein) (Jain, 2002). G-proteins are GTPases and, together with septins, have been found to affect overall colony shape by regulating cell shape as seen in *U. maydis* (Becht et al., 2006; Mahlert et al., 2006). During vegetative growth and membrane expansion, cell wall deposition is mainly confined to hyphal tips, giving hyphae their elongated shape (Harris, 2012). When an entire network of these hyphae comes together, colonies that are symmetrical and evenly shaped are produced (Harris, 2012). Therefore, Ras2 (also a G protein) may be involved in the regulation of hyphal branching and colony shape in *F. circinatum*. Given that the most symmetrical colonies of the wild type and the most asymmetrical colonies in the *ras2* knockout were observed in the dark, light (or absence thereof) is likely a key stimulus for this regulation.

Deletion of *RAS2* did not cause a reduction in the number of conidia produced by *F. circinatum*, which was in contrast to what has been reported for *N. crassa* (Kana-uchi et al., 1997). Compared to the wild type and complementation mutant, the *F. circinatum ras2* knockout mutant produced significantly more conidia. However, this greater number of conidia was largely attributed to

production of macroconida (and mesoconidia), because macroconidium production on PDA is exceedingly rare in *F. circinatum* and many other *Fusarium* species (Leslie and Summerell, 2006). Thus, deletion of *RAS2* enhanced macroconidium production in *F. circinatum*, as these spores represented almost 50% of the conidia produced by the *ras2* knockout mutant. This is contrary to what has been found in *F. graminearum* where deletion of *RAS2* had no negative impact on the production of macroconidia (Bluhm et al. 2007). In a study on *F. verticillioides*, deletion of *Fvmk1* (encoding a MAPK protein) resulted in an 11% increase in macroconidium production relative to the wild type (Zhang et al., 2011). To the best of our knowledge, the present study is the first to report that deletion of *RAS2* in *Fusarium* causes an increase in the production of macroconidia. Consequently, our results suggest that, like *Fvmk1* in *F. verticillioides*, Ras2 negatively regulates macroconidium production in *F. circinatum*. It would be interesting to understand whether this is also in a MAPK pathway-dependent manner, especially given that the cAMP pathway positively regulates macroconidium production in *F. verticillioides* (Zhang et al., 2011).

Similar to observations in *A. fumigatus* and *F. graminearum*, deletion of *RAS2* in *F. circinatum* significantly impacted conidium germination (Fortwendel, 2005; Bluhm et al., 2007). This was evident from the fact that the conidia produced by the *ras2* knockout mutant of *F. circinatum* had significantly shorter germ tubes than the wild type and the complementation mutant. In *A. fumigatus*, deletion of the *RASB* gene (a homologue of *RAS2*) resulted in decreased conidial germination (Fortwendel, 2005). In *F. graminearum*, deletion of *RAS2* caused conidia to germinate much more slowly than those of the wild type strain (Bluhm et al., 2007). Together with the other shared phenotypes between *ras2* knockout mutants of *F. circinatum* and *F. graminearum*, these findings show that the function of *RAS2* has been maintained across 30 million years of evolution (Geiser et al., 2020). Furthermore, conidium production, viability and germination rate represent possibly important fitness traits that are often important during plant infection and disease establishment (Pringle and Taylor, 2002; Agrios et al., 2005). Elucidation of how *RAS2* regulates these properties in *F. circinatum* would thus be invaluable to ultimately understand and potentially manipulate the molecular ecology of this fungus.

Results of this study suggest that Ras2 is required for male fertility in *F. circinatum*. Sexual crosses involving the *ras2* knockout mutant as a male partner to a compatible female partner, generally led to the production of fewer perithecia production than when the wild type was used as a male partner. This is similar to previous observations with *ras2* deletion mutants of *F. graminearum*

and *U. maydis*. In *U. maydis*, *ras2* mutants were defective in pheromone production, which negatively affected mating (Lee and Kronstad, 2002). In *F. graminearum*, Ras2 regulated perithecium production in a MAPK pathway-dependent manner (Bluhm et al., 2007). This was because deletion of the *RAS2* gene in that fungus impaired the activation of Gpmk1, thereby negatively affecting perithecia production (Bluhm et al., 2007). It would be interesting to examine the extent to which *RAS2* affects the overall process of sexual reproduction in *F. circinatum*. Crosses with the current *ras2* knockout mutant to a *ras2* knockout mutant of the female partner could expand our understanding of the role of Ras2 in the mating system of this fungus.

This study has shown that the deletion of the *RAS2* gene impairs the growth and development of *F. circinatum* as well as its virulence on *P. patula* seedlings. We were also able to demonstrate its role in macroconidium production, and apparently perithecia formation. These data are consistent with other functional characterization studies that have shown that the deletion of *RAS2* leads to developmental defects in some fungi (Lee and Kronstad, 2002; Fortwendel, 2005; Bluhm et al., 2007). In recent literature, *RAS* genes are increasingly becoming important targets for anti-fungal chemicals due to their direct role in pathogenicity and development (Hast et al., 2011; Perfect, 2017). Due to these developments and the fact that *F. circinatum* is of global and economical importance, results of this study will be useful in designing management strategies that target fungal genes for the development of anti-fungal chemicals to combat pine pitch canker.

Acknowledgements

We thank S.L. Slinski for guidance provided during the generation of protoplasts in this study. This work was supported by funds from the following South African institutions and funding bodies: the Tree Protection Cooperative Programme (TPCP), the University of Pretoria, and the National Research Foundation (NRF) and Department of Science and Innovation (DSI) via their DSI-NRF Centre of Excellence in Plant Health Biotechnology (CPHB) and the DSI-NRF South African Research Chairs Initiative (SARChI) Chair in Fungal Genomics.

References

Abascal, F., Zardoya, R., Telford, M.J., 2010. TranslatorX: multiple alignment of nucleotide sequences guided by amino acid translations. Nucl. Acids Res. 38, W7-W13.

Agrios, G., 2005. Plant Pathology, fifth ed. Elsevier Academic Press: Amsterdam, Netherlands.

Barbacid, M. Ras genes. Annu. Rev. Biochem. 1987, 56, 779-827.

Becht, P., König, J., Feldbrügge, M., 2006. The RNA-binding protein Rrm4 is essential for polarity in *Ustilago maydis* and shuttles along microtubules. J. Cell Sci. 119, 4964-4973.

Bluhm, B., Zhao, X., Flaherty, J., Xu, J.R., Dunkle, L., 2007. *RAS2* regulates growth and pathogenesis in *Fusarium graminearum*. Mol. Plant-Microbe Interact. 20, 627-636.

Boguski, M.S., McCormick, F., 1993. Proteins regulating Ras and its relatives. Nature. 366, 643.

Bourne, H.R., Sanders, D.A., McCormick, F., 1991. The GTPase superfamily: conserved structure and molecular mechanism. Nature 349, 117.

Bruno, K.S., Aramayo, R., Minke, P.F., Metzenberg, R.L., Plamann, M., 1996. Loss of growth polarity and mislocalization of septa in a *Neurospora* mutant altered in the regulatory subunit of cAMP-dependent protein kinase. EMBO J. 15, 5772-5782.

Campbell, P.M., Der, C.J., 2004. Oncogenic Ras and its role in tumor cell invasion and metastasis. In Seminars in cancer biology (Elsevier) 105-114.

Carroll, A.M., Sweigard, J.A., Valent, B., 1994. Improved vectors for selecting resistance to hygromycin. Fungal Genet. Rep. 41, 22.

Catlett, N.L., Lee, B.N., Yoder, O., Turgeon, B.G., 2003. Split-marker recombination for efficient targeted deletion of fungal genes. Fungal Genet. Rep. 50, 9-11.

Cox, A.D., Der, C.J., 2010. Ras history: The saga continues. Small GTPases. 1, 2-27.

Curran, P., 1980. Effect of temperature, pH, light and dark on the growth of fungi from Irish coastal waters. Mycologia 72, 350-358.

De Vos, L., van der Nest, M.A., van der Merwe, N.A., Myburg, A.A., Wingfield, M.J., Wingfield, B.D., 2011. Genetic analysis of growth, morphology and pathogenicity in the F1 progeny of an interspecific cross between *Fusarium circinatum* and *Fusarium subglutinans*. Fungal Biol. 115, 902-908.

Desjardins, A.E., Plattner, R.D., Gordon, T.R., 2000. *Gibberella fujikuroi* mating population A and *Fusarium subglutinans* from teosinte species and maize from Mexico and Central America. Mycol. Res. 104, 865-872.

Drenkhan, R., Ganley, B., Martín-García, J., Vahalík, P., Adamson, K., Adamčíková, K., Ahumada, R., Blank, L., Bragança, H. and Capretti, P. et al., 2020. Global geographic distribution and host range of *Fusarium circinatum*, the causal agent of Pine Pitch Canker. Forests 11, 1-38.

Edler, D., Klein, J., Antonelli, A., Silvestro, D., 2020. raxmlGUI 2.0: A graphical interface and toolkit for phylogenetic analyses using RAxML. Methods Ecol. Evol. 00, 1-5.

Eisel, D., Seth, O., Grunewald-Janho, S., Krunchen, D, Ruger, B., 2008. Dig Application Manual: For filter hybridization. Roche Diagnostics GmBH 94.

Fillinger, S., Chaveroche, M.K., Shimizu, K., Keller, N., d'Enfert, C., 2002. cAMP and ras signalling independently control spore germination in the filamentous fungus *Aspergillus nidulans*. Mol. Microbiol. 44, 1001-1016.

Fisher, N.L., Burguess, L.W., Toussoun, T.A., et al., 1982. Carnation leaves as a substrate and for preserving cultures of *Fusarium* species. Phytopathol. *72*, 151-153.

Fortwendel J.R., 2005. *Aspergillus fumigatus* Ras homologs regulate vegetative growth, asexual development and virulence. Europe PMC. 100-132.

Geiser, D.M., Al-Hatmi, A., Aoki, T., Arie, T., Balmas, V., Barnes, I., Bergstrom, G.C., Bhattacharyya, M., Blomquist, C.L., Bowden, R., et al., 2020. Phylogenomic analysis of a 55.1 kb 19-gene dataset resolves a monophyletic *Fusarium* that includes the *Fusarium solani* species complex. Phytopathol. https://doi.org/10.1094/PHYTO-08-20-0330-LE

Gourlay, C.W., Ayscough, K.R., 2006. Actin-induced hyperactivation of the Ras signaling pathway leads to apoptosis in *Saccharomyces cerevisiae*. Mol. Cell. Biol. 26, 6487-6501.

Hallen-Adams, H.E., Cavinder, B.L., Trail, F., 2011. *Fusarium graminearum* from expression analysis to functional assays, in: Xu, J., Bluhm, B.H. (Eds.), Fungal Genomics: Methods and Protocols, Methods in Molecular Biology. Springer, Michigan, pp. 79-101.

Harris, S.D., 2012. Molecular Basis of Morphogenesis in Fungi, in: Perez-Martin, J., Di Pietro, A. (Eds.), Morphogenesis and Pathogenicity in Fungi. Springer, New York, pp. 1-20.

Hast, M.A, Nichols, C.B., Armstrong, S.M, Kelly, S.M., Hellinga, H.W., Alspaugh, J.A., Beese, L.S., 2011. Structures of *Cryptococcus neoformans* protein farnesyltransferase reveal strategies for developing inhibitors that target fungal pathogens. J. Biol. Chem. 286, 35149–35162.

Hatanaka, M., Shimoda, C., 2001. The cyclic AMP/PKA signal pathway is required for initiation of spore germination in *Schizosaccharomyces pombe*. Yeast 18, 207-217.

Hrycyna, C.A., Clark, S.S., 1992. Maturation of Isoprenylated Proteins in *Saccharomyces cerevisiae*. J. Biol. Chem. 267, 10457-10464.

Isaac, S., 1995. Moulds, mildews and other fungi are often found in shaded and dark situations – Is their development influenced by light? Mycologist 1, 41-42.

Jain, S., Akiyama, K., Mae, K., Ohguchi, T., Takata, R., 2002. Targeted disruption of a G protein α subunit gene results in reduced pathogenicity in *Fusarium oxysporum*. Curr. Genet. 41, 407-413.

Kana-uchi, A., Yamashiro, C. T., Tanabe, S., Murayama, T., 1997. A *ras* homologue of *Neurospora crassa* regulates morphology. Mol. Gen. Genet. 254, 427-432.

Katoh, K., Misawa, K., Kuma, K.I., Miyata, T., 2002. MAFFT: a novel method for rapid multiple sequence alignment based on fast Fourier transform. Nucleic Acids Res. 30, 3059-3066.

Krishnankutty, R.K., Kukday, S.S., Castleberry, A.J., Breevoort, S.R., Schmidt, W.K., 2009 Proteolytic processing of certain CaaX motifs can occur in the absence of the Rce1p and Ste24p CaaX proteases. Yeast 26, 451–463.

Kronstad, J., Staben, C., 1997. Mating type in filamentous fungi. Annu. Rev. Genet. 31, 245-276.

Larsson, A., 2014. AliView: a fast and lightweight alignment viewer and editor for large data sets. Bioinformatics 30, 3276-3278.

Lee, N., Kronstad, J.W., 2002. *ras2* controls morphogenesis, pheromone response, and pathogenicity in the fungal pathogen *Ustilago maydis*. Eukaryot. Cell 1, 954-966.

Lengeler, K.B., Davidson, R.C., D'Souza, C., Harashima, T., Shen, W., Wang, P., et al., 2000. Signal transduction cascades regulating fungal development and virulence. Microbiol. Mol. Biol. Rev. 64, 746–785.

Leslie, J., Summerell, B., 2006. The *Fusarium* Laboratory Manual. Blackwell Publishing Ltd, Ioha.

Lowy, D.R., Willumsen B.M., 1993. Function and regulation of *RAS*. Annu. Rev. Biochem. 62, 851-91.

Mahlert, M., Leveleki, L., Hlubek, A., Sandrock, B., Bölker, M., 2006. Rac1 and Cdc42 regulate hyphal growth and cytokinesis in the dimorphic fungus *Ustilago maydis*. Mol. Microbiol. 59, 567-578.

Mohsen, L., Al-Janabi, J.K., Jebor, M.A., 2016. The effect of some environmental conditions on the growth and activity of the external enzymes for five sp. Of *Fusarium*. JUBPAS 24, 630-646.

Mosch, H.U., Roberts, R.L., Fink, G.R., 1996. Ras2 signals via the Cdc42/Ste20/mitogen-activated protein kinase module to induce filamentous growth in *Saccharomyces cerevisiae*. Proc. Natl. Acad. Sci. 93, 5352–5356.

Munoz-Adalia, E.J., Fernández, M., Wingfield, B.D., Diez, J. J., 2018a. In silico annotation of five candidate genes associated with pathogenicity in *Fusarium circinatum*. Forest Pathol. 48, e12417.

Munoz-Adalia, E.J., Cañizares, M.C., Fernández, M., Diez, J. J., García-Pedrajas, M. D., 2018b. The *Fusarium circinatum* gene Fcrho1, encoding a putative Rho1 GTPase, is involved in vegetative growth but dispensable for pathogenic development. Forests 9, e684.

Murray, M.G., Thompson, W.F., 1980. Rapid isolation of high molecular weight plant DNA. Nucleic Acids Res. 8, 4321-4326.

Nelson, P.E., 1981. *Fusarium*: Diseases, Biology and Taxonomy. Pennsylvania State University Press, Pennsylvania.

O'Donnell, K., Rooney, A.P., Proctor, R.H., Brown, D.W., McCormick, S.P., Ward, T.J., Frandsen, R.J., Lysøe, E., Rehner, S.A., Aoki, T. and Robert, V.A., 2013. Phylogenetic analyses of RPB1 and RPB2 support a middle Cretaceous origin for a clade comprising all agriculturally and medically important fusaria. Fungal Genet. Biol. *52*, 20-31.

O'Donnell, K., Al-Hatmi, A.M.S., Aoki, T., Brankovics, B., Cano-Lira, J.F., Coleman, J.J., de Hoog, G.S., di Pietro, A., Frandsen, R.J.N., Geiser, D.M., Gibas, C.F.C., Guarro, J., Kim, H.S., Kistler, H.C., Laraba, I., Leslie, J.F., Lopez-Berges, M.S., Lysøe, E., Meis, J.F., Monod, M.M., Proctor, R.H., Rep, M., Ruiz-Roldan, C., Šišić, A., Stajich, J.E., Steenkamp, E.T., Sumerall, B.A., van der Lee, T.A.J., van Diepeningen, A.D., Verweij, P.E., Waalwijk, C., Ward, T.J., Wickes, B.L., Wiederhold, N.P., Wingfield, M.J., Zhang, N., Zhang, S.X., 2020. No to *Neocosmospora*: Phylogenomic and Practical Reasons for Continued Inclusion of the *Fusarium solani* Species Complex in the Genus *Fusarium*. mSphere 5, 00810-20.

Pentland, D.R., Piper-Brown, E., Mühlschlegel, F.A., Gourlay, C.W., 2018. Ras signalling in pathogenic yeasts. Microb. Cell 5, 63.

Perfect, J.R., 2017. The antifungal pipeline: a reality check. Nat. Rev. Drug. Discov. 16, 603-616.

Pringle, A. and Taylor, J.W., 2002. The fitness of filamentous fungi. Trends Microbiol. *10*, 474-481.

Proctor, R.H., Busman, M., Seo, J.A., Lee, Y.W., Plattner, R.D., 2008. A fumonisin biosynthetic gene cluster in *Fusarium oxysporum* strain O-1890 and the genetic basis for B versus C fumonisin production. Fungal Genet. Biol. 45, 1016-1026.

Sambrook, J., Green M. R., 2012. Molecular cloning: A laboratory manual, fourth ed. Cold Spring Harbor Laboratory Press, New York.

Samuels, M.L., Witmer, J.A., 2003. Statistics for the Life sciences, third ed. Pearson.

Schweigkofler, W., O'Donnell, K., Garbelotto, M., 2004. Detection and quantification of airborne conidia of *Fusarium circinatum*, the causal agent of pine pitch canker, from two California sites by using a real-time PCR approach combined with a simple spore trapping method. Appl. Environ. Microbiol. 70, 3512-3520.

Sokolenko, A. P., Imyanitov, E. N., 2018. Molecular diagnostics in clinical oncology. Front. Mol. Biosci. 5, 76.

Spence, R., Casey, P.J., 2001. Mechanism of catalysis by protein farnesyltransferase, in: Tamanoi, F., Sigman, D. (Eds.), The Enzymes. Academic Press, New York, pp. 1-18.

Steenkamp, E., Coutinho, T., Desjardins, A., Wingfield, B., Marasas, W., Wingfield, M., 2001. *Gibberella fujikuroi* mating population E is associated with maize and teosinte. Mol. Plant Path. 2, 215-221.

Steenkamp, E.T., Makhari, O.M., Coutinho, T.A., Wingfield, B.D., Wingfield, M.J., 2014 Evidence for a new introduction of the pitch canker fungus *Fusarium circinatum* in South Africa. Plant Pathol. *63*, 530-538.

Sun, J., Kale, S.P., Childress, A.M., Pinswasdi, C., Jazwinski, S.M., 1994. Divergent roles of *RAS1* and *RAS2* in yeast longevity. J. Biol. Chem. 269, 18638-18645.

Thevelein, J.M., 1984. Cyclic-AMP content and trehalase activation in vegetative cells and ascospores of yeast. Arch. Microbiol. 138, 64-67.

Toda, T., Uno, I., Ishikawa, T. et al., 1985. In yeast, RAS proteins are controlling elements of adenylate cyclase. Cell 40, 27-36.

Uhl, M.A., Biery, M., Craig, N., Johnson, A.D., 2003. Haploin sufficiency-based large-scale forward genetic analysis of filamentous growth in the diploid human fungal pathogen *C. albicans*. EMBO J. 22, 2668-2678.

Van Wyk, S., Wingfield, B.D., De Vos, L., Santana, Q.C., Van der Merwe, N.A., Steenkamp, E. T., 2018. Multiple independent origins for a subtelomeric locus associated with growth rate in *Fusarium circinatum*. IMA fungus 9, 27-36.

Waugh, M.S., Nichols, C.B., DeCesare, C.M., Cox, G.M., Heitman, J., Alspaugh, J.A., 2002. Ras1 and Ras2 contribute shared and unique roles in physiology and virulence of *Cryptococcus neoformans*. Microbiol. 148, 191-201.

Wiemann, P., Sieber, C.M.K., von Bargen, K.W., Studt, L., Niehaus, E.M., et al., 2013. Deciphering the Cryptic Genome: Genome-wide Analyses of the Rice Pathogen *Fusarium fujikuroi* Reveal Complex Regulation of Secondary Metabolism and Novel Metabolites. PloS Pathog. 9, e1003475.

Wingfield, B.D., Steenkamp, E.T., Santana, Q.C., Coetzee, M., Bam S., et al., 2012. First fungal genome sequence from Africa: a preliminary analysis. S. Afr. J. Sci. 108, 1-9.

Wingfield, M., Hammerbacher, A., Ganley, R., Steenkamp, E., Gordon, T., Wingfield, B., Coutinho, T., 2008. Pitch canker caused by *Fusarium circinatum*–a growing threat to pine plantations and forests worldwide. Australas. Plant Path. 37, 319-334.

Young, S.G., Ambroziak, P., Kim, E., Clarke, S., 2001. Postisoprenylation protein processing: CXXX CaaX endoproteases and isoprenylcysteine carboxyl methyltransferase, in: Tamanoi, F., Sigman, D.S. (Eds.), The Enzymes. Academic Press, New York, pp. 155-213.

Zhang Y., Choi Y., Zou X., Xu J., 2011. The FvMK1 mitogen-activated protein kinase gene regulates conidiation, pathogenesis, and fumonisin production in *Fusarium verticillioides*. Fungal Genet. Biol. 48, 71-79.

Zhou, X., Heyer, C., Choi, Y.E., Mehrabi, R., Xu, J.R., 2010. The CID1 cyclin C-like gene is important for plant infection in *Fusarium graminearum*. Fungal Genet. Biol. 47, 143-151.

Zhou, X., Zhao, X., Xue, C., Dai, Y., Xu, J.R., 2014. Bypassing both surface attachment and surface recognition requirements for appressorium formation by overactive Ras signaling in *Magnaporthe oryzae*. Mol. Plant Microbe Interact. 27, 996-1004.

Zhu, Y., Fang, H.M., Wang, Y.M., Zeng, G.S., Zheng, X.D., Wang, Y., 2009. Ras1 and Ras2 play antagonistic roles in regulating cellular cAMP level, stationary-phase entry and stress response in *Candida albicans*. Mol. Microbiol. 74, 862-875.

Tables

Table 1. List of primers used in this study [1].

Primer name	Sequence (5' to 3')	References
*Ras2*U F1	ATTTAAAGTCCACTGGCAGG	This study
*Ras2*U R1	ACTTATTCAGGCGTAGCAACCAGGCAGTTAAGAG GAGGAAAATGAGG	This study
*Ras2*Dw F1	TCAGCATCTTTTACTTTCACCAGCGGAAGAAAGA CGACCCAAGC	This study
*Ras2*Dw R1	CTGATCCCCCTTAAAGAACC	This study
HygF	AACGCTGGTGAAAGTAAAAGATGCTG	This study
HygR	ACGCCTGGTTGCTACGCCTGAATAAGT	This study
hyR	GTATTGACCGATTCCTTGCGGTCCGAA	Zhou et al., 2010
ygF	GATGTAGGAGGGCGTGGATATGTCCT	Zhou et al., 2010
*ras2*F	TACCACACACTT	This study
*ras2*R	TTGGTGGTTCTG	This study
*ras2*_probeF1	CTGGCCGAATGGTGTTAT	This study
*ras2*_ProbeR1	GCCATCACGAATCCATTG	This study
*ras2*left_F1	CGATCTTTACTTTCCTTTCC	This study
*ras2*right_R1	TTCAGCATTCCCCATCCA	This study
Hyg-int-R	CGGCCGTCTGGACCGATGGCTGTGTA	This study
*ras2*allele_F1	TACTCACCTGACACGACTC	This study
*ras2*allele_R	CTCCAAATAATAGCCACAAC	This study
Not_1F_rp619	CTGTTGTGGCTATTATTTGGAGCATGCGGCCGCAT GCCAGTTG	This study
Not_1R_rp620	CATGCGGCCGCAGAGTAAAG	This study
TrpC_Probe_F	CAGATATAGTTCCCGGAG	This study
TrpC_Probe_R	GGATTGATGAAATCAACG	This study
CIRC1A	CTTGGCTCGAGAAGGG	Schweigkofler et al., 2004
CIRC4A	ACCTACCCTACACCTCTCACT	Schweigkofler et al., 2004

[1] See Supplementary file S1 for PCR cycling conditions employed for all primer pairs utilized in this study.

Table 2. Average colony diameter of the three *F. circinatum* strains after seven days of incubation at 25 °C and 15 °C on PDA medium under light and darkness.

Strain	Incubation temperature	Colony diameter (mm) of week-old cultures [1]		Statistical difference in growth under light vs darkness [2]
		Light	Dark	
ΔFcras2	25 °C	57.3 (0.63)*	53.3 (0.58)*	Significant
ΔFcras2C		69.2 (0.76)	57.8 (0.58)*	Significant
FSP34		71.3 (0.27)	73.3 (0.36)	Significant
ΔFcras2	15 °C	36.2 (0.34)*	33.7 (0.39)*	Significant
ΔFcras2C		42.8 (0.43)	42.4 (0.60)	Not significant
FSP34		48.5 (0.26)	43.9 (0.27)	Significant

[1] Values are the average for six replicates per strain, and the Standard Error (expressed in mm) values are shown in brackets. Asterisks indicate values that differ statistically ($P \leq 0.05$) from that of the wild type strain (FSP34) under a specific set of growth conditions.

[2] Statistical significance was tested ($P \leq 0.05$) between growth in light and darkness, using six replicates for each strain at each temperature.

Table 3. Conidial production by the *F. circinatum* wild type and mutant strains after 10 days of incubation at 25°C, under light on PDA medium.

Strain	**Total number of micro- and macroconidia produced (x10^6 spores/ml)** [1]	**Proportion of macroconidia produced (%)** [2]
ΔFcras2	8.48 (0.52) *	48.54 (2.52) *
ΔFcras2C	5.35 (0.59) *	44.74 (3.95) *
FSP34	3.20 (0.47)	3.25 (1.15)

[1] Values are the average for three replicates per strain, and the Standard Error (expressed as a factor of 10^6 spores/ml) values are shown in brackets. Asterisks indicate values that differ statistically ($P \leq 0.05$) from that of the wild type strain, FSP34.

[2] Values represent the average for three replicates per strain. The Standard Error, expressed as percentages, values are shown in brackets. Asterisks show percentages that differ statistically ($P \leq 0.05$) from that of the wild type strain (FSP34).

Table 4: Germination of *F. circinatum* strains at the 24, 48 and 72-hour time points.

Strain	**Germ tube length (µm)** [1]		
	24 h	48 h	72 h
Δ Fcras2	7.7 (0.95) *	24.7 (9.06)*	25.6 (4.35)*
Δ Fcras2C	44.3 (6.39)	125.7 (2.85)	184.3 (31.49)
FSP34	86.6 (20.83)	96.0 (6.85)	133.1 (0.95)

[1] Values are the mean length of the germ tubes/hyphae that emerged from conidia for three replicates per strain, and the Standard Error (expressed in µm) values are shown in brackets. Asterisks indicate values that differ statistically ($P \leq 0.05$) from that of the wild type strain, FSP34.

Figures

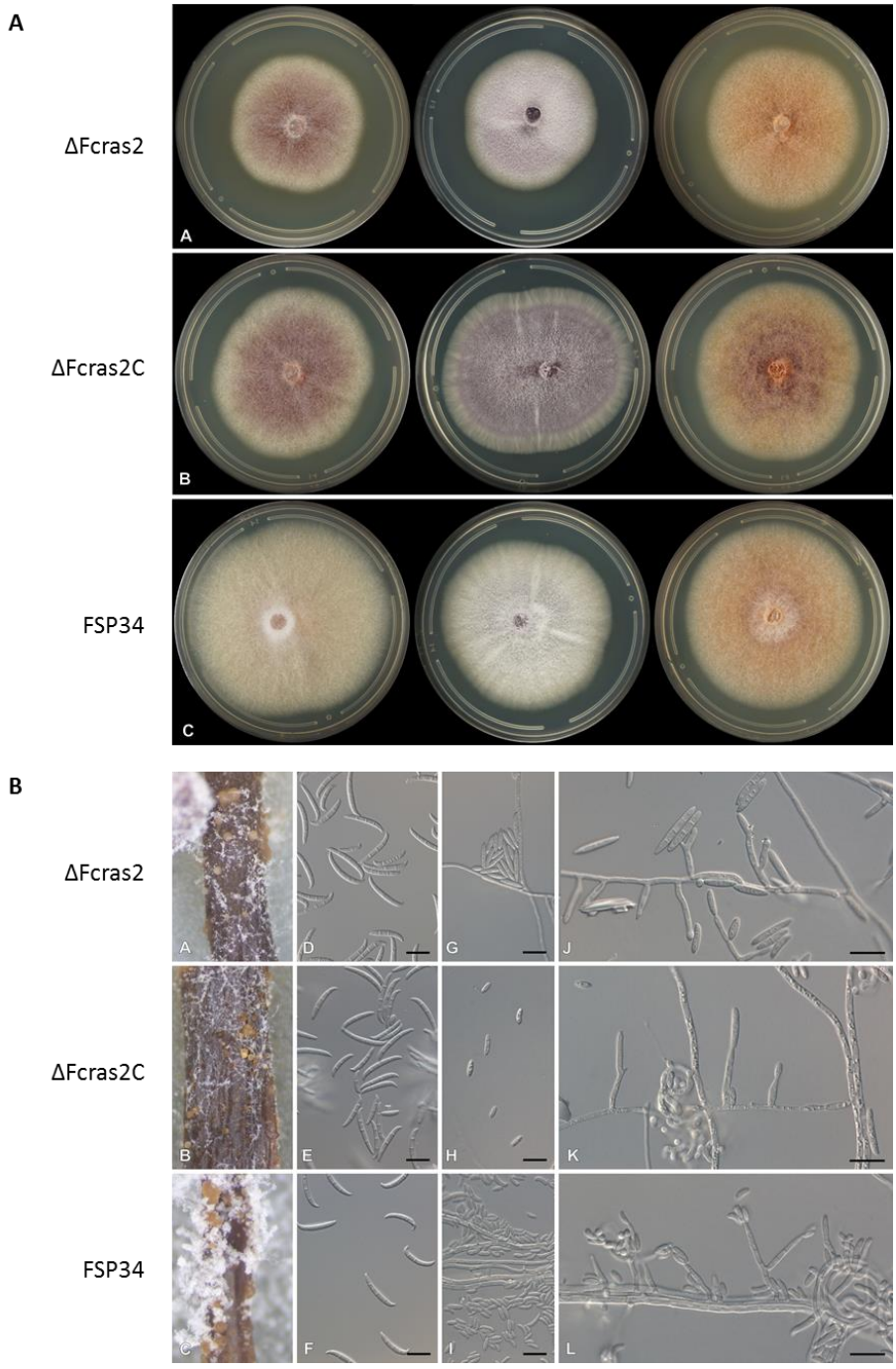

Figure 1. A. Colony morphology of the Knockout mutant strain ΔFcras2 (A), Complement mutant strain ΔFcras2C (B) and Wild type strain FSP34 (C) on PDA after seven days of incubation at 24 °C in the dark, light and near-UV light, respectively. **B.** Sporodochia of ΔFcras2, ΔFcras2C and FSP34 on carnation leaves, A-C respectively. D-F: Sporodochial conidia (macroconidia) of ΔFcras2, ΔFcras2C and FSP34, respectively. G-I: Aerial conidia for of ΔFcras2, ΔFcras2C and FSP34, respectively. J-L: Aerial conidiophores for of ΔFcras2, ΔFcras2C and FSP34, respectively.

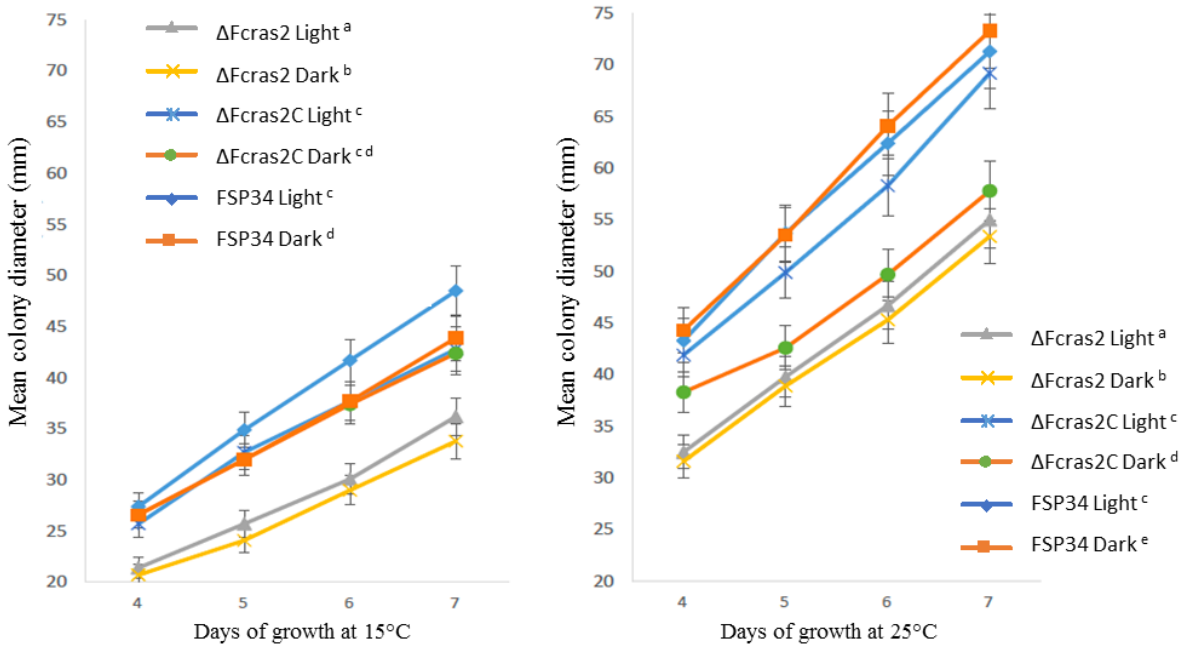

Figure 2. Daily (day four to seven) growth of ΔFcras2, ΔFcras2C and FSP34 at 15 °C and 25 °C under light and dark conditions. Statistical significance between the three strains was tested at $P \leq 0.05$ using six replicates per strain. Strains with different letters show significant difference, while those with the same letter were not significantly different.

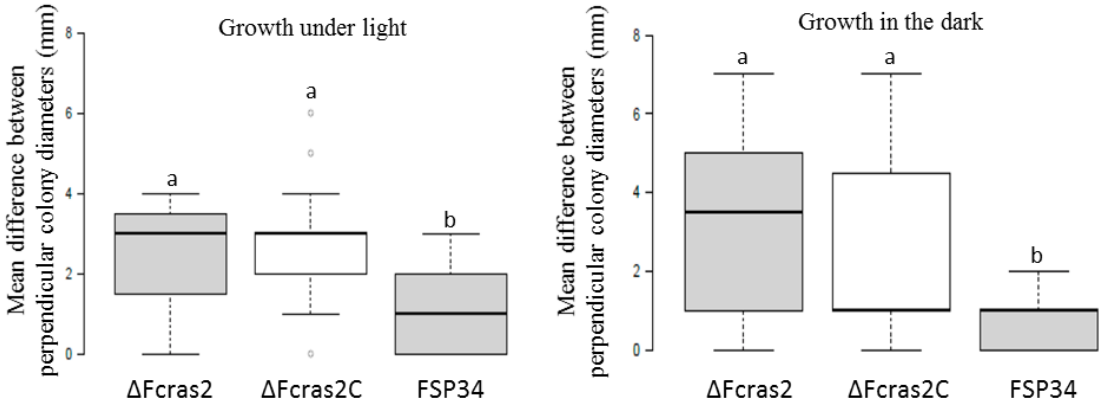

Figure 3. Symmetry of ΔFcras2, ΔFcras2C and FSP34 colonies under light and in the dark at 25 °C. Bottom and top whiskers represent the 1st and 4th quartiles (Q1 and Q4) of the data, respectively. Points outside whiskers represent outliers. Boxes bound the interquartile range (Q2 and Q3) and the solid line in boxes show the median. Wider boxes illustrate asymmetrical colonies whereas narrow and clear boxes display symmetrical colonies. Statistical significance was tested at $P \leq 0.05$ using six replicates per strain. Boxplots with different letters show significant difference, while those with the same letter were not significantly different. Boxplots were constructed using the online tool at http://shiny.chemgrid.org/boxplotr/.

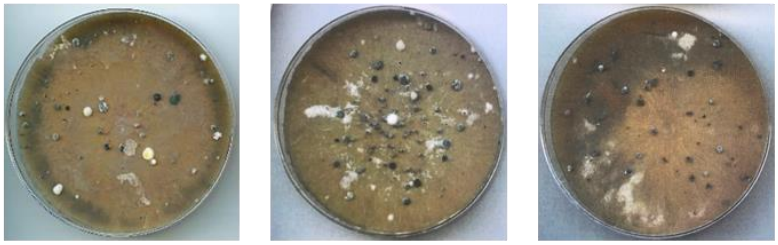

	ΔFcras2 x KS17	ΔFcras2C x KS17	FSP34 x KS17
Replicate 1	*	**	**
Replicate 2	*	**	**
Replicate 3	**	**	**
Replicate 4	**	***	***

<29 perithecia/plate; **30-59 perithecia/plate; *>60 perithecia/plate*

Figure 4. Perithecial production in ΔFcras2, ΔFcras2C and FSP34 on carrot agar. Isolate KS17 was used as a female for these crosses. The crosses were replicated four times for each strain, and these are shown as replicate one to four in the figure. The symbol + is used to indicate the amount of perithecia produced in each cross (+ indicates 0-29 perithecia. ++ indicates 30-59 perithecia. +++ indicates 60-89 perithecia).

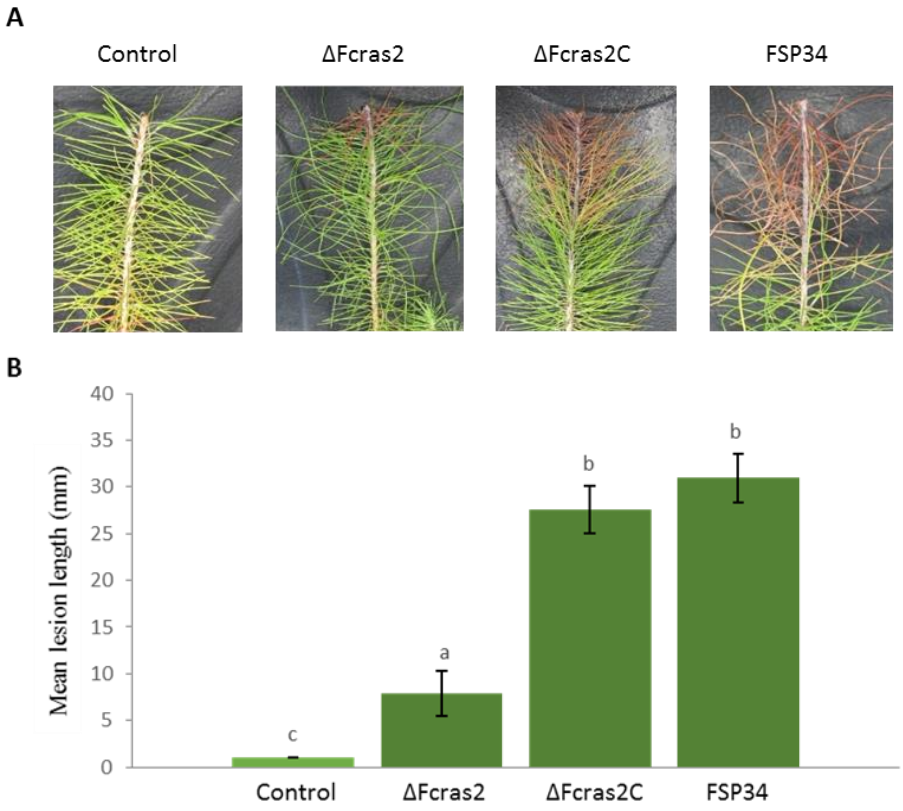

Figure 5. The pathogenicity of ΔFcras2, ΔFcras2C and FSP34 on *P. patula*. **A.** Lesions produced on *P. patula* seedlings after inoculation with 15% glycerol, ΔFcras2, ΔFcras2C and FSP34. **B.** Mean lesion lengths caused by inoculations of *P. patula* with 15% glycerol, ΔFcras2, ΔFcras2C and FSP34. Inoculations were performed on forty seedlings per strain, and statistical significance was tested at $P \leq 0.05$. Means with different error bar letters are significantly different from each other, and those with the same letters are not significantly different from each other.

Supplementary files

Supplementary file S1. Gene knockout and transformation protocol for *Fusarium circinatum* using split-marker constructs.

Detailed protocols and procedures

GENOMIC DNA EXTRACTION

Adapted from Murray and Thompson (1980)

Notes:

i) Handle Phenol and chloroform with care and work in a fume hood

ii) Room temperature (RT) = 22-25 °C.

1. Grow fungal strains on half strength Potato Dextrose Agar (PDA; Becton, Dickinson and Company, Franklin Lakes, NJ, USA) at 25 °C for seven days.

2. Cut a small agar block from the culture and inoculate Difco Potato Dextrose Broth (PDB; Becton, Dickinson and Company, Franklin Lakes, NJ, USA).

3. Incubate with shaking at approximately 200 rpm for seven days at RT.

4. Filter the culture through two layers of Miracloth and freeze dry.

5. Label and unscrew an empty sterile 1.5-ml screw cap tube and place a metal bead in it using sterile tweezers.

6. Using the tweezers, pinch and place about 50-100 mg of the freeze-dried mycelia into the tube.

7. Add 700 µl of TES buffer and homogenize until mycelia are completely ground and then incubate in a deep freezer (−70 to −80 °C) for 10 min, followed by incubation in a water bath at 60 °C for 1 hour.

    - TES buffer: 100 mM Tris-HCL [pH 8.0]; 10 mM EDTA (ethylenediaminetetraacetic acid) [pH 8.0]; and 2 % [w/v] SDS (sodium dodecyl sulfate)

8. Add 230 µl volume CTAB:NaCl mixture, vortex and incubate in a water bath at 65 °C for 10 min.

    - CTAB:NaCl mixture: 2.5 % [w/v] CTAB (cetyltrimethylammonium bromide) and 3.75 M NaCl. These two constituents are made up separately and then combined before use.

9. Add 500 µl of 1:1 [v/v] phenol-chloroform, mix by vortexing, and centrifuge at 11 000 x g for 45 min at RT.

10. Carefully transfer 600 µl of the aqueous (top) phase to a labeled sterile empty tube 1.5-ml Eppendorf tube.

11. Add RNase A 6 µl (Thermo Fisher Scientific, Vilnius, Lithuania) and incubate at 37 °C for 1 hour to eliminate contaminating RNAs.

12. Repeat steps 9-10, but centrifuge for 20 min at RT.

13. Add 300 µl of chloroform, mix by vortexing and centrifuge for 10 min at RT.

14. Carefully transfer the aqueous phase to a new labeled tube 1.5-ml Eppendorf tube.

15. Precipitate DNA by adding 2 X aqueous phase volume of ice-cold 100% ethanol and incubate in a −20 °C freezer overnight.

16. Pellet DNA by centrifugation at 13 200 x g for 30 min at 4 °C.

17. After removing the supernatant, wash pellet by adding 500 µl of 70 % ethanol followed by centrifugation at 13 200 x g for 10 min at 4 °C.

18. Repeat steps 17.

19. Briefly centrifuge (for about 30 sec) to and remove the excess ethanol using a micropipette.

20. Open the tube and place it under a laminar flow until the pellet is dry.

21. Dissolve the pellet by adding 50 µl sterile distilled water and incubating the tube on the laboratory bench for about 30 min.

22. Check the integrity, quality and quantity of the DNA and then store it at −20 °C for later use or use immediately.

OVERVIEW OF THE SPLIT-MARKER APPROACH EMPLOYED

Replacement of *RAS2* in the genome of *F. circinatum* wild type (FSP34) using the split-marker approach (see the diagram below). The *hygR* gene is a hygromycin resistance gene from *Escherichia coli* plasmid pCB1004.

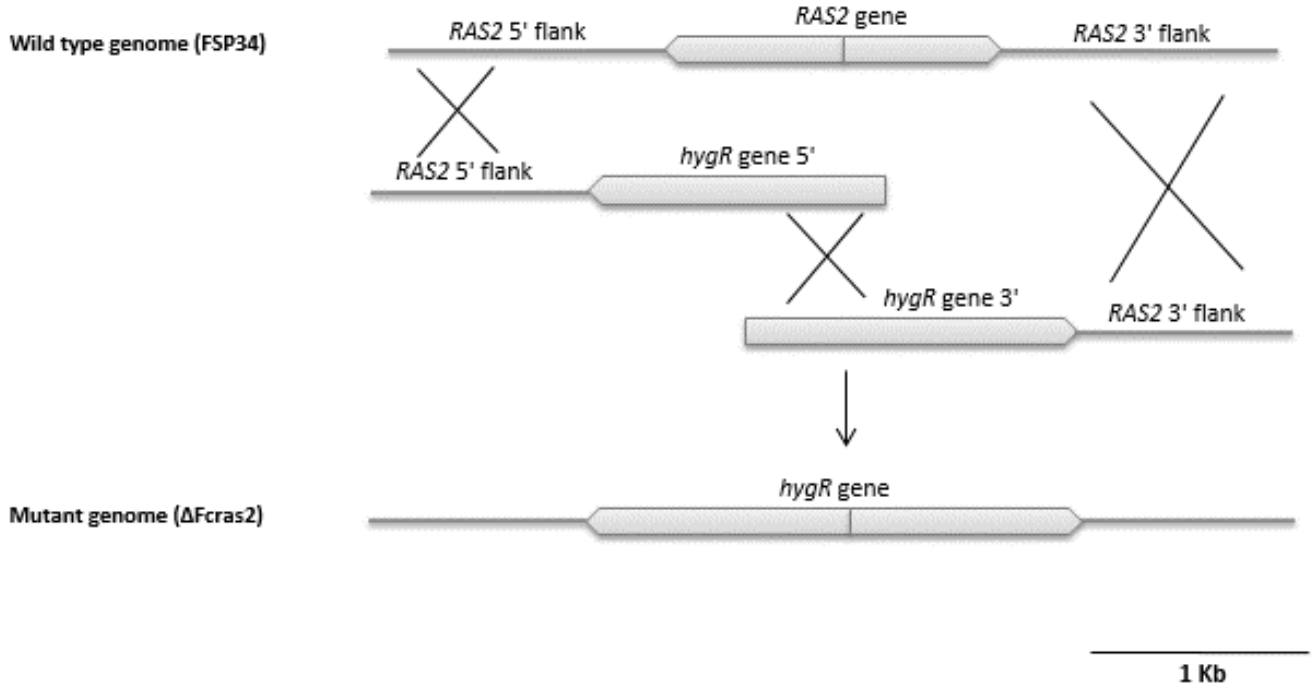

KNOCKOUT AND COMPLEMENT CONSTRUCTS GENERATION

Adapted from Catlett et al. (2003)

Notes:

i) All Polymerase Chain Reactions (PCRs) were performed following manufacturers' protocols (see Appendix A) together with variable melting temperatures corresponding to primers used.

ii) Primer sequences are provided in Table 1 of our research paper.

iii) Unless otherwise stated, primers were used at 10 mM concentration.

iv) About 100-200 ng of template DNA was used in PCR experiments.

Knockout constructs (split-marker constructs)

1. In two independent PCRs, amplify 5' flanking region of the *RAS2* gene from the genomic DNA of *F. circinatum* wild type strain FSP34 using the Phusion High-Fidelity Master Mix (Thermo Fisher Scientific, Vilnius, Lithuania) and primer set *Ras2*U F1 + *Ras2*U R1, the 3' flanking region of the *RAS2* gene using primer set *Ras2*Dw F1 + *Ras2*Dw R1.

2. In two independent PCRs, produce two overlapping amplicons of the hygromycin resistance gene (*hygR*) using the Phusion High-Fidelity Master Mix and primer sets HygR + ygF and HygF + hyR directly on *Escherichia coli* colonies carrying plasmid pCB1004 (Carroll et al., 1994).

3. Fuse the 5' *RAS2* flank to the first *hygR* amplicon using the LongAmp® *Taq* 2X Master Mix (New England BioLabs, Ipswich, MA, USA) and primer set *Ras2*U F1 + ygF.

4. Fuse the 3' *RAS2* flank to the second *hygR* amplicon using the LongAmp® *Taq* 2X Master Mix and primer set *Ras2*Dw R1 and hyR.

Complementation constructs (random integration construct)

1. Amplify the *RAS2* allele from the genomic DNA of *F. circinatum* wild type strain FSP34 (the full gene sequence including the promoter and terminator regions) using Expand™ Long Range dNTPack (Sigma-Aldrich, Mannheim, Germany) with primer set *ras2*allele_F1 + *ras2*allele_R.

2. Amplify the geneticin resistance cassette (i.e., *nptII*; includes promoter and terminator) directly from *E. coli* colonies carrying plasmid pGEN-Not1 (Proctor et al., 2008) using Phusion High-Fidelity Master Mix and the primer set Not_1F_rp619 + Not_1R_rp620.

3. Fuse the *RAS2* allele amplicon to geneticin resistance cassette using LongAmp® *Taq* 2X Master Mix and primers *ras2*allele_F1 and Not_1R_rp620.

PROTOPLASTING AND TRANSFORMATION

Adapted from Hallen-Adams et al. (2011)

Notes:

i) All experiments should be performed in a Biosafety/sterile hood.

ii) Room temperature (RT) = 22 – 25 °C.

1. Inoculate 100 ml of CMC solution in a 250-ml Erlenmeyer flask with an agar block of mycelia or an equivalent amount grown from Potato Dextrose Broth. Incubate for five days on a rotary shaker table at 25 °C at 250 rpm. Prepare two CMC flasks per culture.

- Carboxymethyl cellulose medium (CMC): dissolve 15 g of carboxymethyl cellulose sodium salt (Sigma-Aldrich, St. Louis, MO), 1 g NH_4NO_3, 1 g KH_2PO_4, 0.5 g $MgSO_4 \cdot 7H_2O$, and 1 g yeast extract in 1 l water (carboxymethyl cellulose dissolves slowly, and will need to be heated and stirred). Aliquot 100 ml apiece into 250-ml flasks; autoclave for 20 min.

2. Filter the culture from the two CMC flasks through a sterile Miracloth in a glass funnel into a 50-ml Falcon tube. Rinse with sterile dH_2O. Spin at RT at 4 000 x g in an appropriate rotor for 10 min.

3. Discard all but 2-4 ml of the supernatant and resuspend conidia. Place conidia in 100 ml of YEPD broth in a 250-ml Erlenmeyer flask, and grow in a rotary shaker for 10-12 h at 25 °C at 175 rpm. Timing is critical here as older cultures do not digest well into protoplasts.

    - YEPD: 3 g yeast extract (Difco Laboratories, Detroit, MI); 10 g Bacto peptone (Difco Laboratories, Detroit, MI); 20 g dextrose (anhydrous; = d-glucose); dissolve in 1 ml water, aliquot 100 ml apiece into 250-ml flasks and autoclave.

4. Filter culture from each YEPD flask, through a sterile Miracloth, in a Büchner funnel under vacuum (can use regular glass funnels without vacuum) and collect the mycelial mat. Rinse the mat with sterile dH_2O and allow the water to drain. Place the mat back into the flask from where it was obtained or into a new sterile 250-ml Erlenmeyer flask if needed. Add 30 ml of Protoplasting buffer to each flask (should have already been prepared and filter sterilized).

    - Protoplasting buffer: To 20 ml of 1.2 M KCl, add 500 mg Driselase from Basidiomycetes (Sigma Chemical Co., St. Louis; D8037); 1 mg Chitinase from *Streptomyces griseus* (Sigma Chemical Co., St. Louis; C6137); and 100 mg lysing enzyme from *Trichoderma harzianum* (Sigma Chemical Co., St. Louis; L1412); stir for 30 min and filter sterilize through a 0.45-mm Millex-HA filter (Millipore, Bedford, MA).

5. Digest for 1.5 h on a rotary shaker table at 30 °C at 80 rpm. Check for protoplasts after the first 45 min and then after every 15-20 min.

    - Protoplasts are spherical, while intact *Fusarium* cells occur in a variety of shapes, but are not spherical. Under the microscope, many round protoplasts should be present in the field of view when observed with a 40× objective; if only a few protoplasts are present, continue the reaction. After 2½ h, further incubation will not be of benefit.

6. Filter the digestion mixture through two-three layers of sterile Miracloth into 50-ml Falcon tubes. The filtrate should be turbulent due to the presence of protoplasts. Centrifuge at RT at 3 000 x g for 5 min in an appropriate rotor. Protoplasts are very fragile. Treat them gently.

7. Discard the supernatant and gently resuspend protoplasts in 10 ml of STC Buffer using wide orifice glass pipettes. Spin the solution at 3 000 x g for 5 min.

    - STC buffer: 1.2 M sorbitol; 10 mM Tris–HCl, pH 8.0; 50 mM CaCl2; autoclave. Use 4.1 ml per transformation reaction.

8. Discard the supernatant and gently resuspend protoplasts in 1 ml of STC Buffer using wide orifice pipette tips. Transfer to a 2-ml tube. Spin in a microcentrifuge at RT at 3 500 x g for 5 min. Repeat once.

9. Resuspend protoplasts in a final volume of 200-300 µl. Quantify using a hemocytometer; a good preparation can be expected to yield 106-108 protoplasts/ml. This is your protoplast suspension. Make the following mixture in a 50-ml Falcon tube: 100 µl – protoplast suspension, 100 µl – STC Buffer, 50 µl of 30 % PEG Solution, and PCR product (0.25-0.5 µg for each split-marker constructs). Extra protoplasts can be frozen for later use: add DMSO to 7% volume, aliquot, and freeze at − 80°C. When using frozen stocks, spin to collect and resuspend in STC at least twice before use. Start at step 9.

    - 30% PEG solution: 30% polyethylene glycol (PEG) 8000 (Sigma-Aldrich, St. Louis, MO; P2139); 10 mM Tris–HCl, pH 8.0; 50 mM CaCl2; filter sterilize using a 0.45-µm Millex-HA filter (Millipore, Bedford, MA). Always prepare fresh on the day of use. 2.05 ml is used per reaction.

10. Add 2 ml of 30 % PEG solution and incubate for 5 min.

11. Add 4 ml of STC Buffer and gently mix by inversion.

12. Pour reactions into cooled Regeneration Medium (RM): 9 ml RM per transformation reaction. Incubate at RT overnight (about 18 hours) with agitation at 75 rpm to regenerate protoplasts.

    - Regeneration medium (RM): 135.5 g sucrose in 500 ml water; heat to dissolve, then add 0.5 g yeast extract; 0.5 g N-Z-Amine AS (Sigma-Aldrich, St. Louis, MO), autoclave.

13. Pour 1 ml reactions into 90 mm petri dishes.

14. Pour 10 ml cooled RM agar amended with 150 µg/ml hygromycin B into each petri dish and mix by gently swirling. *RM must be cool enough to touch and hold to the inside of your arm else protoplasts will be killed!* If the medium feels hot, allow it to cool more. The agar should be close to solidifying.

    - RM agar: 135.5 g sucrose in 500 ml water; heat to dissolve, then add 0.5 g yeast extract; 0.5 g N-Z-Amine AS (Sigma-Aldrich, St. Louis, MO; N4517); and 3.72 g agar; autoclave. Keep regeneration medium warm (55-65 °C) and liquid until use.

    - For complementation experiments, amend RM agar with 120 ug/ml of geneticin (G-418 sulfate; Thermo Fisher Scientific, Rockford, IL, USA).

15. Incubate at RT in the dark until protoplasts emerge (usually for 10-14 days).

16. Screen for putative transformants by transferring emerged protoplasts to half strength PDA containing 150 µg/ml hygromycin and incubate at RT in the dark until protoplasts grow (usually for 5-7 days).

    - Half strength PDA: 20 g PDA (Becton, Dickinson and Company, Franklin Lakes, NJ, USA) and 5 g agar in 1 l water; dissolve and autoclave.

- For complementation experiments, augment PDA with 120 ug/ml of geneticin.

SCREENING FOR TRANSFORMANTS

Screening of knockout transformants

1. In two independent PCRs, use LongAmp® *Taq* 2X Master Mix and primer sets *ras*2F + *ras*2R and HygF + HygR to confirm the presence of the *RAS2* and *hygR* genes, respectively directly on the mycelia of putative transformants.
2. Perform a PCR using LongAmp® *Taq* 2X Master Mix and *ras2*left_F1 and *ras2*right_R1 to test for the replacement of *RAS2* by the *hygR* genes in mutants.
3. Screen for copy number of the *hygR* construct in genomes of knockout mutants using Southern Blot capillary analysis. See Appendix B of the protocol.

Screening of complementation transformants

1. Perform colony PCR using LongAmp® *Taq* 2X Master Mix and primer set *Ras2*_probeF1 + *Ras2*_probeR1 to test for the presence of the *RAS2* gene in complementation transformants,
2. Perform the Southern Blot analysis described above to test for copy number of the *ras* gene in genomes of the complementation mutants.

APPENDIX A

CYCLING CONDITIONS FOR THE VARIOUS DNA POLYMERASES AND/OR MASTER MIXES

Phusion High Fidelity Master Mix (Thermo Fisher Scientific, Vilnius, Lithuania)

Step	Temperature	Time	Cycles
Initial Denaturation	98 °C	30 seconds	1
Denaturation	98 °C	5-10 seconds	25-35
Annealing	variable *	10-30 seconds	
Extension	72 °C	15-30 seconds per kb	
Final Extension	72 °C	5-10 minutes	1
Hold	4 °C	∞	

* *Ras2*U F1 + *Ras2*U R1 = 65 °C; *Ras2*Dw F1 + *Ras2*Dw R1 = 65 °C; HygR + ygF = 60 °C and HygF + hyR = 60 °C; Not_1F_rp619 + Not_1R_rp620 = 60 °C; HygF + HygR = 55 °C.

LongAmp® *Taq* 2X Master Mix (New England BioLabs, Ipswich, MA, USA)

Step	Temperature	Time	Cycles
Initial Denaturation	94 °C	30 seconds	1
Denaturation	94 °C	10-30 seconds	30
Annealing	variable *	15-60 seconds	
Extension	65 °C	50 seconds per kb	
Final Extension	65 °C	10 minutes	1
Hold	4-10 °C	hold	

* *Ras2*U F1 + ygF = 65 °C; *Ras2*Dw R1 and hyR = 65 °C; *ras2*allele_F1 and Not_1R_rp620 = 60 °C; *ras*2F + *ras*2R = 53 °C; *Ras2*_probeF1 + *Ras2*_probeR1 = 53 °C; *ras2*left_F1 and *ras2*right_R1 = 50 °C.

Expand™ Long Range dNTPack (Sigma-Aldrich, Mannheim, Germany)

Step	Temperature	Time	Cycles
Initial Denaturation	92 °C	2 minutes	1
Denaturation	94 °C	10 seconds	10
Annealing	60 °C	15 seconds	
Extension	68 °C	60 seconds per kb	
Denaturation	94 °C	10 seconds	15-25
Annealing	60 °C	15 seconds	
Extension	68 °C	60 seconds per kb + 20 seconds cycle for each successive cycle	
Final Extension	68 °C	Up to 7 minutes	1
Hold	4-10 °C	∞	

Taq DNA polymerase and reaction buffer (Roche Diagnostics, Mannheim Germany) *

Step	Temperature	Time	Cycles
Initial Denaturation	98 °C	30 seconds	1
Denaturation	98 °C	30 seconds	30
Annealing	60 °C	30 seconds	
Extension	72 °C	30 seconds	
Final Extension	72 °C	10 minutes	1
Hold	4 °C	∞	

***** This polymerase was used using primers CIRC1A and CIRC4A, and the reaction mixture contained 2.5 mM each dNTP, 25 mM, $MgCl_2$, 10 mM each primer, 50 ng/mL template DNA, 0. 03 U/ mL *Taq* DNA polymerase and reaction buffer.

APPENDIX B
SOUTHERN BLOT ANALYSIS PROTOCOL

Adapted from Sambrook and Green (2012), and Eisel et al. (2008)

1. Synthesize DIG-labeled probe (about 300 bp in this study)

Component	Full volume (50 µl reaction)	Half volume (25 µl reaction)*
H_20	34.25 µl	17.125 µl
Buffer (with $MgCl_2$)	5 µl	2.5 µl
DIG Mix	5 µl	2.5 µl
Primer 1 (10 mM)	1.5 µl	0.75 µl
Primer 2 (10 mM)	1.5 µl	0.75 µl
Enzyme (High fidelity)	0.75 µl	0.375 µl
Template DNA (10 ng/µl)	2 µl	1 µl

*Half volumes were used during the current study, and the LongAmp® *Taq* 2X Master Mix was used together with primer set HygR + Hyg-int-R with an annealing temperature of 66 °C.

- Include non-labeled control (replace DIG mix with normal dNTPs mix).
- Use no more than 100 pg of plasmid DNA or 1-50 ng (10 ng used in this study) of genomic DNA as template for PCR (optimal amount of template is 10 pg for plasmid DNA and 10 ng for genomic DNA). It is better to use plasmid as a template for probe synthesis if available.
- Perform PCR for 35 to 40 cycles. Check for specificity and efficiency of PCR product by loading 2 µl on Agarose gel. DIG-labeled PCR product should run a bit slower when compared with the non-labeled product.
- There is no need to purify the DIG-labeled PCR product. DIG-labeled PCR product can be used directly during hybridization. Store the DIG-labeled PCR product at – 20 °C for later use.

2. Preparation of genomic DNA

Isolate genomic DNA using a method suitable for isolates being examined (the CTAB extraction protocol described on page 1 was used in this study).

- DNA Genomic DNA used for Southern blot needs to be of high quality (high molecular weight, and free of inhibitor for restriction enzymes). Any commercially available DNA isolation kit should be suitable.
- A total of 5 µg of genomic DNA (up to 10 µl for bacteria and fungi) will be used for each lane/restriction enzyme used. Prepare enough genomic DNA for the relevant number of digestion setups.

3. Digest genomic DNA using restriction enzymes relevant to the probe being used for screening (Fast Digest HindIII and BamHI were used in this study - Thermo Fisher Scientific).

Setup digestion restriction(s) following the protocol relevant to the restriction enzymes being used.

- Digest 5 µg of genomic DNA per reaction. If using 10 µg per isolate, use double the volume of all reagents or perform the reaction in 2 tubes. In this study, the following Thermo Fisher Scientific FastDigest protocol was used:

Component	Reagent volume (50 µl total volume reaction)	Double volume (100 µl reaction)*
Nuclease-free water	30 µl	60 µl
10X FastDigest® buffer	5 µl	10 µl
DNA	10 µl (up to 5 µg)	20 µl (up to 10 µg)
FastDigest® enzyme	5 µl	10 µl

*Double volumes were used during the current study.

- Use a PCR machine for incubation if doing 100 µl reactions, and a water bath if doing higher volumes.
- Incubate at appropriate temperature (37 °C in this study) for up to 16 hours. Check digestion progress by running a small volume (~ 0.1 µg of DNA) of the digestion mixture on a 0.75 % agarose gel using after 1 hour of incubation to decide if additional incubation time is required.

After desired incubation time has reached, check for completed digestion by loading a small amount of digestion mixture (~ 0.25 µg of DNA) on a 0.75 % agarose gel. Run and visualize under the UV light.

- Completed digestion can be used immediately or kept in a freezer until use.

Precipitate the digested DNA using the following Ethanol/Sodium Acetate (EtOH/NaOAc) precipitation method (combine reactions if they were divided):

1. Add one tenth of NaOAc to the total digestion reaction (i.e., if the reaction is 100 µl, add 10 µl of NaOAc).
2. Add 2.5 volume of 100% EtOH to the above reaction.
3. Put reaction on ice for 10 min.
4. Spin at 4 °C for 30 min at maximum speed.
5. Discard supernatant.
6. Wash pellet by adding 500 µl 70 % EtOH.
7. Spin at 4 °C for 10 min at maximum speed.
8. Discard supernatant.
9. Repeat steps 6-8.
10. Spin tubes again for 5 min to remove excess EtOH. Use a P20 pipette to remove the excess EtOH.
11. Dry pellet under lamina flow for 5-10 min (assess progress after 4 min to avoid over-drying).
12. Resuspend the pellet in no more than 20 µl (25 µl used in this study) of 1x loading buffer with Gel-red or an equivalent DNA straining dye. Keep on ice until ready to load on Agarose gel for transfer.
13. Pulse spin the above mixture.
14. Incubate at 60 °C for 5-10 min.
15. Keep reaction at 4 °C until loading time.

4. Preparing and running the gel

Prepare 0.75 % agarose gel in 1x TAE (Tris Acetate EDTA) buffer. The thickness of the gel should be just enough (about 5 mm thick) to accommodate the samples' volumes.

Load DIG-labeled marker on the first lane (use 5 µl, mix with loading dye with Gel-red), followed by samples and positive control.

- Use PCR product or linearized plasmid DNA as a positive control, and load no more than 1 ng of it.
- Mix 98 µl of dH_2O with 2 µl of the control PCR product to make 100 µl total volume.
- Only load 2 µl of the above on the Agarose gel (remember to add Gel Red for the loading).

Run the gel at 80 V until the yellow dye gets close to the bottom of the gel (usually about 90 min).

Stop the gel, check and take a picture under UV light.

- Handle gel carefully as it is fragile, and avoid damage to the DNA by longtime UV exposure.

5. Transfer DNA to a membrane.

Note:
Recipes of all solutions used are detailed in the last section of this protocol.

1. Depurinate the DNA by submerging gel in 250 mM HCl with shaking (30 rpm) at RT until the bromophenol blue marker changes from blue to yellow. DO NOT incubate for more than 20 minutes.
2. Rinse the gel briefly with sterile, double distilled water.
3. Submerge the gel in Denaturation Solution (0.5 M NaOH, 1.5 M NaCl) 15 min at RT, with gentle shaking. Repeat once.
4. Rinse the gel briefly with sterile, double distilled water.
5. Submerge the gel in Neutralization Solution (0.5 M Tris-HCL, pH 7.5, 1.5 M NaCl) for 15 min at RT, with gentle shaking. Repeat once.
6. Rinse the gel briefly with sterile, double distilled water.
7. Equilibrate the gel for at least 10 min in 20X SSC (Saline Sodium Citrate).
8. Setup the blot transfer as follows (container, base, paper, membrane and tissue used must be same width and length as gel unless otherwise stated, and avoid the formation of air bubbles):

1 Kg weight/two or three thick stable books
Glass/thick hard-cover book
Stack of tissue paper (15-20 cm thick)
Pour 2 ml 5X SSC on to Whatman filter paper
Whatman filter paper 1 layer (5X SSC)
Whatman filter paper 1 layer
Nylon membrane
Pour 2 ml 20X SSC on gel center
1 cm Parafilm coat at all four gel edges
Gel (inverted)
Pour 20X SSC to drench paper and fill container up to 5 cm
2 layers Whatman filter paper as a bridge (long enough for edges to touch container bottom)
Gel tray inverted as a base (width and length must fit gel)
Container

9. Allow the blot to transfer overnight.
10. Unpacking the blot.
11. Remove ge1 + Whatman filter paper together then make a small cut at the top left edge to mark membrane orientation and cut off edges not containing any DNA.
12. Place the membrane (DNA side facing up) on Whatman 3MM paper that has been soaked with 2x SSC. Expose the membrane to UV light to permanently fix DNA on to the membrane using a Stratalinker UV crosslinker at 1200 mJ.
13. The membrane can now be used directly for hybridization or dried and stored at 4 °C for later use.

6. Pre-hybridize the blotted membrane with DIG Easy Hyb

1. Pre-heat an appropriate volume of DIG Easy Hyb (10 ml/100 cm2 of membrane; a total of 15 ml was used in this study) to hybridization temperature (usually at 42 °C; 68 °C was used) for 20 min.
2. Pre-hybridize the membrane for 30 min in a roller bottle with rotation at 42° C together with
3. Denature DIG-labeled probe by heating at 99 °C for 5 min in a PCR machine and rapidly cool submerged in or using ice-cold water. It is good to adjust the volume of probe to 50 µl with distilled water before denaturing by diluting 15 µl of probe with 35 µl water.
4. Add denatured DIG-labeled probe (15 µl) to the 15 ml pre-heated DIG Easy Hyb above and mix well. Avoid forming bubbles.
5. Pour out the pre-hybridization solution and add the above mixture into the roller with the membrane.
6. Close the cap tightly and incubate overnight with rotation.

7. Wash the membrane

1. Open the hybridization bottle, pour out the hybridization into a falcon tube (this hybridization can be stored at -15 to -20 °C and be reused several times. Freshly denature stored probe by incubating the solution at 68 °C for 10 min before reuse).
2. Wash membrane with 2X washing solution (2X SSC, 0.1 % SDS) at RT with gentle agitation for 5 min. Repeat once.
3. Wash in 0.1X washing solution (0.1X SSC, 0.1% SDS) at 65-68 °C under constant agitation for 5 min, and repeat once.
    - Pre-warm 0.1X washing solution to washing temperature before use.

8. Immunological detection

Notes:

i) Do not let the membrane dry out during the following steps of the detection protocol.

ii) Use the appropriate amount of solutions; do not use more than the necessary amount considering the price of solutions.

1. After washing, rinse the membrane briefly (1-5 min) in 100 ml washing buffer (Maleic acid buffer with 0.3 % Tween 20).
2. Incubate for 30 min (up to 3 hours) in blocking solution with shaking.
3. Incubate for 30 min in 10 ml antibody solution with shaking.
4. Wash min in 100 ml washing buffer (Maleic acid buffer with 0.3 % Tween 20) for 15 min. Repeat once.
5. Equilibrate 1-5 min in detection buffer enough to cover the membrane.
6. Incubate the membrane in 10 ml freshly prepared color substrate solution in an appropriate container in the dark. DO NOT shake during color development.
    - The color precipitate starts to form within a few minutes and the reaction is usually complete after 16 hours. Stop the reaction, when desired spot or band intensities are achieved, by washing the membrane for 5 min with sterile double distilled water or low TE buffer. Immediately photocopy, scan or take picture of the wet membrane.

SOLUTIONS FOR SOUTHERN BLOT ANALYSIS

Depurination solution (200 ml)	250 mM HCL (dilute 3M HCl twelve times in distilled water).
Denaturized solution (500 ml)	NaCl 43.83 g, NaOH 10 g, and distilled water (DW) until 500 ml.
Neutralized solution (500 ml)	NaCl 87.6645 g, Trisma-base 30.275 g, pH to 7.5 with HCl and DW until 500 ml (pH 7.5 with HCl ~ 23 ml).
DIG Easy Hyb	Add 64 ml of sterile double distilled water in two portions to the DIG Easy Hyb Granules; dissolve by stirring immediately for 5 min at 37 °C.
2X Washing solution (1,000 ml)	20X SSC 100 ml: 3M NaCl + 300 mM Sodium Citrate, 10 % SDS 10 ml, and DW 890 ml.
0.1X Washing solution (1,000 ml)	20X SSC 25 ml (5 ml), 10 % SDS 10 ml, and DW 965 ml.
20X SSC (1,000 ml)	NaCl 350.658 g (175.329 g), Sodium citrate 176.460 g (88.23 g), and DW 1,800 ml (900 ml) (pH to 7.0 with HCl) +/- 20 µl of 37% HCL.
5X SSC (1,000 ml)	20X SSC 250 ml and DW 750 ml.
10% SDS (100 ml)	SDS 10 g in 100 DW (heat at 65 ºC for 20 min).
Maleic acid buffer (1,000 ml)	11.61 g Maleic Acid, 8.766 g NaCl. Fill with dH2O. Check pH 7.5 with NaOH pellets (~7 g). Autoclave.
10X Blocking solution	Freshly prepare an appropriate amount of 1x working solution by diluting 10X blocking solution 1:10 with Maleic acid buffer i.e., 10 ml Blocking solution: 90 ml Maleic acid buffer.
Antibody solution	Centrifuge Anti-Digoxigenin-AP for 5 min, 4 °C at 10 000 rpm and pipet the necessary amount from the surface. Dilute Anti-Digoxigenin-AP 1:5000 in blocking solution. Add 10 µl to 50 ml of 10X blocking solution.
Color-substrate solution	Add 1 ml of NBT/BCIP stock solution to 50 ml of detection buffer.
Washing buffer	Add 0.3 % (0.9 ml) Tween 20 to maleic acid buffer using a 1,000 µl tip that is cut at the bottom.
Detection buffer	0.1 M Tris-HCl, 0.1 M NaCl, pH 9.5. Add $MgCl_2.6H_2O$ to a final concentration of 5 mM.
TE buffer	10 mM Tris-HCl, 1 mM EDTA, pH 8.0
Sterile double distilled water	

REFERENCES

Eisel D., Seth O., Grunewald-Janho S., Krunchen D, Ruger B., 2008. Dig Application Manual: For filter hybridization. Roche Diagnostics GmBH 94.

Hallen-Adams, H.E., Cavinder, B.L., Trail, F., 2011. *Fusarium graminearum* from expression analysis to functional assays, in: Xu, J., Bluhm, B.H. (Eds.), Fungal Genomics: Methods and Protocols, Methods in Molecular Biology. Springer, Michigan, pp. 79-101.

Murray, M.G., Thompson, W.F., 1980. Rapid isolation of high molecular weight plant DNA. Nucleic Acids Res. 8, 4321-4326.

Sambrook J., Green M. R., 2012. Molecular cloning: A laboratory manual, fourth ed. Cold Spring Harbor Laboratory Press, New York.

Supplementary figures

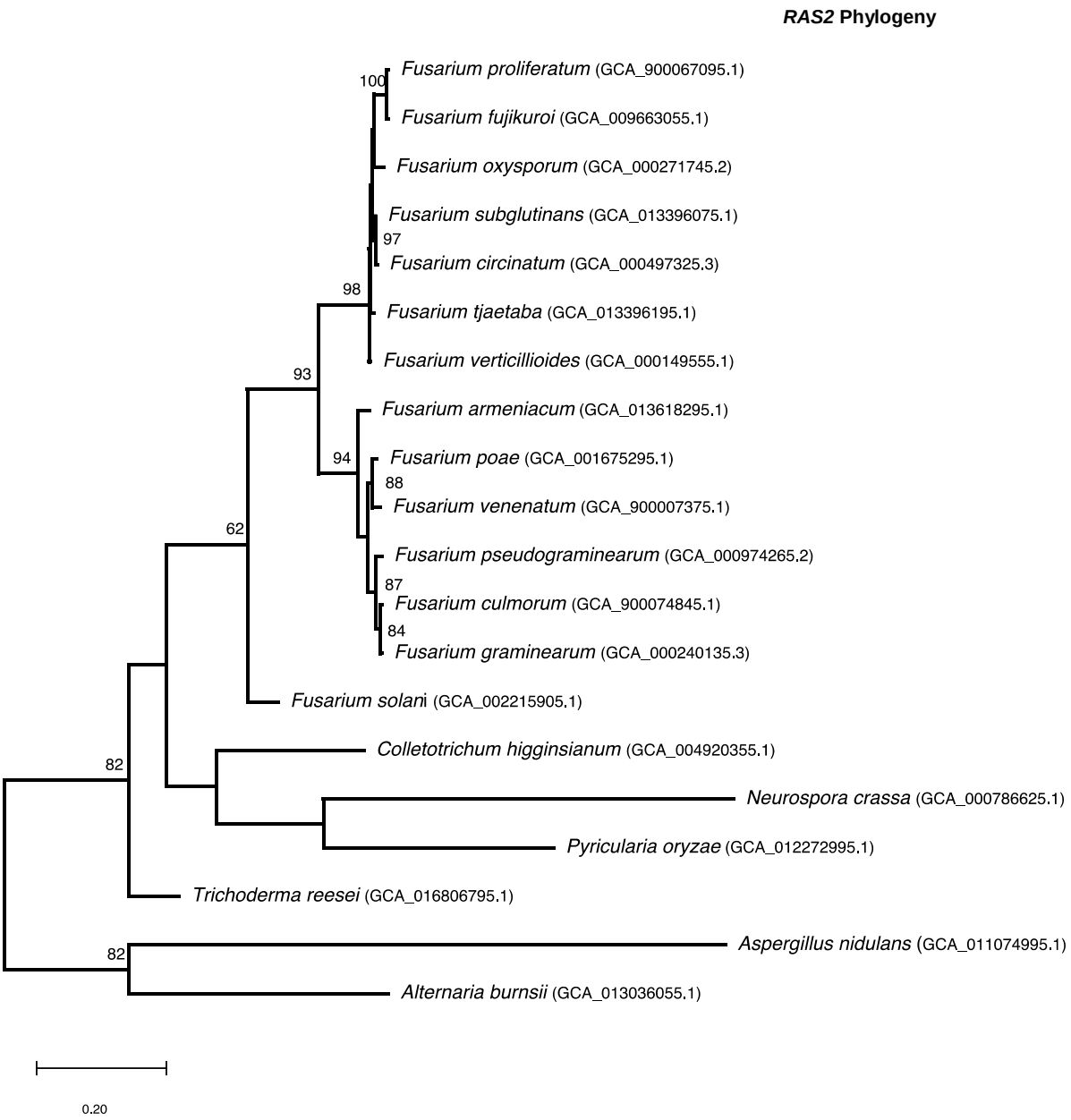

Supplementary figure S1. Maximum likelihood phylogeny for the *RAS2* gene from selected *Fusarium* and closely related fungal species. Bootstrap values above 60% are shown at the nodes, and the scale bar shows substitutions per site. The tree was rooted using *Aspergillus nidulans* and *Alternaria burnsii* as outgroup species. GenBank genome assembly numbers are shown in brackets.

Chapter 3

Deciphering the effect of *FUB1* disruption on fusaric acid production and pathogenicity in *Fusarium circinatum*

Submitted: Phasha, M.M., Wingfield, B.D., Wingfield, M.J., Coetzee, M.P.A., Hammerbacher, A., Steenkamp, E.T., 2021. Deciphering the effect of *FUB1* disruption on fusaric acid production and pathogenicity in *Fusarium circinatum*. Fungal Biol.

Abstract

Fusarium circinatum is an important pathogen of pine trees globally. Despite its economic importance, little is known regarding the molecular processes underlying its pathogenicity and virulence. In this study we explored the potential role of fusaric acid (FA), a known phytotoxin, in the pathogenicity of the fungus. FA is a polyketide secondary metabolite that is produced by the products of the *FUB* biosynthesis gene cluster, containing the genes *FUB1-12.* Of these, *FUB1* encodes the core multimodular polyketide synthase, which we disrupted using the split-marker approach. We then used the resulting mutant strain to investigate whether *FUB1* and FA production might play a role in virulence of *F. circinatum* on *Pinus patula* seedlings. High performance liquid chromatography showed that *FUB1* gene disruption abolished FA production both *in vitro* and i*n planta*. However, bikaverin production was significantly increased in the knockout mutant strain, which was also reflected in RNA-Seq data, where genes of the bikaverin cluster were significantly upregulated in this strain. *FUB1* disruption also corresponded with downregulation of a *F. circinatum* homologue of LaeA, which is known to be a master transcriptional regulator of secondary metabolism. Lesion lengths produced by the *fub1* knockout mutant on inoculated *P. patula* seedlings were significantly smaller than those produced by the wild type strain. Collectively, these results show that *FUB1* gene plays a role in the production of FA in *F. circinatum*, and that this gene contributes to the aggressiveness of *F. circinatum* on *P. patula*. This study will greatly contribute to the limited knowledge we have about the molecular basis of pathogenicity in this fungus.

1. Introduction

The genus *Fusarium* (Class Sordariomycetes, Phylum Ascomycota) accommodates fungi of medicinal, veterinary and agricultural importance (Kowero and Spilsbury, 1997). Its members are also among the most diverse and widely dispersed plant pathogens, causing blights, root rots or wilts on economically important crops (Agrios, 2005; Geiser et al., 2020). For example, the pine pitch canker fungus, *Fusarium circinatum*, causes significant economic losses to forestry industries, globally (Wingfield et al., 2008; Drenkhan et al., 2020). This is because infection by the fungus limits survival of seedlings and young plants, while at the same time reducing the quality of the timber produced (Bezos et al., 2017). Therefore, numerous previous studies have focused on the infection biology of this pathogen (e.g., Sakamoto and Gordon, 2006; Hammerbacher, 2007; Swett et al., 2018), but much remains unknown regarding the molecular mechanisms facilitating its ability to thrive in the forestry setting. Although some *F. circinatum* studies have identified putative virulence factors or effectors involved in pathogenesis and virulence (e.g., Munoz-Adalia et al., 2018, Visser et al., 2019), few have considered the role of secondary metabolites in these processes.

Like other *Fusarium* species, *F. circinatum* produces a variety of secondary metabolites (e.g., mycotoxins, phytotoxins and pigments) during growth in culture and host infection (Wiemann et al., 2013). Some of the best studied *Fusarium* secondary metabolites are beauvericin, bikaverin, fumonisins, fusaric acid (FA), fusarins, fusarubins and gibberellins (Berthiller et al., 2013). Although *F. fujikuroi* is capable of producing all seven of these compounds, most *Fusarium* species produce only some of them (Wiemann et al., 2013). These include well-known species such as *F. verticilliodes* producing only bikaverin, fusarubins, fusarins, beauvericin and FA, and *F. oxysporum,* which produces only bikaverin, beauvericin and FA (Wiemann et al., 2013). Furthermore, presence of a particular biosynthesis gene cluster does not always guarantee the ability of a species to express and produce the corresponding secondary metabolite. For example, the *F. circinatum* genome harbours gene clusters associated with the biosynthesis of six of the seven *F. fujikuroi* secondary metabolites, but it has been reported to produce only bikaverin, beauvericin and FA (Wiemann et al., 2013).

The production of beauvericin is catalysed by a non-ribosomal peptide synthase (Xu et al., 2008), whereas polyketide synthases (PKSs) catalyse the synthesis of bikaverin and FA (Linnemannstons et al., 2002; Brown et al., 2012). Secondary metabolites derived from PKSs are known as polyketides (Muller, 2004) and are involved in various biological processes ranging from growth and development through to pigmentation (Gaffoor et al., 2005; Keller et al., 2005). Polyketide synthesis involves the condensation of short-chain carboxylic acids (i.e., acyl-thioesters derived from acetyl

coenzyme A or malonyl coenzyme A) to form either linear or aromatic products made up of alternating carbonyl and methylene groups (Keller et al., 2005; Gaffoor et al., 2005). A functional PKS must, therefore, contain ketosynthase, acyltranferase and acyl carrier protein domains (Gaffoor et al., 2005). Many PKSs also have additional domains (i.e., ketoreductase, dehydratase and, enoyl reductase) for further modification of the polyketide, thereby adding to the functional diversity of these multidomain enzymes (Fujii et al., 2001; Keller et al., 2005).

FA, one of the earliest known phytotoxins, was first identified in 1937 from *F. heterosporum* (Yabuta et al., 1934). This secondary metabolite is produced by the enzyme PKS6, which is encoded by the *FUB1* gene (Brown et al., 2015). *FUB1* forms part of the *FUB* cluster, which in *F. verticillioides*, *F. fujikuroi*, *F. oxysporum* and *F. graminearum*, contains 12 genes that are positioned in tandem in the genomes of these fungi (Brown et al., 2015). Of these, 11 represent auxiliary genes (i.e., *FUB2* to *FUB12*) that encode acetyltranferases, hydrolases, transcription factors and dehydrogenases, which together with the core PKS6 enzyme produce FA (Brown et al., 2015). Typically, genes that encode secondary metabolites have coordinated expression (Zhang et al., 2004). Such coordination is thought to be achieved by co-regulation (Keller et al., 2005), and has been shown for five of the *FUB* genes of *F. verticillioides* and *F. fujikuroi* using RNA expression data (Brown et al., 2012).

In *Fusarium* species, FA has been shown to fulfil various biological roles. In addition to its cytotoxicity that causes programmed cell death in infected host cells (Samadi and Behboodi, 2006; Jiao et al., 2013), FA has recently been reported to be a chelating agent of metal ions (Lopez-Diaz et al., 2018). This property was discovered in tomato, where plants infected with *F. oxysporum* f. sp. *vasinfectum* had growth inhibition due to metal ion deprivation (Lopez-Diaz et al., 2018). FA has also been hypothesized to enable the fungus to gain advantage over competitors during growth. Here, producers secrete FA into the environment where it chelates metal ions and in so doing inhibits growth of competing microorganisms (Lopez-Diaz et al., 2018). This has been observed in *F. fujikuroi* and *F. oxysporum* f. sp. *vasinfectum*, where FA is transported to the outside environment using Major Facilitator Superfamily transporters (Fub11 and FubT, respectively) to inhibit the growth of other microorganisms (Crutcher et al., 2015; Studt et al., 2016). It has further been suggested that by chelating metal ions, FA could help the producers of this compound to survive toxic levels of it in the environment (Lopez-Diaz et al., 2018). Although the production of FA has been shown to affect the virulence of *F. oxysporum* f. sp. *vasinfectum* on tomato (Lopez-Diaz et al., 2018), it does not play a role in the virulence and pathogenicity of all *F. oxysporum* isolates (e.g., Brown et al., 2015).

The aim of this study was to investigate whether FA might play a role in the pathogenicity of *F. circinatum* on *Pinus patula* seedlings. To achieve this goal, we first identified and characterized the *FUB* gene cluster in the pathogen, and then disrupted the *FUB1* gene using the split-marker gene knockout approach. We also explored the effect of this gene disruption on FA production and gene expression in *F. circinatum*. Results from this study will add to the growing body of knowledge regarding the role of secondary metabolites in the pathogenicity of *F. circinatum* towards its plant hosts, as well as the molecular basis of virulence in this fungus.

2. Materials and Methods

2.1. Strains, growth media, and DNA extraction

Three isolates of *F. circinatum* were used in this study. Of these, one (FSP34) has a full genome sequence available from the database of the National Center for Biotechnology Information (NCBI; https://www.ncbi.nlm.nih.gov) under the accession number AYJV00000000 (Wingfield et al., 2012). This fungus originated from our previous work and is available as strain CMW 53647 from the culture collection of the Forestry and Agricultural Biotechnology Institute, FABI, University of Pretoria, South Africa. The other two isolates used in this study represent *fub1* knockout (Δ*Fcfub1*; CMW 53646) and complement (Δ*Fcfub1C*) mutants of FSP34, which were generated in this study (see below). Fungal strains were routinely grown on half strength Potato Dextrose Agar (PDA; Becton, Dickinson and Company, Franklin Lakes, NJ, USA) at 25 °C for seven days, unless otherwise stated.

For DNA extraction, a small agar block overgrown by the fungus, was cut from a seven-day-old culture and used to inoculate Potato Dextrose Broth (PDB; Betcon, Dickinson and Company, Franklin Lakes, NJ, USA). Following incubation on an Orbishake model 262 orbital shaker (200 rpm; Labotec, Midrand, South Africa) at room temperature for seven days, mycelium was collected by filtration through two layers of Miracloth (Calbiochem, La Jolla, CA, USA) and then freeze-dried. The freeze-dried fungal tissue was subjected to DNA extraction using a modified version of the protocol by Murray and Thompson (1980) that utilizes cetyltrimethylammonium bromide (CTAB) and phenol-chloroform (Phasha et al., 2021).

2.2. Identification of genes and gene clusters

The *FUB1* gene was identified in the *F. circinatum* genome by making use of the *FUB1* (FVEG_12523) gene sequence of *F. verticillioides*. For this purpose, a local BLASTn search against the genome of isolate FSP34 (NCBI accession number AYJV00000000) was done in CLC Genomics Workbench 8 (QIAGEN, Dernmark). To identify the FA cluster in the genome of *F. circinatum*, the DNA sequences for *FUB2* to *FUB12* of *F. verticillioides* (Brown et al., 2015) were used as queries

in BLASTn searches against the FSP34 genome. These BLAST searches were performed using default parameters. Synteny of the putative *FUB* cluster of *F. circinatum* to that of *F. verticillioides* was investigated using antiSMASH 5.0 (Blin et al., 2019). Because of an apparent association between FA and bikaverin production (see below), we also identified the *BIK* cluster involved in the biosynthesis of bikaverin. For this purpose, the *F. fujikuroi* gene sequences for *BIK1* to *BIK6* (Wiemann et al., 2009) were used in BLAST searches as described above.

2.3. *FUB1* gene disruption and complementation

Knockout constructs of *FUB1* were generated using the split-marker construct protocol (Catlett et al., 2003; Supplementary figure S1). Briefly, the 5' and 3' regions flanking *FUB1* were amplified with primer set Fus_UPSTREAM_F1 + Fus_UPSTREAM_R1 and primer set Fus_DOWNSTREAM_F1 + Fus_DOWNSTREAM_R1, respectively (Table 1). Two 5' and 3' overlapping fragments of the hygromycin resistance gene (*hyg*) were amplified directly from colonies of *Escherichia coli* carrying pCB1004 (Carroll et al., 1994), using primer set HygR + ygF and hyR + HygF, respectively (Zhou et al., 2010; Table 1). The 5' *FUB1* flank was fused to the 5' *hyg* overlapping fragment using primer set Fus_UPSTREAM_F1 + ygF, and the 3' *FUB1* flank to the 3' *hyg* overlapping fragment using primer set Fus_DOWNSTREAM_R1 + hygR. All primary amplicons were generated using the Phusion High-Fidelity Master Mix (Thermo Fisher Scientific, Vilnius, Lithuania), while the fusion of amplicons was carried out using LongAmp® *Taq* 2X Master Mix (New England BioLabs, Ipswich, MA, USA). In all cases, amplifications were done using the protocols provided by the manufacturers and primer annealing temperatures listed in Table 1.

A complementation construct was generated for random integration of the *FUB1* gene into the genome of the knockout mutant. This was done by amplifying the full gene sequence (including promoter and terminator regions) using Expand™ Long Range dNTPack (Sigma-Aldrich, Mannheim, Germany) with primer set FUB_1_Allele_F1 + FUB_1_Allele_R primers (Table 1), and fusing them to a geneticin resistance cassette (i.e., *nptII*; Proctor et al., 2008). The geneticin resistance cassette included a promoter and a terminator, and was amplified directly from *E. coli* colonies carrying plasmid pGEN-Not1 (Proctor et al., 2008) using LongAmp® *Taq* 2X Master Mix and primer set Not_1Fub_rp619 + Not_1R_rp620 (Table 1). Fusion of the *FUB1* gene to the geneticin resistance cassette was performed using Expand™ Long Range dNTPack and the primers FUB_1_Allele_F1 + Not_1R_rp620. All these amplifications were also done following the manufacturers' protocols and primer annealing temperatures listed in Table 1.

Protoplasts of *F. circinatum* isolate FSP34 were generated and transformed with the split-marker constructs using a protocol previously developed for *F. graminearum* (Hallen-Adams et al., 2011). This involved co-incubation of constructs and protoplasts, after which potential transformants were

selected based on their ability to grow in the presence of Hygromycin B (Phasha et al., 2021). For putative transformants, we then confirmed the absence and presence of the *FUB1* and *hygR* genes using primer sets FubCheck_F2 + FubCheck_R2 and HygF + HygR, respectively (Table 1). Copy number of the *hygR* construct in genomes of the knockout mutants was determined using Southern blot hybridization as previously described (Phasha et al., 2021), where primer set HygR + Hyg-int-R (Table 1) was used for probe synthesis.

To generate complementation mutants, protoplasts were generated from mutant strain Δ*Fcfub1* and transformed with the complementation construct as described above. The only exception was that putative transformants were identified based on their ability to grow in the presence of geneticin and not Hygromycin B. For these transformants, the presence of the *FUB1* gene in their genomes was confirmed using primer set FubCheck_F2 + FubCheck_R2 (Table 1). All PCRs employed Phusion High-Fidelity Master Mix (Thermo Fisher Scientific, Vilnius, Lithuania), following the manufacturer's protocol and primer annealing temperatures listed in Table 1.

2.4. Secondary metabolite production

We first confirmed the ability of isolate FSP34 to produce FA as previously reported (Wiemann et al., 2013), by making use of an *in planta* assay. For this purpose, an infection trial was conducted on six-month-old *P. patula* seedlings. Inoculum was prepared by flushing a seven- day-old PDA culture of FSP34 with 2 mL of 15 % glycerol, pipetting the glycerol up and down multiple times, and collecting the suspension into 2 mL tubes. Following quantification using a haemocytometer, 10 µL of a 50 000 spores/mL suspension was applied to a wound on a *P. patula* seedling, where the growth tip was removed with sterilized scissors (Mitchell et al., 2012). For the control treatments, 10 µL of 15 % glycerol solution was applied to wounded seedling tips. Each treatment had four replicates. Infected/diseased plant tissue was harvested two, four and five weeks after inoculation. This was done by cutting 2 cm below the developing lesions and collecting the top part of the stem. Following the removal of pine needles, the collected tissue was wrapped in foil, immediately frozen in liquid nitrogen and stored at -80 C for later use.

The collected plant tissue was ground to a fine powder in liquid nitrogen and lyophilized using an adVantage Freeze dryer (SP Scientific, USA) for 24 hours at 20 mbar. Of the dried plant tissue, 50 mg was added to 1.2 mL methanol for extraction of organic compounds by gentle agitation for 3 hours. These samples were then centrifuged at 19 400 x g, after which 10 µL of the supernatant was subjected to high performance liquid chromatography (HPLC) coupled to mass spectrometry analysis. Compound separation was conducted on an Agilent 1100 HPLC system (Agilent Technologies, USA) coupled to a Bruker Daltronics Esquire 3000 ion trap mass spectrometer (Bruker Daltronics, Germany). FA was separated on a Nucleodur Sphinx column (250 x 4.6 mm, 5

µm particle size; Macherey-Nagel, Germany) using a gradient starting from 95 % water containing formic acid (0.1 % v/v; Sigma, USA) to 95 % acetonitrile (Merck, USA) over 25 minutes at a constant flow rate of 0.8 mL/minute. A quarter of the column flow was diverted to enter the mass analyser. FA was analysed in positive mode, scanning $m\ z^{-1}$ between 50 and 1600 with an optimal target mass of 261 $m\ z^{-1}$. The conditions for mass-analysis included: skimmer voltage, 62 V; capillary voltage, 4200 V; nebulizer pressure, 35 psi; drying gas, 11 l min^{-1}; gas temperature, 330 ºC, capillary exit potential at 124 V. FA was identified by comparison with a commercial standard (FA from *Gibberella fujikuroi*; Sigma-Aldrich, Modderfontein, South Africa). Brucker Daltronics Quant Analysis v.3.4 software was used for peak integration and quantification using the following parameters: smoothing width 3 and Peak Detection Algorithm v. 2. An external calibration curve with dilutions of the commercially available FA was used for absolute quantification of the compound.

In vitro production of FA was evaluated in the wild type, knockout and complementation mutant strains. In the case of the knockout mutant and wild type, HPLC was also used to test for the production of bikaverin. For this purpose, the strains were grown in PDB with agitation on an Orbishake model 262 orbital shaker (99 rpm; Labotec, Midrand, South Africa) for five days at 25 °C, after which fungal tissue was removed from the growth medium by filtration through membrane filters with 0.45 µm pore size (Merck, USA). From the filtrates we then extracted organic compounds by first adjusting the pH of each 20 mL-sample to 4 with the addition of 1 mL of glacial acetic acid. This was followed by adding 20 mL of ethyl acetate to each sample. Following mixing by gentle inversion every 15 minutes for one hour, the suspensions were centrifuged (3200 g) at room temp for 10 minutes. The top layer (containing ethyl acetate and organic compounds) of each sample was transferred to clean polypropylene tubes and left open to allow evaporation of the ethyl acetate in a fume hood overnight. The remaining organic extracts were then re-suspended in 0.8 mL methanol, of which 10 µL was subjected to HPLC coupled to mass spectrometry analysis as described above. Bikaverin was assayed and quantified in the same way as FA, except that it was identified based on mass (382 Da) due to unavailability of a commercial standard.

2.5. Pathogenicity assay

To study the effect of *FUB1* on *P. patula* seedlings, pathogenicity assays were conducted. These were done by inoculating six-month-old *P. patula* seedlings with FSP34, mutant strain Δ*Fcfub1* and Δ*Fcfub1* mixed with 1 mg of Simga-Aldrich's FA, as well as 1 mg of FA alone. Inoculation of seedlings was performed as described above. Glycerol was again used in the control treatment, and there were 15 seedlings per treatment. The experiment followed the randomization layout generated using the RAND function of Microsoft® Excel. Seedlings were kept in a phytotron at 23°C, and

watered once every day for six weeks. Lesion lengths produced on the seedlings were measured (in mm) at the end of the six weeks.

To confirm Koch's postulates, isolations were made from the lesions on the infected *P. patula* seedlings and cultured. This was done by cutting diseased stem tips, removing stem pine needles and embedding the stem tips into *Fusarium* selective medium (Leslie and Summerell, 2006). The cultures were then incubated for seven days at 25 °C in the dark, after which fungi resembling *Fusarium* were confirmed to represent *F. circinatum* based on amplification with the specific-primers CIRC1A and CIRC4A (Schweigkofler et al., 2004; Table 1) as previously described (Steenkamp et al., 2014). Also, presence/absence of the *FUB1* and *hygR* genes was tested using primer sets FubCheck_F2 + FubCheck_R2 and HygF and HygR, respectively, as described above.

The lesion length data were subjected to an analysis of variance (ANOVA). This was carried out using the online tools available at http://astatsa.com/OneWay_Anova_with_TukeyHSD/. The null (H_o) hypothesis (that all the isolates did not differ in terms of the lesion lengths produced on the seedlings) was tested using the *F* test (Samuels and Witmer, 2003). For this purpose, the *F* statistic was compared to an *F* distribution critical value at a 95 % confidence level ($P = 0.05$) (Samuels and Witmer, 2003). Tukey's Honestly Significant Difference (HSD) test was used to test for significant differences among means.

2.6. RNA-Seq analysis

An RNA-Seq study was conducted using the wild type isolate FSP34 and the knockout mutant isolate Δ*Fcfub1*. For this purpose, these isolates were grown on half-strength PDA medium layered with cellophane at 25 °C for five days. Three replicates were cultured for both strains. Fungal tissue was then collected from the cellophane and subjected to total RNA extraction using the RNeasy Plant Mini Kit (QIAGEN) following the manufacturer's protocol (HB-0572-002 1101268). To prevent degradation of the extracted RNA, 1 µl of RiboLock (Thermo Fisher Scientific, Vilnius, Lithuania) was added to all extracted RNA samples.

cDNA libraries were then prepared by first capturing mRNA from 100 ng of the total RNA extracted from each sample using the Dynabeads® mRNA DIRECT™ Micro Kit (Thermo Fisher Scientific, Vilnius, Lithuania) following the manufacturer's protocol 61021 Rev. 004 (DynabeadmRNADIRECTMicro_UG_Rev004_20120514). Captured mRNA was eluted in 10 µL nuclease-free water and then used to construct cDNA libraries using the Ion Total RNA-Seq Kit v2 (Thermo Fisher Scientific, Vilnius, Lithuania) following the manufacturer's protocol (MAN00010654_IonTotalRNASeqKit_v2_UG). Briefly, 10 µL of poly(A) RNA was fragmented using RNAse III, purified using a magnetic bead clean-up module, and eluted in 12 µL nuclease-free water. This was then concentrated to a volume of 3 µL and ligated to RNA Xpress Barcoded

adapters (Thermo Fisher Scientific, Vilnius, Lithuania). Subsequently, these adaptor-ligated RNAs were reverse-transcribed to generate first strand cDNA libraries, which were then amplified to generate double stranded cDNA libraries.

The barcoded libraries were each diluted to a concentration of 80 pM and pooled in multiples of three for sequencing-template preparation using the Ion 540™ Chef Kit (Thermo Fisher Scientific, Vilnius, Lithuania). Twenty five microliters of the pooled barcoded library was loaded onto the Ion Chef instrument for template preparation and enrichment using Ion 540™ Chef Reagents, Solutions and Supplies according to the manufacturer's protocol (MAN0010851_Ion_540_Kit_Chef_UG). The templates were then loaded onto an Ion 540™ Chip by the Ion Chef instrument. Sequencing of each chip was performed on the Ion S5™ system using sequencing Solutions and Reagents according to the manufacturer's protocol (MAN0010851_Ion_540_Kit_Chef_UG). Signal processing and base-calling analyses were performed at the Central Analytical Facility at Stellenbosch University using Torrent Suite Software (TSS; version 5.10.0) with default parameters. After each sequencing run, the Ion S5™ system generated Binary Alignment Mapping (BAM) files of the cDNA libraries of the Δ*Fcfub1* and FSP34 strains. These BAM files were filtered for polyclonal reads and trimmed for poor quality nucleotides and barcodes using the TSS.

Following their sequencing, the transcriptomes of the wild type FSP34 and knockout mutant Δ*Fcfub1* strains were analysed. The first step in the analyses of the data was to create a Metadata table containing the BAM file name of each sample and experimental information associated with the BAM file in Microsoft® Excel. This was then imported into CLC Genomics Workbench, after which we imported the BAM files containing the sequencing data together with the reference genome of FSP34 together with its gff annotations.

The RNA-Seq Analysis Tool implemented in CLC Genomics Workbench was used to analyse gene expression in wild type and *fub1* knockout mutant. The tool was run in batch mode to map the reads of each sample (in triplicate) to the reference genome. The Differential Expression Tool was then used to compare the expression levels of the genes in the two isolates in a pairwise manner. Further analyses were only performed on genes that were significantly differentially expressed between the knockout mutant and wild type isolates. Moreover, a pairwise hierarchical clustering analysis was conducted using ClustVis software 2.0 (Metsalu and Vilo, 2015). Genes were considered to be significantly differentially expressed when their mean fold change from all three replicates of each strain used in the study was three or more, with a Bonferroni value of ≤ 0.05. Unless otherwise stated, default parameters were used during all analyses in this study. Furthermore, to assess the validity of the expression data from our study, we analysed the expression of three randomly selected

housekeeping genes (the superoxide dismutase mitochondrial precursor 2, tyrosyl tRNA synthetase and mitochondrial import inner membrane translocase subunit TIM16 genes) in the two strains.

Functional analyses of significantly differentially expressed genes (DEGs) were carried out using the Blast2Go plugin in CLC Genomics Workbench. First, mRNA annotations of the DEGs were extracted from the *F. circinatum* reference genome and converted to protein sequences. A protein BLAST (BLASTp) search against fungal protein sequences in the NCBI database was then performed using the Blast2Go Cloud BLAST function. Results from the BLASTp searches were then used to perform Mapping, Annotation and InterProScan protein domain identification. Unless otherwise stated, default parameters were used during the above analyses.

3. Results

3.1. Genes and gene clusters

The *FUB1* gene was identified in the genome of *F. circinatum* isolate FSP34 using BLASTn analysis with *FUB1* from *F. verticillioides* gene. This resulted in high similarity hits (Expect [E]-value = 0.0) to two predicted genes, each at the end of different contigs (contig 03042 and 02585). These contigs both formed part of Chromosome 3 and joining them yielded the full *FUB1* gene (nucleotide sequence data for this gene are available in the Third Party Annotation Section of the DDBJ/ENA/GenBank databases under the accession number TPA: BK014592). The *F. verticillioides FUB1* gene was 7472 bases in length and that of *F. circinatum* was 7330 bases long. Both genes had four introns located at the same positions. BLAST searches with the 11 accessory genes (*FUB2* to *FUB12*) of the FA cluster also resulted in hits with high similarities ($E \leq 8{,}5 \times 10^{-115}$) to two contigs on Chromosome 3 (see Supplementary file S1). The *FUB2* to *FUB5* genes were on contig 02585, which carried the *FUB1* gene, while *FUB6* to *FUB12* were on another contig (contig 00936). Overall, the *F. circinatum* gene cluster broadly resembled that of *F. verticillioides* (Figure 1A). The main difference was that *FUB1* of *F. circinatum* was located at the beginning of the FA cluster before *FUB2 to FUB5* whereas in *F. verticillioides*, *FUB1* was preceded by *FUB2*, *FUB3*, *FUB4* and *FUB5* (Figure 1A).

Using BLAST, sequences homologous to all six genes (*BIK1* to *BIK6*) of the *BIK* cluster were found in the genome of *F. circinatum* isolate FSP34 (Supplementary file S1). Comparison of these genes to those of the *F. fujikuroi BIK* clusters showed no differences in gene arrangement and orientation between the two clusters (Figure 1B). Nucleotide sequence data for *FUB2-FUB12* and *BIK1-BIK6* of *F. circinatum* have been submitted to the Third Party Annotation Section of the DDBJ/ENA/GenBank databases under accession numbers TPA: BK014554-BK014570.

3.2. *FUB1* gene disruption and complementation

The disruption of *F. circinatum FUB1* resulted in seven potential transformants that grew on PDA supplemented with Hygromycin B. PCR analysis showed that they all encoded for the *hygR* gene, although only three contained the *FUB1* gene. Southern blot analysis further showed only one copy of *hygR* integrated into the genomes of two of the latter transformants (Supplementary figure S2). Of these, one mutant (Δ*Fcfub1*) was selected for further studies. Complementation of Δ*Fcfub1* with the *FUB1* allele resulted in over 20 colonies growing on PDA with geneticin. Two of these tested positive for the presence of *FUB1*, of which one (Δ*Fcfub1C*) was used in the study.

3.3. Production of FA and bikaverin

The results of the *in planta* experiment confirmed that isolate FSP34 of *F. circinatum* is capable of producing FA, as reported previously (Wiemann et al., 2013). The tissues of six-month old *P. patula* seedlings infected with FSP34 contained an average of almost 0.023 mg of FA per gram of infected stem tissue two weeks post inoculation. This amount was significantly different from that in the control treatment ($P = 0.05$). Additionally, the amount of FA produced by isolate FSP34 remained constant up to week five post inoculation (Supplementary figure S3).

The *in vitro* FA assays showed that production of this secondary metabolite was completely lost in the knockout mutant Δ*Fcfub1*, while the wild type isolate FSP34 produced approximately 0.44 mg per mL of FA (Figure 2A). However, FA production was also lost in the complement mutant Δ*Fcfub1C* (Figure 2A), indicating that complementation with *FUB1* did not restore FA production in the knockout mutant.

Cultures of the knockout mutant appeared deep red compared to those of isolate FSP34 (Figure 2B). Previous studies on *F. lycopersici* and *F. fujikuroi* have shown that such red pigmentation is associated with bikaverin production (Kreitman and Nord 1949; Wiemann et al., 2009). An HPLC analysis accordingly revealed that isolate Δ*Fcfub1* produced almost double the amount of bikaverin ($m\ z^{-1}$= 383) as that produced by isolate FSP34 (Figure 2C). An unknown pigment with the same molecular mass was also identified in isolate Δ*Fcfub1* (Figure 2C), but absolute quantification was not possible due to the lack of pure standards.

3.4. Pathogenicity assay

One of the aims of this study was to determine whether the *FUB1* gene is involved in the pathogenicity of *F. circinatum* on *P. patula* seedlings. For this purpose we intended to compare the lesion lengths induced by the wild type, knockout and complementation mutants. However, FA production was not restored in isolate Δ*Fcfub1C*, which negated its use in these experiments. As an alternative, we used synthetic FA combined with the knockout mutant Δ*Fcfub1* as one of the treatments in the inoculation assay to investigate the effect of FA on pathogenicity.

Six weeks after inoculation, needles and stems of all the seedlings, except for those used as control, were wilted, necrotic, and discolored (Figure 3A). PCR with the *F. circinatum*-specific primers on DNA extracted from isolates obtained from diseased seedling tissue confirmed that the symptoms observed were associated with *F. circinatum* infection. Also, presence of amplicons of approximately 1 kb that were generated with primer set FubCheck_F2 + FubCheck_R2 confirmed the presence of the *FUB1* gene only in strain FSP34, while amplicons of approximately 2 kb (generated with primer set HygF + HygR) confirmed the presence of the hygromycin resistance gene only in the knockout mutant strain Δ*Fcfub1*. These results confirmed that differences in disease severity between treatments were as a result of the presence or absence of the *FUB1* gene in the different isolates inoculated.

The knockout mutant strain Δ*Fcfub1* produced significantly smaller lesions than the wild type isolates FSP34 (Figure 3B). The mean lesion length produced by Δ*Fcfub1* was 14.8 mm, which was significantly ($P = 0.05$) smaller than the mean of 20.4 mm produced by FSP34. Although the mean lesion length obtained for the Δ*Fcfub1* + FA treatment (i.e., 12.6 mm) was significantly smaller than that obtained for the Δ*Fcfub1* treatment, it was not significantly different from the results for the FA treatment (i.e., 11.8 mm). However, the lesions produced by the FA and Δ*Fcfub1* + FA treatments appeared bleached, showing that FA was cytotoxic to the seedlings and likely also the inoculated fungus. Likewise, cultures of Δ*Fcfub1* grown on PDA supplemented with 1 mg/mL of FA exhibited no growth after seven days of incubation at 25 °C, revealing that the synthetic FA was also cytotoxic to the *fub1* knockout mutant of *F. circinatum* (results not shown).

3.5. RNA-Seq analysis

Barcode trimming and quality filtering resulted in retention of 70 % of the original data generated from each Ion 540™ Chip. Each strain had at least 23 million reads per replicate with a mean length of 160 bp. Alignment of all reads from the knockout mutant *ΔFcfub1* to the FSP34 reference genome illustrated the disruption of the *FUB1* gene in the knockout mutant (Supplementary figure S4).

Analysis of gene expression patterns in isolates *ΔFcfub1* and FSP34 revealed numerous potentially DEGs. Using a Bonferroni value cut-off of ≤ 0.05, we found 530 significant DEGs. Pairwise hierarchical clustering analysis showed that the majority of these (341) were significantly upregulated in the knockout mutant *ΔFcfub1* (Figure 4; Supplementary file S2). Mean fold changes of the upregulated DEGs from the three replicates used in this study ranged from 2.7 to 235.9 and those of the downregulated DEGs ranged from -2.7 to -291.3 (Supplementary file S2).

Analysis of expression patterns of the three housekeeping genes (FCIRG_06968 encoding superoxide dismutase mitochondrial precursor 2, FCIRG_00112 encoding tyrosyl tRNA synthetase and FCIRG_01366 encoding mitochondrial import inner membrane translocase subunit TIM16)

showed no significant differences (i.e., Bonferroni = 1.00) in expression levels between the knockout mutant and wild type isolates. FCIRG_06968, FCIRG_00112 and FCIRG_01366 had average total counts of 3918, 1238 and 901 reads, respectively, in Δ*Fcfub1*, as opposed to 3514, 1213 and 787 reads, respectively, in FSP34. These data thus demonstrated the reliability of our RNA-Seq data.

Analyses of the domains of proteins encoded by the significant DEGs showed that the disruption of the *FUB1* gene caused a shift in the expression of genes involved in basic and specialized cellular activities. Basic activities included primary metabolic processes associated with vegetative growth (i.e., carbohydrate, lipid, protein and nucleic acid generation and transport), and specialized activities included processes such as secondary metabolism, cell defense, and plant tissue digestion. Although the DEGs included a number of hypothetical and uncharacterized proteins, further analyses were focused only on characterized proteins, specifically those associated with growth, pathogenesis and secondary metabolism due to the potential association of these traits with the disrupted *FUB1* gene and the upregulated *BIK* gene cluster.

Among the proteins encoded by the downregulated DEGs, we identified those involved in mycotoxin biosynthesis, detoxification and defence, membrane integrity, and plant tissue digestion (Table 2; see Supplementary file S3 for GO terms). Mycotoxin biosynthesis proteins included proteins from the *FUB* cluster involved in FA production (Fub10, Fub11 and Fub12), those involved in siderophore biosynthesis, a sterigmatocystin monooxygenase, an AM-toxin-like synthase, a phytoene synthase and the secondary metabolite master transcriptional regulator LaeA. Among these, the gene encoding Fub11 was the most downregulated (at 174.6-fold), and the one encoding AM-toxin-related synthase was the least downregulated (at 5.8-fold). Transcripts involved in detoxification and defence included those encoding catalase-1, an ABC transporter, a drug-binding protein, heat shock protein HSP30 and trichothecene 3-O-acetyltransferase. Genes encoding detoxification proteins were downregulated between 6.4 and 9.8-fold and the one encoding HSP30 was downregulated 20.0-fold. Membrane integrity proteins included those involved in ergosterol biosynthesis, as well as an ankyrin and a cell wall protein. The regulation for genes encoding these proteins was reduced 6.0 to 21.9-fold. Genes encoding products involved in plant tissue digestion included beta-glucosidases and endo-polygalacturonases, and were downregulated 7.8 to 11.2-fold.

Proteins encoded by the upregulated DEGs included those involved in pigmentation and mycotoxin biosynthesis, transcriptional regulation, detoxification, vegetative growth as well as one protein involved in plant tissue digestion (Table 3; see Supplementary file S4 for GO terms). Pigmentation and mycotoxin biosynthesis related DEGs included some belonging to the *BIK* cluster, and those involved in trichothecene and terpene biosynthesis. All the five identified genes of the *BIK* cluster were upregulated (Figure 3). This upregulation was significant for *BIK1*, *BIK2* and *BIK3* but not for

BIK4 and *BIK5*. The *BIK1* gene was upregulated 10.4-fold, *BIK2* 9.4-fold and *BIK3* 14.8-fold. The genes that encode the trichothecene and terpene biosynthesis related proteins were upregulated between 5.6 and 88.7-fold. DEGs involved in transcriptional regulation included transcription factors, as well as those involved in histone modification. Genes for the transcription factors were upregulated 7.2 to 18.2-fold and those encoding the histone modification proteins were upregulated 3.7 to 50.7-fold. Vegetative growth-related DEGs included those encoding a heterokaryon incompatibility protein and a polymer-forming cytoskeletal protein, and were upregulated 10.0 and 11.3-fold, respectively. The DEG involved in plant tissue digestion encoded an endo-polygalacturonase and was upregulated 6.0-fold (Table 3).

4. Discussion

The findings presented in this study demonstrated that the *FUB1* gene of *F. circinatum* plays a key role in FA production and the virulence of this fungus to its *Pinus* host. It encodes the core module of the PKS that synthesizes FA in *F. circinatum*, as is also the case for *F. fujikuroi*, *F. verticillioides* and *F. oxysporum* (Niehaus et al., 2014; Brown et al., 2015; Lopez-Diaz et al., 2018). Expression of this PKS in *F. circinatum* led to the production of FA both *in vitro* and *in planta*. In contrast, the *fub1* knockout mutant of *F. circinatum* generated in this study did not produce any FA, and it induced lesions that were significantly smaller than those caused by the FA-producing wild type isolate. This is different from a report that showed that FA does not play a role in the pathogenicity of *F. oxysporum* during infection of the three-angled cactus (Brown et al., 2015), but is consistent with previous reports where this metabolite was involved in the pathogenesis of isolates and/or species of *Fusarium* (Bacon et al., 1996; Gaumann, 1957). For example, a recent inoculation study using *FUB1* mutant strains of *F. oxysporum* showed that this gene contributes to the virulence of *F. oxysporum* on tomato (Lopez-Diaz et al., 2018). These data suggest a high likelihood that FA affects virulence in a host specific manner.

Our results showed that *FUB1* disruption affected bikaverin production in *F. circinatum*. The *fub1* knockout mutant produced more bikaverin than the wild type, and various genes in the *BIK* cluster of the mutant were upregulated compared to the wild type. The change in bikaverin expression likely contributed to the red colour of the mutant on PDA, consistent with the fact that it has been described as the red pigment produced by a PKS in some fungi including *Fusarium* species (Kreitman and Nord 1949; Wiemann et al., 2009). An increased production of bikaverin due to the disruption of *FUB1* has only been reported in *F. oxysporum*, where growth of a *FUB1* mutant on Czapek-Dox medium caused red pigmentation in the culture (Lopez-Diaz et al., 2018). We postulate that these findings are due to a putative feedback mechanism involved in the regulation of bikaverin and FA production. Feedback regulation has been linked to secondary metabolite production in *Fusarium*,

albeit within a single metabolic cluster (Thewes et al., 2005). In that study, a gene (*carB*) in the *F. fujikuroi* carotenoid biosynthesis cluster was found to negatively regulate biosynthesis of this pigment, because *carB* deletion mutants had overproduction of carotenoids compared to the wild type strain (Thewes et al., 2005). In *F. circinatum,* it remains to be determined which genes are involved in the suggested feedback mechanism between the bikaverin and FA metabolic clusters.

In addition to influencing expression of the *FUB* and *BIK* clusters, disruption of *FUB1* in *F. circinatum* also had significant effects on the expression of genes required for the biosynthesis of other secondary metabolites. These included genes involved in siderophore, sterigmatocystin, AM-like-toxin and phytoene biosynthesis that were downregulated, as well as an upregulated gene involved in terpene biosynthesis. Interestingly, disrupting *FUB1* also caused downregulation of the gene encoding a methyltransferase LaeA-like protein. First described in *Aspergillus nidulans*, LaeA is a master transcriptional regulator of secondary metabolite biosynthesis (Bok and Keller, 2004), and recently, the *laeA* gene was shown to be significantly downregulated in a mutant with impaired aflatoxin production (Gilbert et al., 2016). LaeA is thought to regulate secondary metabolism by mediating chromatin modification (Strauss and Reyes-Dominguez, 2011), and the inactivation of this protein was demonstrated to cause chromatic inaccessibility and repression of transcription at the FA cluster in *F. oxysporum* (Lopez-Diaz et al., 2018). Accordingly, it may be possible that the downregulated *laeA* homolog identified in *F. circinatum* contributed to changes in the multiple secondary metabolites biosynthesis genes observed in this study in a similar fashion that the disruption of *FUB1* led to the downregulation of LaeA. Our future research will explore these hypotheses.

Evidence from RNA-Seq data showed that the disruption of *FUB1* significantly affected the expression of genes known to be linked to virulence. These included two genes encoding endo-polygalacturonases and two encoding beta-glucosidases, which are involved in plant cell wall degradation and hydrolysis of 1,4-beta-linkages in plant cell wall cellulose, respectively (Bateman and Basham, 1976; Sorensen et al., 2013). In addition, genes involved in ergosterol biosynthesis were downregulated, which is consistent with the fact that this compound is needed for membrane integrity and contributes to fungal virulence (Parks et al., 1995; Shin et al., 2018). This is also true for *F. circinatum* in which ergosterol biosynthesis was recently shown to be involved in pathogenicity (Visser et al., 2019). In our *fub1* knockout mutant, genes encoding proteins involved in detoxification and defence (e.g., catalase-1, ABC transporter, a drug-binding protein and HSP30) were also downregulated. Pathogenic fungi typically utilize mechanisms to protect themselves from the toxic compounds secreted by their hosts during infection and colonization (de Waard et al., 2006). Therefore, the observed reduction in expression of detoxification and defence related genes possibly made the *F. circinatum fub1* knockout mutant more susceptible to the defence compounds

secreted by *P. patula* during colonization. Taken collectively, these data suggest that the reduced virulence of the *F. circinatum* mutant on *P. patula* seedlings is a consequence of the combined effects of the downregulation of multiple genes and pathways, caused by the disruption of *FUB1*. Additionally, the fact that genes involved in ergosterol biosynthesis were downregulated in the *F. circinatum fub1* knockout mutant while shown to be upregulated in wild type strain FSP34 *in planta* in the study by Visser et al. (2019) suggests that this mutant is likely to have similar gene expression patterns *in planta*.

As demonstrated by the results of our pathogenicity assays, the *fub1* knockout mutant of *F. circinatum* retained the ability to cause disease on *P. patula* seedlings. Although the lesions caused were significantly smaller than those induced by the wild type, they were longer than expected. Given that bikaverin production was enhanced in the knockout mutant, this secondary metabolite likely contributed to lesion formation by the mutant. This is in agreement with a study on *F. oxysporum* f. sp. *vasinfectum* where increased bikaverin production was associated with increased virulence on cotton (Bell et al., 2003). Additionally bikaverin has been shown to have cytotoxic effects in diverse organisms such as the human parasite *Leishmania brasiliensis*, the pine wood nematode *Bursaphelenchus xylophilus* and the water mold *Phytophthora infestans* (Balan et al., 1970; Kwon et al., 2007; Son et al., 2008). Whether bikaverin contributes to the ability of *F. circinatum* to infect and cause disease on its plant host requires additional research.

We were not able to restore the phenotypes associated with *FUB1* deletion using genetic complementation nor with the application of synthetic FA to the knockout mutant. Random insertion of the complementation construct (containing the *FUB1* allele) into the genome of the knockout mutant did not restore FA production in *F. circinatum*. We hypothesise that this is because expression of the *FUB1* gene is tightly linked to its position in the *FUB* cluster, making expression from other genomic positions unlikely. The addition of synthetic FA to the *fub1* knockout mutant, so as to mimic complementation of FA production during *P. patula* infection, also did not cause lesions similar to those induced by the wild type strain. In fact, these lesions were similar in size to those produced when seedlings were treated with FA alone. Also, cultures of the knockout mutant grown on PDA supplemented with 1 mg/mL of FA exhibited no growth after seven days of incubation. Therefore, lesions induced during the Δ*Fcfub1* + FA treatment of the *P. patula* seedlings was mostly due to the effect of FA on the plants and not of the fungus. Similar cytotoxicity of FA to the fungus producing it has been shown in *F. oxysporum*, where the growth of a *fub1* knockout mutant was inhibited in presence of 0.75 mg/mL FA (Lopez-Diaz et al., 2018). Strains producing FA apparently protect themselves from this toxin by enzyme modification and active export (Crutcher et al., 2015; Studt et al., 2016). It would be interesting to determine how *F. circinatum* to protects itself from the FA it produces.

Apart from being cytotoxic to *F. circinatum*, our results showed that FA is also cytotoxic to *P. patula* tissue. Despite the growing knowledge of how FA contributes to pathogenicity in *Fusarium*, its phytotoxic mechanisms remains poorly defined. Previous studies have reported that plant cell cultures treated with FA displayed unusual accumulation of hydrogen peroxide, release of cytochrome c, chromatin condensation and DNA fragmentation (Samadi and Behboodi, 2006; Jiao et al., 2013). FA apparently causes toxicity in plant cells by inducing such unusual properties, which in turn drive the cells into programmed death (Samadi and Behboodi, 2006; Jiao et al., 2013). In tomato, for example, the chelating properties of FA to copper, iron and zinc caused stem depigmentation, loss of turgor and wilting of the entire plant (Lopez-Diaz et al., 2018). Similar effects such as stem discoloration and bleaching were also observed in the present study following treatment of *P. patula* seedlings with FA. Future studies should focus on determining whether *F. circinatum* uses the same mechanism to cause toxicity on *P. patula*.

5. Conclusions

In this study, we report that the disruption of the *FUB1* gene of the *F. circinatum* wild type strain FSP34 caused this strain to stop producing FA. This disruption also caused a significant reduction in the virulence of FS34 to *P. patula* seedlings. Moreover, the disruption caused significant changes in the expression patterns of genes involved in cell wall and membrane integrity, plant tissue digestion and defence, and in secondary metabolite production beyond FA. These results show that *FUB1* is critical for the production of FA and plays an important role in the pathogenesis of *F. circinatum* during *P. patula* infection. Future studies should concentrate on deciphering the mode of action of FA in *P. patula* cells. Findings from such a study would provide useful information to be considered during the design of strategies to control the spread of *F. circinatum* in pine plantations.

Acknowledgements

We thank A. Wilson and M. Maphosa for advice provided during RNA extraction and RNA-Seq analyses.We thank the Central Analytical Facility at Stellenbosch University for the library preparation and sequencing of the samples used in this study.We also thank the following South African institutions and funding bodies for supporting this work: the Tree Protection Cooperative Programme (TPCP), the University of Pretoria, and the National Research Foundation (NRF) and Department of Science and Innovation (DSI) via their DSI-NRF Centre of Excellence in Plant Health Biotechnology (CPHB) and the DSI-NRF South African Research Chairs Initiative (SARChI) Chair in Fungal Genomics (Grant number: 98353).

References

Agrios, G., 2005. Plant Pathology, fifth ed. Elsevier Academic Press, Amsterdam.

Bacon, C., Porter, J., Norred, W., Leslie, J., 1996. Production of fusaric acid by *Fusarium* species. Appl. Environ. Microbiol. 62, 4039-4043.

Balan, J., Fuska, J., Kuhr, I. Kuhrova, V., 1970. Bikaverin, an antibiotic from *Gibberella fujikuroi*, effective against *Leishmania brasiliensis*. Folia Microbiol. 15, 479-484.

Bell, A.A., Wheeler, M.H., Liu, J., Stipanovic, R.D., Puckhaber, L.S., Orta, H., 2003. United States Department of Agriculture - Agricultural Research Service studies on polyketide toxins of *Fusarium oxysporum* f. sp. *vasinfectum*: potential targets for disease control. Pest Manag. Sci. 59, 736-747.

Bateman, D., Basham, H., 1976. Degradation of plant cell walls and membranes by microbial enzymes, Physiol. Plant Pathol. Springer, 316-355.

Berthiller, F., Crews, C., Dall'Asta, C., De Saeger, S., Haesaert, G., Karlovsky, P., Oswald, I.P., Seefelder, W., Speijers, G., Stroka, J., 2013. Masked mycotoxins: A review. Mol. Nutr. Food Res. 57, 165–186.

Bezos, D., Martinez-Alvarez, P., Fernández, M., Diez, J.J., 2017. Epidemiology and management of pine pitch canker disease in Europe - A Review. Balt. For. 23, 279-293.

Blin, K., Shaw, S., Steinke, K., Villebro, R., Ziemert, N., Lee, S.Y., Medema, M.H., Weber, T., 2019. antiSMASH 5.0: updates to the secondary metabolite genome mining pipeline. Nucl. Acids Res. 47, 81-87.

Bok, J. W. and Keller, N. P., 2004. LaeA, a regulator of secondary metabolism in *Aspergillus* spp. Eukaryot. Cell. 3, 527-535.

Brown, D.W., Butchko, R.A., Busman, M., Proctor, R.H., 2012. Identification of gene clusters associated with fusaric acid, fusarin, and perithecial pigment production in *Fusarium verticillioides*. Fungal Genet. Biol. 49, 521-532.

Brown, D.W., Lee, S.H., Kim, L.H., Ryu, J.G., Lee, S., Seo, Y., Kim, Y.H., Busman, M., Yun, S.H., Proctor, R.H., 2015. Identification of a 12-gene fusaric acid biosynthetic gene cluster in *Fusarium* species through comparative and functional genomics. Mol. Plant Microbe In. 28, 319-332.

Carroll, A.M., Sweigard, J.A., Valent, B., 1994. Improved vectors for selecting resistance to hygromycin. Fungal Genet. Reports. 41, 22.

Catlett, N.L., Lee, B.N., Yoder, O., Turgeon, B.G., 2003. Split-marker recombination for efficient targeted deletion of fungal genes. Fungal Genet. Rep. 50, 9-11.

Crutcher, F.K., Liu, J., Puckhaber, L.S., Stipanovic, R.D., Bell, A.A., Nichols, R.L., 2015. FUBT, a putative MFS transporter, promotes secretion of fusaric acid in the cotton pathogen *Fusarium oxysporum* f. sp. *vasinfectum*. Microbiol. 161, 875-883.

de Waard, M.A., Andrade, A.C., Hayashi, K., Schoonbeek, H., Stergiopoulos, I., Zwiers, L., 2006. Impact of fungal drug transporters on fungicide sensitivity, multidrug resistance and virulence. Pest. Manag. Sci. 62, 195–207.

Drenkhan, R., Ganley, B., Martin-Garcia, J., Vahalik, P., Adamson, K., Adamcikova, K., Ahumada, R., Blank, L., Braganca, H., Capretti, P., Capretti, P., Cleary, M., Cornejo, C., Davydenko, K., Diez J., Lehtiharvi H., Dvorak M., Enderle R., Fourie G., Georgieva M., Ghelardini, L., Hantula, J., Ioos, R., Iturritxa, E., Kanetis, L., Karpun, N., Koltay, A., Landera, E., Markovskaja, S., Mesanza, N., Milenkovic, I., Musolin, D., Musolin, D., Nikolaou, K., Nowakowske, J., Ogris, N., Oskay, F., Oszaka, T., Papazova-Anakieva, I., Paraschiv, M., Pasquali, M., Pecori, F., Rafoss, T., Raitelaityte, K., Raposo, R., Robin, C., Rodas, C., Santini, A., Sanz-Ros, A., Selikhovkin, A., Solla A., Soukainen, M., Soulioti, N., Steenkamp, E., Tsopelas, P., Vemic, A., Vettraino, A., Wingfield, M., Woodward, S., Zamora-Ballesteros, C., Mullet, M.., 2020. Global geographic distribution and host range of *Fusarium circinatum*, the causal agent of Pine Pitch Canker. Forests 11, 724.

Fujii, I., Watanabe, A., Sankawa, U., Ebizuka, Y., 2001. Identification of Claisen cyclase domain in fungal polyketide synthase WA, a naphthopyrone synthase of *Aspergillus nidulans*. Chem. Biol. 8, 189-197.

Gaffoor, I., Brown, D. W., Plattner, R., Proctor, R. H., Qi, W., Trail, F., 2005. Functional analysis of the polyketide synthase genes in the filamentous fungus *Gibberella zeae* (anamorph *Fusarium graminearum*). Eukaryot. Cell. 4, 1926-1933.

Gaumann, E., 1957. Fusaric acid as a wilt toxin. Phytopathology. 47, 342-357.

Gilbert, M. K., Mack, B. M., Wei, Q., Bland, J. M., Bhatnagar, D. and Cary, J. W., 2016. RNA sequencing of an *nsdC* mutant reveals global regulation of secondary metabolic gene clusters in *Aspergillus flavus*. Microbiol. Res. 182, 150-161.

Geiser, D.M., Al-Hatmi, A., Aoki, T., Arie, T., Balmas, V., Barnes, I., Bergstrom, G.C., Bhattacharyya, M., Blomquist, C.L., Bowden, R., et al., 2020. Phylogenomic analysis of a 55.1 kb 19-gene dataset resolves a monophyletic *Fusarium* that includes the *Fusarium solani* species complex. Phytopathol. https://doi.org/10.1094/PHYTO-08-20-0330-LE.

Hallen-Adams, H.E.; Cavinder, B.L., Trail, F., 2011. *Fusarium graminearum* from expression analysis to functional assays, in: Xu, J., Bluhm, B.H., (Eds.), Fungal Genomics: Methods and Protocols, Methods in Molecular Biology. Springer, Michigan, pp. 79-101.

Hammerbacher, A. Biology and epidemiology of *Fusarium circinatum*. University of Pretoria. 2007.

Jiao, J., Zhou, B., Zhu, X., Gao, Z., Liang, Y., 2013. Fusaric acid induction of programmed cell death modulated through nitric oxide signalling in tobacco suspension cells. Planta. 238, 727-737.

Keller, N. P., Turner, G. and Bennett, J. W., 2005. Fungal secondary metabolism—from biochemistry to genomics. Nat. Rev. Microbiol. 3, 937-947.

Kowero, G.S., Spilsbury, M.J., 1997. Capacity for forestry research in the Southern African Development Community. CIFOR. 11, 1-45.

Kreitman, G., Nord, F., 1949. Lycopersin, a pigment from *Fusarium lycopersici*. Arch. Biochem. 21, 457-457.

Kwon, H.R., Son, S.W., Han, H.R., Choi, G.J., Jang, K.S., Choi, Y.H., Lee, S., Sung, N.D., Kim, J.C., 2007. Nematicidal activity of bikaverin and fusaric acid isolated from *Fusarium oxysporum* against pine wood nematode, *Bursaphelenchus xylophilus*. Plant Pathol. J. 23, 318-321.

Leslie, J., Summerell, B., 2006. The *Fusarium* Laboratory Manual. Blackwell Publishing Ltd, Ioha.

Linnemannstons, P., Schulte, J., del Mar Prado, M., Proctor, R. H., Avalos, J. and Tudzynski, B., 2002. The polyketide synthase gene pks4 from *Gibberella fujikuroi* encodes a key enzyme in the biosynthesis of the red pigment bikaverin. Fungal Genet Biol. 37, 134-148.

Lopez-Diaz, C., Rahjoo, V., Sulyok, M., Ghionna, V., Martin-Vicente, A., Capilla, J., Di Pietro, A., Lopez-Berges, M.S., 2018. Fusaric acid contributes to virulence of *Fusarium oxysporum* on plant and mammalian hosts. Mol. Plant Pathol. 19, 440-453.

Metsalu, T., Vilo, J., 2015. ClustVis: a web tool for visualizing clustering of multivariate data using Principal Component Analysis and heatmap. Nucl. Acids Res. 43, 566-570.

Mitchell, R. G., Wingfield, M. J., Steenkamp, E. T. and Coutinho, T. A., 2012. Tolerance of Pinus patula full-sib families to *Fusarium circinatum* in a greenhouse study. Southern Forests: J. For. Sci. 74, 247-252.

Muller, R., 2004., Don't Classify Polyketide Synthases. Chem. Biol. 11, 4-6.

Munoz-Adalia, E. J., Fernandez, M., Wingfield, B. D. and Diez, J. J., 2018. *In silico* annotation of five candidate genes associated with pathogenicity in *Fusarium circinatum*. Forest Pathol. 48, e12417.

Murray, M., Thompson, W. F., 1980. Rapid isolation of high molecular weight plant DNA. Nucl. Acids Res. 8, 4321-4326.

Niehaus, E.M., von Bargen, K.W., Espino, J.J., Pfannmüller, A., Humpf, H.U., Tudzynski, B., 2014. Characterization of the fusaric acid gene cluster in *Fusarium fujikuroi*. Appl. Microbiol. Biot. 98, 1749-1762.

Parks, L.W., Smith S.J., Crowley J.H., 1995. Biochemical and physiological effects of sterol alterations in yeast—A review. Lipids 30, 227-230.

Phasha, M., Wingfield, M., Wingfield, B., Coetzee, M., Hallen-Adams, H., Fru, F., Swalarsk-Parry, B., Yilmaz, N., Duong, T., Steenkamp, E., 2021. Ras2 is important for growth and pathogenicity in *Fusarium circinatum*. Fungal Genet. Biol. 150, 103541-103550.

Proctor, R.H., Busman, M., Seo, J.A., Lee, Y.W., Plattner, R.D., 2008. A fumonisin biosynthetic gene cluster in *Fusarium oxysporum* strain O-1890 and the genetic basis for B versus C fumonisin production. Fungal Genet. Biol. 45, 1016-1026.

Sakamoto, J. M. and Gordon, T., 2006. Factors influencing infection of mechanical wounds by *Fusarium circinatum* on Monterey pines (*Pinus radiata*). Plant Pathol. 55, 130-136.

Samadi, L., Behboodi, B.S., 2006. Fusaric acid induces apoptosis in saffron root-tip cells: roles of caspase-like activity, cytochrome *c*, and H_2O_2. Planta. 225, 223-234.

Samuels, M.L., Witmer, J.A., 2003. Statistics for the Life sciences, third ed. Pearson Education.

Schweigkofler, W., O'Donnell, K., Garbelotto, M., 2004. Detection and quantification of airborne conidia of *Fusarium circinatum*, the causal agent of pine pitch canker, from two California sites by using a real-time PCR approach combined with a simple spore trapping method. Appl. Environ. Microbiol. 70, 3512-3520.

Shin, J., Kim, J., Lee, Y., Son H., 2018. Fungal Cytochrome P450s and the P450 Complement (CYPome) of *Fusarium graminearum*. Toxins *10*, 112-130.

Son, S., Kim, H., Choi, G., Lim, H., Jang, K., Lee, S., Lee, S., Sung, N., Kim, J. C., 2008. Bikaverin and fusaric acid from *Fusarium oxysporum* show antioomycete activity against *Phytophthora infestans*. J. Appl. Microbiol. 104, 692-698.

Sorensen, A., Lubeck, M., Lubeck, P.S., Ahring, B. K., 2013. Fungal beta-glucosidases: a bottleneck in industrial use of lignocellulosic materials. Biomolecules 3, 612-631.

Steenkamp, E.T., Makhari, O.M., Coutinho, T.A., Wingfield, B.D., Wingfield, M.J., 2014 Evidence for a new introduction of the pitch canker fungus *Fusarium circinatum* in South Africa. Plant Pathol. 63, 530-538.

Strauss, J. and Reyes-Dominguez, Y., 2011. Regulation of secondary metabolism by chromatin structure and epigenetic codes. Fungal Genet. Biol. 48, 62.

Studt, L., Janevska, S., Niehaus, E. M., Burkhardt, I., Arndt, B., Sieber, C. M., Humpf, H. U., Dickschat, J. S., Tudzynski, B., 2016. Two separate key enzymes and two pathway-specific transcription factors are involved in fusaric acid biosynthesis in *Fusarium fujikuroi*. Environ. Microbiol. 18, 936-956.

Swett, C., Reynolds, G., Gordon, T., 2018. Infection without wounding and symptomless shoot colonization of *Pinus radiata* by *Fusarium circinatum*, the cause of pitch canker. Forest Pathol. 48, e12422.

Thewes, S., Prado-Cabrero, A., Prado, M.M., Tudzynski, B., Avalos, J., 2005. Characterization of a gene in the car cluster of *Fusarium fujikuroi* that codes for a protein of the carotenoid oxygenase family. Mol. Genet. Genomics. 274, 217-228.

Visser, E.A., Wegrzyn, J.L., Steenkamp, E.T., Myburg, A.A. and Naidoo, S., 2019. Dual RNA-Seq analysis of the pine-*Fusarium circinatum* interaction in resistant (*Pinus tecunumanii*) and susceptible *(Pinus patula*) hosts. Microorganisms 7, 315.

Wiemann, P., Willmann, A., Straeten, M., Kleigrewe, K., Beyer, M., Humpf, H.U. and Tudzynski, B., 2009. Biosynthesis of the red pigment bikaverin in *Fusarium fujikuroi*: genes, their function and regulation, Mol. Microbiol. 72, 931-946.

Wiemann, P., Sieber, C.M.K., von Bargen, K.W., Studt, L., Niehaus, E.M. et al., 2013. Deciphering the Cryptic Genome: Genome-wide Analyses of the Rice Pathogen *Fusarium fujikuroi* Reveal Complex Regulation of Secondary Metabolism and Novel Metabolites. PLoS Pathog. 9, e1003475.

Wingfield, M., Hammerbacher, A., Ganley, R., Steenkamp, E., Gordon, T., Wingfield, B., Coutinho, T., 2008. Pitch canker caused by *Fusarium circinatum* - a growing threat to pine plantations and forests worldwide. Australas. Plant Pathol. 37, 319-334.

Wingfield, B.D., Steenkamp, E.T., Santana, Q.C., Coetzee, M., Bam S., et al., 2012. First fungal genome sequence from Africa: a preliminary analysis. S. Afr. J. Sci. 108, 1-9.

Xu, Y., Orozco, R., Wijeratne, E.K., Gunatilaka, A.L., Stock, S.P., Molnár, I., 2008. Biosynthesis of the cyclooligomer depsipeptide beauvericin, a virulence factor of the entomopathogenic fungus *Beauveria bassiana*, Chem. Biol. 15, 898-907.

Yabuta, T., Kambe, K., Hayashi, T., 1934. Biochemistry of the bakanae fungus. I. Fusarinic acid, a new product of the bakanae fungus. J. Agric. Chem. Soc. Jpn. 10, 1059-1068.

Zhang, Y., Wilkinson, H., Keller, N., Tsitsigiannis, D. and An, Z., 2004. Secondary metabolite gene clusters, in: Zhiqiang A (Ed.), Hand Book of Industrial Mycology. Marcel Dekker, New York, pp. 355-369.

Zhou, X., Heyer, C., Choi, Y.E., Mehrabi, R., Xu, J.R., 2010. The CID1 cyclin C-like gene is important for plant infection in *Fusarium graminearum*. Fungal Genet. Biol. 47, 143-151.

Tables

Table 1. List of primer sequences used in this study.

Primer name	**Sequence (**5' **to** 3'**)**	**Reference**	**Annealing temperature**
Fus_UPSTREAM_F1	GACCATCCATTGTTACCTA	This study	60 °C
Fus_UPSTREAM_R1	ACTTATTCAGGCGTAGCAACCAGGCGAGAGG GAGAGAAAAGAG	This study	60 °C
Fus_DOWNSTREAM_F1	TCAGCATCTTTTACTTTCACCAGCGAACCATC GAAGAGCTCCA	This study	60 °C
Fus_DOWNSTREAM_R1	TGATAGCGGAGAAGTACTTT	This study	60 °C
HygF	AACGCTGGTGAAAGTAAAAGATGCTG	This study	60 °C
HygR	ACGCCTGGTTGCTACGCCTGAATAAGT	This study	60 °C* & 66 °C[@]
hyR	GTATTGACCGATTCCTTGCGGTCCGAA	Zhou et al., 2010	60 °C
ygF	GATGTAGGAGGGCGTGGATATGTCCT	Zhou et al., 2010	60 °C
FubCheck_F2	GGGGGTGCTAACAATGG	This study	55 °C
FubCheck_R2	GAGGAAGGACATGGAGGA	This study	55 °C
FUB_1_Allele_F1	ATGATGTCGATGAGAGTG	This study	55 °C
FUB_1_Allele_R	AAACTGGCTCTTTCGGTC	This study	55 °C
Not_1Fub_rp619	CAAGTTCCGGGACCGAAAGAGCCAGTTTCAT GCGGCCGCATGCCAGTTG	This study	55 °C
Not_1R_rp620	CATGCGGCCGCAGAGTAAAG	This study	55 °C
CIRC1A	CTTGGCTCGAGAAGGG	Schweigkofler et al., 2004	66 °C
CIRC4A	ACCTACCCTACACCTCTCACT)	Schweigkofler et al., 2004	66 °C
Hyg-int-R	CGGCCGTCTGGACCGATGGCTGTGTA	This study	66 °C

* Annealing temperature to determine the presence/absence hygromycin resistance cassette in FSP34 and Δ*Fcfub1*.

@ Annealing temperature used during Southern Blot analysis probe synthesis.

Table 2. Significantly downregulated DEGs involved in mycotoxin biosynthesis, detoxification, membrane integrity, and plant tissue digestion in a *fub1* knockout mutant (Δ*Fcfub1*) of *F. circinatum*.

Biological process [a]	Sequence name [b]	Gene product	Protein length	Number of hits [c]	Expect - value	Similarity mean	Fold change (Δ*Fcfub1* vs. wild type) [d]
Secondary metabolism	FCIRG_03379	Fub11 Major facilitator superfamily (MFS) transporter	593	20	0	98.24	-174.6
	FCIRG_03378	Fub12 Fungal-type Zn(II)2Cys6 TF	647	20	1.48E-135	97.86	-46.3
	FCIRG_14896	Cytochrome P450 monooxygenase trt6	509	20	0	98.68	-21.8
	FCIRG_06985	Phytoene synthase	541	20	5.57E-20	100	-12.0
	FCIRG_10042	Related to aerobactin siderophore biosynthesis protein iucB	457	20	0	97.05	-9.7
	FCIRG_09287	Related to non-ribosomal peptide synthetase	1621	20	0	93.66	-9.4
	FCIRG_12923	Related to methyltransferase LaeA-like	391	20	0	97.46	-7.5
	FCIRG_07289	Related to trichothecene 3-O-acetyltransferase	491	20	0	97.06	-7.4
	FCIRG_03380	Fub10 Fungal-type Zn(II)2Cys6 transcription factor	427	20	0	96.62	-6.0
	FCIRG_10385	Putative sterigmatocystin biosynthesis monooxygenase stcW	584	20	0	98.37	-6.1
	FCIRG_01914	Related to aerobactin siderophore biosynthesis protein iucB	428	20	0	98.62	-6.0
	FCIRG_01916	Related to AM-toxin synthetase (AMT)	2048	20	0	97.21	-5.8
Detoxification and defence	FCIRG_06983	Related to HSP30 heat shock protein Yro1p	307	20	0	98.65	-20.0
	FCIRG_10399	c6 transcription factor	266	20	8.58E-96	59.88	-9.8
	FCIRG_08070	ABC transporter CDR4	1401	20	0	89.93	-9.4
	FCIRG_01447	Catalase-1	734	20	0	97.3	-9.4
	FCIRG_07289	Related to trichothecene 3-O-acetyltransferase	491	20	0	97.06	-7.4
	FCIRG_12408	Related to emopamil-binding protein	211	20	2.81E-149	96.98	-7.2

Table 2. Continued.

Biological process [a]	Sequence name [b]	Gene product	Protein length	Number of hits [c]	Expect - value	Similarity mean	Fold change (Δ*Fcfub1* vs. wild type) [d]
	FCIRG_01913	Related to major facilitator MirA	593	20	0	97	-6.4
Membrane integrity	FCIRG_04319	sterol 24-C-methyltransferase	391	20	0	96.65	-21.9
	FCIRG_11096	NADPH-ferrihemoprotein reductase/ Cytochrome p450 reductase	703	20	0	96.13	-13.9
	FCIRG_02815	Pfs, NACHT and Ankyrin domain protein	612	20	0	64.76	-8.2
	FCIRG_07324	cytochrome P450, family 51	506	20	0	96.7	-8.1
	FCIRG_01340	Related to covalently-linked cell wall protein	407	20	0	95.16	-6.0
Plant tissue digestion	FCIRG_12189	Probable endo-polygalacturonase 6	349	20	0	97.18	-11.2
	FCIRG_05252	Related to glucan 1,3-beta-glucosidase	890	20	0	88.06	-9.8
	FCIRG_02737	Probable PGU1-endo-polygalacturonase	390	20	0	94.59	-7.9
	FCIRG_09516	Related to beta-glucosidase	621	20	0	98.97	-7.8

[a] The proteins in the table were classified into these biological processes based on their Blast2Go descriptions and GO names.

[b] The *F. circinatum* genome used was from the first assembly of this genome assembled using the 454 GS assembler software package, Newbler (Wingfield et al., 2012).

[c] BLASTp searches were done against fungal protein sequences in the NCBI database.

[d] Mean fold change from three replicates of each strain.

Table 3. Significantly upregulated DEGs involved in pigmentation and mycotoxin biosynthesis, transcriptional regulation, detoxification, vegetative growth and plant tissue digestion in a *fub1* knockout mutant (Δ*Fcfub1*) of *F. circinatum*.

Biological process [a]	Sequence name [b]	Gene product	Protein length	Number of hits [c]	Expect - value	Similarity mean	Fold change (Δ*Fcfub1* vs. wild type) [d]
Secondary metabolism	FCIRG_06895	4-coumarate--CoA ligase-like 4	569	20	0	97.63	95.4
	FCIRG_03330	BIK1 Bikaverin cluster-monooxygenase	489	20	0	97.33	10.4
	FCIRG_03329	BIK3 Bikaverin cluster-O-methyltransferase	450	20	0	98.01	14.8
	FCIRG_03331	BIK2 Bikaverin cluster-polyketide synthase	1994	20	0	96.47	9.4
	FCIRG_07084	Geranylgeranyl pyrophosphate synthetase	203	20	1.18E-114	85.1	19.4
	FCIRG_10202	Geranylgeranyl pyrophosphate synthetase	352	20	0	87.3	21.8
	FCIRG_04875	Putative nicotianamine synthase 4	303	20	0	91.89	11.4
	FCIRG_01677	Putative polyketide synthase	4056	20	0	96.57	8.8
	FCIRG_09474	Related to cycloheximide-inducible protein CIP70	557	20	0	91.28	16.3
	FCIRG_00054	Related to gibberellin 20-oxidase	356	20	0	96.77	5.3
	FCIRG_13891	Related to non-ribosomal peptide synthetase	268	20	4.93E-178	94.06	28.5
	FCIRG_13893	Related to TRI13-cytochrome P450	579	20	0	99.02	88.7
	FCIRG_00807	Related to TRI15-putative transcription factor	293	20	0	94.33	5.6
Transcriptional regulation	FCIRG_03317	Protein related to nucleosome binding protein	204	20	2.83E-142	80.4	3.7
	FCIRG_07839	Related to GNAT family acetyltransferase	208	20	9.74E-143	94.95	50.7

Table 3. Continued.

Biological process [a]	Sequence name [b]	Gene product	Protein length	Number of hits [c]	Expect - value	Similarity mean	Fold change (Δ*Fcfub1* vs. wild type) [d]
	FCIRG_04540	Transcription factor	171	20	9.43E-126	94.95	18.2
	FCIRG_09461	Transcription factor	207	20	8.86E-148	93.46	7.2
	FCIRG_14849	Zn2cys6 transcription regulator	221	20	6.47E-160	98.03	10.7
Detoxification and defence	FCIRG_09199	Related to benzoate 4-monooxygenase cytochrome P450	538	20	0	93.03	14.3
	FCIRG_01508	Related to salicylate hydroxylase	411	20	0	88.54	26.6
Vegetative growth	FCIRG_07702	Heterokaryon incompatibility protein 6, OR allele	590	20	0	91.65	10.0
	FCIRG_11230	Polymer-forming cytoskeletal protein	166	20	2.25E-115	94.87	11.3
Plant tissue digestion	FCIRG_02825	Endo-polygalacturonase	359	20	0	98.53	6.0

[a] The proteins in the table were classified into these biological processes based on their Blast2Go descriptions and GO names.

[b] The *F. circinatum* genome used was from the first assembly of this genome assembled using the 454 GS assembler software package, Newbler (Wingfield et al., 2012).

[c] BLASTp searches were done against fungal protein sequences in the NCBI database.

[d] Mean fold change from three replicates of each strain.

Figures

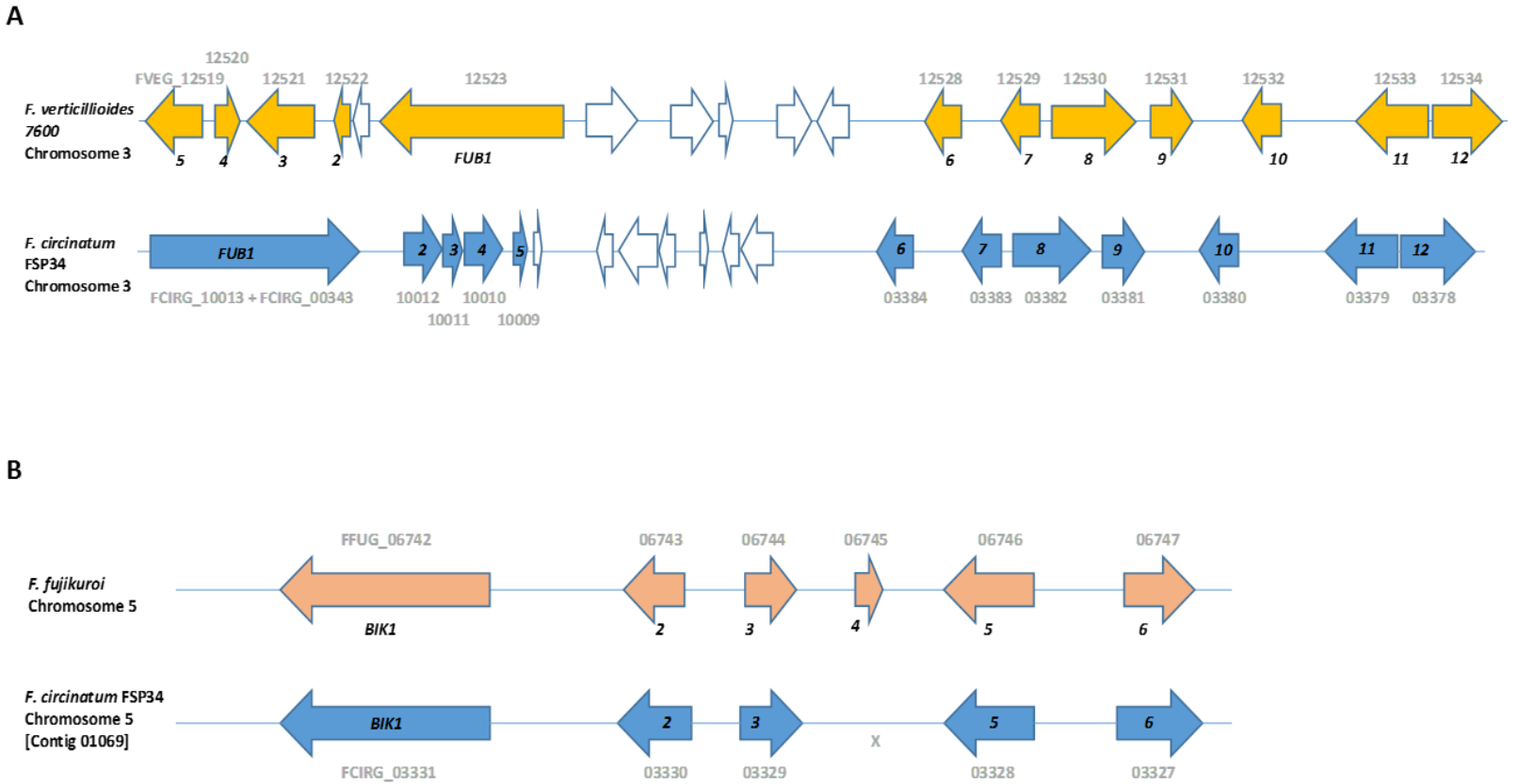

Figure 1. The order of genes in the FA and bikaverin clusters in *F. circinatum*. **A.** The order of *FUB* genes in the *F. circinatum* compared to *F. verticillioides*. Numbers 2 to 12 refer to *FUB2* to *FUB12*. Uncoloured genes are not considered part of the FA cluster. **B.** The order of *BIK* genes in *F. circinatum* and *F. fujikuroi*. The symbol x denotes a missing annotation for *BIK4* in the current annotated version of the *F. circinatum* genome.

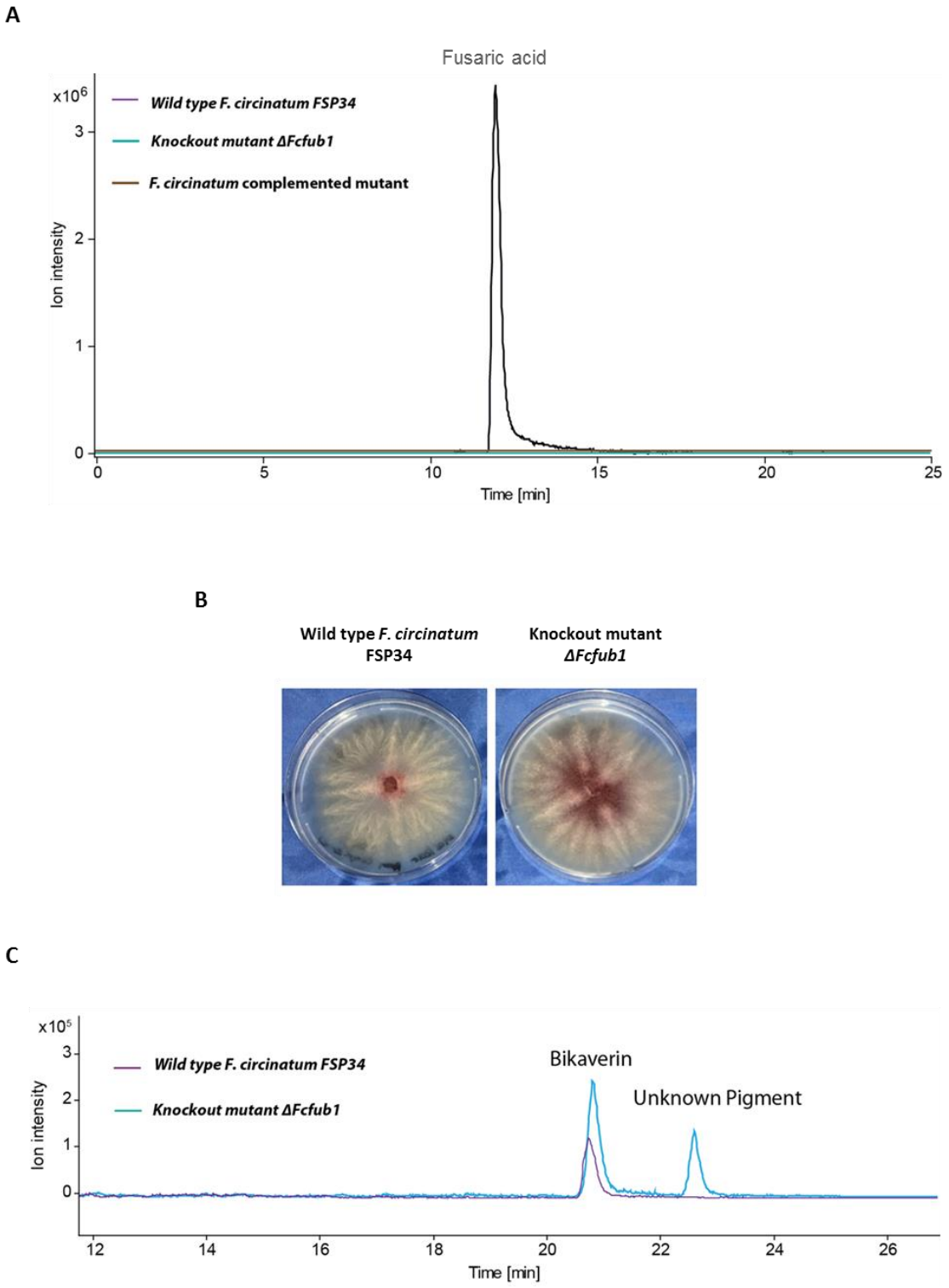

Figure 2. Fusaric acid and bikaverin production in *F. circinatum* wild type (FSP34) and mutant (Δ*Fcfub1*) strains. **A.** A chromatogram of *in vitro* production of FA in *F. circinatum* wild type FSP34, knockout mutant Δ*Fcfub1* and complement mutant Δ*Fcfub1C* strains. **B.** *Fusarium circinatum* wild type and mutant strain colonies after seven days of incubation at 25 °C. **C.** A chromatogram of *in vitro* bikaverin production in *F. circinatum* wild type and mutant strains.

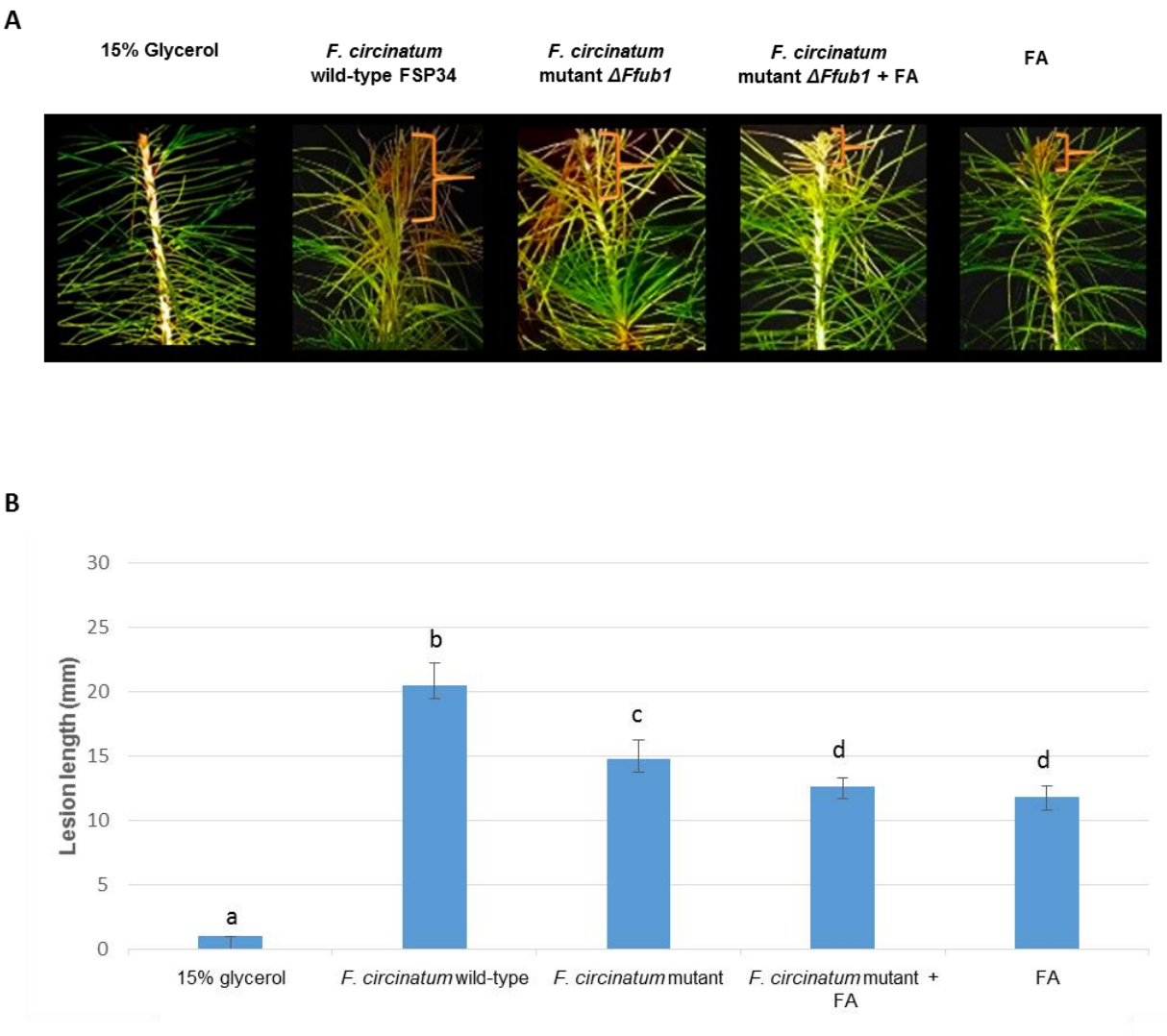

Figure 3. Pathogenicity of *F. circinatum* wild type (FSP34), mutant (Δ*Fcfub1*), mutant + FA and FA on *P. patula*. **A.** Lesions (indicated by curly brackets) produced on *P. patula* seedlings after inoculation with 15 % glycerol, FSP34, mutant (Δ*Fcfub1*), mutant + FA and FA on *P. patula*. **B.** Mean lesion lengths caused by inoculations of *P. patula* with 15 % glycerol, FSP34, mutant, mutant + FA and FA on *P. patula*. Inoculations were performed on thirty seedlings per strain, and statistical significance was tested at $P = 0.05$. Different letters above error bars show significant difference between means of the respective treatments and same letters show no significant difference.

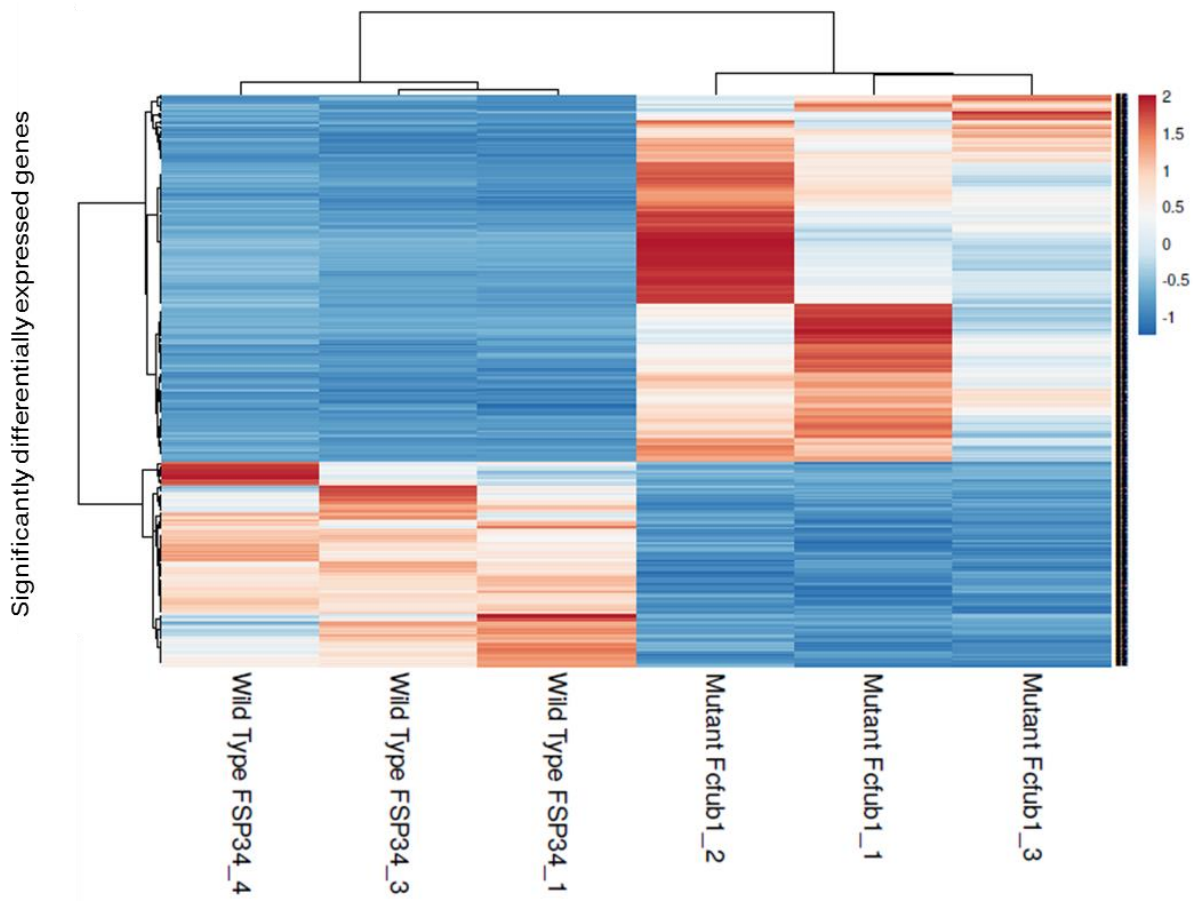

Figure 4. Pairwise hierarchical clustering analysis of significantly differentially expressed genes in *F. circinatum* wild type FSP4 and knockout mutant strain Δ*Fcfub1*.

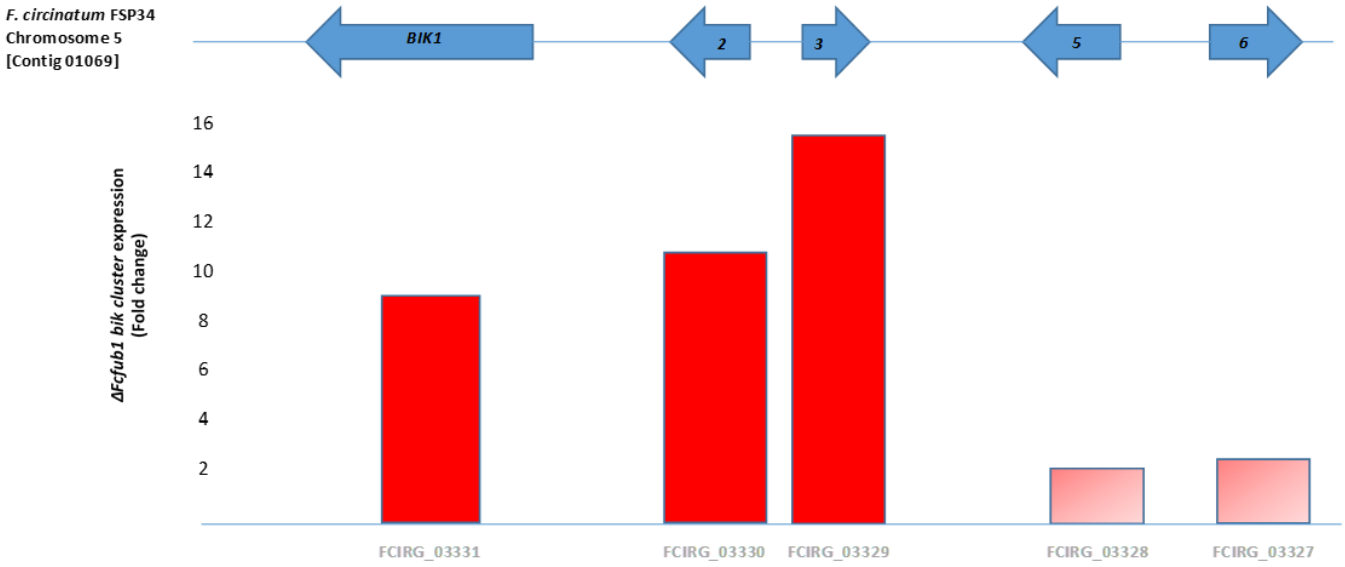

Figure 5. Expression patterns of the *BIK* genes in the *F. circinatum* knockout mutant strain Δ*Fcfub1*. Significantly upregulated genes are represented by dark red bars and those not significantly upregulated are represented by light red bars. Significance was determined using a Bonferroni value of ≤0.05.

Supplementary figures

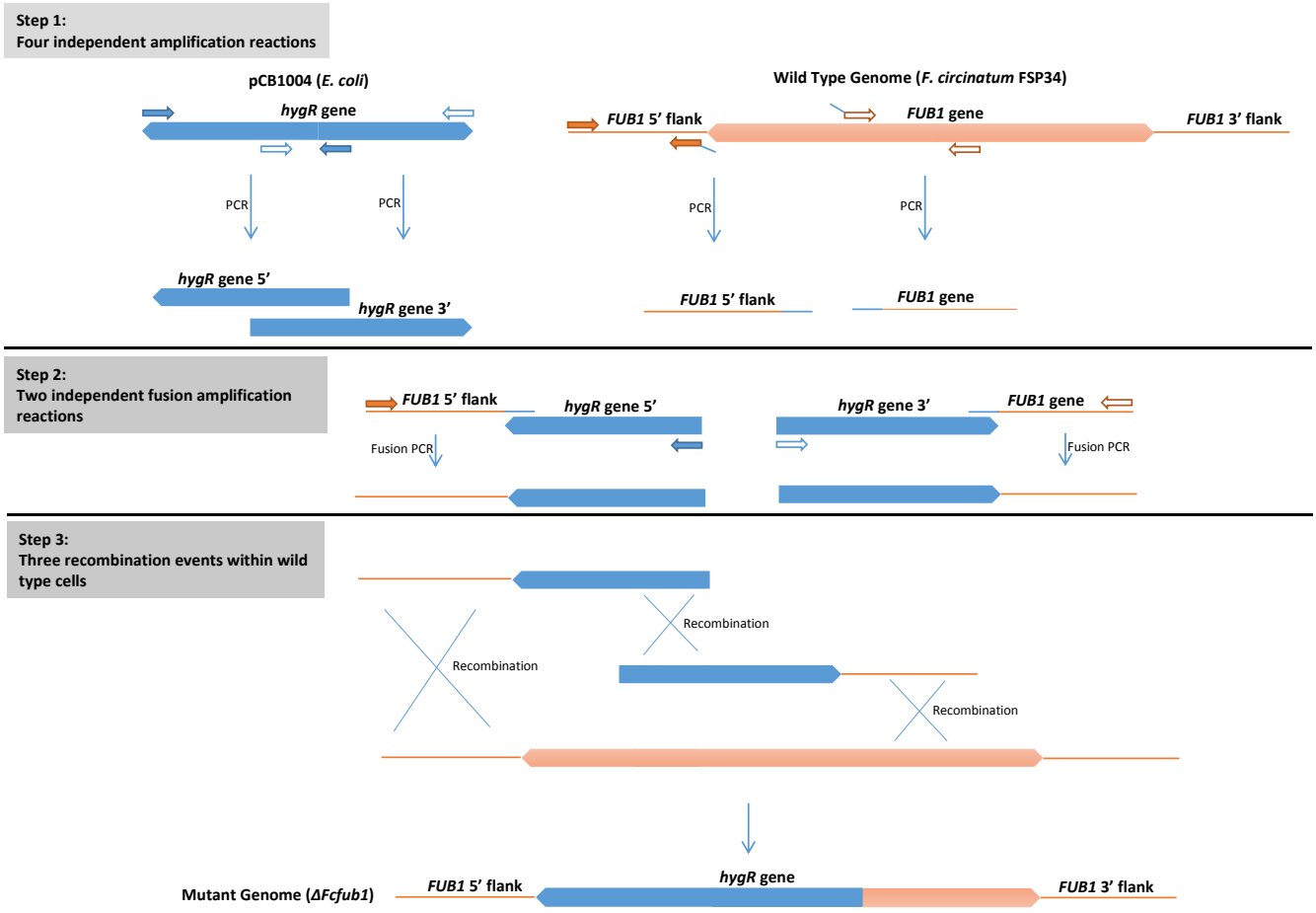

Supplementary figure S1. Split-marker methodology used for the disruption of *FUB1* in the genome of *Fusarium circinatum* wild type (FSP34). Primers pairs used for each amplification reaction are indicated with arrows above and below to the relevant gene region. Blue tails on primers targeting *FUB1* indicate overhangs complementary to the *Escherichia coli* plasmid pCB1004 hygromycin resistance gene (*hygR*).

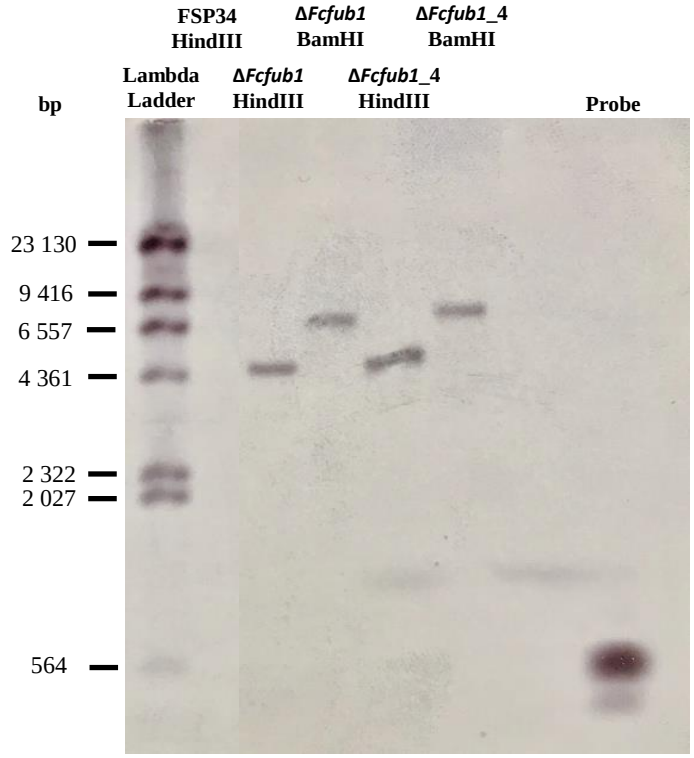

Supplementary figure S2. Southern blot image showing one copy of the hygromycin resistance gene in the genomes of two *F. circinatum fub1* mutants digested with HindIII and BamHI restriction enzymes, and absence of the resistance gene in the genome of the wild type strain FSP34 digested with HindIII.

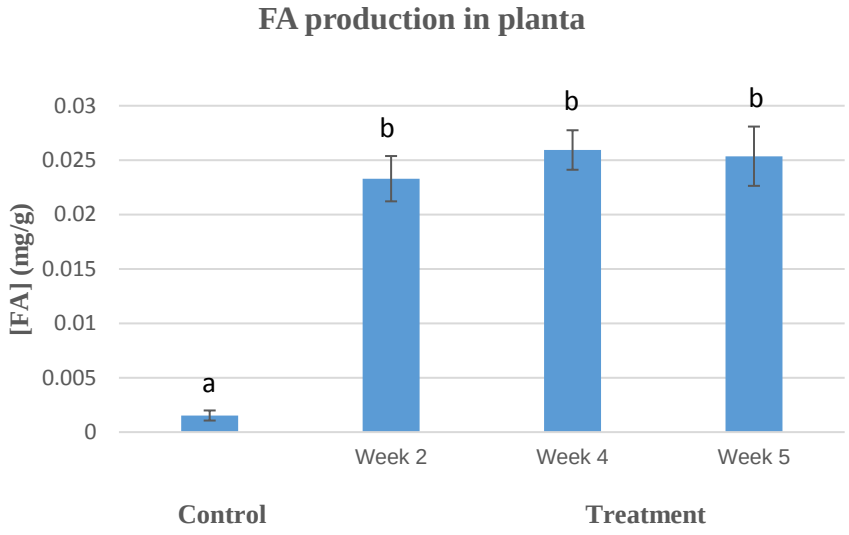

Supplementary figure S3. The amount production of FA produced by *F. circinatum* wild type strain FSP34 in six-month-old *P. patula* seedlings up to five weeks post inoculation. Bars indicate standard error. Different letters above error bars show significant difference between means of the respective treatments and same letters show no significant difference. Statistical significance was tested at $P = 0.05$.

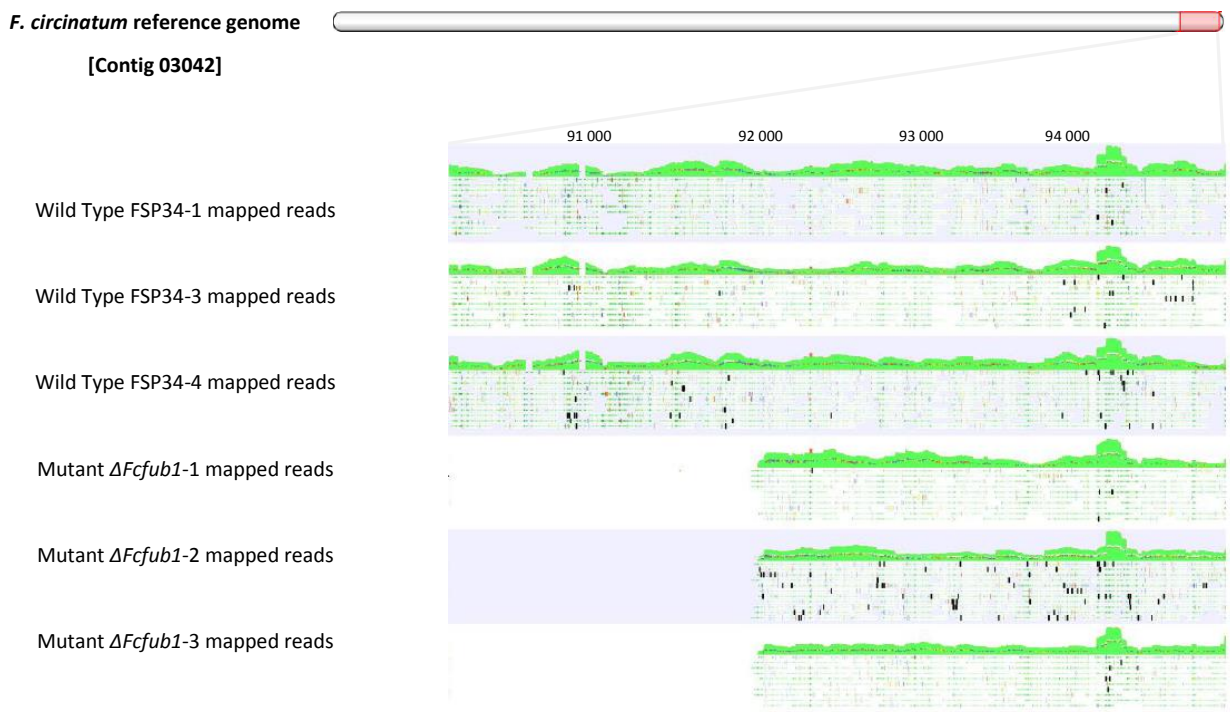

Supplementary figure S4. *F. circinatum* FSP34 wild type and Δ*Fcfub1* knockout mutant RNA-Seq reads mapped to the FSP34 reference genome. The area in knockout mutant strain with no mapped reads demonstrates the disruption of the *FUB1* gene in this strain. Each strain had three replicates. Numbers above aligned reads indicate base position in contig 03042.

Supplementary files

Supplementary file S1. BLAST results of *FUB* and *BIK* genes in the genome of *F. circinatum* using *FUB* and *BIK* gene sequences from *F. verticillioides* and *F. fujikuroi*, respectively.

Supplementary file S2. A file showing significantly downregulated and upregulated DEGs. A Bonferroni value of ≤ 0.05 together with fold change of ≥ 3 for upregulated DEGs and ≤ -3 for downregulated DEGs were used as cut-offs during the identification of genes that were significantly differentially expressed.

Supplementary file S3. A file containing GO terms of downregulated DEGs.

Supplementary file S4. A file containing GO terms of upregulated DEGs.

Chapter 4

Transcriptomic analyses of *ras2* knockout mutant and wild type *Fusarium circinatum* strains: molecular insights into growth, development and virulence

To be submitted to Genes: Phasha, M.M., Wingfield, B.D., Wingfield, M.J., Coetzee, M.P.A., Steenkamp, E.T., 2021.Transcriptomic analyses of *ras2* knockout mutant and wild type *Fusarium circinatum* strains: molecular insights into growth, development and virulence.

Abstract

The fungus *Fusarium circinatum* causes a disease known as pitch canker on *Pinus* spp. in various countries across the globe. Knowledge regarding the molecular basis and mechanisms that govern complex traits such as growth, development, virulence and pathogenicity in this fungus is limited. The Ras2 protein has been reported to regulate these traits in a number of fungi, and this regulation is in a mitogen-activated protein kinase (MAPK) and/or cyclic adenosine monophosphate (cAMP)-dependant manner. The MAPK and cAMP signalling pathways activate many downstream genes that culminate in growth, development, pathogenicity and virulence. The aim of this study was to identify genes under the control of the *RAS2* gene in *F. circinatum* by sequencing and analysing the transcriptomes of a *ras2* knockout mutant (ΔFcras2) and a wild type strain. Comparison of the two transcriptome data sets revealed more than 200 genes that are significantly down regulated in the ΔFcras2. Among these were genes linked to cytokinesis, primary and secondary metabolism and virulence. Particularly interesting genes included a putative gene encoding an ankyrin repeat protein involved in cell structure and shape, genes in the fusaric acid and fusarin C metabolic pathways, a gene encoding the LaeA master transcriptional regulator of metabolic pathways, and candidate virulence genes such as salicylate 1- monooxygenase and trypsin-encoding genes among others. The data also suggest that Ras2 regulates these genes in a MAPK-dependant manner. Collectively, these results will significantly improve our knowledge of the molecular basis and mechanisms of growth, development and virulence in *F. circinatum* and possibly related fungi.

1. Introduction

Fusarium circinatum is a pathogen of *Pinus* species and it is an important threat where these trees grow or are cultivated commercially (Dwinell et al., 1985; Drenkhan et al., 2020). As a result, most previous research on *F. circinatum* sought to identify strategies to reduce its impacts (Wingfield et al. 2008). These studies targeted one or more mechanisms related to pathogenesis in *F. circinatum* (Meng et al., 2009). These include processes relating to the dispersal and arrival of infectious propagules near the *Pinus* host (reviewed by Drenkhan et al., 2020), adhesion to and interaction with the host (e.g., Visser et al., 2019; Swett et al., 2016), as well as infection and invasion of host tissue allowing for symptom development (e.g. Swett et al., 2018; Martín-Rodrigues et al., 2013, Martín-Rodrigues et al., 2015). Genetic studies using sexual crosses of *F. circinatum* further showed that mycelial growth and virulence are quantitatively inherited (De Vos et al. 2011; Slinski et al., 2016). Although this body of work has greatly improved our understanding of the population genetics, infection biology and epidemiology of *F. circinatum*, little is known regarding the molecular mechanisms or particular genes underpinning its ability to cause disease.

The use of forward and reverse genetics has aided the identification and characterization of genes involved in growth, development, pathogenicity and virulence of fungal pathogens (Rauwane et al., 2020). These two, relatively slow, approaches can also be complemented with genomics data to accelerate resolution of the molecular mechanisms underlying fungal pathogenesis. This is especially true given the increasing availability of whole genome sequence information for taxa across the fungal Tree of Life (Grigoriev et al., 2014). Indeed, access to genome sequence information has accelerated the identification of many genes involved in pathogenicity and virulence, as well as disease development in *Fusarium* species (Ma et al., 2010; Ma et al., 2013; Rep and Kistler, 2010).

The process of gene discovery can be fast-tracked with the incorporation of transcriptomic information (Tan et al., 2009; Meijueiro et al., 2014). In this case, the involvement of large sets of genes across the spectrum of pathogenesis-related processes can be gleaned from mRNA expression patterns under controlled conditions (e.g., Ellison et al., 2014; Wang et al., 2009; Gasch et al., 2000). For example, transcriptome studies using different races of the banana pathogen *Fusarium oxysporum* forma specialis *cubense* allowed for the identification of genes involved in pathogenicity and virulence, especially regarding adhesion and invasion of the host, and the molecular signalling pathways mediating these processes (Guo et al., 2104).

One of the effective means of using gene expression studies to understand gene function in pathogens is by utilizing knockout mutants. In *Fusarium*, analyses of such mutants with northern blotting and quantitative reverse-transcriptase polymerase chain reaction (RT-qPCR) have revealed not only gene function, but also entire gene networks implicated in the regulation of growth, pathogenicity and virulence (Wiemann et al., 2009; Bluhm et al., 2007; Brown et al., 2012; Lengeler et al., 2000; Hu et al., 2014). In the case of major regulatory genes, studies of knockout mutants using high-throughput RNA-Seq data are exceptionally powerful in that they enable discovery and detailed analysis of downstream targets and potentially the resolution of entire signalling pathways (e.g., Gilbert et al. 2016; Tannous et al., 2018; Jones et al., 2019). These often include regulators of mitogen-activated protein kinase (MAPK) and cyclic adenosine monophosphate (cAMP) signalling cascades, which play essential roles in many of the pathogenesis mechanisms employed by plant pathogens (e.g., Pham et al., 2015; Li et al., 2017; Wang et al., 2016; Zhang et al., 2020).

Owing to their important biological roles, the MAPK and cAMP pathways are the most widely studied signalling cascades in fungi and other eukaryotes (Lowy, 1993). The individual components (i.e., genes and proteins) of these pathways have received considerable attention in model fungi such as *Saccharomyces cerevisiae* (Toda et al., 1985; Mosch et al., 1996) and *Candida albicans* (Leberer et al., 2001), as well as various pathogens including *Fusarium* species (reviewed by Stepien and Lalak-Kanczugowska, 2020). The cAMP pathway includes adenylate cyclases that catalyse the conversion of adenosine triphosphate into cAMP, an intracellular messenger that activates regulatory proteins such as protein kinase A (PKA), which in turn phosphorylate downstream proteins, including transcription factors, to ultimately modulate one or more physiological processes (Turra et al., 2014). In the MAPK pathway, this modulation of physiological processes is achieved by sets of three protein kinases, whose sequential activation by phosphorylation leads to the activation of downstream proteins, which may also include transcription factors (Turra et al., 2014). Both pathways affect pathogenesis and a range of other processes (e.g., vegetative growth, cellular development, sexual mating) in *Fusarium* (Stepien and Lalak-Kanczugowska, 2020), where they can be activated in parallel or independently depending on the transduced signal (Lengeler et al., 2000).

The MAPK and cAMP pathways can be activated by the Ras2 protein, making it a master regulator of most cellular processes in eukaryotes (Lowy, 1993; Toda et al., 1985; Mosch et al., 1996; Leberer et al., 2001). In some plant pathogenic fungi, the gene encoding Ras2 (*RAS2*) is a well-characterized growth and virulence gene (Lengeler et al., 2000). This is also true for *Fusarium* species such as *F. circinatum*

and *F. graminearum* (Bluhm et al., 2007; Phasha et al., 2021). However, Ras2 may affect these pathways and their individual components differently, depending on the species and conditions (Lengeler et al., 2000). For example, deletion of *RAS2* in *C. albicans* reduces the expression of genes in both MAPK and cAMP pathways, but only one of the three protein kinases in the relevant MAPK module of *F. graminearum* is affected upon *RAS2* deletion (Leberer et al., 2001; Bluhm et al., 2007).

Although *RAS2* behaves as a virulence gene in *F. circinatum* (Phasha et al., 2021), the signalling pathway by which it controls growth and virulence is not known. Thus, knowledge of the downstream molecular processes (especially those involving transcriptional regulators) under the control of Ras2 is lacking for the pathogen. The aim of this study was consequently to identify the genes in which expression is affected by Ras2 in *F. circinatum* and to use these data to determine the signalling pathway(s) by which this protein modulates physiological changes. This was achieved using an RNA-Seq study of a *F. circinatum* wild type strain together with its corresponding *ras2* knockout (ΔFcras2) mutant strain. Results from this study will increase our knowledge and understanding of the molecular basis and mechanisms of growth, development, virulence and pathogenicity, not only in *F. circinatum* but also in fungi in general.

2. Methods

2.1. Fungal strains, RNA extraction, library preparation and sequencing

Three strains of *F. circinatum* were used. These included two mutant strains that were produced previously using wild type strain FSP34 (CMW53647) (Phasha et al., 2021) and the wild type strain FSP34. The mutant strains were assigned isolate CMW53644 that represents the *ras2* knockout mutant strain ΔFcras2 and isolate CMW53645 representing the *ras2* complementation mutant strain ΔFcras2C. Strain ΔFcras2 together with wild type strain FSP34 were the primary strains used in the comparative analyses, while strain ΔFcras2C was used to examine the reliability of expression data analysed. All three isolates used here have been deposited in the culture collection (CMW) of the Forestry and Agricultural Biotechnology Institute (FABI) at the University of Pretoria (Pretoria, South Africa).

For RNA extraction, the strains were grown, in triplicate, on half-strength Potato Dextrose agar medium with a layer of cellophane placed on the agar surface for five days at room temperature (25°C). Total RNA was extracted from each of the cultures using the RNeasy Plant Mini Kit (Qiagen) and to prevent degradation of the extracted RNA, 1 µl of Ribo Lock (Thermo Fisher Scientific) was added to each sample. From 100 ng of total RNA, mRNA was then extracted using the Dynabeads® mRNA DIRECT™ Micro Kit (Thermo Fisher Scientific). The captured mRNA was eluted in 10 µl nuclease-free water and

used to construct cDNA libraries. This was done using the Ion Total RNA-Seq Kit v2 (Thermo Fisher Scientific), which involved fragmentation of 10 µl of poly(A) RNA with RNAse III, purification of the fragmented RNA using a magnetic bead clean-up module and elution in 12 µl nuclease-free water. The purified RNA was then concentrated to a 3 µl volume and ligated to RNA Xpress Barcoded adapters. The adaptor-ligated RNA was reverse transcribed to generate first strand cDNA libraries, after which the cDNA products were amplified to generate double stranded cDNA libraries. The libraries were assessed for quantity and fragment size distribution on a BioAnalyser 2100 using the High Sensitivity DNA chip and reagent kit (Agilent Technologies).

The barcoded cDNA libraries were converted to single stranded libraries and enriched to prepare them for sequencing. To achieve this, the barcoded libraries were each diluted to a concentration of 80 pM and pooled in multiples of three for template preparation using the Ion Torrent™ Ion 540™ Chef Kit (Thermo Fisher Scientific). For each of these pools, a volume of 25 µl was loaded onto the Ion Chef instrument for template preparation and enrichment using Ion 540™ Chef reagents, solutions and supplies protocol (Thermo Fisher Scientific). Enriched templates were loaded onto an Ion 540™ Chip using the Ion Chef instrument (Thermo Fisher Scientific). Sequencing of each chip was performed on an Ion S5™ System (Thermo Fisher Scientific) at the Central Analytical Facility of Stellenbosch University. Signal processing and base-calling analyses were also performed at this facility using the Torrent Suite Software (TSS; version 5.10.0) with default parameters.

2.2. RNA-Seq data and differential expression analysis

For each sequencing run, Binary Alignment Mapping (BAM) files were filtered for polyclonal reads and trimmed for poor quality nucleotides and barcodes using the Torrent Suite Version 5.10.0 Software. A metadata table was then constructed in Microsoft Excel that contained the BAM file name of each sample and experimental information associated with the BAM file. The metadata table, together with the BAM files containing sequence data were then imported into the CLC Genomics Workbench 12.0 (Qiagen). In addition, the reference genome of *F. circinatum* strain FSP34 (NCBI accession AYJV00000000), along with its gff annotations, were imported into CLC Genomics Workbench.

The RNA-Seq Analysis Tool in CLC Genomics Workbench was used with default parameters to quantify and analyse gene expression in the wild type, knockout mutant and complement mutant strains. This tool enabled mapping the reads for each sample (in triplicate) to the FSP34 reference genome. The Differential Expression Tool with default parameters was then used to compare the expression levels of the genes of

the three strains in a pairwise manner. Further analyses were mainly performed on genes that were significantly differentially expressed between the knockout mutant and wild type strains.

A relatively conservative approach was used to identify differentially expressed genes (DEGs), and only those for which the three replicate samples yielded a mean fold change of ≥3 and a Bonferroni value of ≤0.05 were considered. To assess the reliability of the expression data, we analysed expression for the *RAS2* gene (FCIRG_08573) as well as three randomly selected housekeeping genes (FCIRG_06968, FCIRG_00112 and FCIRG_01366) encoding superoxide dismutase mitochondrial precursor 2, tyrosyl tRNA synthetase and mitochondrial import inner membrane translocase subunit TIM16, respectively, in the three strains. We also investigated the arrangement of DEGs in the genome of *F. circinatum*. For this purpose, the contigs on which DEGs were found were analysed. Contigs harbouring the DEGs were linked to chromosomes using a scaffold version of the *F. circinatum* genome.

2.3. Functional annotation of DEGs

Protein families and molecular functions (MFs) encoded by DEGs were determined. This was done using the Blast2Go plugin in CLC Genomics Workbench. First, mRNA annotations of the DEGs were extracted from the *F. circinatum* reference genome using the Annotations Tool. This was followed by conversion of the transcripts to protein sequences, after which the protein sequence list was converted into a Blast2GO Project. These sequences were then compared to known fungal protein sequences in the database of the National Center for Biotechnology Information (NCBI; https://www.ncbi.nlm.nih.gov/guide/proteins/) using the Blast2Go Cloud Blast function. Results from these Blastp searches were then used to perform InterProScan analysis, gene ontology (GO) mapping, and gene annotation. To obtain graphical representations of these results, the Statistics Tool of Blast2Go was used.

2.4. DEGs with potential roles in pathogenesis

Using the results generated from Blast2Go, DEGs potentially encoding proteins involved in *F. circinatum* pathogenesis were identified. For this purpose, the focus was on genes in which expression was negatively impacted by the deletion of *RAS2* (i.e., downregulated) and were thus likely involved in growth, development, virulence and pathogenicity. This was done by analysing the fold change levels of the DEGs, coupled with the descriptions of the proteins within the Blast2Go results. The possible function of candidate proteins was then further deciphered by considering their roles in other fungal species.

2.5. Analysis of MAPK and cAMP pathway components

The putative pathways used by Ras2 to regulate growth, development, virulence and pathogenicity in *F. circinatum* were investigated. To achieve this, genes that encode proteins forming part of the MAPK and cAMP pathways associated with growth, development and pathogenicity in *Fusarium* other fungi were searched in the *F. circinatum* genome using CLC Genomics Workbench's local BLASTn tool, and their expression patterns were analysed in the knockout mutant and wild type strains. Three genes encoding the main proteins of the MAPK pathway, and two encoding the main components of the cAMP pathway in other *Fusarium* species were used. The three genes of the MAPK pathway included *F. fujikuroi* MAPKKK gene FFUJ_13563, *F. fujikuroi* MAPKK gene FFUJ_08617, and *F. verticillioides* MAPK gene FVEG_03043. The two genes of the cAMP pathway included the *F. oxysporum* adenylate cyclase gene FOYG_07227 and the *F. oxysporum* PKA gene FOYG_02727. Furthermore, we searched for and analysed the expression of two genes known to play a role in gene expression regulation. They included *laeA* that encodes the master transcriptional regulation LaeA (Bok and Keller, 2004) and the gene that encodes arginyl tRNA synthetase that is known to form complexes with Ras2 in eukaryotes (Park et al., 2008).

3. Results

3.1. RNA-Seq data and identification of DEGs

Barcode trimming and quality filtering resulted in the retention of 72 % of the original sequence data generated per Ion 540™ Chip. Each strain had at least 17 million reads per replicate, and the mean length of the reads was 152 bp. RNA-Seq analysis of these data showed numerous genes that appeared to be differentially expressed between the knockout mutant strain ΔFcras2 and the wild type strain FSP34 using the three replicates of each strain. Of these, the majority were downregulated in the knockout mutant strain ΔFcras2 (Figure 1; Supplementary file S1). In total, 436 genes displayed mean fold changes of ≥3 and Bonferroni values of ≤0.05. Of these DEGs, 300 were downregulated (-3.0 to -652.3 mean fold change) and 136 upregulated (3.1 to 63.4 mean fold change) in the knockout mutant (Supplementary file S2). Together, these genes accounted for approximately 3% of the *F. circinatum* genome. The *RAS2* gene (FCIRG_08573) was not expressed in the knockout mutant (Table 1) as no true reads were detected for the gene in the three replicates of this strain (Supplementary file S2). By contrast, the replicates of the complement mutant strain ΔFcras2C had an average of 725 reads, while those of the wild type strain had 1062 reads on average for the *RAS2* gene. Expression data of the three housekeeping genes assessed in this study (FCIRG_06968, FCIRG_00112 and FCIRG_01366 encoding superoxide dismutase mitochondrial precursor 2, tyrosyl tRNA synthetase and mitochondrial import inner membrane

translocase subunit TIM16, respectively) showed that there were no significant differences (i.e., Bonferroni = 1.00, Table 1) when the knockout and complement strains were each compared to the wild type strain in all replicates (Table 1). Collectively, the expression data of the *RAS2* and housekeeping genes illustrate the reliability of the RNA-Seq data generated in this study.

Analysis of the arrangement of DEGs in the genome of *F. circinatum* showed that nearly 50% (141 out of 300) of the downregulated DEGs were located next to each other. These DEGs were distributed across 51 contigs (Supplementary file S3), which were located across the 11 chromosomes of *F. circinatum* (Figure 2). The downregulated DEGs were arranged in clusters of two to nine genes, either in tandem or separated by one or a few other genes (Supplementary file S3). Chromosome 3 had the greatest number of such clusters and chromosome 2 had the least (Figure 2). There were eight clusters (constituting of 32 downregulated DEGs) on chromosome 3, and only one with two genes on chromosome 2 (Supplementary file S3; Figure 2). The fusarin C and fusaric acid biosynthesis gene clusters (see below) reside on Chromosome 3, and were separated by seven genes (FCIRG_00344 to FCIRG_00350), none of which were differentially expressed. Fold change levels of downregulated DEGs belonging to the same cluster followed a similar trend in numerous cases (Figure 2; Supplementary file S3).

A small number (18%) of upregulated DEGs arranged contiguously were found. Nine contigs contained clusters of upregulated DEGs (Figure 2; Supplementary file S3), and these were distributed across the chromosomes of *F. circinatum* excluding chromosomes 3, 6 and 10 (Figure 2; Supplementary file S3). In total, 25 upregulated DEGs were located across the nine contigs, and were arranged in clusters of two to six genes, mostly separated by other genes (Supplementary file S3). All chromosomes had only one cluster except chromosome 4, which had two (Supplementary file S3; Figure 2). The upregulated DEGs belonging to the same cluster mostly had dissimilar levels of expression (Supplementary file S3).

3.2. Functional annotation of DEGs

Blast2GO analysis allowed functional annotation of only 177 of the 436 DEGs, with the remaining 259 lacking GO terms or sufficient annotation data. InterProScan analyses of the former showed that the downregulated and upregulated DEGs formed part of 19 protein families (Figure 3). Overall, the downregulated and upregulated DEGs had fold change patterns ranging between -4.4 to -18.5 and 3.5 to 16.2, respectively. (Table 2; see Supplementary file S4 for GO terms of the downregulated and upregulated DEGs). For the domains encoded, there was some overlap between these two groups as both included a number of proteins with domains belonging to the flavin/nicotinamide adenine (phosphate)

(FAD/NAD[P])-binding domain, major facilitator and cytochrome P450 superfamilies. Families unique to the downregulated DEGs included the NADP-dependent oxidoreductase domain superfamily, sugar transporters, acyl carrier protein (ACP)-like superfamily, as well as methyl and acetyl transferases (Figure 3A). On the other hand, flavin monooxygenases, zinc zipper protein 1 (ZPR1), as well as peptidoglycan and glycoside deacetylases were among the protein families unique to the upregulated DEGs (Figure 3B).

Blast2GO identified 20 MFs among the proteins encoded by the downregulated DEGs (Figure 4 Graph A), while 10 MFs were identified for the upregulated DEGs (Figure 4 Graph B). MFs in common between the two groups of DEGs were ion binding, oxidoreduction, ligation, lysis, proteolysis, hydrolysis, transmembrane transport and DNA binding. Among these, there were 49 downregulated oxidoreductase genes with fold changes of between -3.0 and -35.8, while only 12 oxidoreductase genes were upregulated with fold changes ranging from 3.5 to 22.4 (Supplementary file S5). Similar patterns were observed for ligases, lyases, peptidases, hydrolases, transmembrane and ion binding MF groups where the number of downregulated DEGs were more than that of upregulated DEGs. The DNA binding MF group was an exception as there were three upregulated DEGs and only two downregulated DEGs (Figure 4). Furthermore, the downregulated DEGs encoded proteins of other MF groups that were not found in the upregulated DEGs (Figure 4). These unique MF groups included proteins such as ATPases, transferases, isomerases, nucleases and RNA binding proteins (Figure 4). Genes encoding these proteins had fold changes ranging from -3.0 to -40.1 (Table 3), and those encoding proteins with transferase activity were the highest in number (Table 3). The upregulated DEGs did not encode proteins with unique molecular functions.

3.3. DEGs with potential roles in pathogenesis

DEGs that encode putative proteins involved in the growth, development, virulence and pathogenicity of *F. circinatum* were identified (Figure 5). Among DEGs downregulated in the *ras2* knockout mutant, six encoded products potentially involved in growth (i.e., hyphal growth, cytokinesis, protein synthesis and conidiation) (Osherov and May, 2000; Zhang et al., 2016; Roberts and Yanofsky, 1989; Jeong et al., 2001). These included a putative protein- related to vegetative incompatibility protein HET-E-1 (encoded by FCIRG_05857), a putative structural constituent of ribosome (SCR) protein (FCIRG_03394), a putative methyltransferase LaeA encoded by *laeA* (FCIRG_12923), as well as a putative conidiation-specific expression (CSE) protein (FCIRG_10564). These proteins were downregulated 12.5, 15.7, 12.8-fold, and 10.2, respectively. The remaining two growth-linked DEGs encoded a putative ankyrin repeat

protein (FCIRG_05938) and an ankyrin protein linked to membrane biogenesis (FCIRG_10318), with fold changes of -652.3 and -11.37, respectively.

At least 20 DEGs were shown to encode products potentially involved in secondary metabolism. Four DEGs involved in secondary metabolism included a putative non-ribosomal peptide synthetase (NRPS; FCIRG_09287), a putative NRPS MxcG (component of the myxochelin iron transport regulon; FCIRG_03382), a putative enniatin synthetase (FCIRG_01589), and a putative KP4 killer toxin (FCIRG_05861) downregulated 3.8-, 10.8-, 19.5- and 17.7-fold, respectively. The remaining secondary metabolism-linked DEGs all encoded components of the fusaric acid and fusarin C biosynthesis gene clusters (Table 4). DEGs in the fusarin C cluster were downregulated at fold changes of between -3.0 to -6.3 and those of the fusaric acid cluster were downregulated 6.1- to 11.2-fold in the *ras2* knockout mutant. In both these cases, the DEGs included those encoding the core biosynthesis enzymes, i.e., polyketide synthase/NRPS Fus1 (FCIRG_00355, -3.7 fold change) and polyketide synthase Fub1 (FCIRG_10013 and FCIRG_00343, -7.8 fold change), respectively.

At least 12 DEGs encoded products potentially involved in plant tissue digestion, cellular defence response and transport (Asai and Shirasu, 2015; Dubovenko et al., 2010; Buswell et al., 1979; Bateman and Basham, 1976; Sorensen et al., 2013; Andrew et al., 2009; de Waard et al., 2006). Those involved in plant tissue digestion included a putative salicylate 1-monooxygenase (FCIRG_02254), a putative trypsin (FCIRG_03855), a putative 5-carboxyvanillate decarboxylase (FCIRG_02256), a probable endo-polygalacturonase 6 (FCIRG_12189), a putative beta-glucosidase (FCIRG_09516), a probable beta-glucosidase 1 precursor (FCIRG_00913), and a putative protein related to aliphatic nitrilase (FCIRG_01666). Of these, the salicylate 1-monooxygenase was the most downregulated at 90.3-fold, followed by trypsin and the endo-polygalacturonase 6 at 55.9- and 49.0-fold, respectively, in the *ras2* knockout mutant. The NRRL 32931 beta-glucosidase and beta-glucosidase 1 precursor were downregulated 27.3- and 16.1-fold while the aliphatic nitrilase had a fold change of -13.4. DEGs encoding proteins with functions in cell defence response and transport included an ABC transporter CDR4 (FCIRG_08070), a putative tartrate transporter (FCIRG_08690), a putative protein related to benzoate 4-monooxygenase cytochrome P450 (FCIRG_08224), a putative multidrug resistance protein (FCIRG_01587), a putative protein related to glutathione S-transferase II (FCIRG_00004), and a putative chymotrypsin-elastase inhibitor ixodidin (FCIRG_12139), which had fold changes of -10.8,-42.4, -14.4, -9.2, -15.5 and -15.8, respectively.

3.4. Analysis of MAPK and cAMP pathway components

Three genes constituting the MAPK pathway (Hou et al., 2002; Zhang et al., 2011; Ding et al., 2015), and two constituting the cAMP pathway (Choi and Xu, 2010; Kim et al., 2001) that are associated with growth, development and pathogenicity in other *Fusarium* species were identified in the genome of *F. circinatum*. For the MAPK pathway, gene FCIRG_11025 (homologous to the *F. fujikuroi* MAPKKK gene), gene FCIRG_10336 (homologous to the *F. fujikuroi* MAPKK gene), and gene FCIRG_04394 (homologous to the *F. verticillioides* MAPK gene) were identified (Figure 6). For the cAMP pathway, gene FCIRG_06741 (homologous to the *F. oxysporum* adenylate cyclase gene) and gene FCIRG_14034 (homologous to the *F. oxysporum* PKA gene) were identified (Figure 6).

Because of the stringent criteria used for identifying genes that are differentially expressed in this study, none of the significant DEGs identified included the aforementioned genes. However, analysis of the RNA-Seq data suggested that the signalling pathway through which the Ras2 protein controls growth, development, virulence and pathogenicity in *F. circinatum* is the MAPK pathway. This is because expression of the gene encoding MAPK (FCIRG_04394) was 2.5 times less expressed in the *ras2* knockout mutant than in the wild type, which represented a significant difference at a False Discovery Rate (FDR; Benjamini and Hochberg, 1995) p-value of 0.00028 (Table 5; Supplementary file S1). By contrast, the PKA gene (FCIRG_14034) of the cAMP pathway appeared to be downregulated 1.2 times in the mutant, but this was not statistically significant with a FDR p-value of 0.582573 (Table 5; Supplementary file S1). Further analysis of the total read counts of the MAPK and PKA genes in the three replicates of the knockout mutant and wild type strains showed that the MAPK gene had reduced expression in all three replicates (i.e., 771, 1476 and 812) of the knockout mutant compared to the wild type strain (i.e., 2515, 3741 and 5797), while this was not the case for the PKA gene (i.e., 776, 917, 1135 for the mutant and 1113, 2097 and 2244 for the wild type; Table 5, Supplementary file S1). Furthermore, analysis of the RNA-Seq data suggested the other genes of the two pathways were not differentially expressed when FDR p-values and total read counts of all replicates of each strain were taken into account (Table 5; Supplementary file S1).

Two genes encoding products known to interact with Ras2 were significantly downregulated in the *ras2* knockout mutant. The one was FCIRG_12923 that is a homolog of *laeA* encoding the methyltransferase LaeA transcriptional regulator (Bok and Keller, 2004; Figure 6). The other was FCIRG_00125 which encodes a homolog of the arginyl tRNA synthetase that reportedly forms complexes with Ras2 in eukaryotic cells (Park et al., 2008, Figure 6). The *laeA* gene was downregulated 12.8-fold in the *ras2*

knockout mutant, while the arginyl tRNA synthetase gene was not expressed in this strain, corresponding to a fold change of -213.0 (Supplementary file S1). In FSP34, the latter gene had an average of 135 reads for the three replicates (Supplementary file S1).

4. Discussion

In this study, the genes regulated by Ras2 in *F. circinatum* were investigated using transcriptomic data from a *ras2* knockout mutant strain (ΔFcras2) alongside the wild type strain FSP34. The Ras2 protein is a master regulator of cellular processes in eukaryotes **(**Boguski and McCormick, 1993**)** and a number of fungal *ras2* mutants have been generated and their phenotypes studied (Leberer et al., 2001; Lengeler et al., 2000; Bluhm et al., 2007; Phasha et al., 2021). However, in most cases, the downstream genes regulated by Ras2 have not been well catalogued. Results of the present study thus enabled the identification of a large number of *F. circinatum* genes downstream of, and consequently regulated by, Ras2.

RNA-Seq analysis of the *F. circinatum ras2* knockout mutant and wild type strains revealed that the expression of more than 400 genes, with diverse functions, differed significantly between the two strains. Studies in other fungi based on RNA-Seq analyses of knockout mutants have also reported significant down- and upregulation of several genes when master transcriptional regulators were knocked out (Gilbert et al. 2016; Tannous et al., 2018; Jones et al., 2019). For example, a study on a mutant of the global regulator of carbon catabolism CreA in *Penicillium expansum* found that 399 genes under the control of this protein were differentially expressed between the mutant and wild type strains (Tannous et al., 2018).

Of the *F. circinatum* DEGs identified, 70% were downregulated in the mutant strain. This was not surprising because the phenotypes controlled by *RAS2*, especially growth and pathogenicity, are known to be multigenic traits in *F. circinatum* (De Vos et al., 2011; Slinski et al., 2016). The fact that 30% of the DEGs were upregulated in the *ras2* knockout mutant was also not unexpected as similar findings have been reported for deletion of regulatory genes in other fungi (Choi and Shim, 2008; Wang et al., 2014). It is thought that upregulated genes following gene deletion usually compensate for downregulated genes with a similar function, especially if their products belong to the same protein family (Kafri et al., 2009). Examples emerging from the present study are those encoding products belonging to the FAD/NAD(P)-binding domain, major facilitator and cytochrome P450 superfamilies for which some were upregulated and others downregulated, at similar levels of expression. These results suggest that while the deletion of the *RAS2* caused downregulation of genes encoding certain proteins, those encoded by the upregulated

genes likely compensated for the primary metabolism and transport functions lost, thereby keeping the knockout mutant viable.

Protein families unique to the downregulated and upregulated DEGs were identified in this study. Families unique to the downregulated DEGs included the ACP (acyl carrier protein)-like superfamily as well as the methyl and acetyl transferase superfamilies. ACP-like superfamily proteins play a role in fatty acid synthesis and activation of polyketides such as toxins (Hopwood and Sherman, 1990), while acetyl and methyl transferases play a role in the formation of euchromatin and heterochromatin, which are the active and inactive states of DNA allowing or inhibiting transcription, respectively (Javaid and Choi, 2017). Families unique to upregulated DEGs included a flavin monooxygenase, peptidoglycan deacetylase and ZPR1 (zinc zipper protein). Flavin monooxygenases are involved in detoxification and secondary metabolism (Van Berkel et al., 2006), while peptidoglycan deacetylases are involved in cell wall structure and evasion of host defence response (Aragunde et al., 2018). ZPR1 proteins are signalling molecules and activators of cell growth and proliferation (Gangwani et al., 1998; Nakamura et al., 2012). Therefore, the unique downregulated genes might explain why the knockout mutant strain (Phasha et al., 2021) is not as virulent in comparison to the wild type strain, while the unique upregulated DEGs provided the mutant strain with a sufficient molecular arsenal to infect and colonize the host to a certain extent as reported in our previous study (Phasha et al., 2021).

Functional annotation of DEGs revealed a number of genes and molecular processes potentially underlying the conidiation and conidium germination phenotypes previously observed in a *RAS2* deletion mutant of *F. circinatum* (Phasha et al., 2021). Although *RAS* genes, and specifically *RAS2*, are known to play roles in these two processes in various fungi (e.g., Som and Kolaparthi 1994; Van Leeuwen et al., 2013), the mechanisms and downstream genes they control are generally not well resolved. However, our collection of DEGs contained three proteins for which expression is dependent on Ras2 and might determine these phenotypes. The three DEGs encode the following putative proteins: a CSE protein, a methyltransferase LaeA, and a SCR protein, which were respectively downregulated 10 to 15-fold in the *ras2* knockout mutant. The *F. circinatum* CSE protein was most homologous to the *con10* gene product of *F. austroafricanum*, although the two proteins were identical in only the first 19 amino acids, which likely represents an important functional motif for this protein (Roberts and Yanofsky, 1989). Homologs of the CSE gene also play a role in conidial development in *Neurospora crassa* (Roberts et al., 1988), as well as hyphal growth in *Aspergillus nidulans* (Miller et al., 1987). LaeA is essential for conidiation in asexual development in *Penicillium oxalicum*, where deletion of the *laeA* gene impairs conidiation

(Zhang et al., 2016). In terms of conidial germination, neither *laeA* nor *con10* appears to play a role in the process (Van Leeuwen et al., 2013; Zhi et al., 2019), but protein synthesis is essential for conidial germination (Osherov and May, 2000) and potentially involves the SCR protein. Therefore, possible roles for *laeA, con10* and the SCR gene in conidial germination in *F. circinatum* remain to be examined using functional genetic studies, especially experiments exploring their activities in *RAS2* mutant and wild type backgrounds.

The reduction in growth rate and virulence caused by deletion of *RAS2* in *F. circinatum* (Phasha et al., 2021) may be due to the role Ras2 plays in regulating ankyrin-related genes involved in cytokinesis. One of the DEGs identified encodes a putative ankyrin protein linked to membrane biogenesis, which was downregulated 11-fold in the knockout mutant. Also, the most downregulated (652-fold) DEG in the mutant encoded a putative ankyrin repeat protein homologous to Cdc10 of *S. cerevisiae,* which has septin activity, thus forming filaments that become part of the cytoplasmic membrane during cytokinesis (Jeong et al., 2001). In *F. graminearum,* Cdc10 is involved in the control of septum formation and nuclear division (Chen et al., 2016). In *Ustilago maydis* septins, together with G-proteins such as Ras, further determine cell shape (Becht et al., 2006; Mahlert et al., 2006). Indeed, the asymmetrical colonies formed by our *ras2* knockout mutant of *F. circinatum* points towards a cell shape defect (Phasha et al., 2021). Therefore, via these ankyrin proteins, Ras2 likely determines the division and structure of cells for efficient growth and ultimately host infection and disease progression in *F. circinatum* (Wang and Lin, 2012).

Results of this study suggest that Ras2 is an important regulator of secondary metabolism in *F. circinatum*. It potentially affects the expression of as many as six secondary metabolites. Evidence for this was in the reduced expression in the *ras2* knockout mutant of transcripts coding for proteins known to be involved in the uptake and/or secretion of ions into and out of fungal cells (Silakowski et al., 2000; Gage et al., 2001; Prosperini et al., 2017; Khan et al., 2018; Lopez-Diaz et al., 2018). These included a putative MxcG NRPS known to produce a siderophore that binds and stores iron (Silakowski et al., 2000; Khan et al., 2018), polyketide synthase producing fusaric acid that chelates metal ions in host cells (Lopez-Diaz et al., 2018), enniatin synthetase producing an ionophore that pumps cations across membranes (Prosperini et al., 2017), and KP4 killer toxin that chelates calcium to block its uptake (Gage et al., 2001). These compounds potentially provide *F. circinatum* with a competitive advantage during interactions with other organisms, particularly its host plant, by either restricting their access to essential ions or by affecting ionic gradients across their cell membranes (Gage et al., 2001; Prosperini et al., 2017;

Lopez-Diaz et al., 2018). Such processes, together with their phytotoxic effects on plant cells, likely also contribute to the role of these compounds in virulence, because deletion of genes responsible for their production negatively affects the ability of pathogens to induce disease symptoms (Herrmann et al., 1996a; Lopez-Diaz et al., 2018; Eranthodi et al., 2020; Lu and Faris, 2019). Collectively, these data suggest that Ras2 contributes to the virulence of *F. circinatum* by regulating the expression of secondary metabolites that give the fungus an advantage during infection.

Although less downregulated compared to the other genes encoding the proteins discussed above, it was surprising that genes of the fusarin C biosynthesis gene cluster were altogether downregulated in the *ras2* knockout mutant of *F. circinatum*. Wiemann et al. (2013), as well as a preliminary study conducted by us, found that *F. circinatum* wild type strain FSP34 does not produce fusarin C. It is worth noting that these studies were performed in culture, therefore it is possible that production of fusarin C does occur *in planta*. If detected *in planta*, it would be interesting to determine whether this metabolite contributes to *F. circinatum* pathogenicity because, to the best of our knowledge, fusarin C is a mutagen with no proven role in the pathogenesis of its producers such as *F. fujikuroi* and *F. verticillioides* (Gelderblom et al., 1986; Diaz-Sanchez et al., 2012; Brown et al., 2012; Ismaiel and Papenbrock, 2015).

The RNA-Seq data presented here showed that *F. circinatum* Ras2 likely regulates an arsenal of proteins involved in the digestion of plant-derived compounds. One of the genes that was most highly downregulated in the *ras2* knockout mutant encoded a putative salicylate 1-monooxygenase, which is known to degrade the plant hormone salicylic acid (Katagiri et al., 1966). Such an impairment of the plant's defence response by utilizing the hormone as carbon source (Metraux et al., 1990; Asai and Shirasu, 2015) might thus contribute to the virulence of *F. circinatum* and its ability to colonize host tissue. However, digestion of salicylic acid in this way is positively correlated with virulence only in some fungi (Wadke et al., 2016; Rabe et al., 2013; Rocheleau et al., 2019). Other digestive enzymes that are apparently dependent on Ras2 for expression in *F. circinatum* includes peptidases such as trypsin and enzymes that depolymerize plant cell wall components such as cellulose, lignin and pectin (i.e., 5-carboxyvanillate decarboxylase, beta-glucosidase and beta-glucosidase, and endo-polygalacturonase, respectively). These enzymes are known to contribute to a pathogen's ability to penetrate and colonize its plant host (Dubovenko et al., 2010; Have et al., 1998; Buswell et al., 1979; Peng et al., 2002; Bateman and Basham, 1976; Sorensen et al., 2013). Future research should therefore seek to characterize the exact role of these proteins and how (if any) their activities contribute to virulence in *F. circinatum*.

The findings presented here suggest that *F. circinatum* requires Ras2 for protecting itself from harmful compounds in the environment or secreted by competitors and its hosts during infection and colonisation (de Waard et al., 2006). We found five highly downregulated DEGs in the knockout mutant that encode putative products involved in the defence against or detoxification of such compounds (de Waard et al., 2006). These included genes coding for homologs of the ABC transporter CDR4, glutathione S-transferase II, benzoate 4-monooxygenase cytochrome P450, a multidrug resistance protein, and a chymotrypsin-elastase inhibitor ixodidin. Except for the latter protein, all these proteins are involved in detoxification and, in some cases, also contribute to virulence, as have been described in fungi such as *A. nidulans*, *Nectria haematococca*, *Magnaporthe grisea*, *Botrytis cinerea*, (Andrade et al., 2000; Prins et al., 2000; Coleman et al., 2011; Sun et al., 2006; de Waard et al., 2006). Apart from being reported as an antimicrobial compound in ticks (Fogaca et al., 2006), nothing is known regarding the role of an ixodidin-like protein would play in fungi. Functional studies on this gene would thus be invaluable for not only shedding light on the mechanisms underlying pathogenesis in *F. circinatum*, but likely also the molecular basis of its interactions with other organisms.

Interestingly and related to the potential mechanisms for *F. circinatum* protecting itself from external factors, one of the significantly downregulated (-12.5 fold) DEGs identified in the *ras2* knockout mutant of *F. circinatum* encoded a homolog of vegetative incompatibility protein HET-E-1. This protein was first identified in *Podospora anserina*, where it plays a role in self/non-self recognition by mediating programmed cell death when cells of genetically unlike individuals fuse (Paoletti and Clave 2007). A link between Ras2 and this protein has not been reported in literature, but it would not be inconceivable as HET-E-1 contains multiple domains implicated in signal transduction (Chevanne et al., 2009). Future work should thus explore the possibility that Ras2 affects vegetative compatibility, at least in *P. anserina*, as the molecular basis of self/non-self recognition has not yet been resolved in *F. circinatum*. Whatever the case may be, should such a link indeed exist, Ras2 would also be involved in the regulation of the *het-e-1* homolog in *F. circinatum*.

Expression patterns of components of the MAPK and cAMP signalling pathways linked to fungal growth, development and virulence (Kim et al., 2001; Hou et al., 2002; Choi and Xu, 2010; Zhang et al., 2011; Ding et al., 2015) suggest that *F. circinatum* Ras2 regulates these processes in a MAPK-dependant manner. Although the MAPK (FCIRG_04394) and PKA genes appeared downregulated in the knockout mutant, only the MAPK gene showed consistent downregulation in all replicates tested, and thus significant. It is known that Ras2 can regulate cellular processes such as fungal growth, development and

virulence in a MAPK- and/or cAMP-dependant manner (Zhao et al., 2007). In fungi such as *Cryptococcus neoformans* and *C. albicans*, both pathways have been reported to be involved in hyphal growth and virulence (Wang et al., 1999; Leberer et al., 2001; Huang et al., 2019), however, deletion of the *RAS2* gene in *F. graminearum* only affected the MAPK pathway (Bluhm et al., 2007). Additionally, and consistent with our findings, only the MAPK gene was affected in that fungus (Bluhm et al., 2007). A study based on the deletion of the *F. circinatum* MAPK gene FCIRG_04394 would confirm the suggestion that Ras2 regulates the affected processes in a MAPK-dependent manner in this fungus.

Among the downstream proteins regulated by Ras2, the transcriptional regulator LaeA is one of its likely targets in *F. circinatum*. The gene encoding a homolog of this protein was downregulated 12.8-fold in the *ras2* knockout mutant of *F. circinatum*. LaeA is best known as a master transcriptional regulator of secondary metabolism in various fungi (Bok and Keller, 2004). For example, an RNA-Seq study conducted in *A. flavus* found significant downregulation of the *laeA* gene in a mutant that had reduced aflatoxin production (Gilbert et al., 2016). Accordingly, the downregulation of *laeA* in the current study alongside that of secondary metabolites, suggests a possible role of LaeA in the regulation of secondary metabolism in *F. circinatum*. There is more than one reported mechanism by which LaeA regulates the production of secondary metabolites (Shimizu et al., 2003; Strauss and Reyes-Dominguez, 2011). A study conducted in *A. nidulans* found that LaeA interacts with, and thus activates, the Zn(II)2Cys6 transcription factor AflR that directly activates genes responsible for Sterigmatocystin production, whereby AflR is itself regulated by Ras (Shimizu et al., 2003). Another reported mechanism is that LaeA regulates transcription by channelling chromatin modification at loci where secondary metabolite genes are found thereby inducing the transcription of a number of genes (often clustered) simultaneously (Gasch et al., 2000; Strauss and Reyes-Dominguez, 2011; Ellison et al. 2014). Interestingly, about 50% of the genes that were downregulated, including those involved in secondary metabolism, were clustered and had similar fold change patterns, which suggests a possible mechanism for LaeA regulation in secondary metabolism and possibly other genes.

In addition to regulating the expression of transcriptional regulators, Ras2 may also control cellular processes in *F. circinatum* by binding to other regulatory proteins. For example, expression of the gene encoding arginyl tRNA synthetase was completely halted in the *ras2* knockout mutant. Arginyl tRNA synthetase ordinarily catalyses the ligation of amino acids to their corresponding tRNAs, but in humans it also forms a complex with Ras2 (Park et al., 2008). Although the exact mechanism is not known, the interaction between this protein and Ras2 is thought to contribute to the role of Ras2 in its activation of

cellular processes (Park et al., 2008). To the best of our knowledge, the association of arginyl tRNA synthetases with Ras proteins has not been reported in fungi, therefore functional characterization of the arginyl tRNA synthetase gene reported here will shed light on whether its product has associations with Ras proteins in *F. circinatum* and other fungi, and thereby possibly contributing to growth, development and virulence.

5. Conclusions

In this study, we identified biologically important candidate genes (i.e., linked to the growth, development and virulence) under the control of Ras2 in *F. circinatum*. Analyses of RNA-Seq data from the *ras2* knockout mutant and wild type strains of this fungus showed that the disruption of *RAS2* affected (negatively) the expression of enzymes that degrade plant cell wall components, which are also known to contribute to fungal virulence and pathogenicity. The expression of genes associated with hyphal growth, cytokinesis, and conidiation was also affected. A number of genes that encode proteins with ATPase, transferase and isomerase activities, which are linked to secondary metabolism, were also identified. These genes were downregulated alongside the transcriptional regulator LaeA, suggesting its possible role in secondary metabolism regulation in *F. circinatum*. Genes such as those encoding chymotrypsin-elastase inhibitor ixodidin, arginyl tRNA synthetase, and HET-E-1 not previously shown to play a role in fungal pathogenesis, but that were significantly downregulated in the *ras2* knockout mutant were also found. Furthermore, the expression data suggested that Ras2 controls the latter cellular processes in a MAPK-dependant manner. To the best of our knowledge, this is the first study to catalogue genes under the control of Ras2 using a *ras2* knockout mutant, thus shedding light on the molecular basis and mechanisms of virulence and pathogenesis in *F. circinatum* and possibly other fungi.

Acknowledgements

We thank the following South African institutions and funding bodies for supporting this work: the University of Pretoria, the National Research Foundation (NRF), the Forestry and Agricultural Biotechnology Institute (FABI), the Tree Protection Cooperative Programme (TPCP), the DST-NRF Centre of Excellence in Plant Health Biotechnology (CPHB) and the DSI-NRF South African Research Chairs Initiative (SARChI) Chair in Fungal Genomics. We also thank the Central Analytical Facility at Stellenbosch University for the library preparation and sequencing of the samples used in this study.

References

Andrade, A.C., Del Sorbo, G., Van Nistelrooy, J.G., de Waard, M.A., 2000. The ABC transporter AtrB from *Aspergillus nidulans* mediates resistance to all major classes of fungicides and some natural toxic compounds. Microbiology, 146, 1987-1997.

Aragunde, H., Biarnés, X., Planas, A., 2018. Substrate recognition and specificity of chitin deacetylases and related family 4 carbohydrate esterases. Int. J. Mol. Sci. 19, 412.

Asai, S., Shirasu, K., 2015. Plant cells under siege: plant immune system versus pathogen effectors. Curr. Opin. Plant Biol. 28, 1-8.

Bateman, D., Basham, H., 1976. Degradation of plant cell walls and membranes by microbial enzymes. Physiol. Plant Pathol: Springer, 316-355.

Becht, P., König, J., Feldbrügge, M., 2006. The RNA-binding protein Rrm4 is essential for polarity in *Ustilago maydis* and shuttles along microtubules. J. Cell Sci. 119, 4964-4973.

Benjamini, Y., Hochberg, Y., 1995. Controlling the false discovery rate: a practical and powerful approach to multiple testing. J. R. Stat. Soc: Ser. B (Methodological) 57, 289-300.

Bluhm, B., Zhao, X., Flaherty, J., Xu, J.R., Dunkle, L., 2007. RAS2 regulates growth and pathogenesis in *Fusarium graminearum*. Mol. Plant-Microbe Interact. 20, 627-636.

Boguski, M. S., McCormick, F., 1993. Proteins regulating Ras and its relatives. Nature 366, 643-654.

Bok, J.W., Keller, N.P., 2004. LaeA, a regulator of secondary metabolism in *Aspergillus* spp. Eukaryot. Cell 3, 527-535.

Brown, D.W., Butchko, R.A., Busman, M., Proctor, R.H., 2012. Identification of gene clusters associated with fusaric acid, fusarin, and perithecial pigment production in *Fusarium verticillioides*. Fungal Genet. Biol. 49, 521-532.

Buswell, J., Ander, P., Pettersson, B., Eriksson, K.E., 1979. Oxidative decarboxylation of vanillic acid by *Sporotrichum pulverulentum*. FEBS Lett. 103, 98-101.

Chen, A., Xie, Q., Lin, Y., Xu, H., Shang, W., Zhang, J., Zhang, D., Zheng, W., Li, G., Wang, Z., 2016. Septins are involved in nuclear division, morphogenesis and pathogenicity in *Fusarium graminearum*. Fungal Genet. Biol. 94, 79-87.

Chevanne, D., Bastiaans, E., Debets, A., Saupe, S.J., Clavé, C., Paoletti, M., 2009. Identification of the het-r vegetative incompatibility gene of *Podospora anserina* as a member of the fast evolving HNWD gene family. Curr. Genet. 55, 93-102.

Choi, Y.E., Shim, W.B., 2008. Functional characterization of *Fusarium verticillioides* CPP1, a gene encoding a putative protein phosphatase 2A catalytic subunit. Microbiology, 154, 326-336.

Choi, Y.E., Xu, J.R., 2010. The cAMP signaling pathway in *Fusarium verticillioides* is important for conidiation, plant infection, and stress responses but not fumonisin production. Mol. Plant-Microbe Interact. 23, 522-533.

Coleman, J.J., White, G.J., Rodriguez-Carres, M., VanEtten, H.D., 2011. An ABC transporter and a cytochrome P450 of *Nectria haematococca* MPVI are virulence factors on pea and are the major tolerance mechanisms to the phytoalexin pisatin. Mol. Plant-Microbe Interact. 24, 368-376.

De Vos, L., van der Nest, M.A., van der Merwe, N.A., Myburg, A.A., Wingfield, M.J., Wingfield, B.D., 2011. Genetic analysis of growth, morphology and pathogenicity in the F1 progeny of an interspecific cross between *Fusarium circinatum* and *Fusarium subglutinans*. Fungal Biol. 115, 902-908.

de Waard, M.A., Andrade, A.C., Hayashi, K., Schoonbeek, H.J., Stergiopoulos, I., Zwiers, L. H., 2006. Impact of fungal drug transporters on fungicide sensitivity, multidrug resistance and virulence. Pest Manag. Sci. 62, 195-207.

Diaz-Sanchez, V., Avalos, J., Limón, M.C., 2012. Identification and regulation of fusA, the polyketide synthase gene responsible for fusarin production in *Fusarium fujikuroi*. Appl. Environ. Microbiol. 78, 7258-7266.

Ding, Z., Li, M., Sun, F., Xi, P., Sun, L., Zhang, L., Jiang, Z., 2015. Mitogen-activated protein kinases are associated with the regulation of physiological traits and virulence in *Fusarium oxysporum* f. sp. *cubense*. PLoS One, 10, e0122634.

Drenkhan R, Ganley B, Martin-Garcia J, Vahalik P, Adamson K, Adamcikova K, Ahumada R, Blank L, Braganca H, Capretti P, Capretti P, Cleary M, Cornejo C, Davydenko K, Diez J, Lehtiharvi H, Dvorak M, Enderle R, Fourie G, Georgieva M, Ghelardini L, Hantula J, Ioos R, Iturritxa E, Kanetis L, Karpun N, Koltay A, Landera E, Markovskaja S, Mesanza N, Milenkovic I, Musolin D, Musolin D, Nikolaou K, Nowakowske J, Ogris N, Oskay F, Oszaka T, Papazova-Anakieva I, Paraschiv M, Pasquali M, Pecori F, Rafoss T, Raitelaityte K, Raposo R, Robin C, Rodas C, Santini A, Sanz-Ros A, Selikhovkin A, Solla A, Soukainen M, Soulioti N, Steenkamp E, Tsopelas P, Vemic A, Vettraino A, Wingfield M, Woodward S,

Zamora-Ballesteros C, Mullet M., 2020. Global geographic distribution and host range of *Fusarium circinatum*, the causal agent of Pine Pitch Canker. Forests 11, 724.

Dubovenko, A.G., Dunaevsky, Y.E., Belozersky, M.A., Oppert, B., Lord, J.C., Elpidina, E.N., 2010. Trypsin-like proteins of the fungi as possible markers of pathogenicity. Fungal Boil. 114, 151-159.

Dwinell, L.D., Barrows-Broaddus, J.B., Kuhlman, E.G., 1985. Pitch canker: a disease complex. Plant Dis. 69, 270-276.

Ellison, C.E., Kowbel, D., Glass, N.L., Taylor, J.W., Brem, R.B., 2014. Discovering functions of unannotated genes from a transcriptome survey of wild fungal isolates. MBio 5.

Eranthodi, A., Schneiderman, D., Harris, L.J., Witte, T. E., Sproule, A., Hermans, A., Overy, D. P., Chatterton, S., Liu, J., Li, T., 2020. Enniatin Production Influences *Fusarium avenaceum* Virulence on Potato Tubers, but not on Durum Wheat or Peas. Pathogens 9, 75.

Freimoser, F.M., Hu, G., St Leger, R. J., 2005. Variation in gene expression patterns as the insect pathogen *Metarhizium anisopliae* adapts to different host cuticles or nutrient deprivation in vitro. Microbiology 151, 361-371.

Fogaca, A.C., Almeida, I.C., Eberlin, M.N., Tanaka, A.S., Bulet, P., Daffre, S., 2006. Ixodidin, a novel antimicrobial peptide from the hemocytes of the cattle tick *Boophilus microplus* with inhibitory activity against serine proteinases. Peptides 27, 667-674.

Gage, M.J., Bruenn, J., Fischer, M., Sanders, D., Smith, T.J., 2001. KP4 fungal toxin inhibits growth in *Ustilago maydis* by blocking calcium uptake. Mol. Microbiol. 4, 775-785.

Gangwani, L., Mikrut, M., Galcheva-Gargova, Z., Davis, R.J., 1998. Interaction of ZPR1 with translation elongation factor-1α in proliferating cells. J. Cell Biol. 143, 1471-1484.

Gasch, A.P., Spellman, P.T., Kao, C.M., Carmel-Harel, O., Eisen, M.B., Storz, G., Botstein, D., Brown, P.O., 2000. Genomic expression programs in the response of yeast cells to environmental changes. Mol. Biol. Cell 11, 4241-4257.

Gelderblom, W., Thiel, P., Jaskiewicz, K., Marasas, W., 1986. Investigations on the carcinogenicity of fusarin C—a mutagenic metabolite of *Fusarium moniliforme*. Carcinogenesis 7, 1899-1901.

Gilbert, M.K., Mack, B.M., Wei, Q., Bland, J.M., Bhatnagar, D., Cary, J.W., 2016. RNA sequencing of an *nsdC* mutant reveals global regulation of secondary metabolic gene clusters in *Aspergillus flavus*. Microbiol. Res. 182, 150-161.

Greenshields, D.L., Liu, G., Feng, J., Selvaraj, G., Wei, Y., 2007. The siderophore biosynthetic gene SID1, but not the ferroxidase gene *FET3*, is required for full *Fusarium graminearum* virulence. Mol. Plant Pathol. 8, 411-421.

Grigoriev, I.V., Nikitin, R., Haridas, S., Kuo, A., Ohm, R., Otillar, R., Riley, R., Salamov, A., Zhao, X., Korzeniewski, F., Smirnova, T., Nordberg, H., Dubchak, I., Shabalov, I., 2014. MycoCosm portal: gearing up for 1000 fungal genomes. Nucl. Acids Res. 42, 699-704.

Guo, L., Han, L., Yang, L., Zeng, H., Fan, D., Zhu, Y., Feng, Y., Wang, G., Peng, C., Jiang, X., Zhou, D., 2014. Genome and transcriptome analysis of the fungal pathogen *Fusarium oxysporum* f. sp. *cubense* causing banana vascular wilt disease. PLoS One 9, .e95543.

Herrmann, M., Zocher, R., Haese, A., 1996a. Effect of disruption of the enniatin synthetase gene on the virulence of *Fusarium avenaceum*. Mol. Plant-Microbe Interact. 9, 226-232.

Herrmann, M., Zocher, R., Haese, A., 1996b. Enniatin production by *Fusarium* strains and its effect on potato tuber tissue. Appl. Environ. Microbiol. 62, 393-398.

Hopwood, D. A., Sherman, D. H., 1990. Molecular genetics of polyketides and its comparison to fatty acid biosynthesis. Annu. Rev. Genet. 24, 37-62.

Hou, Z., Xue, C., Peng, Y., Katan, T., Kistler, H.C., Xu, J.-R., 2002. A mitogen-activated protein kinase gene (MGV1. in *Fusarium graminearum* is required for female fertility, heterokaryon formation, and plant infection. Mol. Plant-Microbe Interact. 15, 1119-1127.

Hu, S., Zhou, X., Gu, X., Cao, S., Wang, C., Xu, J.R., 2014. The cAMP-PKA pathway regulates growth, sexual and asexual differentiation, and pathogenesis in *Fusarium graminearum*. Mol. Plant-Microbe Interact. 27, 557-566.

Huang, G., Huang, Q., Wei, Y., Wang, Y., Du, H., 2019. Multiple roles and diverse regulation of the Ras/cAMP/protein kinase A pathway in *Candida albicans*. Mol. Microbiol. 111, 6-16.

Ismaiel, A.A., Papenbrock, J., 2015. Mycotoxins: producing fungi and mechanisms of phytotoxicity. Agriculture 5, 492-537.

Javaid, N., Choi, S., 2017. Acetylation-and methylation-related epigenetic proteins in the context of their targets. Genes 8, 196.

Jeong, J.W., Kim, D.H., Choi, S.Y., Kim, H.B., 2001a. Characterization of the CDC10 product and the timing of events of the budding site of *Saccharomyces cerevisiae*. Molecules & Cells (Springer Science & Business Media BV) 12.

Jones, D.A., John, E., Rybak, K., Phan, H.T., Singh, K.B., Lin, S.Y., Solomon, P.S., Oliver, R.P., Tan, K.C., 2019. A specific fungal transcription factor controls effector gene expression and orchestrates the establishment of the necrotrophic pathogen lifestyle on wheat. Sci. Rep. 9, 1-13.

Kafri, R., Springer, M., Pilpel, Y., 2009. Genetic redundancy: new tricks for old genes. Cell 136, 389-392.

Katagiri, M., Takemori, S., Suzuki, K., Yasuda, H., 1966. Mechanism of the salicylate hydroxylase reaction. J. Biol. Chem. 241, 5675-5677.

Kim, H.S., Park, S.Y., Lee, S., Adams, E.L., Czymmek, K., Kang, S., 2011. Loss of cAMP-dependent protein kinase A affects multiple traits important for root pathogenesis by *Fusarium oxysporum*. Mol. Plant-Microbe Interact. 24, 719-732.

Leberer, E., Harcus, D., Dignard, D., Johnson, L., Ushinsky, S., Thomas, D.Y., Schröppel, K., 2001. Ras links cellular morphogenesis to virulence by regulation of the MAP kinase and cAMP signalling pathways in the pathogenic fungus *Candida albicans*. Mol. Microbiol. 42, 673-687.

Leger, R.S., Charnley, A., Cooper, R., 1986. Cuticle-degrading enzymes of entomopathogenic fungi: synthesis in culture on cuticle. J. Invert. Pathol. 48, 85-95.

Lengeler, K.B., Davidson, R.C., Dsouza, C., Harashima, T., Shen, W.C., Wang, P., Pan, X., Waugh, M., Heitman, J., 2000. Signal transduction cascades regulating fungal development and virulence. Microbiol. Mol. Biol. Rev. 64, 746-785.

Leslie, J.F., 1993. Fungal vegetative compatibility. Annu. Rev. Phytopathol. 31, 127-150.

Li, X., Wu, Y., Liu, Z., Zhang, C., 2017. The function and transcriptome analysis of a bZIP transcription factor *CgAP1* in *Colletotrichum gloeosporioides*. Microbiol. Res. 197, 39-48.

Lowy, D.R., Willumsen, B.M., 1993. Function and regulation of *ras*. Annu. Rev. Biochem. 62, 851-891.

Lu, S., Faris, J.D., 2019. *Fusarium graminearum* KP4-like proteins possess root growth-inhibiting activity against wheat and potentially contribute to fungal virulence in seedling rot. Fungal Genet. Biol. 123, 1-13.

Lopez-Diaz, C., Rahjoo, V., Sulyok, M., Ghionna, V., Martín-Vicente, A., Capilla, J., Di Pietro, A., Lopez-Berges, M.S., 2018. Fusaric acid contributes to virulence of *Fusarium oxysporum* on plant and mammalian hosts. Mol. Plant Pathol. 19, 440-453.

Ma, L.J., Geiser, D.M., Proctor, R.H., Rooney, A.P., O'Donnell, K., Trail, F., Gardiner, D.M., Manners, J.M., Kazan, K., 2013. *Fusarium* pathogenomics. Annu. Rev. Microbiol. 67, 399-416.

Mahlert, M., Leveleki, L., Hlubek, A., Sandrock, B., Bölker, M., 2006. Rac1 and Cdc42 regulate hyphal growth and cytokinesis in the dimorphic fungus *Ustilago maydis*. Mol. Microbiol. 59, 567-578.

Martín-Rodrigues, N., Espinel, S., Sanchez-Zabala, J., Ortíz, A., González-Murua, C., Duñabeitia, M.K., 2013. Spatial and temporal dynamics of the colonization of Pinus radiata by *Fusarium circinatum*, of conidiophora development in the pith and of traumatic resin duct formation. New Phytol. 198, 1215-1227.

Martín-Rodrigues, N., Sanchez-Zabala, J., Salcedo, I., Majada, J., González-Murua, C., Duñabeitia, M.K., 2015. New insights into radiata pine seedling root infection by *Fusarium circinatum*. Plant Pathol. 64, 1336-1348.

Meijueiro, M.L., Santoyo, F., Ramírez, L., Pisabarro, A.G., 2014. Transcriptome characteristics of filamentous fungi deduced using high-throughput analytical technologies. Brief. Funct. Genom. 13, 440-450.

Meng, S., Torto-Alalibo, T., Chibucos, M.C., Tyler, B.M., Dean, R.A., 2009. Common processes in pathogenesis by fungal and oomycete plant pathogens, described with Gene Ontology terms. BMC Microbiol. 9, S7.

Miller, B., Miller, K., Roberti, K., Timberlake, W., 1987. Position-dependent and-independent mechanisms regulate cell-specific expression of the SpoC1 gene cluster of *Aspergillus nidulans*. Mol. Cellul. Biol. 7, 427-434.

Metraux, J., Signer, H., Ryals, J., Ward, E., Wyss-Benz, M., Gaudin, J., Raschdorf, K., Schmid, E., Blum, W., Inverardi, B., 1990. Increase in salicylic acid at the onset of systemic acquired resistance in cucumber. Science 250, 1004-1006.

Mosch, H.U., Roberts, R.L., Fink, G.R., 1996. Ras2 signals via the Cdc42/Ste20/mitogen-activated protein kinase module to induce filamentous growth in *Saccharomyces cerevisiae*. Proc. Natl. Acad. Sci. 93, 5352-5356.

Nakamura, T., Ichinose, H., Wariishi, H., 2012. Flavin-containing monooxygenases from *Phanerochaete chrysosporium* responsible for fungal metabolism of phenolic compounds, *Biodegradation*, 23(3), 343-350.

Osherov, N., May, G., 2000. Conidial germination in *Aspergillus nidulans* requires RAS signaling and protein synthesis. Genetics 155, 647-656.

Park, S. G., Schimmel, P., Kim, S., 2008. Aminoacyl tRNA synthetases and their connections to disease. Proc. Natl. Acad. Sci. 105, 11043-11049.

Paoletti, M., Clave, C., (2007. The fungus-specific HET domain mediates programmed cell death in *Podospora anserine*. Eukaryot. Cell 6, 2001-2008.

Peng, X., Masai, E., Kitayama, H., Harada, K., Katayama, Y., Fukuda, M., 2002. Characterization of the 5-carboxyvanillate decarboxylase gene and its role in lignin-related biphenyl catabolism in *Sphingomonas paucimobilis* SYK-6. Appl. Environ. Microbiol. 68, 4407-4415.

Pham, K.T.M., Inoue, Y., Vu, B.V., Nguyen, H.H., Nakayashiki, T., Ikeda, K.I., Nakayashiki, H., 2015. MoSET1 (histone H3K4 methyltransferase in *Magnaporthe oryzae*. regulates global gene expression during infection-related morphogenesis. PLoS Genet. 11, e1005385.

Phasha, M., Wingfield, M., Wingfield, B., Coetzee, M., Hallen-Adams, H., Fru, F., Swalarsk-Parry, B., Yilmaz, N., Duong, T., Steenkamp, E., 2021. Ras2 is important for growth and pathogenicity in *Fusarium circinatum*. Fungal Genet. Biol. 150, 103541-103550.

Prins, T. W., Wagemakers, L., Schouten, A., Van Kan, J.A., 2000b. Cloning and characterization of a glutathione S-transferase homologue from the plant pathogenic fungus *Botrytis cinerea*. Mol. Plant Pathol. 1, 169-178.

Prosperini, A., Berrada, H., Ruiz, M.J., Caloni, F., Coccini, T., Spicer, L.J., Perego, M.C., Lafranconi, A., 2017. A review of the mycotoxin enniatin B. Front. Public Health 5, 304.

Rabe, F., Ajami-Rashidi, Z., Doehlemann, G., Kahmann, R., Djamei, A., 2013. Degradation of the plant defence hormone salicylic acid by the biotrophic fungus *Ustilago maydis*. Mol. Microbiol. 89, 179-188.

Rauwane, M.E., Ogugua, U.V., Kalu, C. M., Ledwaba, L.K., Woldesemayat, A.A., Ntushelo, K., 2020. Pathogenicity and Virulence Factors of *Fusarium graminearum* Including Factors Discovered Using Next Generation Sequencing Technologies and Proteomics. Microorganisms 8, 305-333.

Rep, M., Kistler, H.C., 2010. The genomic organization of plant pathogenicity in *Fusarium* species. Curr. Opin. Plant Biol. 13, 420-426.

Roberts, A., Berlin, V., Hager, K., Yanofsky, C., 1988. Molecular analysis of a *Neurospora crassa* gene expressed during conidiation. Mol. Cell. Biol. 8, 2411-2418.

Roberts, A. N., Yanofsky, C., 1989. Genes expressed during conidiation in *Neurospora crassa*: characterization of con-8. Nucl. Acids Res. 17, 197-214.

Rocheleau, H., Al-harthi, R., Ouellet, T., 2019. Degradation of salicylic acid by *Fusarium graminearum*. Fungal Biol. 123, 77-86.

Schrettl, M., Bignell, E., Kragl, C., Joechl, C., Rogers, T., Arst Jr, H.N., Haynes, K., Haas, H., 2004. Siderophore biosynthesis but not reductive iron assimilation is essential for *Aspergillus fumigatus* virulence. J. Exp. Med. 200, 1213-1219.

Shimizu, K., Hicks, J.K., Huang, T.P., Keller, N.P., 2003. Pka, Ras and RGS protein interactions regulate activity of AflR, a Zn (II. 2Cys6 transcription factor in *Aspergillus nidulans*. Genetics 165, 1095-1104.

Silakowski, B., Kunze, B., Nordsiek, G., Blöcker, H., Höfle, G., Müller, R., 2000. The myxochelin iron transport regulon of the myxobacterium *Stigmatella aurantiaca* Sg a15. Eur. J. Chem. 267, 6476-6485.

Slinski, S., Kirkpatrick, S., Gordon, T., 2016. Inheritance of virulence in *Fusarium circinatum*, the cause of pitch canker in pines. Plant Pathol. 65, 1292-1296.

Som, T., Kolaparthi, V., 1994. Developmental decisions in *Aspergillus nidulans* are modulated by Ras activity. Mol. Cellul. Biol. 14, 5333-5348.

St Leger, R.J., Joshi, L., Roberts, D.W., 1997. Adaptation of proteases and carbohydrases of saprophytic, phytopathogenic and entomopathogenic fungi to the requirements of their ecological niches. Microbiol. 143, 1983-1992.

Stepien, L., Lalak-Kanczugowska, J., 2020. Signalling pathways involved in virulence and stress response of plant-pathogenic *Fusarium* species. Fungal Biol. Rev. 35, 27-39.

Strauss, J., Reyes-Dominguez, Y., 2011. Regulation of secondary metabolism by chromatin structure and epigenetic codes. Fungal Genet. Biol. 48(1), 62.

Sorensen, A., Lübeck, M., Lübeck, P.S., Ahring, B.K., 2013. Fungal beta-glucosidases: a bottleneck in industrial use of lignocellulosic materials. Biomolecules 3, 612-631.

Sun, C.B., Suresh, A., Deng, Y.Z., Naqvi, N.I., 2006. A multidrug resistance transporter in *Magnaporthe* is required for host penetration and for survival during oxidative stress. The Plant Cell 18, 3686-3705.

Tan, K.C., Ipcho, S.V., Trengove, R.D., Oliver, R.P., Solomon, P.S., 2009. Assessing the impact of transcriptomics, proteomics and metabolomics on fungal phytopathology. Mol. Plant Pathol. 10, 703-715.

Turra, D., Segorbe, D., and Di Pietro, A., 2014. Protein kinases in plant-pathogenic fungi: conserved regulators of infection. Annu. Rev. Phytopathol. 52, 267-288.

Swett, C.L., Kirkpatrick, S.C., Gordon, T.R., 2016. Evidence for a hemibiotrophic association of the pitch canker pathogen *Fusarium circinatum* with *Pinus radiata*. Plant Dis. 100, 79-84.

Swett, C.L., Reynolds, G.J., Gordon, T.R., 2018. Infection without wounding and symptomless shoot colonization of *Pinus radiata* by *Fusarium circinatum*, the cause of pitch canker. For. Pathol. 48, e12422.

Tannous, J., Kumar, D., Sela, N., Sionov, E., Prusky, D., Keller, N.P., 2018. Fungal attack and host defence pathways unveiled in near-avirulent interactions of *Penicillium expansum creA* mutants on apples. Mol. Plant Pathol. 19, 2635-2650.

Toda, T., Uno, I., Ishikawa, T., Powers, S., Kataoka, T., Broek, D., Cameron, S., Broach, J., Matsumoto, K., Wigler, M., 1985. In yeast, RAS proteins are controlling elements of adenylate cyclase. Cell 40, 27-36.

Visser, E.A., Wegrzyn, J.L., Steenkamp, E.T., Myburg, A.A., Naidoo, S., 2019. Dual RNA-Seq analysis of the pine-*Fusarium circinatum* interaction in resistant (*Pinus tecunumanii*) and susceptible (*Pinus patula*) hosts. Microorganisms, 7, 315.

Van Berkel, W., Kamerbeek, N., Fraaije, M., 2006. Flavoprotein monooxygenases, a diverse class of oxidative biocatalysts. J. Biotech. 124, 670-689.

Van Leeuwen, M., Krijgsheld, P., Bleichrodt, R., Menke, H., Stam, H., Stark, J., Wösten, H., Dijksterhuis, J., 2013. Germination of conidia of *Aspergillus niger* is accompanied by major changes in RNA profiles. Stud. Mycol. 74, 59-70.

Wadke, N., Kandasamy, D., Vogel, H., Lah, L., Wingfield, B.D., Paetz, C., Wright, L.P., Gershenzon, J., Hammerbacher, A., 2016. The bark-beetle-associated fungus, *Endoconidiophora polonica*, utilizes the phenolic defense compounds of its host as a carbon source. Plant Physiol. 171, 914-931.

Wang, L., Lin, X., 2012. Morphogenesis in fungal pathogenicity: shape, size, and surface. PLoS Pathog. 8, e1003027.

Wang, P., Heitman, J., 1999. Signal transduction cascades regulating mating, filamentation, and virulence in *Cryptococcus neoformans*. Curr. Opin. Microbiol. 2, 358-362.

Wang, Z., Gerstein, M., Snyder, M., 2009. RNA-Seq: a revolutionary tool for transcriptomics. Nat. Rev. Genet. 10, 57-63.

Wang, Z., Lopez-Giraldez, F., Lehr, N., Farré, M., Common, R., Trail, F., Townsend, J.P., 2014. Global gene expression and focused knockout analysis reveals genes associated with fungal fruiting body development in *Neurospora crassa*. Eukaryot. Cell 13, 154-169.

Wang, Y., Zhang, X., Zhou, Q., Zhang, X., Wei, J., 2015. Comparative transcriptome analysis of the lichen-forming fungus *Endocarpon pusillum* elucidates its drought adaptation mechanisms. Sci. China Life Sci. 58, 89-100.

Wang, Y., Tian, L., Xiong, D., Klosterman, S.J., Xiao, S., Tian, C., 2016. The mitogen-activated protein kinase gene, *VdHog1*, regulates osmotic stress response, microsclerotia formation and virulence in *Verticillium dahliae*. Fungal Genet. Biol. 88, 13-23.

Wiemann, P., Sieber, C.M., Von Bargen, K.W., Studt, L., Niehaus, E.M., Espino, J.J., Huß, K., Michielse, C. B., Albermann, S., Wagner, D., 2013. Deciphering the cryptic genome: genome-wide analyses of the rice pathogen *Fusarium fujikuroi* reveal complex regulation of secondary metabolism and novel metabolites. PLoS Pathog. 9, e1003475.

Wiemann, P., Willmann, A., Straeten, M., Kleigrewe, K., Beyer, M., Humpf, H.U., Tudzynski, B., 2009. Biosynthesis of the red pigment bikaverin in *Fusarium fujikuroi*: genes, their function and regulation. Mol. Microbiol. 72, 931-946.

Zhang, M.Z., Sun, C.H., Liu, Y., Feng, H.Q., Chang, H.W., Cao, S.N., Li, G.H., Yang, S., Hou, J., Zhu-Salzman, K., Zhang, H., 2020. Transcriptome analysis and functional validation reveal a novel gene, BcCGF1, that enhances fungal virulence by promoting infection-related development and host penetration. Mol. Plant Pathol. 21, 834-853.

Zhang, X., Zhu, Y., Bao, L., Gao, L., Yao, G., Li, Y., Yang, Z., Li, Z., Zhong, Y., Li, F., 2016. Putative methyltransferase LaeA and transcription factor CreA are necessary for proper asexual development and controlling secondary metabolic gene cluster expression. Fungal Genet. Biol. 94, 32-46.

Zhang, Y., Choi, Y.E., Zou, X., Xu, J.R., 2011. The FvMK1 mitogen-activated protein kinase gene regulates conidiation, pathogenesis, and fumonisin production in *Fusarium verticillioides*. Fungal Genet. Biol. 48, 71-79.

Zhao, X., Mehrabi, R., Xu, J.R., 2007. Mitogen-activated protein kinase pathways and fungal pathogenesis. Eukaryot. Cell 6, 1701-1714.

Zhi, Q., He, L., Li, J., Li, J., Wang, Z., He, G., He, Z.M., 2019. The kinetochore protein Spc105, a novel interaction partner of LaeA, regulates development and secondary metabolism in *Aspergillus flavus*. Front. Biol. 10, 1881.

Tables

Table 1. Expression data of *RAS2* and three housekeeping genes in *F. circinatum* knockout and complement mutant strains Δ*Fcras2* and Δ*Fcras2C* (respectively) vs. wild type strain FSP34.

Gene (encoded protein)	***ras2* knockout mutant vs. wild type expression**		**Total number of transcripts**					
	Bonferroni*	**Fold change [@]**	**ΔFcras2_1[#]**	**ΔFcras2_2**	**ΔFcras2_3**	**FSP34_1**	**FSP34_3**	**FSP34_4**
FCIRG_08573 (GTPase Ras2)	0.00	-626.67	2.00	1.00	0.00	852.00	1327.00	1007.00
FCIRG_06968 (Superoxide dismutase mitochondrial precursor 2)	1.00	-1.91	1295.00	1430.00	784.00	1823.00	4253.00	4465.00
FCIRG_00112 (Tyrosyl tRNA synthetase)	1.00	1.34	958.00	1557.00	822.00	1222.00	1534.00	938.00
FCIRG_01366 (Mitochondrial import inner membrane translocase subunit TIM16)	1.00	-1.32	404.00	374.00	273.00	715.00	782.00	609.00
	***ras2* complement mutant vs. wild type expression**							
	Bonferroni*	**Fold change[@]**	**ΔFcras2C_1[#]**	**ΔFcras2C_6**	**ΔFcras2C_7**	**FSP34_1**	**FSP34_3**	**FSP34_4**
FCIRG_08573 (GTPase Ras2)	1.00	1.00	580.00	808.00	786.00	852.00	1327.00	1007.00
FCIRG_06968 (Superoxide dismutase mitochondrial precursor 2)	1.00	-1.62	883.00	1215.00	2333.00	1823.00	4253.00	4465.00
FCIRG_00112 (Tyrosyl tRNA synthetase)	1.00	-1.24	599.00	757.00	694.00	1222.00	1534.00	938.00
FCIRG_01366 (Mitochondrial import inner membrane translocase subunit TIM16)	1.00	-1.69	239.00	370.00	259.00	715.00	782.00	609.00

***** Bonferroni value taking all three replicates into account.

[@] Fold change from the three replicates of each strain.

[#] The underscored number denotes the replicate of each strain.

Table 2. Expression fold change in overlapping protein families between downregulated and upregulated DEGs.

Gene category	Protein Family [a]	Sequence ID [b]	Fold change [c]
Downregulated genes	NADP binding	FCIRG_12923	-12.8
		FCIRG_08851	-10.3
		FCIRG_01668	-12.8
		FCIRG_13824	-8.7
		FCIRG_01511	-7.6
	FAD binding	FCIRG_00313	-6.6
		FCIRG_00490	-10.3
		FCIRG_02823	-9.5
		FCIRG_15065	-8.9
		FCIRG_02944	-8.8
		FCIRG_02254	-90.3
	MFS transporter	FCIRG_14017	-18.5
	Cytochrome	FCIRG_03381	-4.4
		FCIRG_07324	-9.2
		FCIRG_08224	-14.5
Upregulated genes	NADP binding	FCIRG_00989	3.5
		FCIRG_13424	7.3
		FCIRG_13738	11.0
		FCIRG_14749	9.0
	FAD binding	FCIRG_00061	6.5
		FCIRG_00064	5.5
	MFS transporter	FCIRG_00062	8.4
	Cytochrome	FCIRG_01680	6.6
		FCIRG_09199	7.4
		FCIRG_12824	9.2
		FCIRG_13893	16.2

[a] InterProScan proteins families.

[b] The *F. circinatum* genome used was from the first assembly of this genome assembled using the 454 GS assembler software package, Newbler (Wingfield et al., 2012).

[c] Mean fold change from three replicates of each strain.

Table 3. Proteins encoded by downregulated DEGs with unique molecular functions in *F. circinatum ras2* knockout mutant (ΔFcras2).

Molecular function [a]	Protein description [b]	Sequence ID [c]	Fold change [d]
ATPase	ABC transporter CDR4	FCIRG_08070	-10.8
	Related to multidrug resistance protein	FCIRG_09288	-8.2
	Multidrug resistance protein 1B	FCIRG_14202	-10.1
	Related to multidrug resistance protein	FCIRG_01587	-9.2
	Related to TOB3 (member of AAA-atpase family)	FCIRG_12090	-9.9
Transferase	Cytochrome P450, family 51 (sterol 14-demethylase)	FCIRG_07324	-9.2
	Related to hard surface induced protein 3 (sterol glycosyl transferase)	FCIRG_10833	-12.1
	Related to alpha-1,6-mannosyltransferase HOC1	FCIRG_10834	-5.8
	Related to beta-1,4-mannosyl-glycoprotein 4-beta-N-acetylglucosaminyltransferase	FCIRG_10969	-4.7
	Related to methyltransferase LaeA-like	FCIRG_12923	-12.8
	Fusarin C cluster-methyltransferase	FCIRG_00359	-3.0
	Fusarin C cluster-polyketide synthase/NRPS	FCIRG_00355	-3.7
	Related to Glutathione S-transferase II	FCIRG_00004	-15.5
	Probable CDP-alcohol phosphatidyltransferase	FCIRG_00927	-6.0
	Trichothecene 3-O-acetyltransferase	FCIRG_02427	-4.9
	Hypothetical protein	FCIRG_01665	-7.9
	Related to NAM7-nonsense-mediated mRNA decay protein (rdrp)	FCIRG_01527	-4.5
	Uncharacterized protein	FCIRG_03683	-40.1
	Probable delta(24)-sterol c-methyltransferase (ERG6)	FCIRG_04319	-21.8
	Homoserine O-acetyltransferase	FCIRG_10009	-6.1
Isomerase	Phytoene synthase	FCIRG_06985	-6.6
	Maleylacetoacetate isomerase	FCIRG_13172	-11.7
	Fusarin C cluster-polyketide synthase/NRPS	FCIRG_00355	-3.7
Nuclease	Related to endonuclease/exonuclease/phosphatase family protein	FCIRG_14970	-15.5
RNA binding	Hypothetical protein	FCIRG_03394	-15.7
	Fusarin C cluster-translation Elongation factor	FCIRG_00353	-4.7

[a] Blast2Go molecular functions. [b] Blast2Go protein descriptions. [c] The *F. circinatum* genome used was from the first assembly of this genome assembled using the 454 GS assembler software package, Newbler (Wingfield et al., 2012). [d] Mean fold change from three replicates .of each strain.

Table 4. Fold change of downregulated DEGs encoding proteins of the fusaric acid and fusarin C metabolic clusters in *F. circinatum ras2* knockout mutant (ΔFcras2).

Secondary metabolite	Protein description [a]	Sequence ID [b]	Fold change [c]
Fusaric acid	Polyketide synthase Fub1	FCIRG_10013 and FCIRG_00343	-7.8
	Uncharacterized protein Fub2	FCIRG_10012	-8.8
	Aspartate kinase Fub3	FCIRG_10011	-7.1
	Serine hydrolase Fub4	FCIRG_10010	-6.8
	Homoserine O-acetyltransferase Fub5	FCIRG_10009	-6.1
	NAD(P)-dependent dehydrogenase Fub6	FCIRG_03384	-11.2
	O-acetylhomoserine (thiol-)lyase Fub7	FCIRG_03383	-6.7
	Non-ribosomal peptide synthetase (NRPS)-like enzyme Fub8	FCIRG_03382	-10.8
	FMN-dependent dehydrogenase Fub9	FCIRG_03381	-4.4
Fusarin C	Oxidoreductase Fus5	FCIRG_00351	-4.4
	Translation elongation factor Fus3	FCIRG_00353	-4.8
	Hydrolase Fus2	FCIRG_00354	-3.6
	Polyketide synthase/NRPS Fus1	FCIRG_00355	-3.7
	Transporter Fus6	FCIRG_00356	-3.9
	Dehydrogenase Fus7	FCIRG_00357	-6.3
	Methyltransferase Fus9	FCIRG_00359	-3.0

[a] Blast2Go protein descriptions.

[b] The *F. circinatum* genome used was from the first assembly of this genome assembled using the 454 GS assembler software package, Newbler (Wingfield et al., 2012).

[c] Mean fold change from three replicates of each strain.

Table 5. Expression data of components of the MAPK and cAMP pathways in the *F. circinatum ras2* knockout mutant (ΔFcras2) vs. the wild type strain FSP34.

Gene (Protein name)	*ras2* knockout mutant vs. wild type expression		Total number of transcripts					
	Fold change*	FDR p-value[@]	ΔFcras2_1[#]	ΔFcras2_2	ΔFcras2_3	FSP34_1	FSP34_3	FSP34_4
FCIRG_11025 (MAPKKK)	1.720972	0.081089	968	811	972	624	1147	836
FCIRG_10336 (MAPKK)	1.118938	0.780014	1113	1121	965	1303	1715	1426
FCIRG_04394 (MAPK)	-2.54785	0.00028	812	1476	771	2515	5797	3741
FCIRG_06741 (Adenylate cyclase)	1.832216	0.038488	2953	2955	2978	1988	2927	2767
FCIRG_14034 (PKA)	-1.22856	0.582574	917	1135	776	1113	2244	2097

* Fold change from the three replicates of each strain.

[@] False Discovery Rate p-value taking all replicates into account.

[#] The underscored number denotes the replicate of each strain.

.

Figures

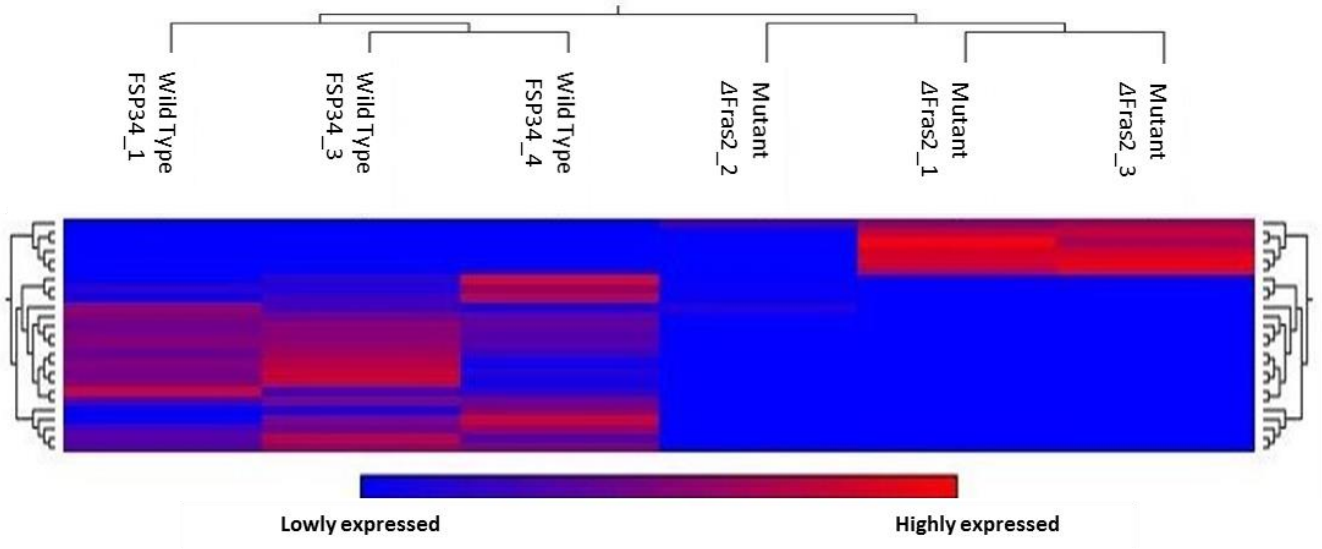

Figure 1. Heatmap showing hierachical clustering of genes in the *F. circinatum* knockout mutant strain ΔFcras2 and the wild type strain FSP34 according to their levels of expression. Each strain had three replicates. Genes with similar expression levels are close to each other and those that differ in expression levels are further apart. Blue indicates lowly expressed genes and highly expressed genes are in red.

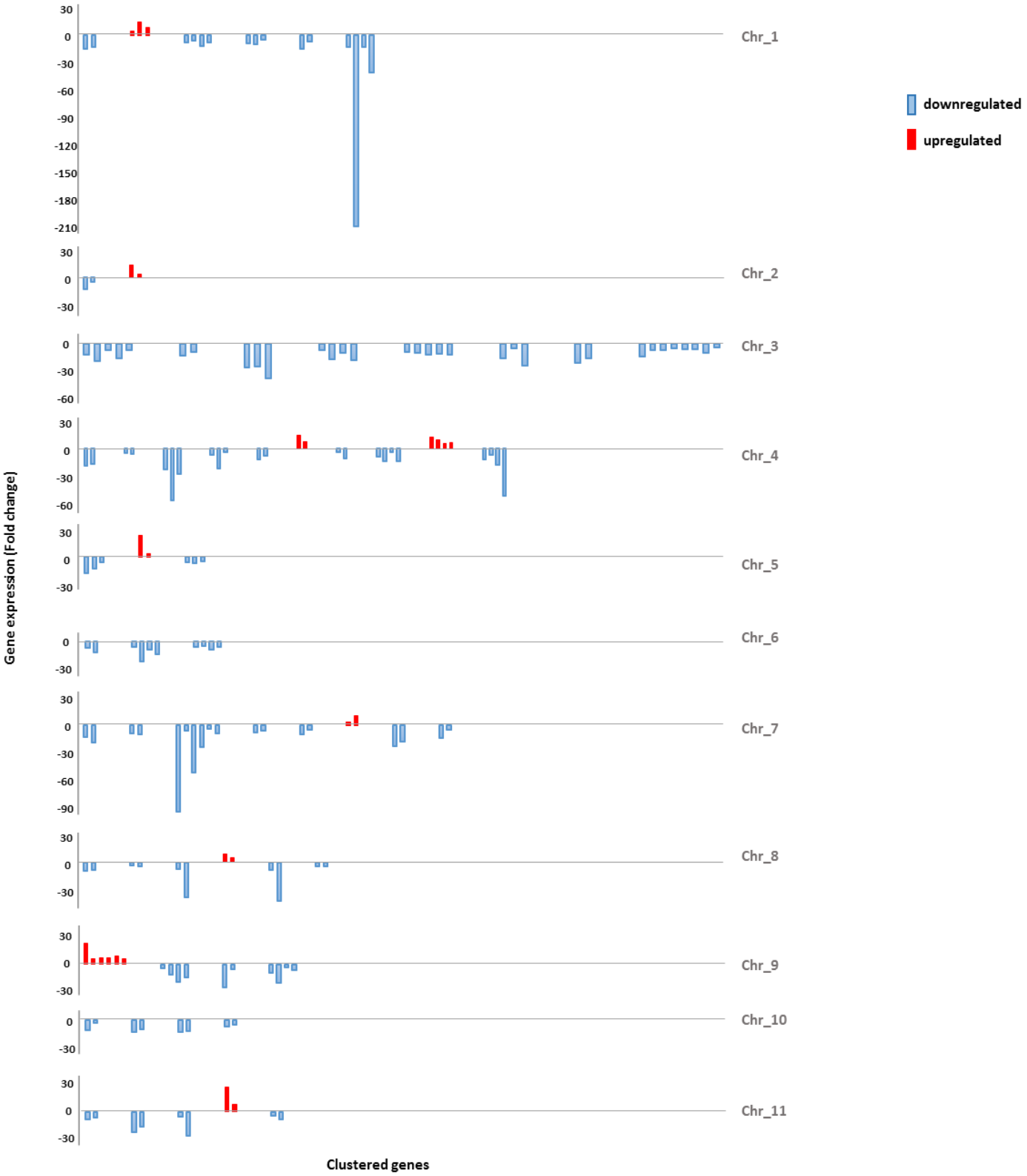

Figure 2. The arrangement of the differentially expressed genes in the genome of *F. circinatum*. The x-axis represents fold change (see supplementary file 4 for actual fold change values), and the y-axis represents gene clusters. Downregulated DEG clusters are indicated in blue while upregulated clusters in red. Chromosomes are drawn to an arbitrary scale. Chr = Chromosome.

A

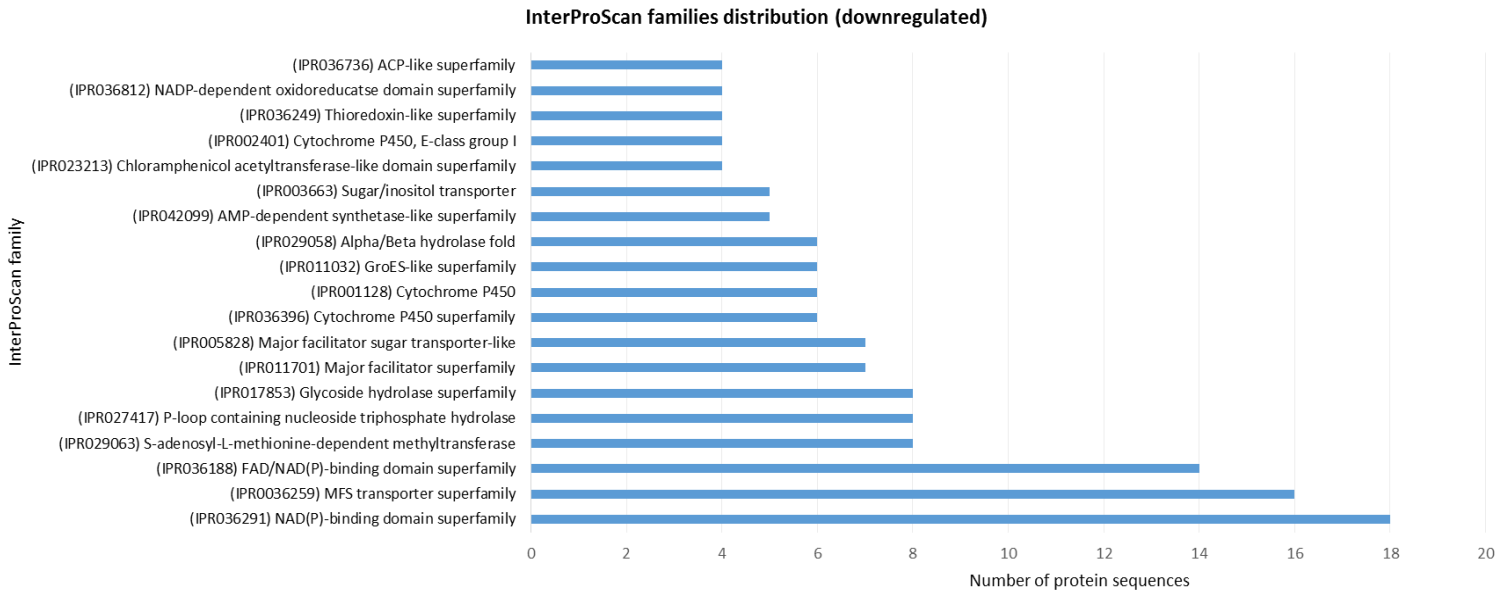

B

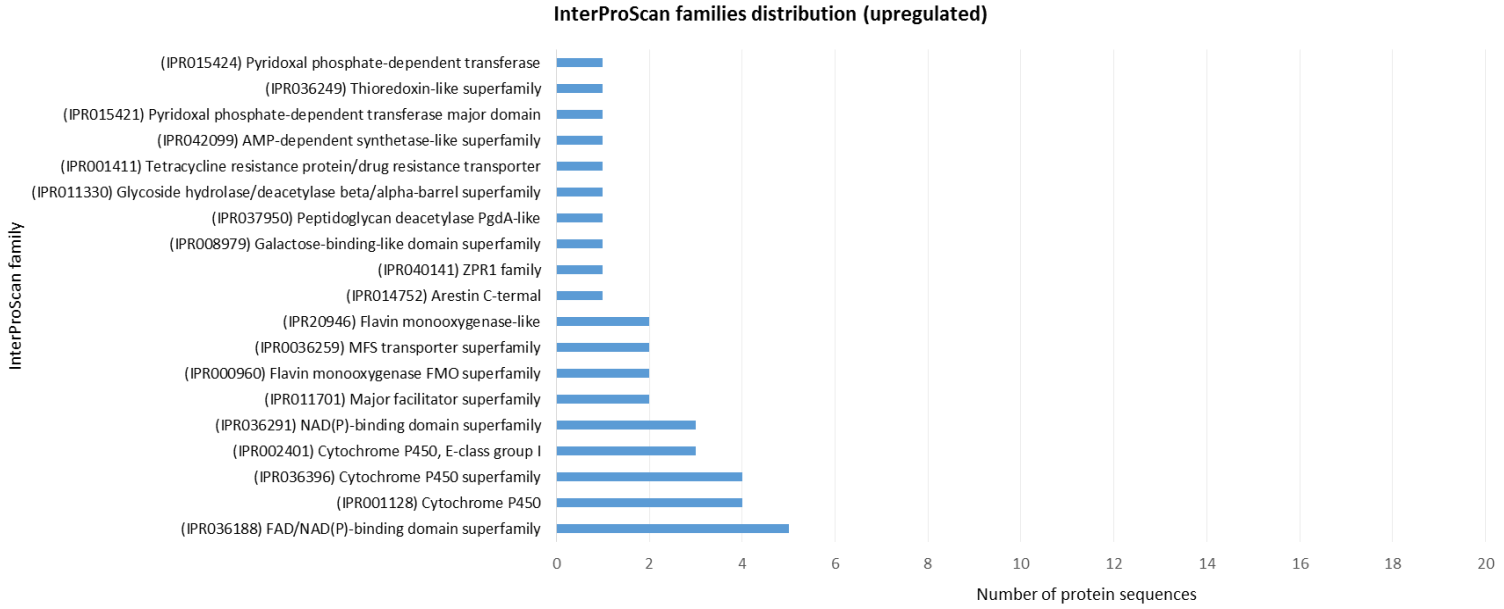

Figure 3. Graphs showing the distribution of InterProScan families for downregulated (**A**) and upregulated (**B**) genes of *F. circinatum* knockout mutant ΔFcras2.

A

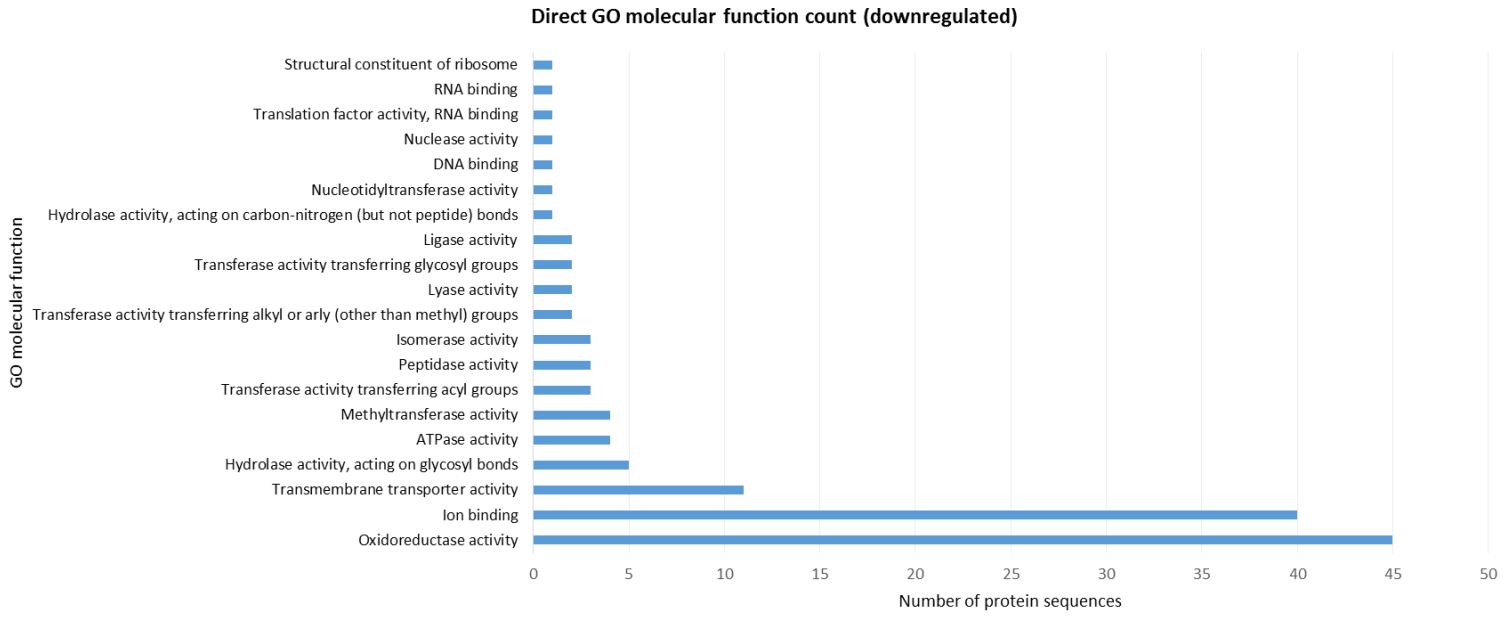

B

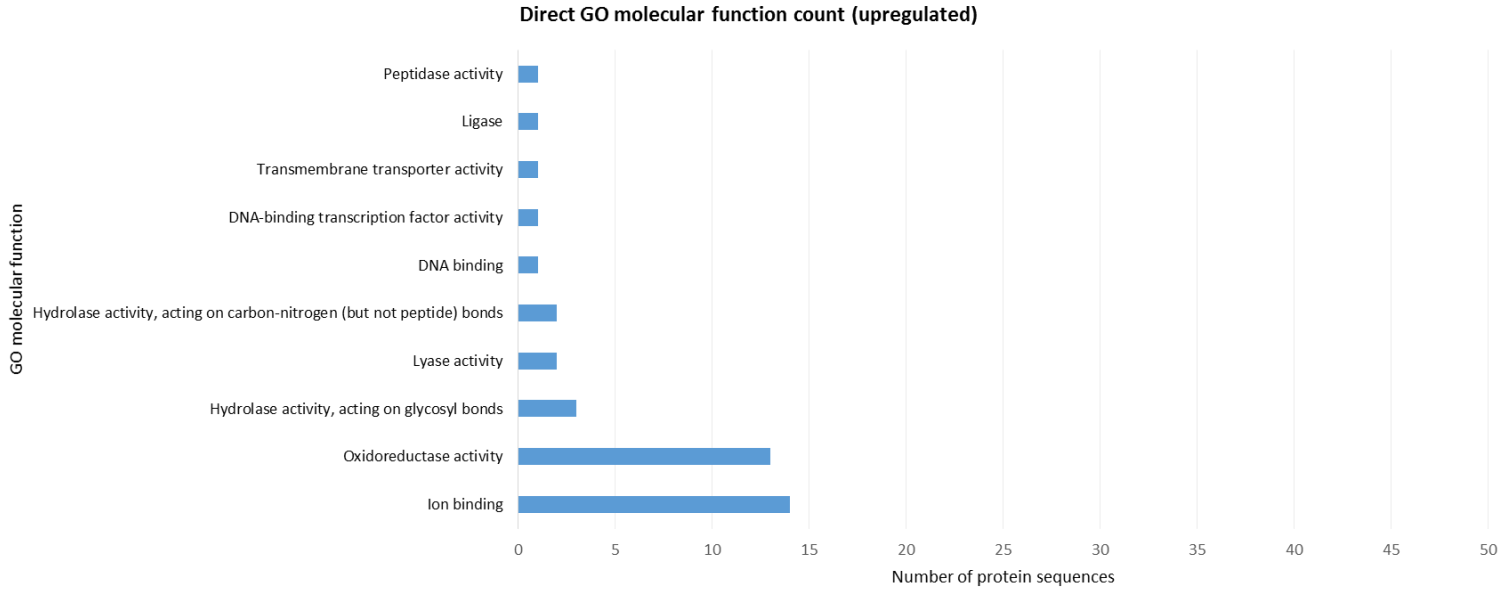

Figure 4. Graphs showing the distribution of InterProScan molecular functions for downregulated (**A**) and upregulated (**B**) genes of *F. circinatum* knockout mutant ΔFcras2.

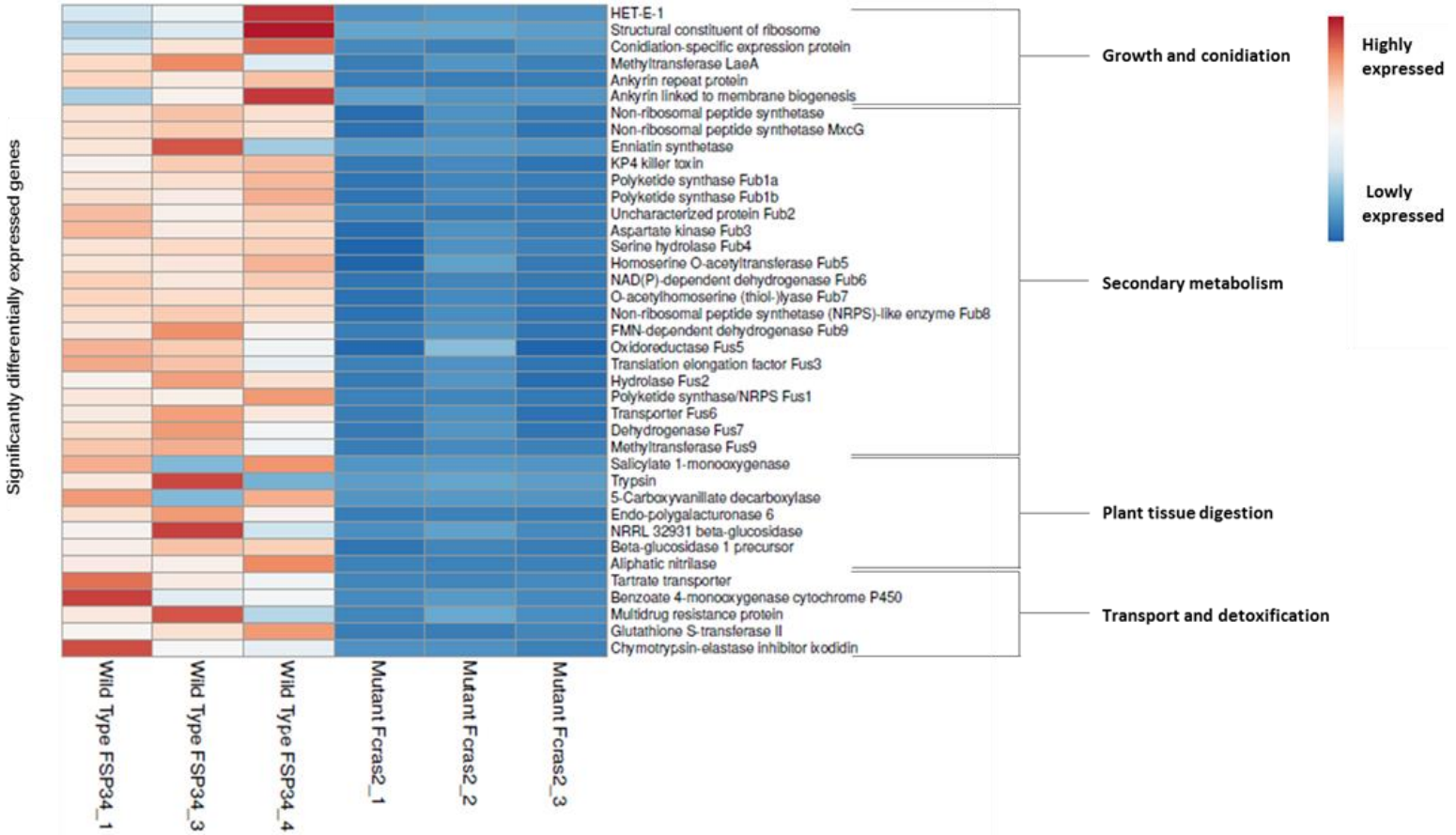

Figure 5. Heatmap showing expression patterns of proteins linked to hyphal growth, cytokinesis, protein synthesis, conidiation, secondary metabolism, plant tissue digestion, and cell defence response and transport in the *F. circinatum* knockout mutant ΔFcras2 and the wild type FSP34 strains. Each strain had three replicates. Strains are represented by columns, and proteins are shown in rows. Proteins displayed in blue are lowly expressed genes and while those in red are highly expressed.

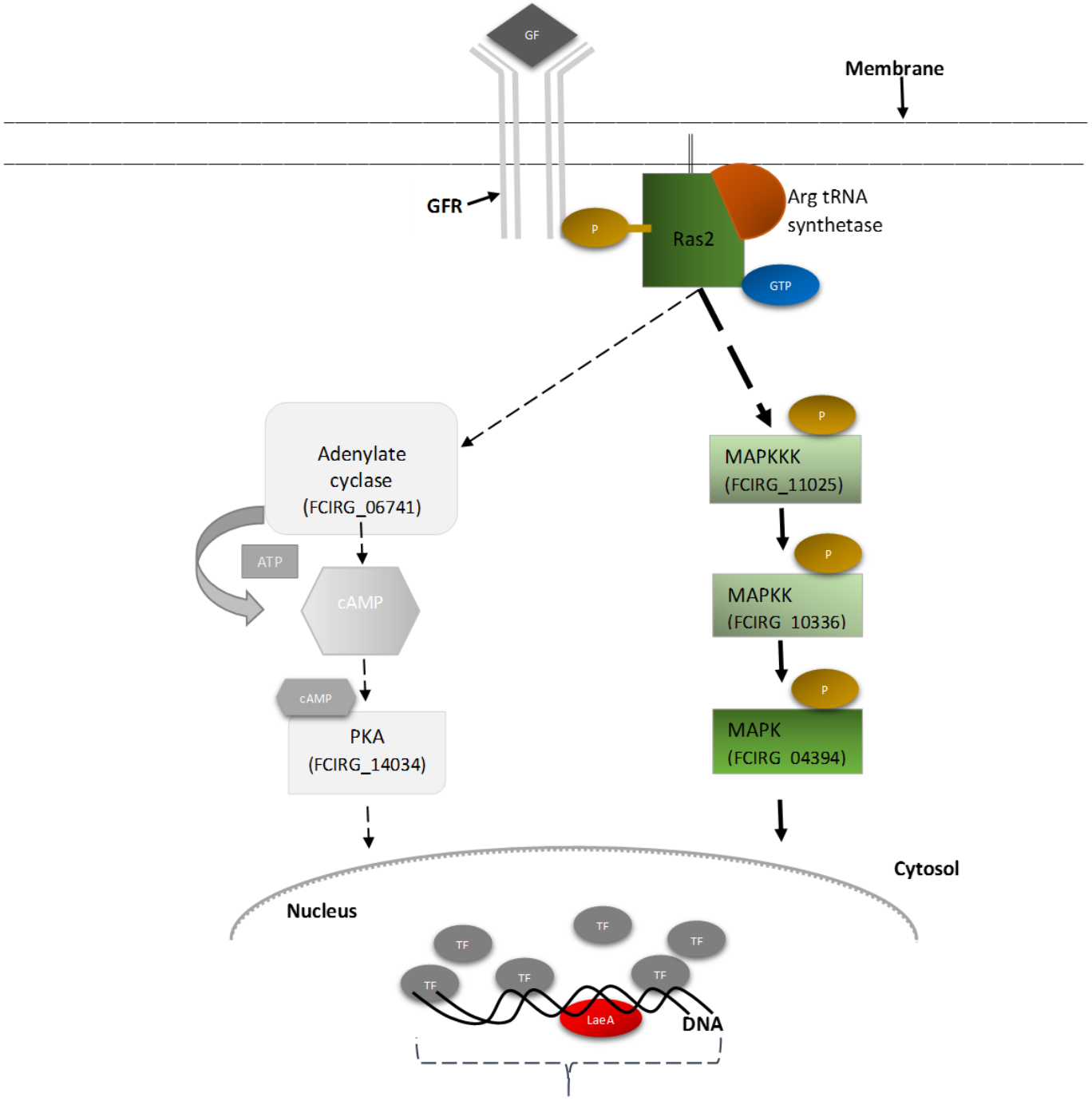

Figure 6. Putative components of the MAPK and cAMP signalling pathways associated with growth, development and pathogenicity in *F. circinatum*. GF = growth factor, GFR = growth factor receptor, P = Phosphate, Arg = arginyl, ATP = adenosine tri phosphate, cAMP = cyclic adenosine mono phosphate, PKA = protein kinase A, MAPKKK = mitogen-activated protein kinase kinase kinase, MAPKK = mitogen-activated protein kinase kinase, MAPK = mitogen-activated protein kinase, and TF = transcription factor, LaeA =

Supplementary files

Supplementary file S1. A file showing raw expression data of all the genes of *F. circinatum* in the knockout mutant strain ΔFcras2 and wild type strain FSP34.

Supplementary file S2. A file showing significantly downregulated and upregulated DEGs in *F. circinatum* knockout mutant strain ΔFcras2. A Bonferroni value of ≤ 0.05 together with fold change of at least 3 (i.e., ≥ 3 for upregulated DEGs and ≤ -3 for downregulated DEGs) were used as cut-offs during the identification of genes that were significantly differentially expressed.

Supplementary file S3. A file showing a list of clustered DEGs reported in the current study.

Supplementary file S4. A file showing GO terms and InterProScan IDs of downregulated and upregulated DEGs.

Supplementary file S5. Expression fold change in proteins with overlapping molecular functions between downregulated and upregulated DEGs in *F. circinatum ras2* knockout mutant.

Summary

The genus *Fusarium* includes some of the most destructive pathogens of agricultural and forestry crops. Within this genus, *Fusarium circinatum* is an important pathogen that causes severe disease on pine plants of all ages and is thus responsible for huge economic losses to forestry industries worldwide. In this thesis, the roles of putative pathogenicity genes (*RAS2* and *FUB1*) were investigated in *F. circinatum*. This was done by generating *ras2* and *fub1* knockout mutants, and studying their phenotypes alongside *F. circinatum* wild type strain FSP34. The phenotypes included hyphal growth, conidiation, fertility, secondary metabolite production and virulence. Transcriptomes of these mutants and the wild type strain were also sequenced, and gene expression patterns were compared. Results from the phenotypic studies showed that deletion of *RAS2* caused reduced growth of *F. circinatum* colonies as well as reduced virulence of the fungus on *Pinus patula* seedlings. The results also showed that the lack of the *RAS2* gene in the knockout mutant strain slowed conidia germination, and resulted in fewer perithecia being produced in a sexual cross where this strain was a female. Phenotypic studies with the *fub1* knockout mutant showed that disruption of the *FUB1* gene caused an abolishment in the production of the fusaric acid secondary metabolite by *F. circinatum*. This disruption also caused the *fub1* knockout mutant to produce smaller lesions on *P. patula* seedlings than the wild type strain. Analyses of gene expression patterns in the *ras2* knockout mutant and wild type strain revealed that the deletion of *RAS2* caused downregulation in numerous genes putatively involved in *F. circinatum* development and pathogenesis including transcriptional regulators and components of the mitogen-activated protein kinase (MAPK) signalling pathway. Results from analyses of gene expression patterns in the *fub1* knockout mutant and the wild type strains also revealed a number of downregulated genes possibly involved in pathogenesis, and an upregulation genes of the bikaverin biosynthetic cluster. Collectively, the findings from this thesis show that *RAS2* and *FUB1* are virulence factor genes in *F. circinatum*. The findings also suggest that the Ras2 protein is a master regulator that controls growth, development and virulence in this fungus, and that it does so in a MAPK-dependent manner. This work will contribute to our knowledge of the molecular basis and mechanisms used by fungi in general to cause disease on their hosts.

Conclusions

Fusarium circinatum is an important pathogen of pines that causes severe disease and thus huge economic losses to forestry industries. Although the genome sequence of this fungus has been determined, little is known about the molecular basis and mechanisms of pathogenesis in this fungus. This study focused on the functional characterization of two putative virulence genes (*RAS2* and *FUB1*) and the identification of other pathogenesis-related genes potentially under their control and/or linked to them. To characterize the *RAS2* and *FUB1* genes, *F. circinatum* knockout mutants of the two genes were generated and their phenotypes (i.e., growth, development and virulence) were compared to those of a wild type strain (FSP34) of the fungus. To determine genes potentially under the control of *RAS2* and those linked to *FUB1*, the transcriptomes of the *ras2* and *fub1* knockout mutant strains were sequenced and compared to that of the wild type strain. Results showed that *RAS2* and *FUB1* are important for the virulence of *F. circinatum* on *Pinus patula* seedlings. Transcriptomic analyses revealed numerous genes under the control of *RAS2* and genes that were affected by the disruption of *FUB1*.

Chapter 1 of this thesis discussed the role of known pathogenicity and virulence factor genes in filamentous fungal phytopathogens during infection of various agriculturally and economically important crops. From the available literature discussed, it was evident that homologous pathogenicity and virulence genes can have different functions during infection, often depending on the host. Therefore, lessons learnt from one pathosystem cannot always be applied to another. It is also apparent that putative pathogenicity and virulence factor genes need to be functionally characterized in any fungal pathogen of interest. The value of current and future sequencing technologies for identifying previously unknown pathogenicity and virulence factor genes in non-model phytopathogenic fungi was also explored and emphasized.

The *RAS2* gene, which was the focus of Chapter 2, encodes a GTPase (Ras2) known to regulate numerous cellular processes in eukaryotes. In phytopathogenic fungi, Ras2 has been shown to control growth, aspects of development and virulence. The *F. circinatum ras2* knockout strain generated in this study had reduced hyphal growth, asymmetric colonies and slow conidial germination compared to wild type strain FSP34. Sexual crosses between the *ras2* knockout strain and a male strain of this fungus resulted in fewer perithecia than when FSP34 was crossed with this male strain. *Pinus patula* seedling infection studies showed the knockout strain produced

shorter lesions than FSP34. These results showed that Ras2 controls growth, development and virulence in *F. circinatum*.

The *FUB1* gene, studied in Chapter 3, encodes a polyketide synthase that is involved in the biosynthesis of fusaric acid, which is a phytotoxin in some *Fusarium* species. The *fub1* knockout mutant generated here did not produce fusaric acid and had reduced virulence on *P. patula* seedlings compared to wild type strain FSP34. The disruption of *FUB1* also caused an overproduction of another phytotoxin (i.e., bikaverin). Transcriptome data revealed downregulation of other genes that form part of the *FUB* gene cluster as well as of a gene (*laeA*) that encodes LaeA methyltransferase, which is a known master transcriptional regulator of secondary metabolism in various fungi. Genes involved in detoxification and cell defence, membrane integrity and plant cell wall degradation were also downregulated.

In Chapter 4, the transcriptomic analyses of the *ras2* knockout strain alongside wild type strain FSP34 revealed that Ras2 likely controls growth, development and pathogenesis via the mitogen-activated protein kinase (MAPK) signalling pathway. This was shown by downregulation of the core MAPK gene in the *ras2* knockout mutant. Numerous other downregulated genes in the *ras2* knockout mutant were also observed, which included specific genes encoding products involved in cytokinesis, cell defense, plant cell wall degradation, hyphal growth and phytotoxin production.

Taken together, this study showed that Ras2 and fusaric acid are virulence factors in *F. circinatum*. It was also demonstrated that growth, development and virulence are traits encoded by multiple genes in this fungus. The genes catalogued using the transcriptomics significantly improve current knowledge, not only of the molecular basis, but also of molecular mechanisms used by *F. circinatum* during pathogenesis and disease development. Functional characterization of this catalogue of genes, and infection trials, thus will be vital for understanding exactly how the genetic information encoded by *F. circinatum* allows the fungus to cause disease on its pine host, while at the same time evading the host's defense mechanisms. In addition to what we now understand about the role of *RAS2* and *FUB1* in this fungus, knowledge of the exact roles of the other identified genes will help us design effective management strategies to control the fungus in pine nurseries and plantations.